ABSTRACT

FRANKL, BERNARD ANTHONY. Structural Behavior of Insulated Precast Prestressed Concrete Sandwich Panels Reinforced with CFRP Grid. (Under the direction of Sami H. Rizkalla, Ph.D.)

Precast prestressed concrete sandwich wall panels are typically used for the construction of building envelopes. Such panels consist of two layers of concrete separated by a layer of rigid foam insulation. Panels are typically designed to carry gravity loads from floors and roofs, to resist transverse lateral loads due to wind, to insulate a structure, and to provide specific interior and exterior finished wall surfaces.

Insulated concrete sandwich panels may be designed to resist gravity and lateral loads in a non-composite, partially composite or fully composite action. A fully composite panel is designed to allow utilization of the two concrete wythes acting in composite action to resist the applied loads. For panels designed as fully non-composite, each of the concrete wythes act independently to resist the applied loads. The partially composite panel has an intermediate behavior.

This thesis summarizes a research program undertaken to study the behavior of prestressed concrete sandwich panels reinforced with carbon fiber reinforced polymer (CFRP) shear grid to achieve the composite action between the two concrete wythes. The experimental program consists of six precast prestressed concrete sandwich panels measuring 20 ft tall by 12 ft wide by 8 in thick that were tested vertically in a steel frame. The panels were subjected to gravity loads and reverse-cyclic lateral loading to simulate 50 years service life of the structure. The various parameters considered in the experimental program were the type of foam core, the wythe and core thicknesses, the quantity of the carbon shear grid

and the presence of solid concrete zones. Each panel was instrumented to measure gravity and lateral loads, lateral deflections, and concrete strains to evaluate the behavior as affected by these parameters.

Test results and observed behavior of the panels under applied load indicates that the stiffness and the panel degradation behavior are dependant on the relative wythe thicknesses, the quantity of carbon shear grid and the type of foam. In general, an increase in relative wythe thickness or quantity of carbon shear grid increases the stiffness and reduces the degradation behavior. Ultimate load carrying capacity and composite action can be increased by using Expanded Polystyrene foam (EPS) in comparison to Extruded Polystyrene foam (XPS).

Typical failure mode was characterized by failure at the top of the panel near the corbels. Failure of the adequately reinforced panels with CFRP grid exhibited simultaneous flexural-shear cracking followed by separation of the concrete wythes.

The degree of composite action was evaluated with respect to deflection. The percent composite action with respect to deflection is based on comparing the measured deflection to the theoretical composite and non-composite deflections of the panel. Results indicated that EPS foam exhibited superior bond than XPS foam resulting in a higher level of composite action. It was also found that a 4-2-2 configuration (4 inch inner concrete wythe thickness) significantly showed improved behavior in comparison to a 2-4-2 (2 inch inner concrete wythe thickness) configuration and solid zones of concrete were the most structurally efficient shear transfer mechanism.

Structural Behavior of Insulated Precast Prestressed Concrete Sandwich Panels Reinforced with CFRP Grid

by
Bernard Anthony Frankl

A thesis submitted to the Graduate Faculty of
North Carolina State University
in partial fulfillment of the
requirements for the Degree of
Master of Science

Civil Engineering

Raleigh, North Carolina

2008

APPROVED BY:

_____	_____
Rudolf Seracino, Ph.D.	Michael L. Leming, Ph.D.

_____
Sami H. Rizkalla, Ph.D. (Chair)

DEDICATION

To my loving wife *Nicole Marie Carr Frankl* and my son *Keith Driver Frankl*. Without the love and support of my family, this thesis would not have been possible. They are the light, meaning and inspiration of my life. I would also like to dedicate this thesis to my parents, Patrick Frankl and Sandra Frankl, for their love, support and guidance.

BIOGRAPHY

Bernard Anthony Frankl received his Master of Science in Civil Engineering (MSCE) at North Carolina State University (NCSU), Summa Cum Laude, in 2008, with an emphasis in structural design. He received his Bachelor of Science in Civil Engineering (BSCE) at South Dakota School of Mines and Technology (SDSM&T), Summa Cum Laude, in 2006, with an emphasis in structural and geotechnical design.

Bernard had the opportunity to develop his technical skills when he began working for Dick Anderson Construction in Montana the summers of 2000 through 2003. With construction experience and excellent grades, he was honored by interning with Morrison-Maierle Inc. the summer of 2004. While his primary duties included site survey work, he learned the value of design specifications, construction oversight, and technical data collection. He then accepted a research position at SDSM&T with Dr. Sangchul Bang as well as with the Advanced Materials Processing Center. Along with planning and executing research experiments, he had the opportunity to develop his teaming and leadership abilities by becoming a leader of the SDSM&T organization Center of Excellence for Advanced Manufacture and Production (CAMP), as well as accepting a leadership role within the ASCE Steel Bridge team. These activities ultimately lead to his induction into the SDSM&T Leadership Hall of Fame in 2006. Along with technical, teaming and leadership achievements, Bernard received his Fundamentals of Engineering certification in the spring of 2006 and his ACI Concrete Field Testing Technician – Grade 1 certification in 2004.

ACKNOWLEDGEMENTS

I would like to extend my highest appreciation to my graduate advisor, Dr. Sami Rizkalla, as well as Dr. Rudolf Seracino and Dr. Michael Leming. They have been supportive and understanding throughout my experience at North Carolina State University. I am also ever grateful to my undergraduate research advisors at South Dakota School of Mines and Technology, Dr. Sangchul Bang, Dr. Anil Patnaik, and Bill Arbegast who presented me the opportunity to conduct undergraduate research, for which I inspired to pursue my graduate degree in Civil Engineering.

I would like to thank Greg Lucier for his guidance in the laboratory as well as advising me in my analytical pursuits. I would also like to extend my gratitude to Harry Gleich of Metromont Corporation and Steve Brock of Gate Precast who produced the wall panels as well as Altus Group for providing the research funding to investigate the behavior of precast prestressed concrete sandwich panels.

Finally I would like to thank the Constructed Facilities Laboratory personnel. Without their help and assistance, this research would not have been possible.

Jerry Atkinson – Providing day to day assistance in the laboratory

Bill Dunleavy – Providing electronic assistance in capturing test data

Lee Nelson – Providing technical assistance during testing

Amy Yonai – General office paper work support and purchase order assistance

Diana Lotito– General office paper work support and purchase order assistance

Work study students – Assisting me in test setup and test executions

TABLE OF CONTENTS

LIST OF TABLES

LIST OF FIGURES

LIST OF SYMBOLS

a_1 = top of panel to height of axial load

a_2 = end of panel to height of lateral load (four point bending)

a_3 = inner wythe surface to point of axial load

A_c = composite concrete area

$A_{c,o}$ = outer wythe concrete area

$A_{c,i}$ = inner wythe concrete area

$A_{p,o}$ = prestressing steel area for outer wythe

$A_{p,c}$ = prestressing steel area for composite section

$A_{p,i}$ = prestressing steel area for inner wythe

$A_{s,c}$ = mild steel area for composite section

$A_{s,nc}$ = mild steel area for each wythe (assumed same area for inner and outer wythe)

b = panel width

C = compression force

d_1 = top extreme fiber of composite section to inner wythe steel

d_2 = top extreme fiber of composite section to outer wythe steel

d_o = composite elastic centroid to outer wythe elastic centroid

$d_{p,o}$ = outer wythe prestressing depth from outer wythe top extreme fiber

$d_{p,c}$ = fully composite prestressing depth from top extreme fiber

$d_{p,i}$ = inner wythe prestressing depth from inner wythe top extreme fiber

$d_{s,o}$ = outer wythe mild steel depth from outer wythe top extreme fiber

$d_{s,c}$ = fully composite mild steel depth from top extreme fiber

$d_{s,i}$ = inner wythe mild steel depth from inner wythe top extreme fiber

d_i = composite elastic centroid to inner wythe elastic centroid

$e_{a,o}$ = outer wythe axial load eccentricity

$e_{a,c}$ = composite section axial load eccentricity

$e_{a,i}$ = inner wythe axial load eccentricity

E_c = concrete modulus of elasticity day of testing

E_{ci} = initial concrete modulus of elasticity

e_i = initial panel bow

$e_{p,o}$ = outer wythe prestressing eccentricity

$e_{p,c}$ = fully composite prestressing eccentricity

$e_{p,i}$ = inner wythe prestressing eccentricity

E_{ps} = prestressing steel modulus of elasticity

E_s = mild steel modulus of elasticity

f_c = concrete strength day of testing

f_{ci}' = initial concrete strength

f_{pi} = initial prestressing jacking stress

f_{ps} = prestressing strand stress

f_{pu} = prestressing strand ultimate strength

f_{py} = prestressing strand yield strength

f_r = concrete tension modulus

f_{sy} = mild steel yield strength

H' = bottom of panel to height of axial load

H = height of panel

I = inner wythe stiffness

I_c = fully composite moment of inertia

$I_{cr,.o}$ = outer wythe cracked moment of inertia

$I_{cr,c}$ = composite section cracked moment of inertia

$I_{cr,i}$ = inner wythe cracked moment of inertia

I_{eff} = effective moment of inertia

I_{nc} = non-composite moment of inertia

$I_{nc,o}$ = outer wythe moment of inertia

$I_{nc,i}$ = inner wythe moment of inertia

k = friction loss coefficient associated with prestressing

k_{cr} = creep coefficient associated with prestressing

k_{sh} = shrinkage coefficient associated with prestressing

M_a = effective applied moment

$M_{cr,o}$ = outer wythe cracking moment

$M_{cr,c}$ = composite section cracking moment

$M_{cr,i}$ = inner wythe cracking moment

$M_{e,o}$ = outer wythe moment due to axial load

$M_{e,c}$ = composite section moment due to axial load

$M_{e,i}$ = inner wythe moment due to axial load

M_n = nominal moment capacity

M_{SD} = moment due to super imposed dead loads

n = effective prestressing modular ratio

n_i = initial prestressing modular ratio

O = outer wythe stiffness

P_a = composite axial load

$P_{a,o}$ = outer wythe axial load

$P_{a,i}$ = inner wythe axial load

$P_{e,o}$ = effective outer wythe prestressing force

$P_{e,c}$ = effective composite prestressing force

$P_{e,i}$ = effective inner wythe prestressing force

$P_{i,o}$ = initial outer wythe prestressing force

$P_{i,c}$ = initial composite prestressing force

$P_{i,i}$ = initial inner wythe prestressing force

P_{lat} = lateral load applied per point load in four point bending

P_n = nominal axial load capacity

R = percent prestressing force retained after losses

RH = relative humidity associated with prestressing

t = panel thickness

T = tension force

t_1 = equivalent inner wythe thickness

t_2 = equivalent outer wythe thickness

t_3 = equivalent core thickness

t_{relax} = time from casting to testing

t_{set} = time of casting to release of prestressing strands

V/S = concrete volume divided by concrete surface area

x = top of panel to height used for deflection percent composite action

x_1 = bottom of panel to height used for deflection percent composite action

x_2 = bottom of panel to height of maximum moment

x_3 = top of panel to height of maximum moment

$y_{b,o}$ = outer wythe elastic centroid to bottom extreme fiber of outer wythe

$y_{b,c}$ = composite elastic centroid to bottom extreme fiber of composite section

$y_{b,i}$ = inner wythe elastic centroid to bottom extreme fiber of inner wythe

$y_{t,o}$ = outer wythe elastic centroid to top extreme fiber of outer wythe

$y_{t,c}$ = composite elastic centroid to top extreme fiber of composite section

$y_{t,i}$ = inner wythe elastic centroid to top extreme fiber of inner wythe

Δ_A = anchorage seating associated with prestressing

Δ_{app} = panel lateral deflection due to applied loads

Δf_{pA} = prestressing losses due to anchorage seating

Δf_{pCR} = prestressing losses due to concrete creep

Δf_{pES} = prestressing losses due to concrete elastic shortening

Δf_{pF} = prestressing losses due to friction

Δf_{pR} = prestressing losses due to strand relaxation

Δf_{pSD} = prestressing losses due to super imposed dead loads

Δf_{pSH} = prestressing losses due to concrete shrinkage

$\Delta_{P\text{-}\Delta}$ = panel lateral deflection due to eccentrically applied axial load

α = wobble coefficient associated with prestressing

β_1 = neutral axis depth coefficient

ε_1 = effective strain in strand due to prestressing

ε_2 = effective strain in strand at decompression of section

ε_3 = effective strain in strand compatible with ultimate compression strain

ε_{cu} = concrete crushing strain

ϕ_f = flexural strength reduction factor

ϕ_v = shear strength reduction factor

$\gamma\sqrt{f_c}$ = concrete tension modulus coefficient

γ_c = concrete unit weight

μ = friction coefficient associated with prestressing

1 INTRODUCTION

1.1 BACKGROUND

Precast concrete insulated sandwich wall panels, commonly known as concrete sandwich panels, are typically used for building envelopes. Such panels consist of two outer layers of concrete separated by an inner foam core. Panels can serve to carry gravity loads from floors or roofs, to resist normal or transverse lateral loads caused by wind, to insulate a structure and to provide the interior and exterior finished wall surfaces.

Typical panels are fabricated with heights up to 45 feet and widths up to 12 feet. Wythe thickness ranges from 2 inches to 6 inches with overall panel thicknesses ranging from 5 inches to 12 inches. Prestressing is normally provided for both concrete wythes.

Insulated concrete sandwich panels may be designed as one of three types: non-composite, partially composite and fully composite. Some panels are also designed to be non-composite during service but fully composite during handling in order to reduce the amount of shear transfer mechanism used within the panel. The degree of composite action depends on the nature of the connections between the two concrete wythes. Connections between wythes have traditionally been made using solid zones of concrete, bent reinforcing bars, or various specially-designed steel shear connectors. Increasing the degree of composite action between wythes increases the structural capacity of a given panel, making it more structurally efficient. However, traditional composite shear connections have the negative consequence of thermally bridging the two concrete wythes, thus decreasing the thermal efficiency.

In order to achieve the most structural efficiency provided by a composite panel, while avoiding the thermal bridges created by traditional means of shear transfer, Altus Group has recently begun utilizing a carbon-fiber shear connection grid. Since carbon fiber has a relatively low thermal conductivity of $0.9x10^{-6}$/°F (Altus Group 2008) in comparison to steel of $6.6x10^{-6}$/°F (Hibbler 2003), connecting concrete wythes with carbon grid allows a panel to develop composite structural action without developing thermal bridges; therefore, maintaining the insulating value of the panel. Optimal design practices for using carbon grid shear connectors are still being developed.

This thesis describes an experimental program conducted at the Constructed Facilities Laboratory at North Carolina State University to investigate the behavior of 20 foot Altus precast prestressed concrete sandwich wall panels reinforced with carbon-fiber shear grid, commercially knows as C-GRID.

The experimental program consisted of six 20 foot precast prestressed concrete sandwich wall panels composed of two prestressed outer concrete wythes and an internal layer of foam insulation with shear grid reinforcment placed through the core into each concrete wythe. The various parameters considered are the type of foam, presence of solid concrete zones, panel configuration, and shear grid reinforcement ratio to achieve composite action. The two types of foam considered are expanded polystyrene (EPS) foam and extruded polystyrene (XPS) foam. Each panel consisted of three layers including an inner wythe, internal foam core and an outer wythe. Panel identification contains three numbers corresponding to each layer's thickness in inches.

The first two panels tested were identical panels consisting of a 2-4-2 configuration with an EPS foam core. Both panels consisted of 90 linear feet of shear grid running along the

panel height. The last four panels all contained XPS foam but all varied in the panel configuration, presence of solid concrete zones and the quantity of shear grid. The first XPS foam panel had the same configuration and shear grid quantity as the EPS foam panels; however, it also contained several discretely located solid concrete zones while the second XPS panel consisted of a 4-2-2 configuration with no solid concrete zones. The third XPS foam panel was identical to both EPS panels with the exception of the foam core. The last panel tested was similar to the third XPS panel with an additional 30 feet of shear grid.

This thesis presents test results, analysis of the test results of the experimental program which was used to identify the structural behavior as well as to develop design guidelines for these types of panels.

1.2 RESEARCH OBJECTIVE

The primary objective of the testing program was to determine the structural performance of full-size precast EPS and XPS insulated sandwich wall panels reinforced with carbon fiber reinforced polymer shear mechanism subjected to combined axial and reverse cyclic lateral loads. The loading sequence for each panel was selected to simulate the effect of service gravity and wind loads for a 50 year lifespan. Load and support conditions were designed to mimic field conditions. Test results of the experimental program were compared to theoretical calculations to evaluate the percent composite action and assess the optimum panel configuration to maximize the efficiencies of these types of panels. Based on the findings, a design guideline is presented.

1.3 PROGRAM SCOPE

In order to achieve the research objectives described above, the following stages were pursued:

1. An extensive literature review was conducted investigating the history and development of precast insulated sandwich wall panels and their benefits. These findings were compared to extract various panel characteristics and their respective advantages and disadvantages. Industry and innovative design methods were investigated and compared indicating the importance and definitions of percent composite action.
2. Six panels containing several testing variables were subjected to a rigorous loading regimen simulating a 50 year service life. Panel behavior was recorded throughout testing to monitor the panels' response to the applied loads over time.
3. Test results were analyzed characterizing each panel's behavior. The behavior was used to develop a thorough understanding of the effect of each variable on the percent composite action of the panel.
4. Analytical modeling was conducted to evaluate the percent composite action for each panel.
5. The findings were used to develop a design guideline for these types of panels.

2 LITERATURE REVIEW

Precast prestressed concrete insulated sandwich wall panels have become increasingly popular within the precast concrete industry. Wall panels were first introduced in the 1960's with the use of double tees. Double tees were soon replaced by flat slabs to optimize structural performance and cost. Shear transfer mechanisms evolved from solid concrete zones to steel truss mechanisms to FRP truss mechanisms improving the thermal performance of wall panel system.

Wall panel systems can consists of various parameters including foam core material, type of shear transfer mechanisms and arrangement of concrete wythes and foam cores. Utilizing different variations of the wall panel parameters, the structural performance can vary from a fully non-composite behavior to a fully composite behavior. Various shear transfer mechanisms have been investigated quantifying their structural contribution to the wall panel system along with their thermal performance.

Several design philosophies have been developed for various panel behaviors and shear transfer mechanisms. Percent composite actions have been correlated by comparing experimental results to the theoretical design boundaries. Optimization of the design procedures have been achieved by utilizing the percentage of composite action. Material consumption, fabrication costs and construction costs were also significantly reduced by optimizing the design method.

2.1 DEVELOPMENT OF SANDWICH WALL PANELS

Wall panels were first introduced during the 1960's with double tee sandwich panels (Gleich, 2007). Solid concrete zones were used between the double tees in order to develop

the composite action. Double tees sandwich panels provided a robust structural wall, but sacrificed the potential thermal savings. Flat concrete slabs soon replaced double tees as the concrete wythes to reduce concrete material, optimize the structural performance and reduce overall costs (Gleich 2007). The use of solid concrete zones created thermal bridges between the wythes and could lead to a thermally deficient structural wall system.

Recently, steel ties, connecting the two concrete wythes were used to replaced solid concrete zones in an attempt to enhance the thermal performance of wall panels. It was found that the use of steel ties significantly improved the thermal efficiency in comparison to solid concrete zones; however, it could also create thermal bridges between the two concrete wythes (Gleich 2007).

Non-composite panels were introduced in the 1980's addressing the thermal deficiencies created by thermal bridges (Gleich 2007). Non-composite panels contained minimal shear connectors for handling loads only, but the lack of shear transfer compromised the structural integrity of the system. Despite the lower structural capacity, non-composite panels became popular due to their thermal savings and architectural characteristics.

In 1997, Salmon et. al. introduced the use of FRP bars formed in a truss orientation in place of metal wire trusses. They concluded that the use of FRP in a truss like mechanism can achieve a high level of composite action and can provide good thermal benefits similar to non-composite insulated sandwich wall panels. Following the same concept, Altus Group developed Carbon Fiber Reinforced Polymer Grid, commercially known as C-GRID, in 2003. Altus group utilized the C-GRID in an orthogonal layout parallel to the long axis of the wall panels. Orienting the C-GRID in a truss like orientation provides adequate shear transfer between the concrete wythes while maintaining the thermal benefits.

2.2 BENEFITS OF PRECAST INSULATED WALL PANELS

Losch (2005) investigated the use and benefits of precast insulated sandwich panels. Losch (2005) indicated that the use of a wall panel system provides several benefits over traditional wall construction. Some of the benefits are:

a. Increased thermal efficiency
b. Increased design flexibility
c. Increased speed of erection
d. Competitive costs

Precast insulated wall panels have been identified to be one of the most structural efficient systems in terms of low material consumption and highly thermal efficient systems. Bush and Stine (1994) and GoStructural (2008) stated that the use of insulated precast wall panels can increase the thermal efficiency of concrete sandwich panels nearly 30 percent over that of a stud wall system. These thermally efficient systems can save nearly 20 percent in energy cost compared to framed walls (Gleich 2007). Insulated concrete sandwich panels with polystyrene cores can exhibit R-values up to a value of 30 in comparison to a stud wall system with an R-value of 5 to 10 (Christian & Kosny 1999). The presence of steel or concrete thermal bridges can reduce the R-value up to 40 percent resulting in R-values from 12 to 16 (Lee & Pessiki 2004, Bush & Stine 1994).

Lee and Pessiki (2004) investigated the thermal efficiency of three wythe wall panels in comparison to two wythe panels in an attempt to enhance the R-value while still providing structurally efficient concrete solid zones. Lee and Pessiki (2004) showed that:

a. Three wythe panels have greater thermal efficiency than a two wythe panel
b. Concrete wythe thickness does not affect the R-values
c. Three wythe panels produces higher thermal savings in comparison to a two wythe panel with more core insulation.

Three wythe wall panel systems exhibit enhanced thermal behavior due to the increased thermal path from the inner wythe to outer wythe. It should be noted Lee and Pessiki's (2004) study was only conducted with extruded polystyrene foam. Within this study, Lee and Pessiki (2004) conducted finite elements modeling (FEM) to analyze the thermal predictions of three wythe concrete insulated sandwich panels. They found that using solid elements for modeling concrete and foam while using shell elements for modeling steel plates produced results with 95% accuracy. For this level of accuracy, thermal properties must be known of the concrete, foam core and thermal barriers such as the shear transfer mechanisms. FEM was found to represent thermal performance better than the isothermal plane method and parallel flow method. Isothermal plane method and parallel flow method yielded results within 88% and 58% accuracy, respectively.

The amount of thermal savings is dependant on the type of foam core used within the panel. Currently, there are two foam cores commonly used for insulated sandwich panels, expanded polystyrene (EPS) foam and extruded polystyrene (XPS) foam. EPS foam consists of 0.07 inch to 0.12 inch polystyrene beads that are expanded and fused together to form a solid insulation block (Horvath 1994). XPS foam is produced from a solid mass of molten material resulting in a dense consistency in comparison to EPS foam (PCA 2008). Comparisons of XPS and EPS microstructure are shown in Figure 2-1(a) and (b), respectively. EPS foam densities range from 0.6 pcf to 2.5 pcf in comparison to XPS foam which exhibits densities up to 3 pcf (Horvath 1994, PCA 2008, ASTM C578 2007). Consequently, EPS foam can retain an R-value up to 4.35 per inch thickness in comparison to XPS foam with an R-value up to 5 per inch thickness (PCA 2008). It should be noted that material properties of polystyrene foam are highly variable.

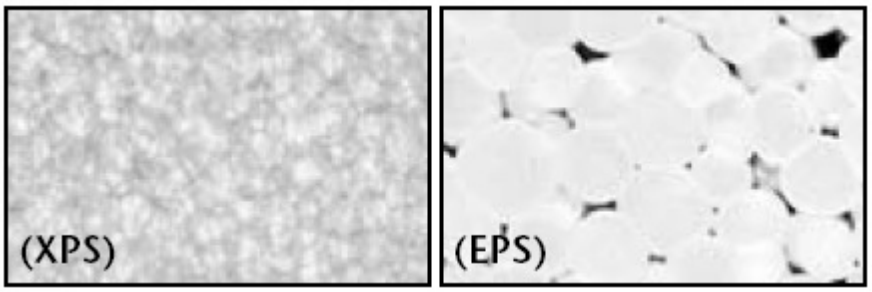

(a) (b)

Figure 2-1: Foam core microstructure
(Dow Chemical Company, 2008)

Precast concrete sandwich wall panels not only enhance the thermal efficiency, but also decreases the structural costs. An insulated wall panel can withstand equivalent flexural strength to a solid wall yet consume nearly half the concrete material; however, if the compression zone is greater than the thickness of the compression wythe, then a lower flexural strength may be experienced. Wall panels can exhibit higher ductility than solid concrete walls due to the reduction of the moment of inertia. As a result of high ductility, panels should be carefully designed to minimize the lateral deflections.

Wall panels can also provide a lighter system which is critical for the construction industry. Precast wall panels provide a quick and efficient construction system when construction costs are critical or the job site is subjected to harsh construction environments. Panels can be cast in a controlled environment ensuring structural quality, and then placed in the field with less labor than an in-situ wall (Losch 2005).

These panels not only provide structural and thermal benefits but also provide architectural benefits. It is common to provide an architectural overlay to the structural wythes making the panels aesthetically pleasing. Not only can these panels be overlaid, but wythe surface textures can be customized to the particular job and architect (Losch 2005).

2.3 PRECAST INSULATED WALL PANEL CHARACTERISTICS

Precast insulated wall panels generally consist of three layers.

a. Outer wythe
b. Foam core
c. Inner wythe

Panel identification consists of three numbers corresponding to each layer thickness in inches. A 2-4-2 panel designation consists of a 2 inch outer wythe, a 4 inch foam core and a 2 inch inner wythe. Panels can consist of additional layers. Lee and Pessiki (2004) investigated the advantages of a three wythe sandwich panel in comparison to a two wythe sandwich panel. A three wythed wall panel will consist of five numbers corresponding to the following layer thicknesses in inches:

a. Outer wythe
b. Outer foam core
c. Middle wythe
d. Inner foam core
e. Inner wythe

Lee and Pessiki (2004) concluded a three wythe system provides several potential benefits over a two wythe panel. These benefits include:

a. Improved thermal performance
b. Composite action can be achieved with solid concrete zones without sacrificing thermal efficiency
c. Locations of thickened concrete regions can be used for placements of embedded hardware
d. All prestressing can be located within the center concrete wythe

Lee and Pessiki (2008) investigated the structural behavior of a three wythe structural system under flexure only. Flexural behavior of three wythe panels showed that staggered solid concrete zones exhibits behavior similar to that of a fully composite panel. Along with high flexural capacity, these systems exhibit a ductile flexural behavior for proportionally reinforced panels. Panel ductility is attributed to the formation of a uniformly distributed

crack system along the height of the panel and yielding of the longitudinal reinforcement. It was also observed that release of the prestressing force induced cracks in the concrete wythes parallel to the prestressing strands. A Finite Element Modeling (FEM) analysis was conducted to investigate the prestressing forces during release. A comparison of experimental results and FEM results showed that modeling the concrete and the foam insulation with solid block elements provided close results to the measured values. FEM analysis was then utilized to conduct a parametric study. FEM results revealed that increasing the concrete area near the end regions of the panel reduces the number of cracks induced during prestressing.

Losch (2005) noted that induced cracking can also be reduced by providing relatively equal wythe thicknesses. Equal wythe thicknesses induces equal concrete curing of the wythes reducing shrinkage stresses.

Wall panels are generally assumed to behave as a one way system due to their height to width aspect ratios. Benayoune et. al. (2008) stated a two way system exists when the height to width aspect ratio is less than one. A one way system exists when the height to width aspect ratio is greater than 2.67. Consequently, intermediate aspect ratios yields intermediate behavior. Benalyoune et. al. (2008) showed FEM accurately represents one way systems using 2-D isoperimetric plane stress elements. The FEM is a 2-D system representing the behavior of the wall panel per foot width. Similar results for a two way system can be obtained by using 3-D thin shell elements. A two way system has to be analyzed using a 3-D model to capture behavior along the width and height of the panel. Results were confirmed by comparing the FEM deflection and strain behavior with experimental results. It was found that FEM models can exhibit increased stiffness in comparison to experimental tests.

Lee and Pessiki (2007) also found that assuming perfect bond between the foam core and the concrete surface yields similar results to a non-linear model where the foam core resists only compression and the wythe connectors resist only tensile forces.

Traditionally, sandwich wall panels are assumed to behave as either fully composite or fully non-composite systems. Fully composite panels are designed so that the two concrete wythes act together as a single unit to resist lateral loads. The decisive indication of composite behavior is a through-thickness strain profile that remains continuous at all locations along the height and width of a panel. A linear strain profile across the thickness of the panel is identified by a single neutral axis. Fully non-composite behavior results from each wythe acting independently to resist applied loads. Fully non-composite panels will have independent strain profiles and unique neutral axes for each wythe. Strain profiles for a theoretically composite and theoretically non-composite panel are shown in Figure 2-2 (a) and Figure 2-2 (b), respectively. Panel orientation with respect to the strain profile is shown in Figure 2-2 (c).

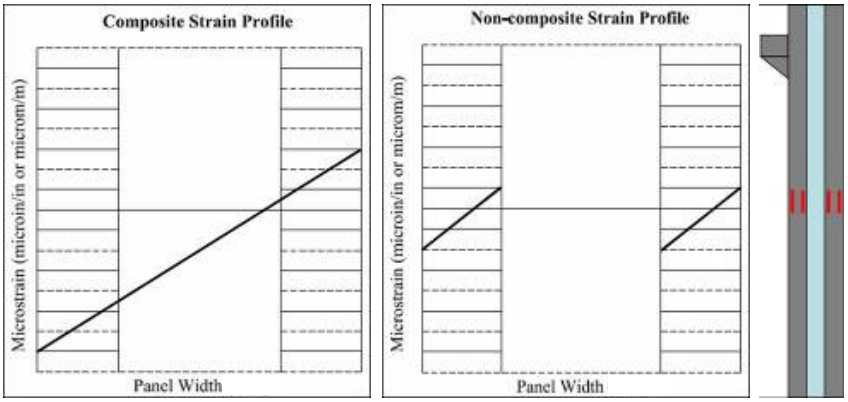

(a) (b) (c)

Figure 2-2: Theoretical fully composite and fully non-composite strain profiles

The term "partially composite" action has been introduced by several authors including Pessiki & Mylnarczyk (2003) and Lee & Pessiki (2007). Partial composite action describes a

sandwich panel behavior between the two extremes of composite and non-composite behavior.

The typical design method for precast sandwich panels assumes non-composite action (PCI 1997). In practice, panels generally exhibit partially composite behavior (Pessiki and Mylnarczyk 2003, Lee and Pessiki 2007, Bush and Stine 1994). Tests have shown that generally some level of shear transfer occurs between the wythes (Pessiki and Mylnarczyk 2003, Lee and Pessiki 2007, Bush and Stine 1994). Utilizing partial degree of composite action in the design could significantly reduce costs.

Several shear transfer mechanisms have been developed in order to increase the partial composite behavior. Several common mechanisms described in *State-of-the-Art of Precast/Prestressed Sandwich Wall Panels* (PCI 1997) are wire truss connectors, bent wire connectors, and solid zones of concrete penetrating the foam core as detailed in Figure 2-3 (a), (b) and (c), respectively.

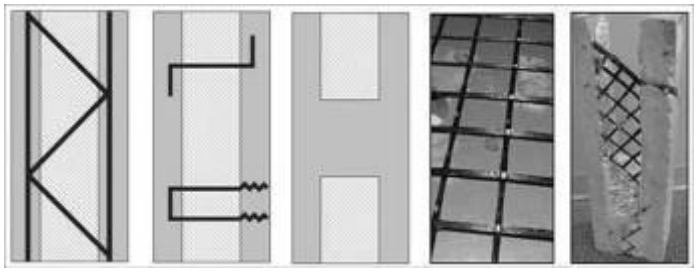

(a) (b) (c) (d) (e)

Figure 2-3: Typical shear transfer mechanisms

Wire truss connectors provide diagonal steel to transmit longitudinal shear forces from one wythe to another. Bent wire connectors rely on the shear strength of ties perpendicular to the panel faces to transfer forces. Mechanisms such as wire truss connectors provide adequate shear resistance to achieve the composite action and are commonly referred to as shear connectors. Connectors such as bent wire connectors do not provide sufficient shear

resistance and are referred to as non-shear connectors. Connectors with diagonally oriented members are more efficient than connectors with only normal oriented members in transferring longitudinal shear.

Bush and Stine (1994) investigated the efficiency of a steel truss connector in comparison to a bent wire connector. Shear specimens were tested to investigate the shear resistance of each connector. Three wythe specimens were cast with the steel connectors extending into each concrete wythe. The two outer wythes were restrained from vertical and horizontal translation and the center wythe was loaded. The three wythe configuration subjected the foam core to pure shear revealing the shear resistance of the system. Bush and Stine (1994) showed that a truss orientation increased the shear stiffness up to approximately 70% in comparison to bent wire connectors. It should be noted that solid concrete zones provide the simplest and most structurally efficient longitudinal shear transfer mechanism (Pessiki and Mylnarczyk 2003).

One major criticism of traditional shear transfer mechanisms are they allow heat to bridge the foam core. Thermal efficiency is dramatically compromised when heat is allowed to travel through the panel core.

Fiber reinforced polymer (FRP) shear transfer mechanisms have been developed as early as 1997 (Salmon et al 1997). FRP systems were developed to improve deficient thermal characteristics of traditional shear transfer mechanisms. Two notable carbon fiber reinforced polymer (CFRP) systems have been introduced. The first system was introduced in 1997 by Salmon et. al. This system uses CFRP bars in a truss orientation to transmit shear forces from the inner wythe to outer wythe. The second system was developed by Altus Group in 2003 (Gleich 2007). This system consists of carbon fiber polymer strips approximately ¼”

(6 mm) wide by $^{1}/_{16}$" (2 mm) thick arranged in an orthogonal pattern. The finished grid is oriented at a 45° angle and developed in each concrete wythe, allowing for a truss mechanism to developed. The truss orientation engages the tensile properties of the FRP grid. A grid oriented within a wall panel section is shown in Figure 2-3 (d) and Figure 2-3 (e).

Foam core thickness and surface roughness also significantly affects the shear flow capacity. An EPS foam core will exhibit increased shear resistance in comparison to an XPS foam core. EPS foam exhibits a higher surface roughness in comparison to XPS foam. A high surface roughness enhances the concrete to foam bond engaging the foam shear strength. XPS foam, however, has up to 20% higher shear strength than an EPS foam (PCA 2008). As a result, the shear resistance of XPS foam can be greater than EPS foam if the XPS foam surface is roughened to match or exceed EPS foam surface roughness.

As the foam core thickness increases, the shear flow capacity reduces while the induced shear flow from applied forces increases. Consequently, additional shear transfer mechanisms have to be provided to achieve greater composite action.

Panel shear demands are greatly affected by the loading scheme the panel is subjected to. Panels are typically designated as load bearing or non-load bearing systems. Load bearing walls carry associated gravity loads introducing an axial force into the wall panel system. Non-load bearing walls resist only lateral loads requiring another system to transmit gravity loads to the foundation. Non-composite panels are commonly non-load bearing walls due to their structural inefficiencies while composite panels are generally designed as load bearing systems. Therefore, to utilize sandwich wall panels to their full potential, composite action generally has to be achieved at service load allowing for cost savings and improved service life.

2.4 DESIGN PHILISOPHIES

The behavior of precast insulated sandwich wall panels is continually changing with the advancements of different shear transfer mechanisms. As a result, a unified design procedure has not been accepted throughout industry. There are currently several methods of design in use. Currently, design methods vary depending on the shear transfer mechanism and the precast plant designing the panels.

Precast/Prestressed Concrete Institute (PCI) published a design guideline in 1997 summarizing fully composite and fully non-composite design philosophies of concrete sandwich panels. This design philosophy consists of three behavioral variations.

a. Fully composite
b. Semi-composite
c. Fully non-composite

Fully composite assumes the panel resists applied forces as a single unit. Semi-composite assumes the panel behaves compositely during handling and erection and fully non-composite under service loads. A fully non-composite behavior assumes each wythe resists the applied moments individually and the moment is distributed between the wythes with respect to their uncracked stiffness.

PCI accounts for four load conditions: service, stripping and handling, travel and erection. The maximum applied moment is due to the largest moment of these four loading conditions. Moments due to applied service loads consists of two parts: moment due to applied forces and secondary P-δ effects due to axial loads. Once the ultimate moment is acquired, the prestressing strands are selected in accordance to ACI 318. If axial load is present, the load is assumed to act through the elastic centroid of the composite cross section for a fully composite panel and through the elastic centroid of the axially loaded wythe for fully non-

composite. Panel deflections include flexural deflections along with secondary P-δ deflections.

The shear transfer mechanism has to resist the induced shear forces throughout the height and width of the panel in order to develop a fully composite behavior. Shear flow resistance must be greater than the induced shear flow (Salmon et. al. 1997). Shear flow capacity must be provided through testing or by the shear transfer mechanism provider. If solid concrete zones are present, then the shear strength of the concrete is assumed to be $80A_c$ (psi) as specified by ACI 318-05 section 17.5.3. The concrete shear strength can then be distributed over the tributary height in order to develop the shear flow resistance. An alternative method of shear reinforcement design is to develop horizontal shear strength across the panel core greater than the smaller of the tension force or compressive force extracted from strain equilibrium of the cross-section at ultimate condition (Lee & Pessiki 2008).

The drawbacks to the PCI design method is that it does not account for partial composite action or shear deformations. Shearing deformation can be accounted for in a composite panel if the shear modulus and shear strength of the panel core is known. Some precasters have developed shear properties to account for the shearing deformation in composite panels for a particular type of shear transfer mechanism.

Bush and Stine (1994) showed that nearly all panels will exhibit some level of composite action through three shear mechanisms: concrete to foam interface, shear strength of the shear transfer mechanism and the shear strength of the foam core. Strain profile discontinuities have to be accounted for when accounting for partial composite action. . Accounting for the level of discontinuity becomes very difficult and varies with the panel configuration, shear mechanism, and type of foam.

As stated by Pessiki and Mlynarczyk (2003) the definition of percent composite action is inconsistent throughout industry. Pessiki and Mlynarczyk (2003) developed a method of interpolation between the two extremes of fully composite and fully non-composite to evaluate the percent composite action. Their resulting interpretation is given in Equation 2-1.

$$\kappa = \frac{I_{\exp} - I_{nc}}{I_c - I_{nc}}(100) \qquad \textbf{Equation 2-1}$$

Where
- κ is the percent composite action
- I_{exp} is the moment of inertia extrapolated from the test data
- I_{nc} is the non-composite moment of inertia
- I_c is the composite moment of inertia

Since the percent composite action is dependant on the experimental load deflection behavior to extrapolate the experimental moment of inertia, the percent composite action is dependant on the type of shear resistance (Pessiki and Mlynarczyk 2003). Consequently, the percent composite action has to be specified for the type and quantity of shear transfer mechanism as well as the type of foam used.

Percent composite action values for two and three wythe panels have been developed by Pessiki and Mlynarczyk (2003) and Lee and Pessiki (2008), respectively. Variables addressed within the analysis include: panel configuration, type of shear transfer mechanism and foam type. The studies included in Table 2-1 all contained XPS foam cores.

Table 2-1: Percent composite action

Panel Configuration	Shear Transfer Mechanism	Percent Composite Action
3-2-3	Solid Concrete Regions, M-ties and XPS Foam Bond	100%
3-2-3	Solid Concrete Regions only	92%
3-2-3	M-ties only	10%
3-2-3	XPS Foam Bond only	5%
2-1-2-1-2	Solid Concrete Regions and XPS Foam Bond[1]	79%
2-1-2-1-3	Solid Concrete Regions and XPS Foam Bond[2]	94%

Note: 2 has more evenly distributed solid concrete zones in comparison to 1

Pessiki and Mlynarczyk (2003) and Lee and Pessiki (2008) found the percent composite action of solid concrete zones exhibits significantly higher percent composite action than XPS foam to concrete bond and M-ties as shown inTable 2-1. More evenly distributed shear reinforcement was found to increase the percent composite action as shown with the two three wythe panels in Table 2-1 It was also shown two wythe panels with equivalent shear reinforcement as three wythe panels exhibited similar percent composite action values.

An alternative method for accounting for the percent composite action, presented by Benayoune et. al. (2005) and Salmon et. al. (1997), was developed by taking the ratio of the experimental behavior with respect to the fully composite behavior. The experimental to composite ratio allows for the maximum applied moment to be increased and the panel designed for fully composite behavior. Benayoune et. al.(2005) tested a series of small scale, two wythe panels under one way and two way bending reinforced with a wire truss shear transfer mechanism and polystyrene foam. The type of polystyrene foam was not specified. The experimental moment of inertia was compared to the fully composite uncracked moment of inertia resulting in percent composite actions ranging from 70% to 90% by doubling the shear transfer reinforcement ratio.

2.5 CONCLUSIONS

After review of previous research, several conclusions were developed summarizing the behavior of precast insulated sandwich panels.

1. Wall panels exhibit improved thermal properties in comparison to a stud wall system
2. Three-wythed panel exhibits improved thermal performance in comparison to a two-wythed panel
3. FEM can be utilized to accurately represent strength and thermal behavior of insulated wall panels

3 EXPERIMENTAL PROGRAM

3.1 TEST PROGRAM

3.1.1 Test Panels

A total of six precast prestressed concrete sandwich wall panels were tested in this experimental program. The typical dimension of the tested panels is 8 inches thick, 12 feet wide and 20 feet tall. Designation of the tested sandwich panel generally consists of three numbers referring to the inner wythe concrete thickness, the foam thickness and the outer wythe concrete thickness as shown in Figure 3-1.

For the purpose of this thesis, the corbel wythe will be referred to as the inner wythe and the non-corbel wythe will be referred to as the outer wythe as given in Figure 3-1.

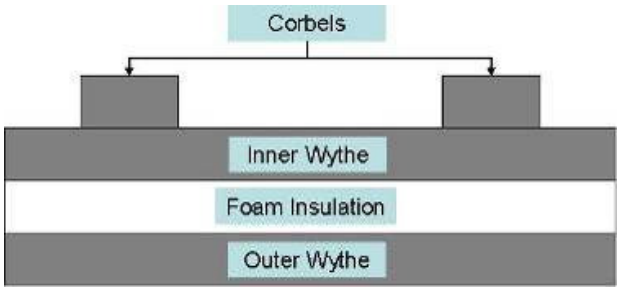

Figure 3-1: Cross-section labels

This study included panels fabricated with two different foam types. The first foam type is expanded polystyrene foam (EPS). Expanded polystyrene foam consists of a beaded material with a high void ratio. The second foam used is extruded polystyrene foam (XPS) which consists of a dense hard foam material with a low void ratio.

Five panels consisted of a 2-4-2 configuration with 4 inches of an insulation core, and the inner wythe had two 2 inch thick by 24 inch wide pilasters at quarter widths spanning the total height of the panels as shown in Figure 3-2. These pilasters were provided to work with the corbels to carry the gravity load to the foundation.

The concrete wythes are reinforced with welded wire reinforcement, 16 x 10 - W2.1 x W3.0, located at one inch from the outer surface of each wythe. A total of ten 3/8 inch diameter 270k low-lax prestressing strands were used to prestress the concrete to a stress equivalent to 202.5 ksi. Locations of the strands are shown in Figure 3-2 and Figure 3-3.The strand locations were:

- 2 strands spaced at 5 ¾" from each end, 1" from each surface
- 2 strands spaced at 9 ¾" from each end, 1" from each surface
- 2 strands spaced at mid width, 1" from each surface

Each strand was stressed to 75% of ultimate, providing an initial prestressing force (before losses) of 17,200 lbs/strand.

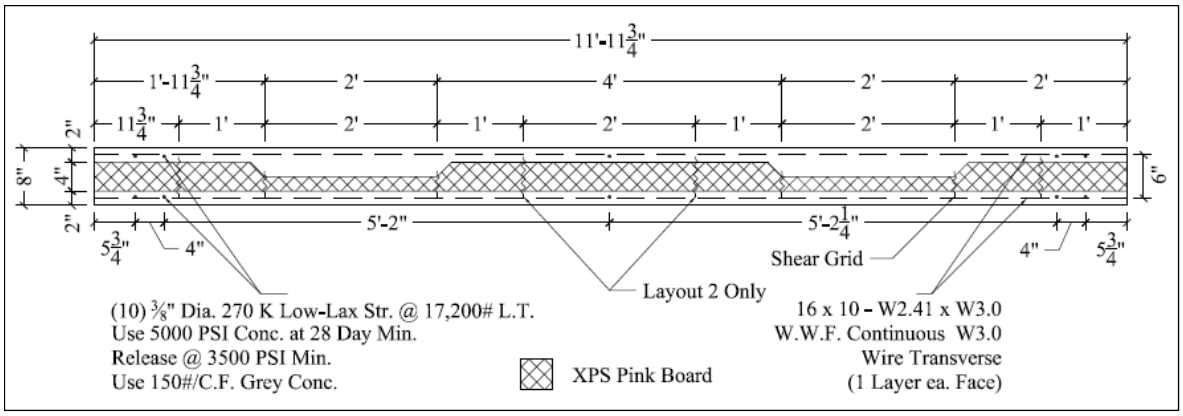

Figure 3-2: Typical 2-4-2 specimen cross section

Figure 3-3: Photograph of cut 2-4-2 panel showing an internal pilaster

The 4-2-2 panel consist of a 4 inch thick inner wythe throughout the width of the panel followed by a constant 2 inch foam layer and a 2 inch concrete outer wythe as shown in Figure 3-4 and Figure 3-5. Welded wire fabric sheets of 16x10-W2.1xW3.0 were also used at the center of each wythe, adjacent to the prestressing strands. A total of five 3/8 inch diameter 270k low-lax prestressing strands were used to stress the 2 inch concrete wythe and five 1/2 inch diameter 270k low-lax prestressing strands were used to stress the 4 inch concrete wythe as shown in Figure 3-4. Strand locations were provided as follows:

-2 strands 7 7/8" from each end, centered in each concrete wythe
-2 strands 3'-3 7/8" from each end, centered in each concrete wythe
-2 strands 5'-11 7/8" from either end (in center width), centered in each concrete wythe

Each strand was stressed to 75% of ultimate, providing an initial prestressing force (before losses) of 17,200 lbs/strand.

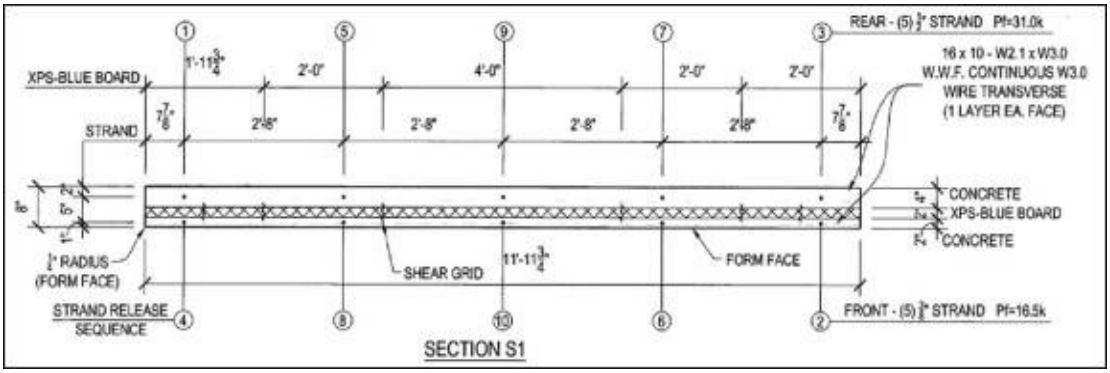

Figure 3-4: Typical 4-2-2 specimen cross section

Figure 3-5: Photograph of cut 4-2-2 panel showing wythe thickness

Carbon fiber C-GRID was provided between the two wythes to transfer the shear stresses across the foam and to develop a composite action between the wythes. This carbon grid was provided in strips running parallel to the long axis of each panel at the locations shown in Figure 3-6, (a). Panels EPS 1, EPS 2, XPS 1, XPS 2, and XPS 3 contained the same grid layout totaling 90 linear feet of C-GRID per panel. Panel XPS 4 contained an additional 30 foot of C-GRID totaling 120 linear feet of C-GRID as shown in the Layout 2 in Figure 3-6, (b). Panel XPS 1 also contained 10 discretely placed solid concrete zones for additional shear transfer between the two wythes. In addition, four 18 inch by 18 inch sections of C-GRID were placed parallel to the panel surface at each lifting point to reinforce the concrete during the installation process.

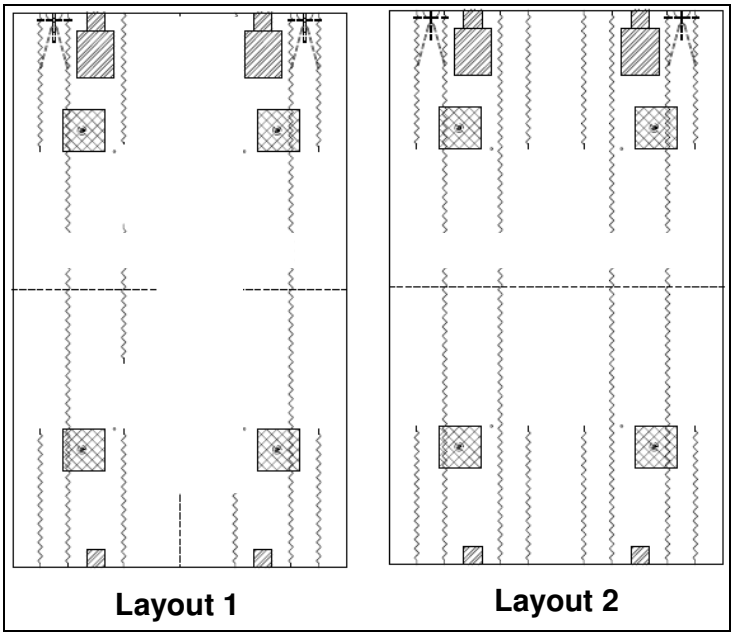

Figure 3-6: Specimen elevation C-GRID layouts

3.1.2 Construction of Wall Panels

The various parameters considered in this study are:

a. Type of foam core (EPS and XPS)
b. Configuration of the panel (2-4-2 and 4-2-2)
c. Percentage of C-GRID to achieve composite action
d. Use of solid concrete in addition to the C-GRID to achieve composite action

Panels consisting of expanded polystyrene (EPS) cores were fabricated for Altus Group by Metromont Corporation of Greenville, SC and all panels consisting of extruded polystyrene (XPS) cores were fabricated for Altus Group by Gate Precast Company of Ashland City, TN. Overall dimensions, foam types, thickness configurations, solid zones, C-GRID layout, concrete strength, cast dates and test dates of all tested panels are summarized in Table 3-1.

Table 3-1: Test specimens

Panel	Foam	Configuration	Solid Zones	C-GRID Layout	28 Day Concrete Strength (psi)	Dates Cast	Dates Tested
EPS 1	EPS	2-4-2	No	Layout 1	6410	10/17/2006	1/16/2007
EPS 2	EPS	2-4-2	No	Layout 1	6410	10/17/2006	1/31/2007
XPS 1	XPS	2-4-2	Yes	Layout 1	9190	2/7/2007	5/28/2007
XPS 2	XPS	4-2-2	No	Layout 1	7930	2/6/2007	6/8/2007
XPS 3	XPS	2-4-2	No	Layout 1	6870	9/9/2007	12/4/2007
XPS 4	XPS	2-4-2	No	Layout 2	6660	9/10/2007	11/19/2007

Sandwich panels are cast in a flat orientation in long-line production forms. Fabrication began by stressing the strands and laying reinforcement for the outer concrete wythe. After casting the first wythe, foam insulation was placed on top followed by placing the C-GRID through the foam into the wet concrete wythe beneath. With adequate shear grid projecting from the insulation, the top prestressing strands and the reinforcement of the inner wythe placed and the top concrete wythe is cast. After curing and stripping the forms, steel angles

were welded to the upper embed plates used for the corbel reinforcement and top surface. Figure 3-7 depicts a sample of the C-GRID used for shear reinforcement.

The compressive strength at time of testing was estimated based on the measured compressive stress at 28 days of 4 inch by 8 inch cylinders given in Table 3-2.

The strength on day of testing was evaluated by equation 3-1 (Mehta & Monteiro, 1993).

$$f_c(t) = f_{c28}\left(\frac{t}{4 + 0.85t}\right) \qquad \textbf{Equation 3-1}$$

Where
- $f_c(t)$ is the concrete strength at the day of interest
- f_{c28} is the 28 day concrete strength
- t is the time in days

Table 3-2: Concrete strength during tests

Panel	Test Day Concrete Strength
EPS 1	7620
EPS 2	7670
XPS 1	10080
XPS 2	8790
XPS 3	7670
XPS 4	7340

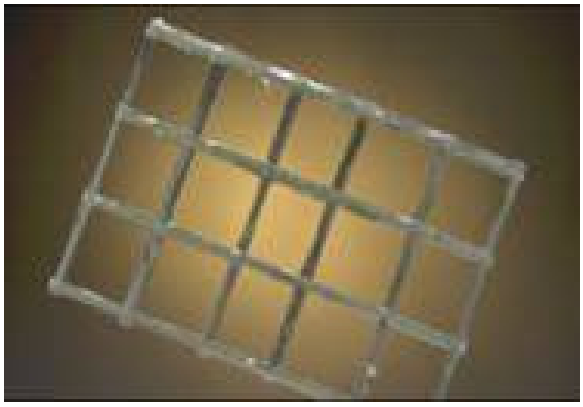

Figure 3-7: C-GRID sample
(photo courtesy of www.altusprecast.com)

3.2 LOAD SEQUENCE

The proposed loading sequence for the testing program consists of combined axial gravity load and reversed cyclic lateral load for approximately 4,000 cycles. Typical loading sequence is summarized in Table 3-3. One full load cycle consist of loading the panel laterally from zero lateral load to the specified lateral load level in both directions and back to zero lateral load. Panels EPS 1, XPS 1, XPS 2, XPS 3, and XPS 4 simulated a lateral load equivalent to a 120 MPH wind speed while panel EPS 2 simulated a lateral load equivalent to a 150 MPH wind speed.

Table 3-3: Proposed loading sequence

Step	**Vertical Load**		**Lateral Load**		
(#)	**Level**	**Load per Corbel (kips)**	**Level**	**Magnitude (kips)** (EPS 2)	**Cycles at Step (#)**
1	D	13.5	0	0	0
2	D+L	18.9	0	0	0
3	1.2D+0.5L	18.9	0	0	0
4	1.2D+0.5L	18.9	45% x 1.6W	5.0 (7.8)	3710
5	1.2D+0.5L	18.9	50% x 1.6W	5.6 (8.6)	177
6	1.2D+0.5L	18.9	60% x 1.6W	6.7 (10.4)	1
7	1.2D+0.5L	18.9	80% x 1.6W	9.0 (13.8)	1
8	1.2D+0.5L	18.9	100% x 1.6W	11.2 (17.3)	1
9	1.2D+0.5L	18.9	up to Failure	up to 20 (up to 30)	1

3.2.1 Gravity Loads

The axial load level was calculated based on the assumption that a 12 foot wide panel is supporting 60 foot of a 10DT24 double-tee roof deck. In addition to the self weight of the deck, an additional 30 psf dead load and a roof live load, L_r, of 30 psf was used. The service load case, $D+L_r$, is equal to 18.9 kips per corbel. For the required design load of $1.2D+0.5L_r+1.6W$, the factored axial load of $1.2D+0.5L_r$ is equal to 18.9 kips per corbel.

3.2.2 Lateral Loads

Lateral wind loadings were determined in accordance to ASCE 7-02 assuming a building classification of II, an exposure category of C, a building width of 200 feet, a building length of 250 feet and an exterior wall and a flat roof with a mean height of 20 feet. The topographic factor was assumed to be 1.0 and the directionality factor was assumed to be 0.85. For these conditions and a design wind speed of 120 MPH, the analytical procedure of ASCE 7-02 section 6.5 predicts a wind pressure (windward force) of 25 psf and a wind suction (leeward force) of 29 psf over the surface of the panel. The 29 psf wind suction is equivalent to a total factored concentrated lateral wind load ($1.6W_{120}$) of 11.2 kips total lateral load. This lateral load was assumed to act equally in both directions (ie: wind pressure and suction are both assumed to equal the most severe value), so loads of the same magnitude could be applied in both directions for each cycle.

3.2.3 Fatigue Cycles

In order to simulate the effects of wind loading over 50-year design lifetime of a panel, it was desired to subject each panel to a fatigue loading regimen. A Weibull distribution function was employed to rationally select the load increments and number of cycles for fatigue loading based on published work (Hau 2000, Xu 1995, Manwell 2002).

The wind variation for a typical site is described using the Weibull distribution to model the probability of occurrence for given wind speeds, where the probability distribution function is defined below.

$$P(U) = 1 - \exp\left[-\left(\frac{U}{c}\right)^{k}\right] \qquad \textbf{Equation 3-2}$$

Where:
-P(U) is the Weibull probability distribution function
-U is the wind speed being evaluated
-k and c are the shape factor and scale factor, respectively.

The shape factor and scale factor both depend on the mean wind speed and on the standard deviation of wind speeds. Both can be determined from field-recorded wind data and vary according to specific geographical location. In the absence of field-recorded data, it is generally acceptable to assume a shape factor of 2.0 (Hau 2000, Xu 1995). This choice creates a special form of the Weibull Distribution known as the Rayleigh Distribution where the ratio of standard deviation to mean will be constant. This constant relationship allows the Rayleigh Distribution to take the following form, dependent only on average mean wind speed.

$$P(V) = 1 - \exp\left[-\frac{\Pi}{4}\left(\frac{V}{\overline{V}} \right)^2 \right] \qquad \textbf{Equation 3-3}$$

Where:
-P(V) is the Rayleigh probability distribution function
-V is the wind speed under consideration
- $\overline{V}$ is the average mean wind speed for the location under consideration

The Rayleigh distribution versus wind speed is shown in Figure 3-8 for a mean wind speed between 13 and 14 mph.

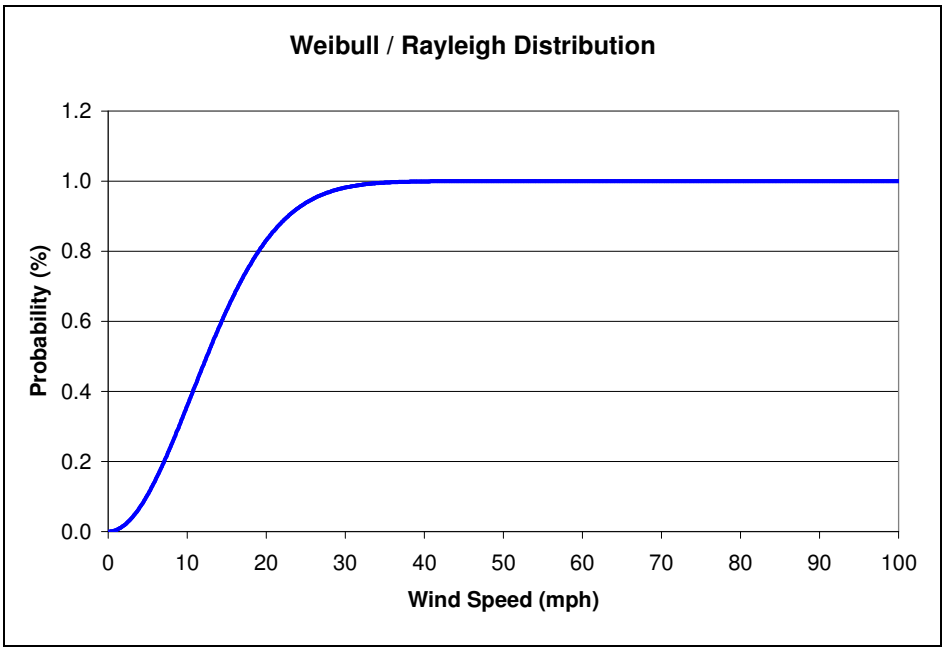

Figure 3-8: Probability distribution function

Once the distribution function was determined, the number of cycles likely to occur in a design lifetime could be estimated. Noting that P(V) is the probability of a wind gust of a given strength or less occurring at a given moment, one can conclude that [1-P(V)] is the probability of a wind gust of a given strength or more occurring at any given moment. Thus:

[1-P(V)] * Lifetime = Probable exposure time at or above a given wind speed

If the lifetime is taken in seconds, probable exposure time will be in seconds.

Assuming a set of conditions including a 50-year design lifetime, a 120 mph design wind speed, and a mean annual wind speed between 13 and 14 mph, one can estimate the number of cycles likely to occur at or above a given wind speed by multiplying the probable exposure time in seconds by the expected vibration frequency of the panel. If it is conservatively assumed that 1 full cycle (full load reversal on the panel) will occur for every second of exposure (1 Hz), the number of cycles expected will be equal to the probable seconds of

exposure over a given design lifetime. The number of cycles predicted by the Rayleigh distribution at or above several given wind speeds are given in Table 3-4.

Table 3-4: Rayleigh probability of exposure at or above given wind speeds

% of 120 mph Design Wind Speed	Given Wind Speed	1-F(V)	Probable # of Cycles
(%)	(mph)	(% Probability)	(#)
10	12	52.72973%	831442389
20	24	7.73076%	121898627
30	36	0.31514%	4969087
40	48	0.00357%	56320
45	54	0.00024%	3710
50	60	0.00001%	177
60	72	0.00000%	0.2
70	84	0.00000%	0.0
80	96	0.00000%	0.0
90	108	0.00000%	0.0
100	120	0.00000%	0.0

Note that the Rayleigh distribution is not dependent on the design wind speed. Thus, the probability of occurrence for a given wind speed does not change with an increase in design wind speed.

3.3 TEST SETUP

The test setup was designed and constructed to allow testing of the panels in a vertical configuration. Vertical (axial) load was applied to each corbel using pressure-regulating jacks and lateral load was applied to the panel using a computer-controlled hydraulic actuator.

3.3.1 General Setup and Loading

One braced steel frame was provided on each side of the panel to support an upper cross-beam. This cross-beam in turn provided the upper lateral reaction. The top of the cross beam was located approximately 2 inches above the top of the panel, allowing for sufficient room to place a hinge assembly. The entire setup was constructed on a testing floor which was used to anchor the frames and to provide a vertical reaction for the axial loads. A

reaction wall, located adjacent to the testing setup, was used as a reaction for the hydraulic actuator producing the lateral load. An overview of the test setup is given in Figure 3-9.

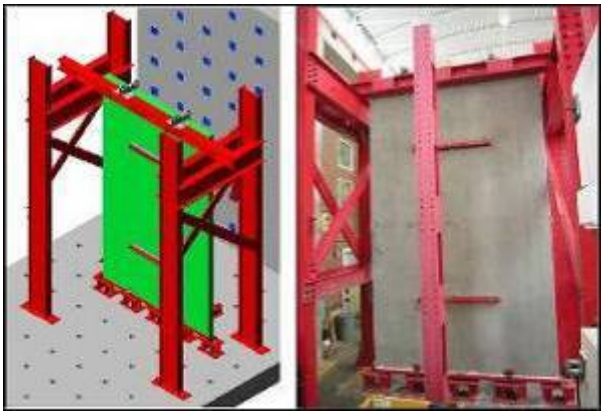

Figure 3-9: Overview of test setup

Vertical loads were applied to the top of each corbel by the jacks shown Figure 3-10. These loads were provided to simulate the effects of a double-tee roof system and associated gravity loads. The jacks were connected to the strong floor and cables which ran through holes in each corbel. One hole was centered in each corbel, 6 inches away from the face of the inner wythe. The holes were sufficiently large enough to prevent the cable from touching the inside of the hole. In addition, the cables ran through a spherical bearing placed on top of each corbel prior to being secured with strand chucks. The spherical bearing was provided to insure that the applied load would remain vertical even as the panel deformed laterally. The inset photograph in Figure 3-10 shows a close-up view of this spherical bearing detail.

Figure 3-10: Details of the inner wythe loading system

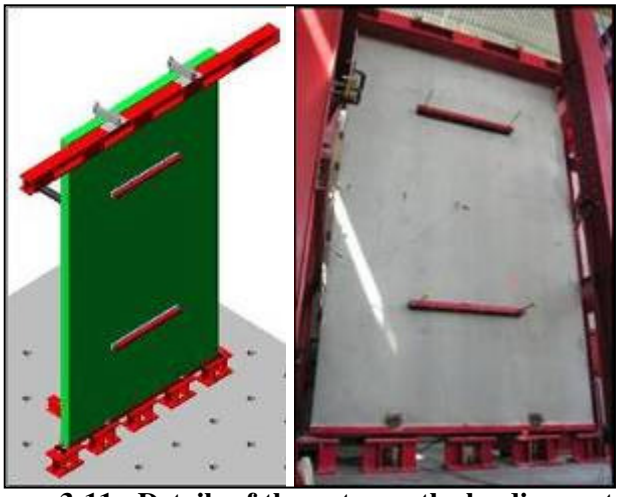

Figure 3-11: Details of the outer wythe loading system

Lateral loads were applied using an MTS hydraulic actuator shown in Figure 3-10. Lateral loading was provided to simulate wind fatigue cycles (pressure and suction), and thus the spreader beam system connecting the actuator to the panel was designed to allow tension and compression loadings. Two loading lines were provided at both quarter-height locations, creating a condition of four point lateral bending. At each of the two loading lines, two 4 inch by 4 inch by 60 inch square steel tubes were placed on the panel, one on each wythe, as shown in Figure 3-11. The tubes were bolted together through holes drilled in the panel to allow the use of bearing pads to transfer the loads to the panel in either lateral direction.

Neoprene pads were placed between the concrete surfaces and the loading tubes to account for surface irregularities and to allow the loading tubes to rotate as the panel deformed. In addition, the holes through the panel were sized so that the threaded rods connecting the loading tubes would not touch the panel itself.

A vertical spreader beam was connected to both of the inner wythe loading tubes. The actuator piston was connected to the center of this spreader beam. While the top loading tube was fixed rigidly to the spreader beam, the bottom loading tube was connected through a system of stainless steel plates and Teflon-coated bearing pads as shown in Figure 3-12. This configuration prevented horizontal motion at the lower spreader beam connection, but allowed for vertical movement. It was intended that this special lower connection, along with the neoprene pads, would prevent the loading system from contributing to the composite action between the concrete wythes.

Figure 3-12: Spreader beam orientation and lower boundary condition

A 55-kip capacity hydraulic actuator was mounted to the strong wall and the spreader beam. This allowed application of reversed lateral cyclic loading to the panel.

3.3.2 Bottom Boundary Conditions

The bottom panel was supported by a pure hinge supporting system as shown in Figure 3-13. The hinge was designed to restrain panel movement in the horizontal and vertical directions and allow rotation only. In order to provide an even surface for the panel to sit on, 5 support bases were leveled and post-tensioned to the strong floor. A continuous piece of 2 inch diameter round stock was welded to the center of 12 foot long W10x30 C-Channel. One inch square pieces of bar stock were welded to the support bases 2 inches apart creating a trough for the round bar and connected channel to ride in. The round bar protruded from both ends of the channel, allowing the assembly to be anchored at the ends to prevent sliding or uplift. The precast sandwich panel was then set between the upward-facing channel flanges and welded in place at the connection points using flexible angle clips at four locations. Fast setting grout was then poured between the panel and the channel section providing uniform reactions in both directions along the entire panel width. This configuration created a robust pined connection at the bottom of the panel.

Figure 3-13: Bottom panel support

3.3.3 Top Boundary Condition

To maintain a simply supported condition in the lateral direction, a roller was provided at the top of each panel to complement the lower hinge. The roller was fabricated by welding a vertical steel plate to a connection point above each corbel at the top of the panel. Top hinge panel plates for Panel EPS 1 were welded only to the top 8 inch by 8 inch weld plate. This configuration was altered for all other panels so the weld top hinge panel plate extended to the top of the corbel where additional weld material was placed. The bottom corner of the plate was notched to fit around the spherical bearing plate as well as the prestressing chucks. These details are shown for panel EPS 1 and EPS 2, XPS 1, XPS 2, XPS 3 and XPS 4 in Figure 3-14 right and left, respectively and Figure 3-15 right and left, respectively.

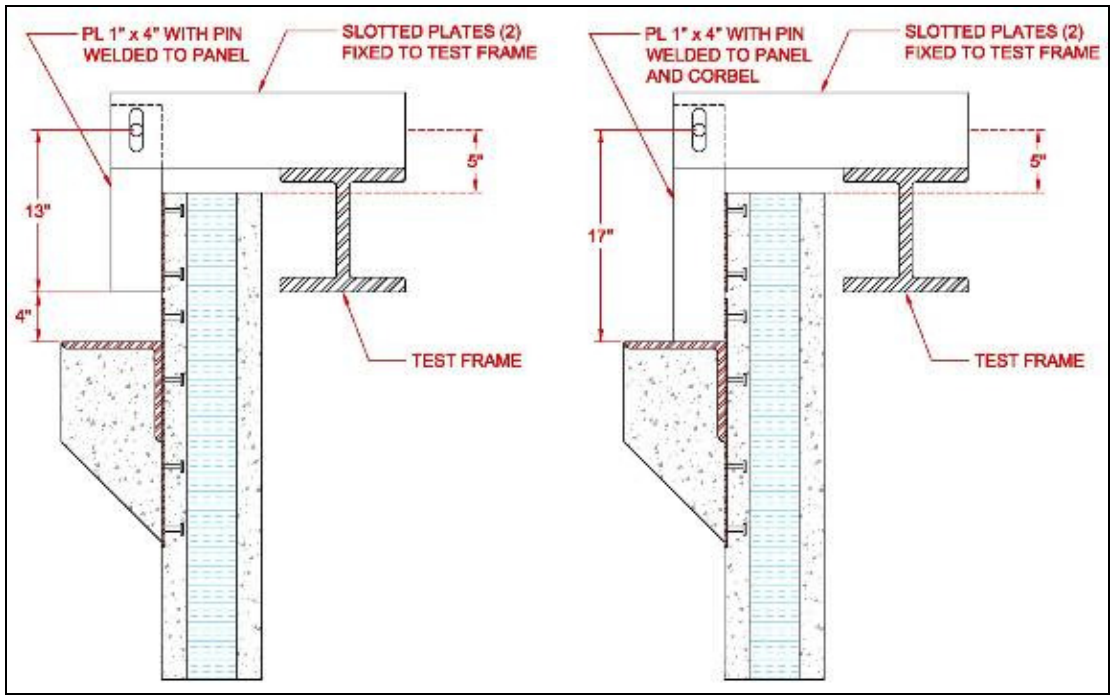

Figure 3-14: Top hinge configurations
EPS 1 configuration (left) Altered configuration (right)

Figure 3-15: Top hinge system

This vertical plate was drilled 5 inches above the top surface of the panel. The hole was aligned with vertical slots in two plates fixed rigidly to the test frame and cantilevered over the top of the panel. A pin was inserted through the first slot, the vertical plate hole, and then through the second slot creating a roller that restrained horizontal panel motion while allowing for vertical deformation.

3.4 INSTRUMENTATION

A variety of instruments were used during testing to measure panel behavior. Several different types of instrumentation were implemented to monitor deflections, loads and strains. The instrumentation used included:

1. Load cells
2. String potentiometers (string pots)
3. Linear potentiometers (linear pots)
4. PI-Gauges (reusable surface-applied wire-arch strain gauges)
5. Surface applied concrete strain gauges TML PL-60-11

Surface applied concrete strain gauges were only used for panels XPS 3 and XPS 4. All instruments were wired to an electronic data acquisition system. Data were recorded continuously at a sample rate of 1 Hz during static loading and 10 Hz during fatigue loading.

3.4.1 Load Cells

One load cell was integrally mounted to the hydraulic actuator and to each hydraulic jack. These load cells were used to independently monitor the lateral load applied to the panel and the vertical load applied to each corbel.

3.4.2 String pots

Lateral deflections of the panel and the supporting frames were monitored throughout the testing with string potentiometers.

These locations included:

1. Support deflection at top of panel
2. Deflection at top of panel, mid-width
3. Deflection at 7/8-height of panel, mid-width
4. Deflection at 3/4-height of panel, mid-width
5. Deflection at mid-height of panel, mid-width
6. Deflection at mid-height of panel, right edge
7. Deflection at quarter-height of panel, mid-width
8. Deflection of bottom of panel, mid-width
9. Support deflection at bottom of panel

String pots at 7/8-height and 3/4-height were only used during the testing of XPS 3 and XPS 4. Measured support deflections were used to determine the net lateral deflection measurements of the panel. All presented data are adjusted to eliminate the effects of support and frame motion. Locations of lateral deflection measurements are given in Figure 3-16. Sign convention is also provided along with conventions for “left,” “right,” “inner” and “outer”.

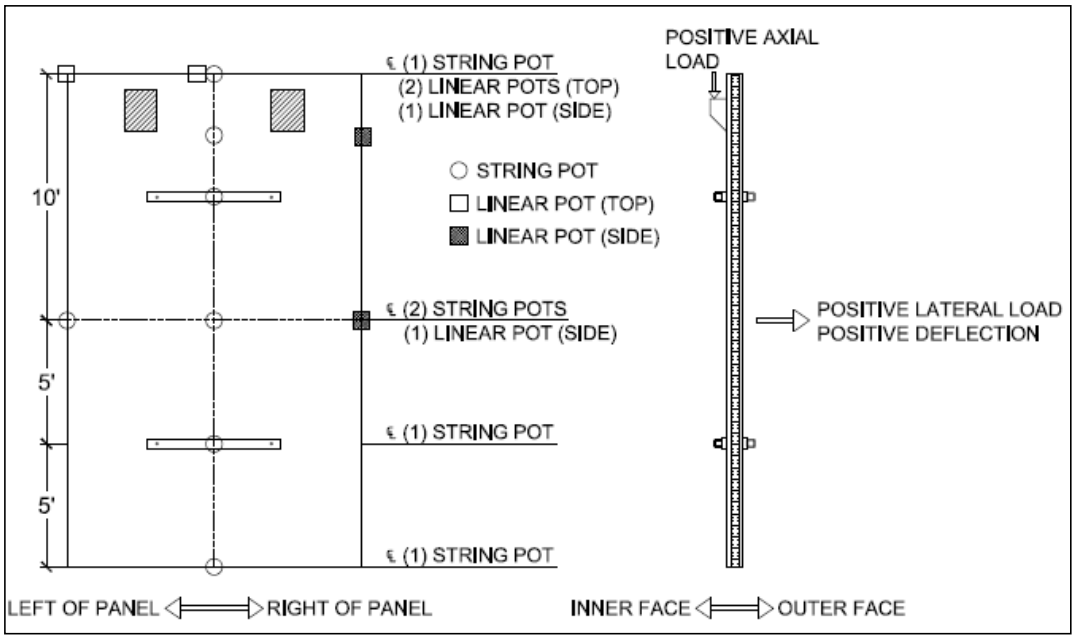

Figure 3-16: Location of deflection instruments

3.4.3 Linear Potentiometers

Two linear potentiometers were used to measure the relative vertical slip between the two concrete wythes at the top of each panel. A support was fixed to the center of the outer wythe at the mid-width and the outside edge of each panel. A linear potentiometer was fixed to this support and the top center of the inner wythe. The locations of these instruments are given in Figure 3-16. The configuration of the potentiometers is shown in Figure 3-17.

Figure 3-17: LVDT to measure relative vertical displacement

Linear potentiometers were also placed at mid-height for XPS 2 and 7/8-height and mid-height for XPS 3 and XPS 4 to measure relative horizontal displacement between wythes. These potentiometers were located on the outside of the panel measuring the relative movement between centers of concrete wythes. The locations of these instruments are shown in Figure 3-18. These potentiometers were supported by ½ inch by 2 inch by 2 inch plywood squares glued to the center of each wythe by appropriate fast setting adhesive.

Figure 3-18: LVDT to measure relative horizontal displacement for XPS 3 and 4

3.4.4 PI-Gauges

In total, 18 PI-gauges were used to monitor surface strains at various locations. Six 100-mm gauge-length instruments were placed on the inner and outer panel faces to monitor the flexural strains on the panel surfaces. Twelve 200-mm gauge-length instruments were placed in groups of four gauges at three panel heights to capture through-thickness strain profiles during each test.

Surface PI gauges were mounted at the mid-height of the panel faces at three locations. A gauge was mounted on the inner and outer face 6 inch from the outer edge of the panel, at 3 feet from the outer edge and 5 foot 6 inches from the outer edge. All PI-gauges were

configured to measure strain in the vertical direction with tension strain being considered as positive. The locations of PI-gauges mounted on the faces of the panel are given in Figure 3-19, and Figure 3-20 (a).

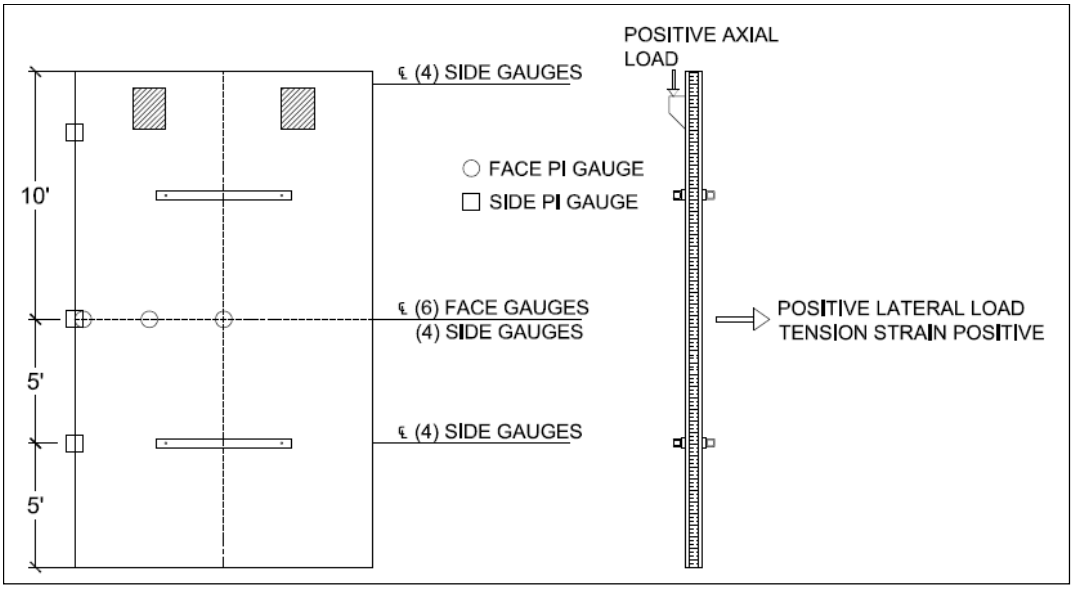

Figure 3-19: Locations of stain measurements

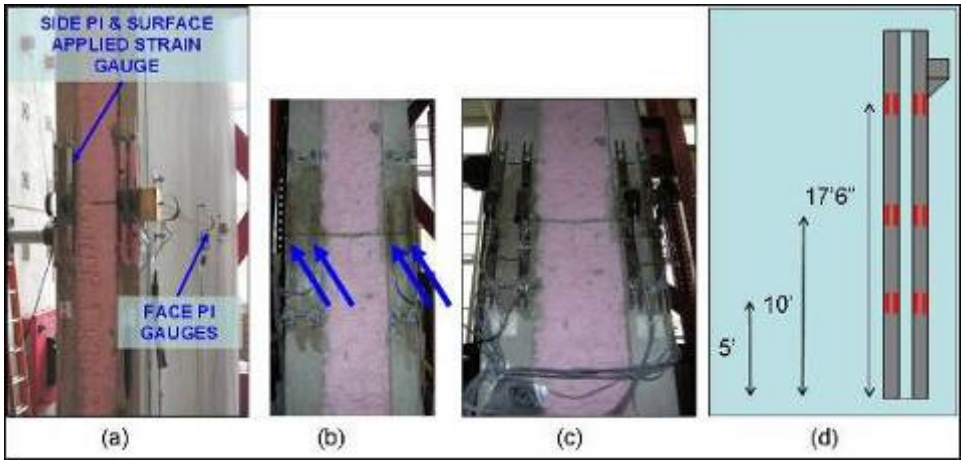

Figure 3-20: Typical PI-gauges on a panel

The PI-gauges provided on the side of each panel are also shown in Figure 3-19 and Figure 3-20 (c). Groups of four gauges were installed on the side of each panel at quarter and mid-height. Additional gauges were provided at 7/8-height for panels XPS 3 and 4 to capture additional panel behavior. Gauge locations are shown in Figure 3-19 and Figure

3-20 (d). In each of these locations, a gauge was provided at ¼ inch from each edge of each wythe. All side PI-gauges were also configured to measure strains in the vertical direction with tension strain being considered positive.

3.4.5 Surface Strain

Electronic resistance strain gauges were applied on the surface of panels XPS 3 and XPS 4. A total of 12 electronic resistance strain gauges were located in groups of four at three locations along the panel height. Strain gauges were applied at the same location of the side PI-Gauge as shown in Figure 3-20 (b) and (c). Side strain measurements were monitored by both PI-Gauges and electronic resistance strain gauges due to the anticipated small strains.

3.5 FAILURE MODES AND CRACK PATTERNS

The proposed loading sequence presented in section 3.2 was followed as a guideline for all panels. Each fatigue cycle consisted of a windward load (negative direction) and a leeward load (positive direction) of equal magnitudes respectively. All tests were conducted in load control throughout the fatigue cycles at a loading rate of 10 Hz. Controls were changed to displacement control through the final failure cycle. The final failure cycle was applied in a leeward direction to account for worse case scenario.

3.5.1 Panel EPS 1

Panel EPS 1 was loaded up to a combined load of $1.2D+0.5L_r+2.8W_{120}$ which was the maximum measured load before failure, as given in Table 3-5. This failure is equivalent to a load level of 18.9 kips gravity load per corbel and 19.3 kip lateral load. Lateral loads for panel EPS 1 correspond to a design wind speed of 120 MPH.

Table 3-5: Loading sequence for EPS 1

Step	Vertical Load		Lateral Load		
(#)	Level	Load per Corbel	Level	Magnitude (kips)	# of Cycles at Step
1	D	13.5	0	0	0
2	D+L	18.9	0	0	0
3	1.2D+0.5Lr	18.9	0	0	0
4	1.2D+0.5Lr	18.9	45% x 1.6W120	5.0	3710
5	1.2D+0.5Lr	18.9	50% x 1.6W120	5.6	177
6	1.2D+0.5Lr	18.9	60% x 1.6W120	6.7	1
7	1.2D+0.5Lr	18.9	80% x 1.6W120	9.0	1
8	1.2D+0.5Lr	18.9	100% x 1.6W120	11.2	1
9	1.2D+0.5Lr	18.9	111% x 1.6W120	12.4	1
10	1.2D+0.5Lr	18.9	140% x 1.6W120	15.5	1
11	1.2D+0.5Lr	18.9	172% x 1.6W120	19.3	Connection Failure

Failure occurred due to localized pullout of the upper embedded connection plates. Panel failure was observed corresponding to an abrupt drop in lateral load. A radial crack pattern extending from the top of the corbel to the top of the panel was observed and is shown in Figure 3-21 and Figure 3-22. It should be noted that some diagonal cracking was observed before testing due to transportation and handling.

Figure 3-21: Failure of EPS 1

Figure 3-22: Views of EPS 1 at failure

3.5.2 Panel EPS 2

The lateral load used for testing EPS 1 test was increased to simulate a 150 MPH design wind speed. Consequently, the load increments were increased while the number of cycles executed at each increment remained the same as given in Table 3-6. The constant axial load level was also identical to the value used for testing EPS 1. Failure of panel EPS 2 was global in nature at a load equivalent to $1.2D+0.5L_r+1.8W_{150}$ after a series of higher level fatigue cycles.

Table 3-6: Loading sequence for EPS 2

Step	Vertical Load		Lateral Load		
(#)	Level	Load per Corbel	Level	Magnitude (kips)	# of Cycles at Step
1	D	13.5	0	0	0
2	D+L	18.9	0	0	0
3	$1.2D+0.5L_r$	18.9	0	0	0
4	$1.2D+0.5L_r$	18.9	45% x $1.6W_{150}$	7.8	3710
5	$1.2D+0.5L_r$	18.9	50% x $1.6W_{150}$	8.6	177
6	$1.2D+0.5L_r$	18.9	60% x $1.6W_{150}$	10.4	1
7	$1.2D+0.5L_r$	18.9	80% x $1.6W_{150}$	13.8	1
8	$1.2D+0.5L_r$	18.9	100% x $1.6W_{150}$	17.3	1
9	$1.2D+0.5L_r$	18.9	113% x $1.6W_{150}$	19.8	Flexural-shear Failure

In order to prevent the localized failure observed in EPS 1, the upper roller detail for panel EPS 2 was modified slightly to reinforce the connection as described in 3.3 TEST

SETUP. The top hinge plate was extended and welded to the upper surface of the corbel in an attempt to avoid premature connection failure.

Failure of EPS 2 occurred due to flexural-shear cracking of the outer wythe at approximately 7/8 panel height during the static cycle following the fatigue regimen as shown in Figure 3-23 and Figure 3-24. Simultaneously, diagonal cracks developed on the inner wythe radiating from the upper loading beam as shown in Figure 3-23. Failure of EPS 2 was identified by a gradual decay in load carrying capacity.

Figure 3-23: Crack pattern of ESP 2 outer (Left) and inner (Right) wythes at failure

Figure 3-24: Close-up photograph of upper shear crack at failure for EPS 2

Significant cracking was also noticed along the top of EPS 2 as shown in Figure 3-25. Cracking occurred primarily between the foam core and the inner wythe producing a 0.2 inch crack along the panel width.

Figure 3-25: Crack width at top of ESP 2

3.5.3 Panel XPS 1

Panel XPS 1 experienced failure at a load level equivalent to $1.2D+0.5L_r+1.6W_{120}$, corresponding to a 120 MPH wind speed as given in Table 3-7. Consequently, the failure load was equal to the ultimate design load of $1.2D+0.5L_r+1.6W_{120}$. Thus, a localized failure occurred at an applied load of 18.9 kips gravity load and a lateral load 11.2 kips.

Table 3-7: Loading sequence for XPS 1

Step	Vertical Load		Lateral Load		
(#)	Level	Load per Corbel	Level	Magnitude (kips)	# of Cycles at Step
1	D	13.5	0	0	0
2	D+L	18.9	0	0	0
3	$1.2D+0.5L_r$	18.9	0	0	0
4	$1.2D+0.5L_r$	18.9	45% x $1.6W_{120}$	5.0	3710
5	$1.2D+0.5L_r$	18.9	50% x $1.6W_{120}$	5.6	177
6	$1.2D+0.5L_r$	18.9	60% x $1.6W_{120}$	6.7	1
7	$1.2D+0.5L_r$	18.9	80% x $1.6W_{120}$	9.0	1
8	$1.2D+0.5L_r$	18.9	100% x $1.6W_{120}$	11.2	1
9	$1.2D+0.5L_r$	18.9	100% x $1.6W_{120}$	11.2	Localized Failure

Failure of panel XPS 1 occurred around the corbels during the leeward stroke (positive direction). Panel damage was isolated to separation of the inner wythe and the inner foam core at the top of the panel. These cracks extended from the outside of each corbel protruding through the inner wythe at approximately 30° as shown in Figure 3-26 and Figure 3-27.

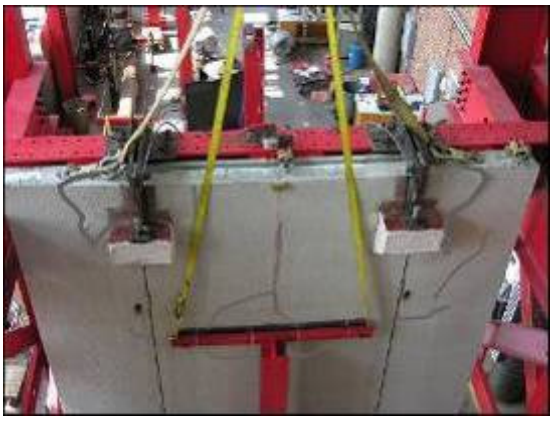

Figure 3-26: Failure of XPS 1

Figure 3-27: Top views of XPS 1 at failure

3.5.4 Panel XPS 2

Panel XPS 2 was tested with the same gravity loads as previous panels and a lateral load simulating a 120 MPH wind speed as given in Table 3-8. Panel XPS 2 withstood nearly twice the ultimate design lateral load as XPS 1 with the same foam core and C-GRID layout. A localized failure occurred at a load level of $1.2D+0.5L_r+3.2W_{120}$, equivalent to an applied load of 18.9 kips lateral load with factored gravity load of 18.9 kips per corbel.

Table 3-8: Loading sequence for XPS 2

Step	Vertical Load		Lateral Load		
(#)	Level	Load per Corbel	Level	Magnitude (kips)	# of Cycles at Step
1	D	13.5	0	0	0
2	D+L	18.9	0	0	0
3	$1.2D+0.5L_r$	18.9	0	0	0
4	$1.2D+0.5L_r$	18.9	$45\% \times 1.6W_{120}$	5.0	3710
5	$1.2D+0.5L_r$	18.9	$50\% \times 1.6W_{120}$	5.6	177
6	$1.2D+0.5L_r$	18.9	$60\% \times 1.6W_{120}$	6.7	1
7	$1.2D+0.5L_r$	18.9	$80\% \times 1.6W_{120}$	9.0	1
8	$1.2D+0.5L_r$	18.9	$100\% \times 1.6W_{120}$	11.2	1
9	$1.2D+0.5L_r$	18.9	$201\% \times 1.6W_{120}$	22.5	Localized Failure

Failure was observed with an abrupt loss in lateral load carrying capacity due to localized failure around each corbel on the inner wythe as shown in Figure 3-28. Four cracks, one on each side of both corbels, extended from the top of the panel to the bottom of each corbel. As shown in Figure 3-29, some hour glass shaped cracking was observed on the outer wythe extending from 1/8 panel height to 7/8 panel height; however, a majority of these cracks were sustained during handling and placement and they did not contribute to the panel failure.

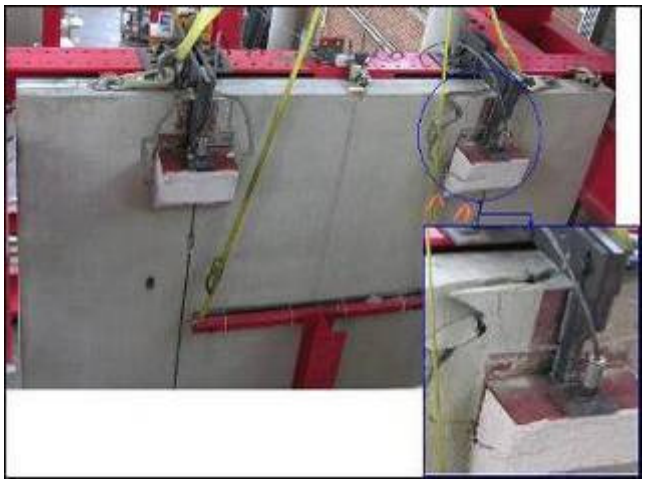

Figure 3-28: Crack pattern of XSP 2 localized failure

Figure 3-29: Outer wythe cracking at connection failure of XPS 2

3.5.5 Panel XPS 3

Failure of panel XPS 3 occurred after completion of 1282 cycles a total lateral load of 5 kips and gravity load of 18.9 kips at each corbel. Panel XPS 3 experienced a flexural shear failure simultaneously with separation of the wythes at the top of the panel at a load equivalent to $1.2D+0.5L_r+45\% \times 1.6W_{120}$ as given in Table 3-9.

Table 3-9: Loading sequence for XPS 3

Step	Vertical Load		Lateral Load		
(#)	Level	Load per Corbel	Level	Magnitude (kips)	# of Cycles at Step
1	D	13.5	0	0	0
2	D+L	18.9	0	0	0
3	$1.2D+0.5L_r$	18.9	0	0	0
4	$1.2D+0.5L_r$	18.9	$45\% \times 1.6W_{120}$	5.0	1282 Flexural Shear/ Separation Failure

Panel XPS 3 experienced significant increase in deflection before failure after completion of 1282 cycles due to the formation of flexural shear cracking across the outer wythe at 7/8 of the panel height. At this stage, separation of the top of the panel was observed across the full width of the panel. The separation continued approximately 2 feet down from the top of

the panel as shown in Figure 3-30. Partial rupture and pull out of the C-GRID from the inner surface of the outside wythe was observed as shown in Figure 3-31.

Figure 3-30: Failure of XPS 3

Figure 3-31: Internal view of XPS 3 at failure

Post-failure investigation of the top of XPS 3, included removing the top 2 feet of the panel is shown in Figure 3-32. The investigation confirmed rupture of the C-GRID at the top of the panel at 7/8 of the panel height.

Figure 3-32: C-GRID failure investigation of XPS 3

3.5.6 Panel XPS 4

Panel XPS 4 was tested with the same lateral and gravity loads as well as the same design wind speed as panels EPS 1, XPS 1, XPS 2, and XPS 3. Panel XPS 4 withstood the proposed loading sequence with an additional ultimate design load cycle as given in Table 3-10. Failure occurred due to flexural shear cracking at 7/8 panel height simultaneously with separation of the wythes at the top of the panel. Failure occurred at gravity load of 18.9 kips per corbel plus a lateral load of 12.6 kips, which is equivalent to $1.2D+0.5L_r+1.8W_{120}$.

Table 3-10: Loading sequence for XPS 4

Step	Vertical Load		Lateral Load		
(#)	Level	Load per Corbel	Level	Magnitude (kips)	# of Cycles at Step
1	D	13.5	0	0	0
2	D+L	18.9	0	0	0
3	$1.2D+0.5L_r$	18.9	0	0	0
4	$1.2D+0.5L_r$	18.9	45% x $1.6W_{120}$	5.0	3710
5	$1.2D+0.5L_r$	18.9	50% x $1.6W_{120}$	5.6	177
6	$1.2D+0.5L_r$	18.9	60% x $1.6W_{120}$	6.7	1
7	$1.2D+0.5L_r$	18.9	80% x $1.6W_{120}$	9.0	1
8	$1.2D+0.5L_r$	18.9	100% x $1.6W_{120}$	11.2	2
9	$1.2D+0.5L_r$	18.9	113% x $1.6W_{120}$	12.6	Flexural Shear/ Separation Failure

Failure occurred due to formation of a flexural shear crack across the outer wythe at 7/8 of the panel height. At failure, the concrete separated approximately 1 inch from the foam across the panel width as shown in Figure 3-33. In addition to the flexural-shear cracking across the outer wythe, vertical cracks were also observed around each corbel and extended approximately 2 feet in length as shown in Figure 3-34.

Figure 3-33: Failure of XPS 4

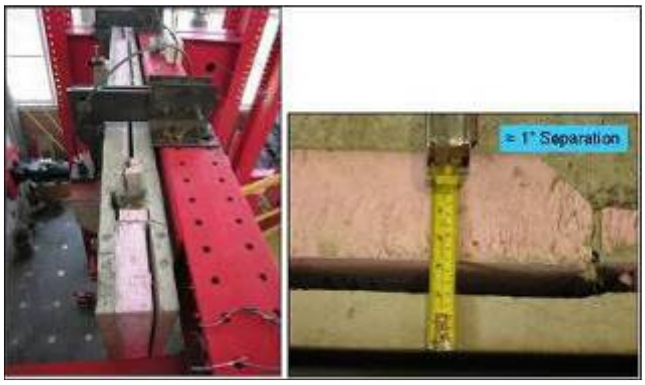

Figure 3-34: Top view of XPS 4 failure

Test results of the entire experimental program are given inTable 3-11. The table includes test designation, deflections at service load, maximum measured lateral load, and failure modes for each test.

Table 3-11: Summary of test results

Panel	Service Load Deflection $D+L_r+W$	Failure Load $[1.2D+0.5L_r+]$	Lateral Failure Load (kip)	Failure Mode
EPS 1	h/460	$2.8W_{120}$	19.3	Localized Failure Around Corbels
EPS 2	h/500	$1.8W_{150}$	19.8	Flexural Shear Failure
XPS 1	h/1480	$1.6W_{120}$	11.2	Localized Failure Around Corbels
XPS 2	h/755	$3.2W_{120}$	22.5	Localized Failure Around Corbels
XPS 3	N/A	$0.7W_{120}$	5 (Cycle 1282)	Flexural Shear Cracks & Separation Failure
XPS 4	h/700	$1.8W_{120}$	12.6	Flexural Shear Cracks & Separation Failure

3.6 LATERAL DEFLECTIONS

Lateral deflections were measured at several locations using string potentiometers attached to the outer concrete wythe. The deflections were measured from a stationary column independent from the panel. All data presented in the subsequent sections account for self deflection of the testing frame as well as movement of the connections. Maximum deflections at service load due to the total applied loads are compared to the specified values by ACI 533 of h/360.

Deflection profiles were created along the height and width of the panels. These profiles were established based upon the measured deflections at mid-height center, quarter-height center, and mid-height edge. In these figures, the left side of each panel was assumed to have the same deflection as the right side of the panel and the 3/4-height was assumed to have the same deflection value as the 1/4-height except where 3/4-height and 7/8-height readings were available. Positive deflection is considered as movement from the inner to outer wythe.

Deflection profiles were created at several key load levels corresponding to factored gravity load only, first service load cycle, first ultimate design load cycle and failure load level, corresponding to $1.2D+0.5L_r$, $1.2D+0.5L_{r+}W$, $1.2D+0.5L_r+1.6W$ and $1.2D+0.5L_r+$ lateral failure load, respectively.

3.6.1 Panel EPS 1

Measured lateral deflections along the mid-height center, mid-height left-edge and quarter-height center of panel EPS 1 are shown in Figure 3-35 (a), (b) and (c), respectively. Deflections along the panel edge at mid-height are also shown. All panel deflections are combined in APPENDIX A, Figure 7-1 for comparison purposes. Initial deflections at zero lateral load was due to the applied axial load of 18.9 kips per corbel, which is equivalent to

1.2D+0.5L_r. Throughout the cyclic lateral load fatigue cycles, some panel degradation was observed, but the panel stiffness remained constant through the fatigue regimen. Panel stiffness remained constant up to a laterally applied load of 15 kips, at which concrete cracking occurred causing reduction of the stiffness as shown in Figure 3-35. The localized corbel zone failure occurred at a lateral load of 19.3 kips with applied factored gravity loads. At this stage, the panel experienced abrupt failure and the test was terminated. Observed service load deflection was 0.53 which is equivalent to h/460. These deflections were well within the ACI 533 limit of h/360.

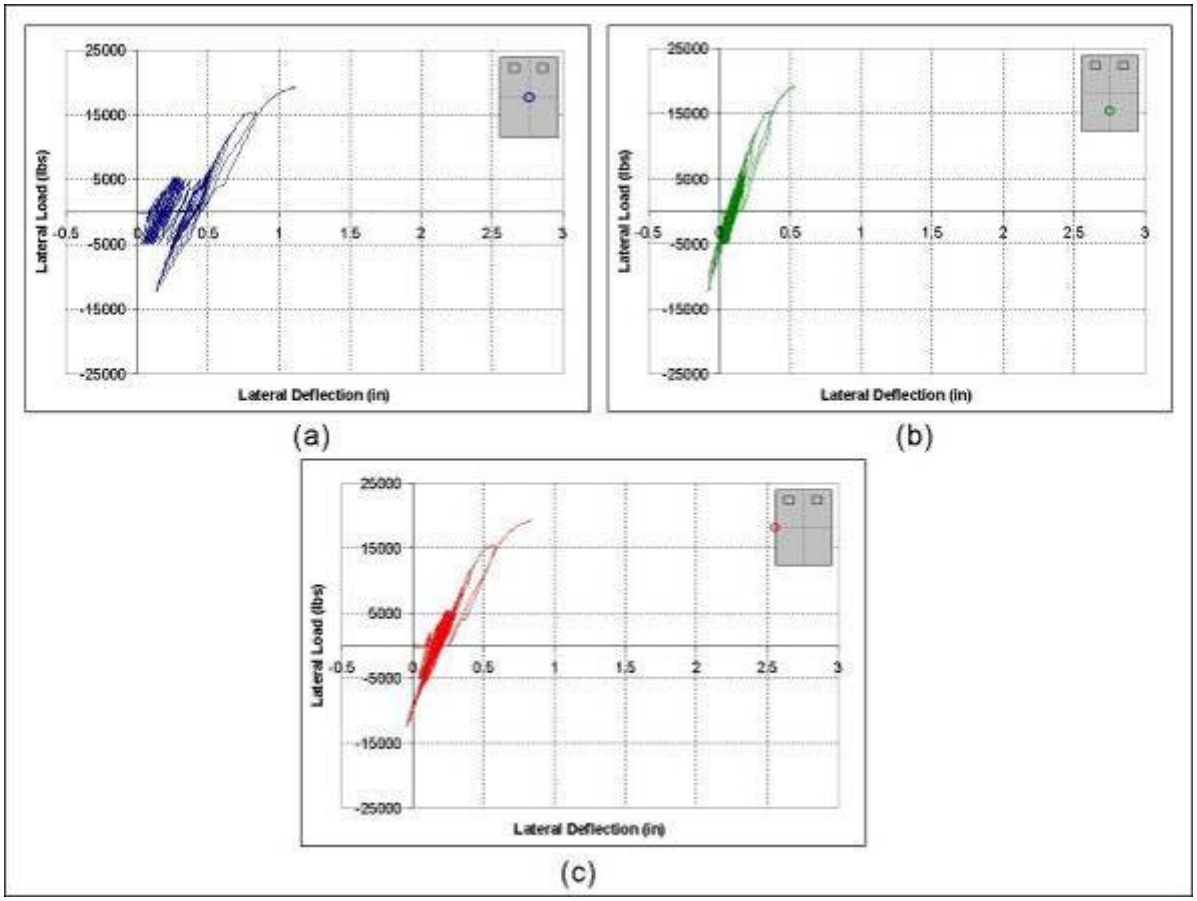

Figure 3-35: Individual lateral displacement of EPS 1

Deflection profiles along the panel height and width of panel EPS 1 are shown in Figure 3-36 (a) and (b), respectively. Measurements show that panel EPS 1 experienced maximum

deflections at mid-height center. Panel EPS 1 experienced curvature along the width of the panel which suggests unequal distribution of the applied moment across the width of the panel. Deflection profiles exhibited a linear behavior from panel edge to panel center as shown in Figure 3-36. Maximum measured deflections at mid-height center for gravity loads only, service load, design load, and failure load were 0.19 inches, 0.53 inches, 0.63 inches and 1.11 inches, respectively.

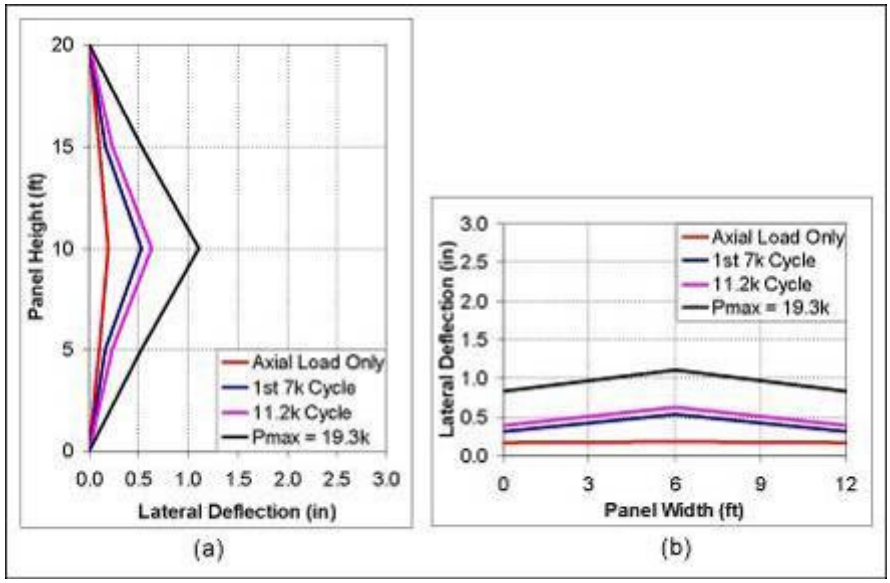

Figure 3-36: Deflection profiles of EPS 1

3.6.2 Panel EPS 2

Measurements of individual lateral deflections at mid-height center, mid-height left-edge and quarter-height center of panel EPS 2 are shown in Figure 3-37 (a), (b) and (c), respectively and were combined in APPENDIX A, Figure 7-2 for comparison purposes. Lateral deflection behavior of panel EPS 2 was very similar to panel EPS 1. Following the initiation of flexural shear cracking of the EPS panels, the panel was tested until significant reduction of the lateral load carrying capacity was observed. Measured deflection at center of the panel at service load was 0.47 which is equivalent to h/500.

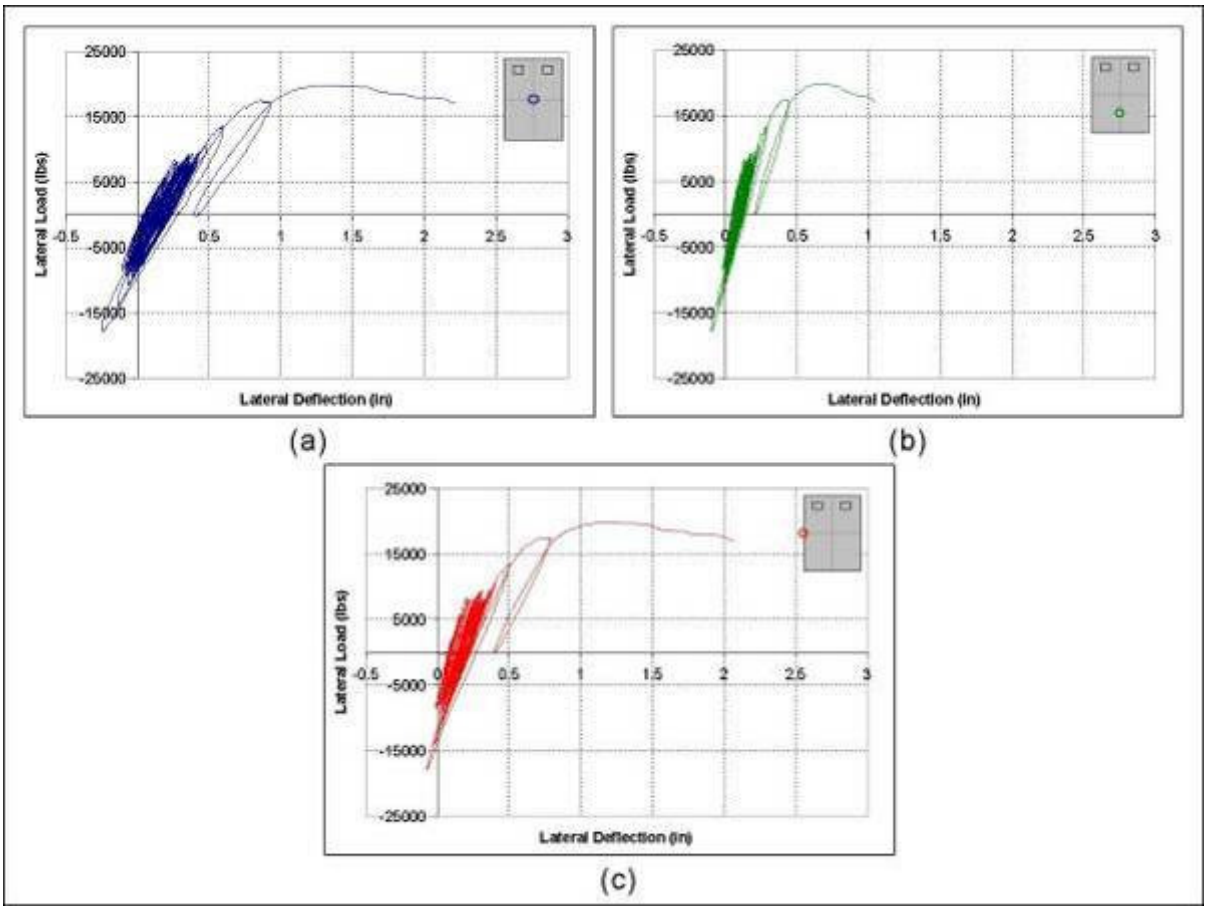

Figure 3-37: Individual lateral displacement of EPS 2

Similar to EPS 1, the deflection along the height and width of the panel exhibited a linear trend with curvature in both the vertical and horizontal directions as shown in Figure 3-38 (a) and (b), respectively. Maximum measured deflections at mid-height center for gravity loads only, service load, design load, and failure load were 0.06 inches, 0.47 inches, 0.85 inches and 1.27 inches, respectively.

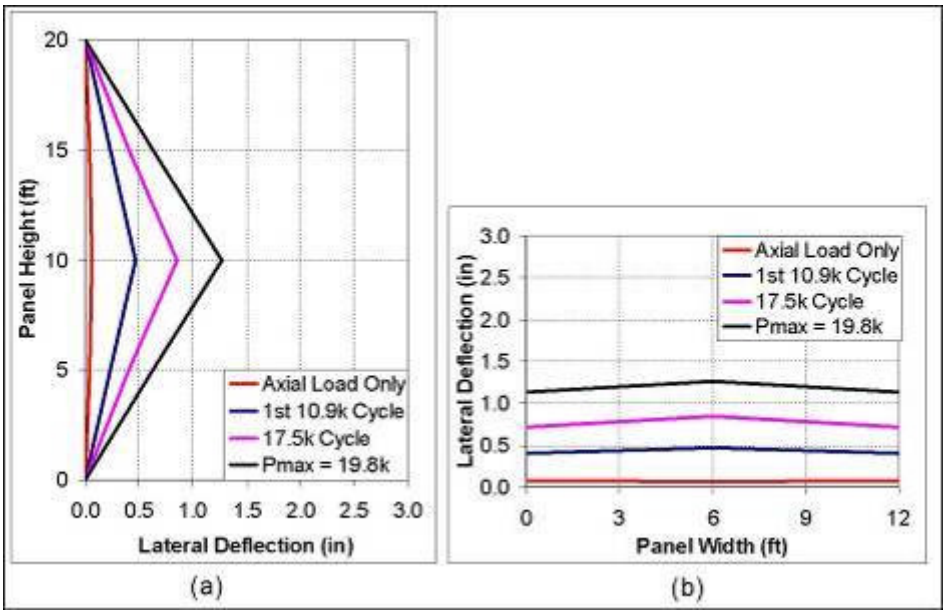

Figure 3-38: Deflection profiles of EPS 2

3.6.3 Panel XPS 1

Measured lateral deflections at mid-height center, mid-height right-edge and quarter-height center of panel XPS 1 are shown in Figure 3-39 (a), (b) and (c), respectively and were combined in APPENDIX A, Figure 7-3 for comparison purposes. The measured initial deflections at zero lateral loads were due to the applied gravity load of $1.2D+0.5L_r$. Throughout the loading sequence, minimal panel degradation was observed due to the presence of the solid concrete zones. At a load combination equivalent to $1.2D+0.5L_r+1.6W_{120}$, the panel experienced an abrupt localized corbel zone failure within the linear range of the panel. Consequently, observed panel deflections were significantly less than panels without solid concrete zones. Lateral deflections at service load were 0.16, equivalent to h/1480.

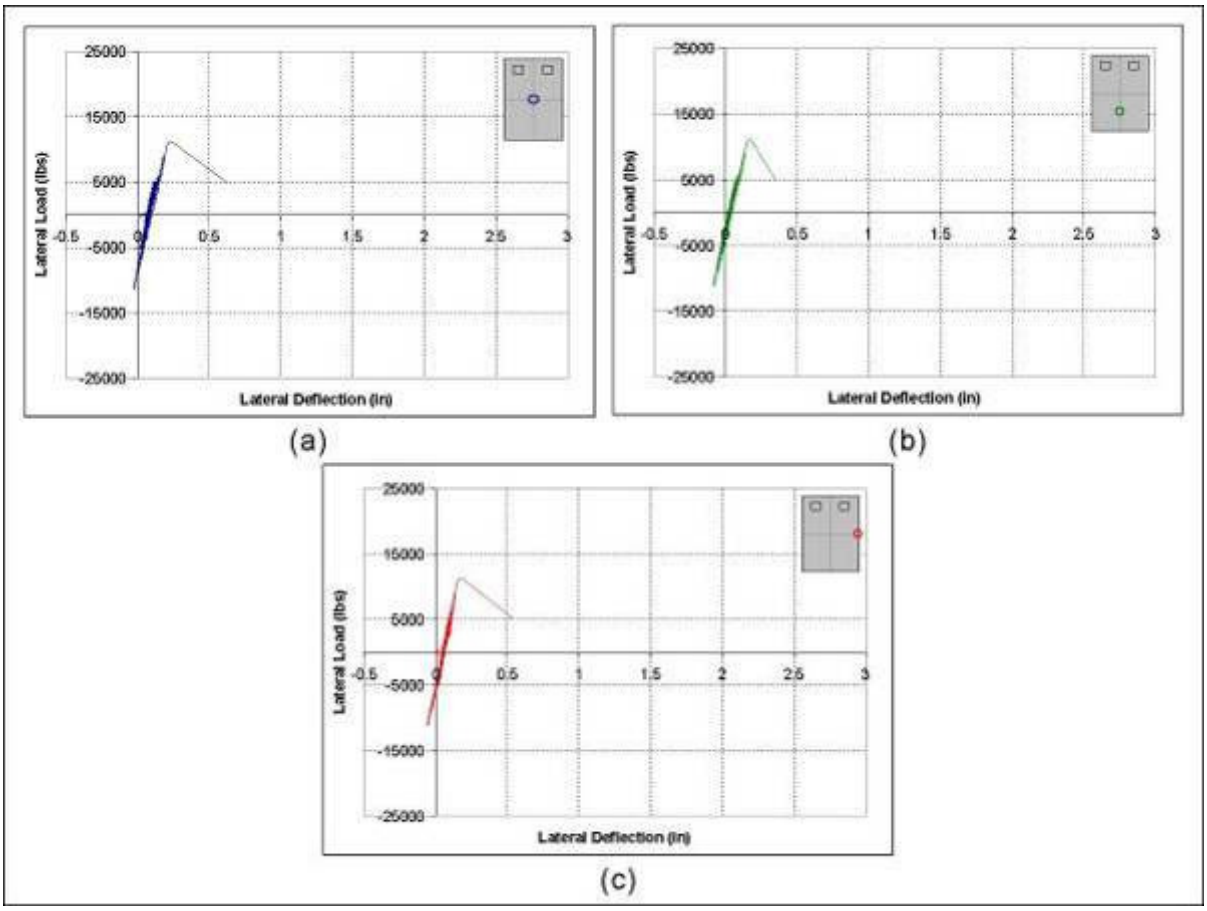

Figure 3-39: Individual lateral displacement of XPS 1

Deflection profiles show that panel XPS 1 experienced maximum deflections at mid-height center. Panel XPS 1 also experienced curvature along the height and width of the panel as shown in Figure 3-40 (a) and (b), respectively. Panel XPS 1 deflection profiles exhibited a parabolic trend from panel edge to panel center exhibited significantly lower deflection values as panels without solid concrete zones. Maximum measured deflections at mid-height center for gravity loads only, service load, and design load were 0.06 inches, 0.16 inches, and 0.22 inches, respectively.

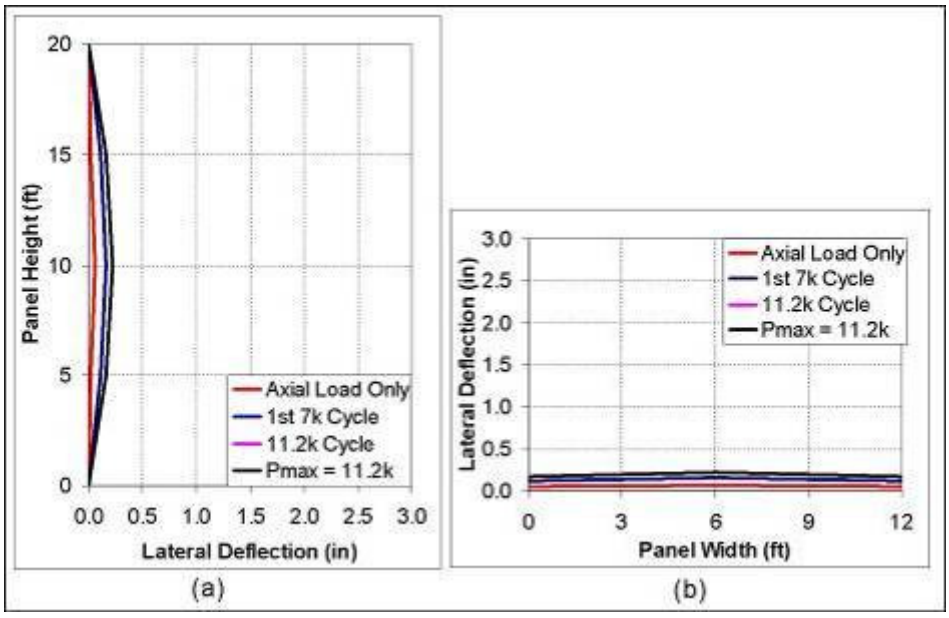

Figure 3-40: Deflection profiles of XPS 1

3.6.4 Panel XPS 2

Measured lateral deflections of panel XPS 2 at mid-height center, quarter-height center and mid-height edge are shown in Figure 3-41 (a), (b) and (c), respectively and were combined in APPENDIX A Figure 7-4 for comparison purposes. Initial deflections were due to the applied factored gravity loads equivalent to $1.2D+0.5L_r$. Though panel XPS 2 experienced minimal lateral load degradation, the increase in lateral load throughout the fatigue cycles was noticeably more than panel XPS 1, particularly during the higher lateral load fatigue cycles. Panel behavior remained linear up to a lateral load of approximately 15 kips with factored gravity loads. At this stage, the panel experienced continual concrete cracking reducing the panel stiffness until failure at a lateral load of 22.5 kips lateral load with factored gravity loads. These applied loads are equivalent to $1.2D+0.5L_r+3.2W_{120}$. Observed service load deflections of panel XPS 2 was 0.32, equivalent to h/755, well within the ACI 533 limit of h/360.

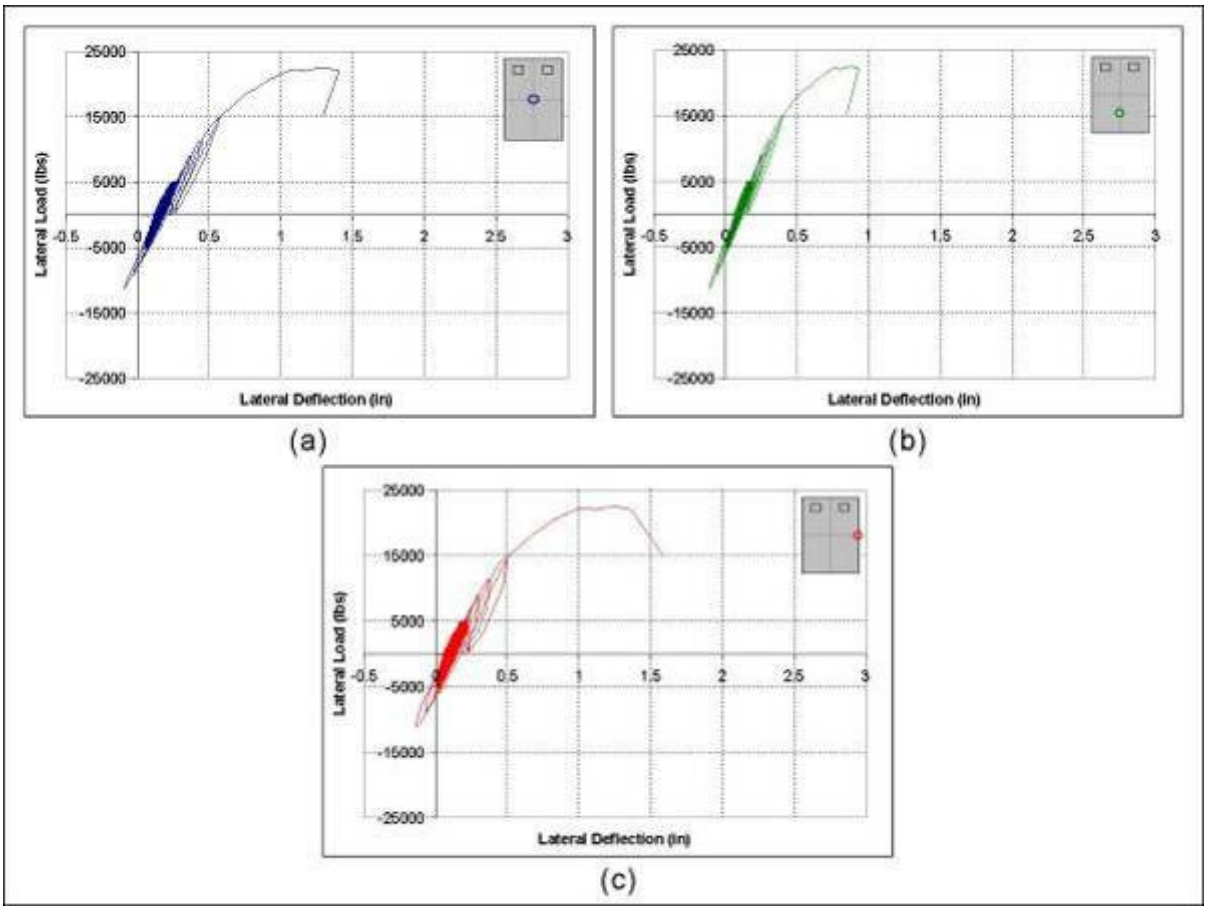

Figure 3-41: Individual lateral displacement of XPS 2

Deflection profiles show that panel XPS 2 also experienced curvature along the height and width of the panel as shown in Figure 3-42 (a) and (b), respectively. Similar to XPS 1, XPS 2 deflection profiles exhibited a parabolic trend from panel edge to panel center. Deflection values at corresponding load levels were significantly higher than panel XPS 1. Maximum measured deflections at mid-height center for gravity loads only, service load, design load, and maximum load with were 0.08 inches, 0.32 inches, 0.43 inches and 1.34 inches, respectively.

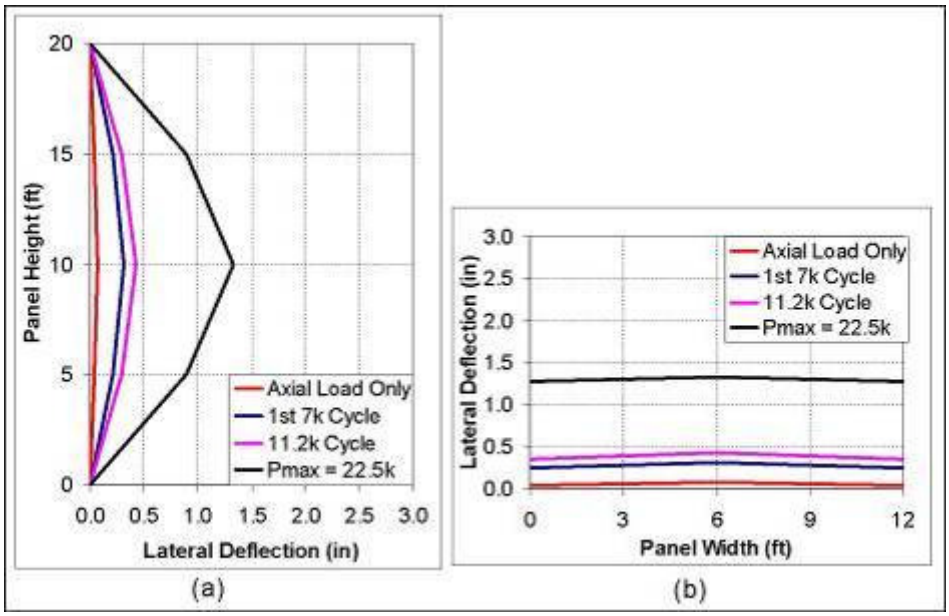

Figure 3-42: Deflection profiles of XPS 2

3.6.5 Panel XPS 3

The measured deflections along the center of the panel at 7/8-height center, 3/4-height center, mid-height center, quarter-height center and quarter-height right-edge are shown in Figure 3-43 (a), (b), (c), (d) and (e), respectively. All measured deflections were combined and shown in APPENDIX A, Figure 7-5 for comparison purposes. In each figure, initial deflections at zero lateral load are due to the applied axial load of 18.9 kips per corbel, which is equivalent to gravity load of $1.2D+0.5L_r$. Test results suggest that accumulated degradation was substantial and larger in magnitude in comparison to previous panels.

Failure occurred after completion of 1282 cycles of lateral load of 5 kips and gravity load of 18.9 kips per corbel. This load combination is equivalent to a load of $1.2D+0.5L_r+0.7W_{120}$. At this stage, significant deflection was measured which indicate significant reduction of the overall stiffness of the panel. Deflection at service is not given in Table 3-11 since failure occurred before reaching the design service load.

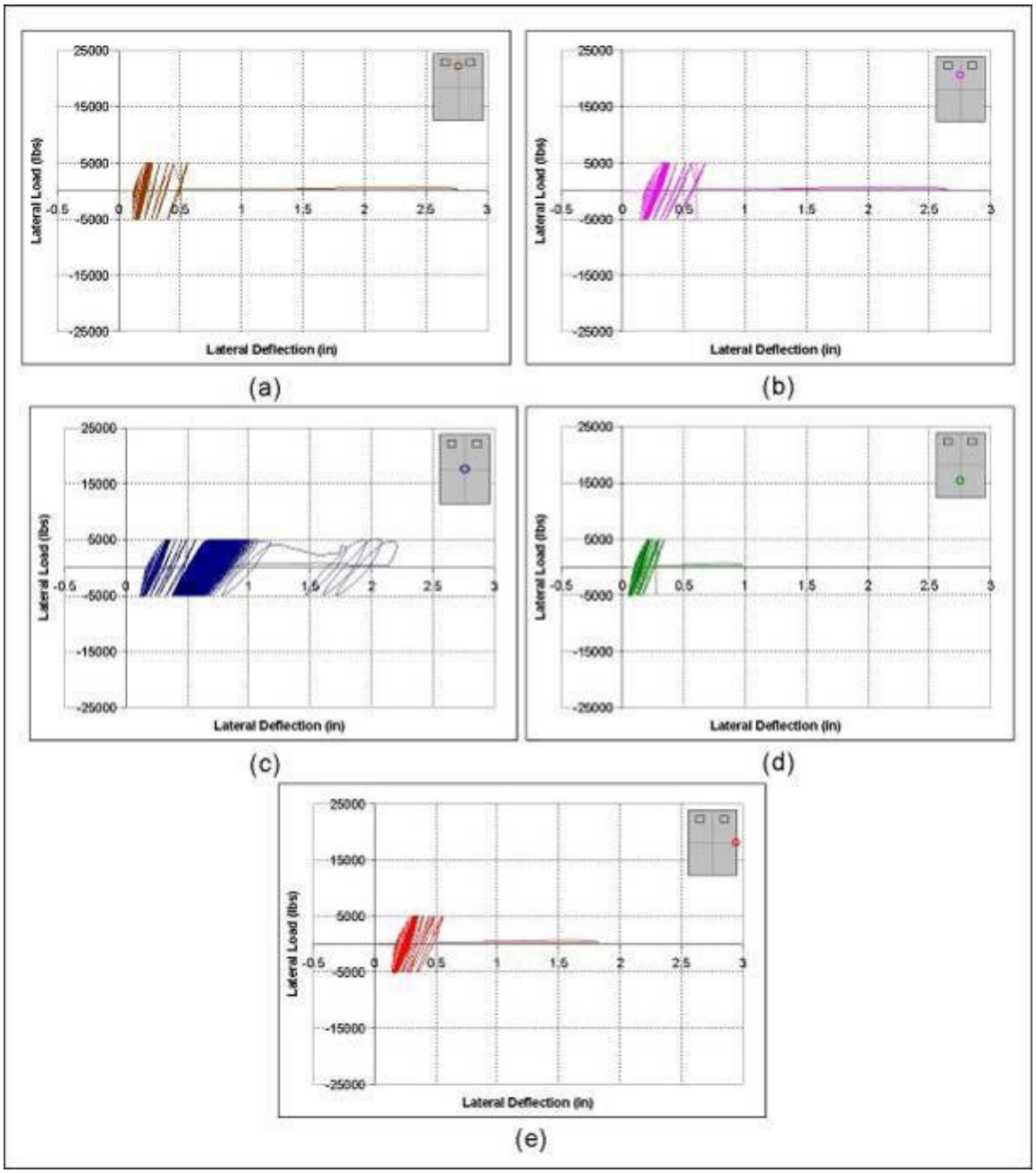

Figure 3-43: Individual lateral displacement of XPS 3

Since panel XPS 3 failed before reaching the service load level, deflection profiles along the panel height and width are provided up to a lateral load of 5 kips and gravity load of 18.9 kips on each corbel as shown in Figure 3-44 (a) and (b), respectively. This combination is equivalent to $1.2D+0.5L_r+0.7W_{120}$. The profiles are given after completion of the first cycle

and after 1005 cycles. Test results indicate that the maximum deflection occurred at 3/4-height of the panel throughout the cyclic loading until failure. Maximum recorded deflection for the first 5 kip lateral load cycle and after completion of the 1005th 5 kip lateral load cycle were 0.32 inches and 0.68 inches, respectively.

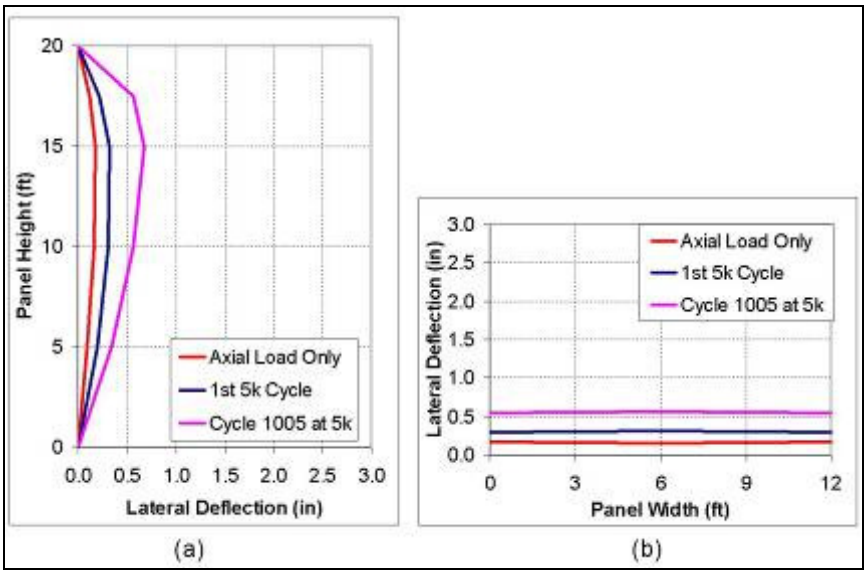

Figure 3-44: Deflection profiles of XPS 3

3.6.6 Panel XPS 4

All measured lateral deflections along the height of the panel at 7/8-height center, 3/4-height center, mid-height center, quarter-height center and quarter-height right-edge are shown in Figure 3-45 (a), (b), (c), (d) and (e), respectively. Measured values indicate very little accumulated degradation in comparison to XPS 3. All measured lateral deflections were linear up to lateral load approximately 10 kips, after which, the panel stiffness decreased noticeably throughout the load cycles. The measured lateral deflection at mid-height and mid-width of the panel, under service load was 0.34 inches, which is equivalent to h/700. The deflection at service load was within the ACI 533 limits of h/360. All measured deflections were combined and shown in APPENDIX A, Figure 7-6 for comparison purposes.

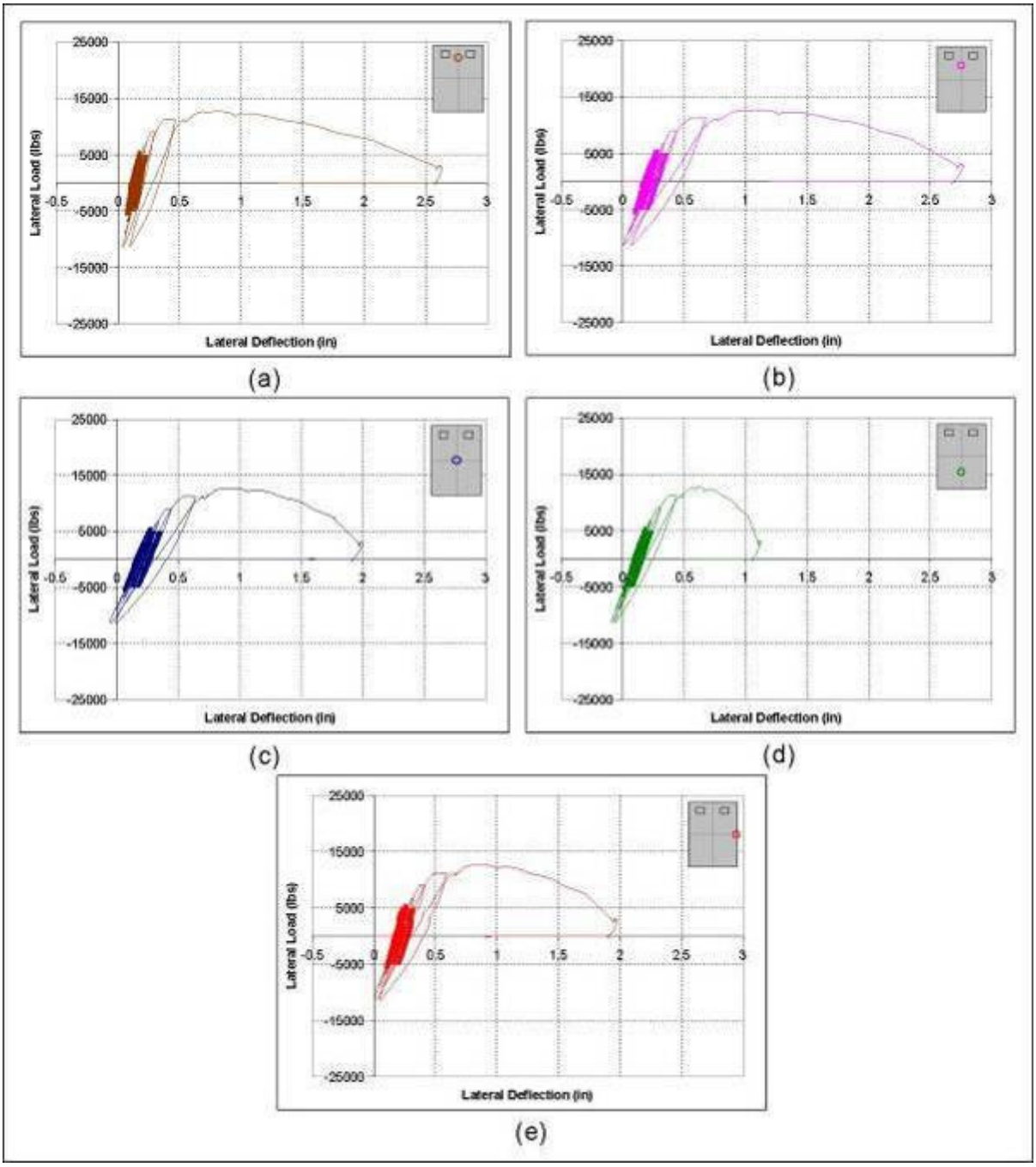

Figure 3-45: Individual lateral displacement of XPS 4

Deflection profiles for panel XPS 4 were created at load levels equivalent to $D+L_r+W_{120}$, $1.2D+0.5L_r+1.6W_{120}$, and $1.2D+0.5L_r+1.8W_{120}$, respectively. The deflection profiles indicate that the maximum deflection located at the mid-height for service load was shifted to

3/4-height at failure as shown in Figure 3-46 (a). It was also observed that panel XPS 4 experienced slight curvature across the width of the panel as shown in Figure 3-46 (b). Maximum measured deflections for service load, design load, and maximum load were 0.34 inches, 0.58 inches, and 0.98 inches, respectively.

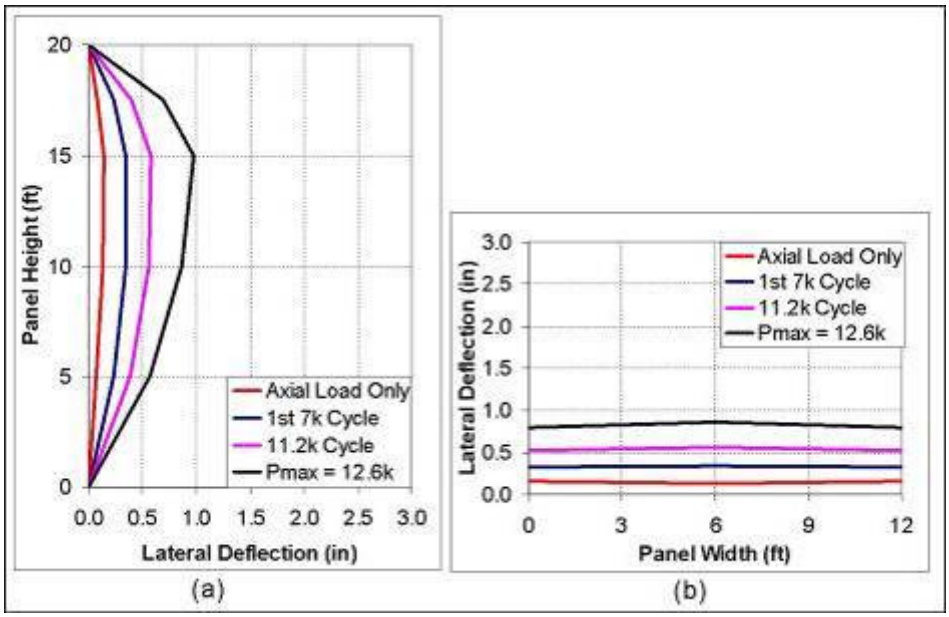

Figure 3-46: Deflection profiles of XPS 4

3.7 RELATIVE VERTICAL AND HORIZONTAL DISPLACEMENTS

The measured relative vertical displacements refer to the relative movement of the inner wythe with respect to the outer wythe. Positive motion represents relative movement of the inner wythe downward with respect to the outer wythe. Relative vertical measurements were measured at the top of each panel near the mid-width and edge of the panel.

The relative horizontal displacement between the two concrete wythes was monitored at 7/8 of the panel height and mid-height at the edge for panels XPS 3 and XPS 4 only. This displacement was also monitored at mid-height for XPS 2. Positive relative motion reflects separation of the wythes from each other.

3.7.1 Panel EPS 1

The center of panel EPS 1 experienced nearly 0.01 inches of elastic shortening during the application of the axial load while the edge of the panel experienced nearly no effect. Throughout the fatigue cycles, the center of the panel experienced approximately 0.01 inches of relative vertical panel degradation while the edge of the panel experienced nearly half that degradation as shown in Figure 3-47 (a) and (b), respectively. During the application of the higher level fatigue cycle, the center instrument went offline while the panel edge instrument measured increased load effects. Throughout these cycles, the inner wythe experienced greater elastic shortening due to leeward forces and less elastic shortening due to windward forces. As the panel approached failure, the magnitude of panel degradation significantly increased indicating that the inner wythe resisted increased axial load with an increase in lateral load indicating the panel did not experience fully composite behavior.

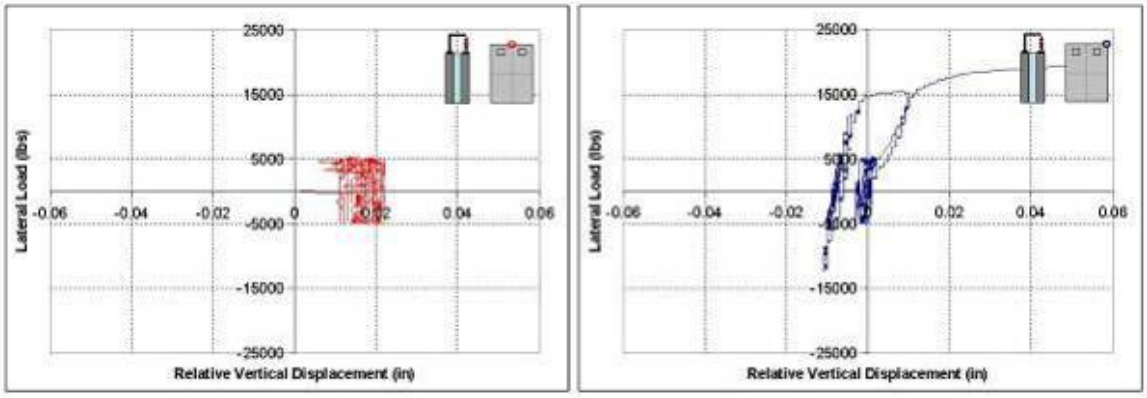

(a) (b)

Figure 3-47: Relative vertical displacement of EPS 1

3.7.2 Panel EPS 2

Panel EPS 2 experienced a positive relative vertical displacement during the application of the factored gravity loads indicating that the inner wythe experienced a greater level of elastic shortening. Throughout the fatigue cycles, the panel experienced an increase in

relative vertical displacement due to leeward forces and a decrease in relative vertical displacement due to windward forces as shown in Figure 3-48. Throughout these cycles, the panel experienced significant panel degradation at both the center of the panel and the edge of the panel as shown in Figure 3-48 (a) and (b), respectively. Note that the positive scale of displacement is scaled to 0.14 inches for EPS 2 versus 0.06 inches for other panels due to the significant panel degradation with increased lateral loads.

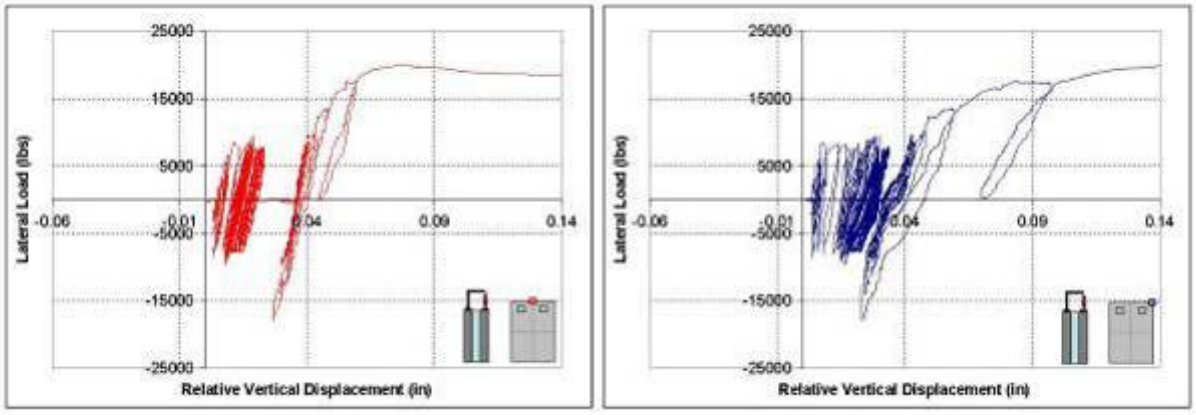

(a) (b)

Figure 3-48: Relative vertical displacement of EPS 2

3.7.3 Panel XPS 1

The effect of relative vertical displacement for XPS 1 was minimal in comparison to all other panels. XPS 1 experienced some positive relative vertical displacement during the application of the axial load indicating that the inner wythe resisted more axial load than the outer wythe as indicated in the center and edge of the panel as shown in Figure 3-49 (a) and (b), respectively. Throughout the fatigue cycles, the effect on the panel was minimal in comparison with other panels indicating that solid concrete zones increases the degree of composite action.

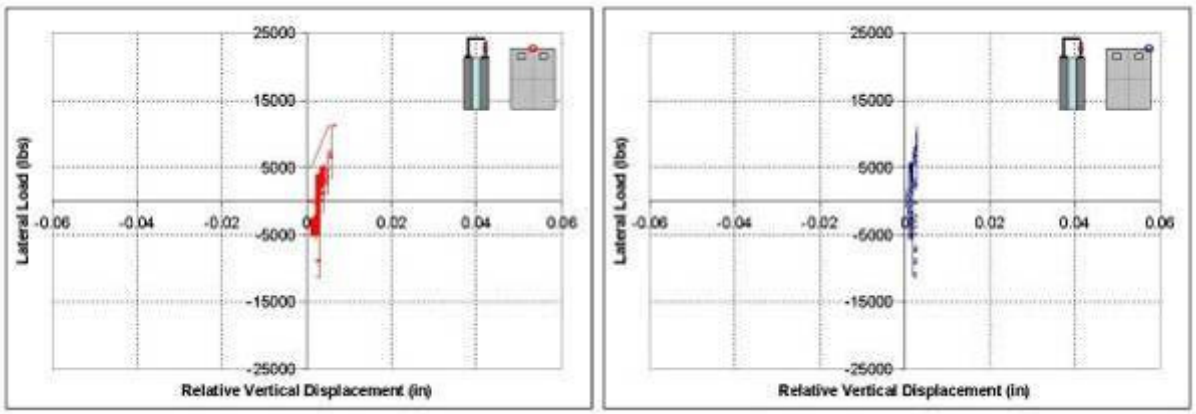

(a) (b)

Figure 3-49: Relative vertical displacement of XPS 1

3.7.4 Panel XPS 2

Panel XPS 2 experienced approximately 0.05 inches of relative vertical displacement across the panel width due to the application of the gravity loads. Throughout the fatigue cycles, the magnitude of displacement increased due to leeward forces and decreased due to windward forces. The amplitude of displacement variation from push to pull stroke was noticeably higher of other panels. The center of the panel experienced approximately twice the amplitude than the edge of the panel throughout the maximum and minimum loads of a given cycle as shown in Figure 3-50 (a) and (b), respectively.

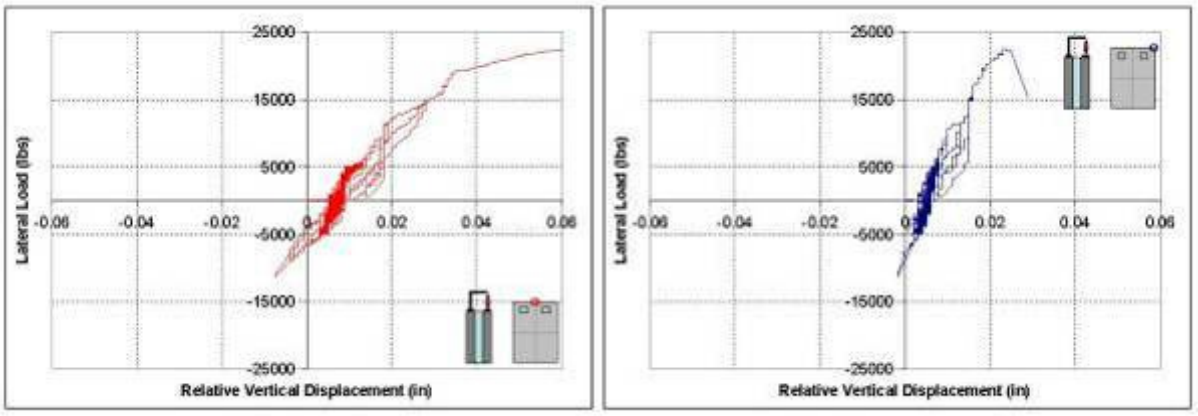

(a) (b)

Figure 3-50: Relative vertical displacement of XPS 2

Panel XPS 2 experienced nearly 0.01 inches of wythe separation at mid-height due to the application of the gravity loads. Throughout the fatigue regimen, the panel experienced wythe compression due to leeward forces and wythe separation due to windward forces as shown in Figure 3-51. As the lateral load approached 15 kips with factored gravity loads, the wythe separation became non-linear indicating a degradation in composite action. Final panel compression was nearly 0.06 inches at the failure load of $1.2D+0.5L_r+3.2W_{120}$.

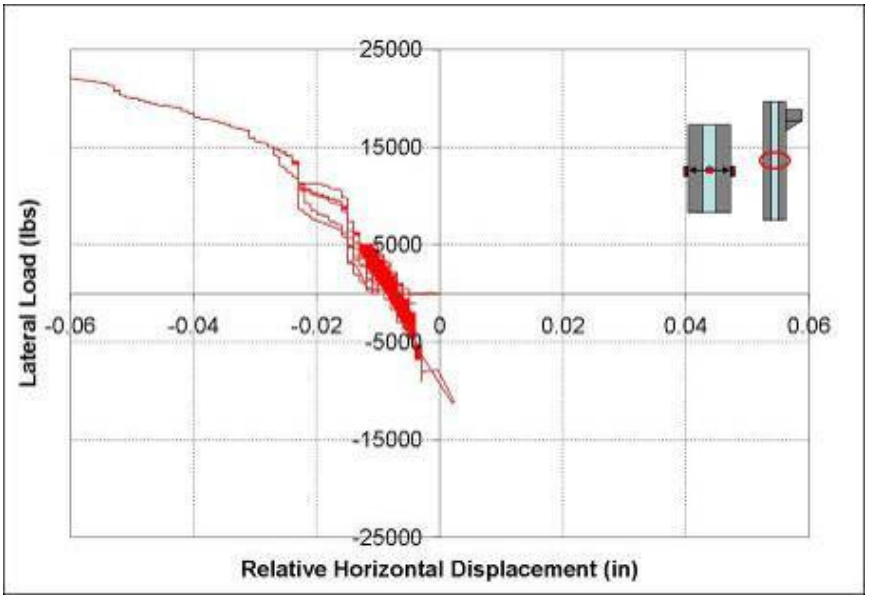

Figure 3-51: Relative horizontal displacement at mid-height of XPS 2

3.7.5 Panel XPS 3

The measured small positive relative vertical displacements during testing of XPS 3 indicated that the inner wythe experienced slightly more elastic shortening during the application of factored gravity loads than the outer wythe. Throughout the fatigue cycles, measurements at the center of the panel degradation as the relative vertical displacement increased from approximately 0.004 to 0.02 inches as shown in Figure 3-52 (a). During the application of lateral loads, windward forces (negative direction) showed a decrease in the relative vertical displacement while leeward forces (positive direction) showed an increase in

relative vertical displacement as shown in Figure 3-52 (b). The relative vertical displacement degradation at the panel edge throughout the fatigue regimen was greater than at the center of the panel.

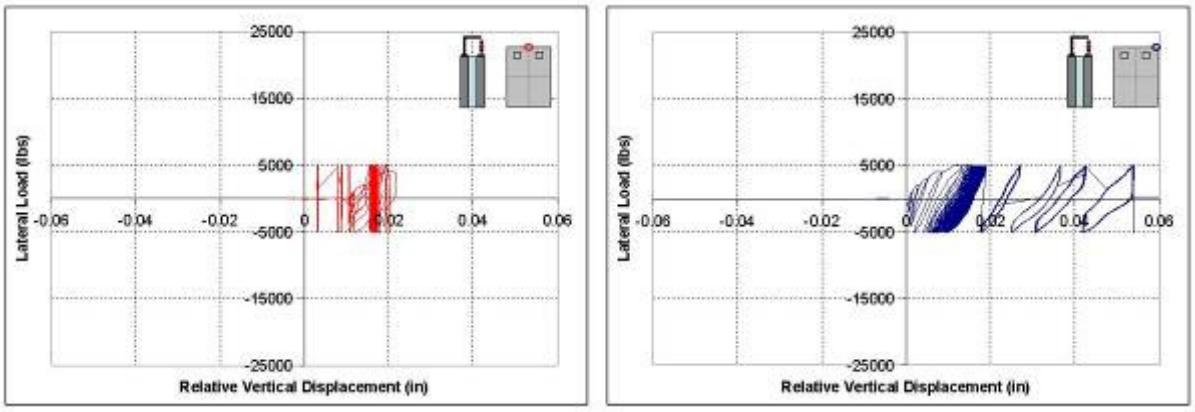

(a) (b)

Figure 3-52: Relative vertical displacement of XPS 3

The measurements at 7/8 of the panel height showed the wythes compressed towards each other with the application of the factored gravity loads while the mid height of the panel experienced no motion due to these loads. With the application of lateral loads, the measured values showed that the panel compressed during leeward forces and separated during windward forces. With increased lateral load cycles, the top of the panel experienced very little degradation while the mid height of the panel did not show any sign of degradation throughout the fatigue regimen as shown in Figure 3-53 (a) and (b), respectively.

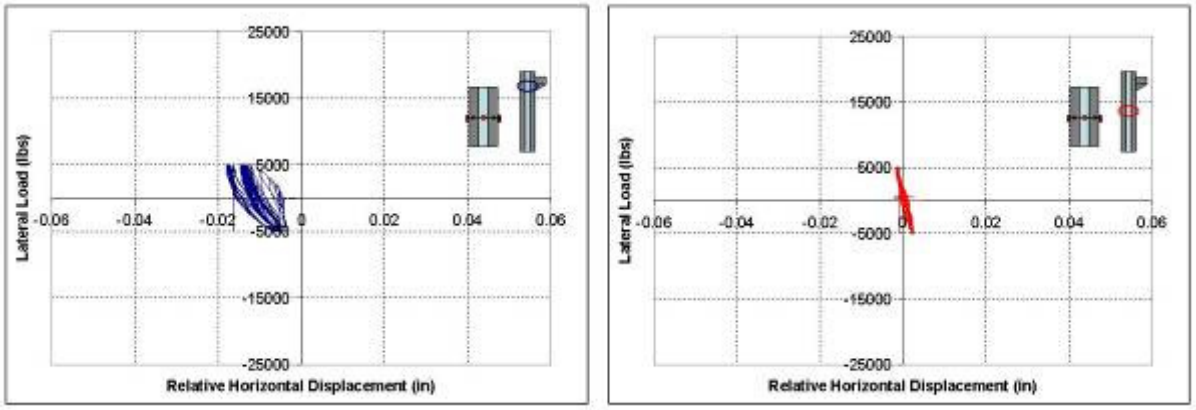

(a) (b)

Figure 3-53: Relative horizontal displacement of XPS 3

3.7.6 Panel XPS 4

Positive relative vertical displacements measured during testing of XPS 4 showed that the center of the inner wythe experienced slightly more elastic shortening during the application of factored gravity loads than the outer wythe. Throughout the fatigue cycles, the panel experienced a decrease in relative vertical displacement due to windward forces and an increase in relative vertical displacement due to leeward forces. The panel experienced very little degradation across the panel width throughout the fatigue regimen as shown in Figure 3-54 (a) and Figure 3-54 (b).

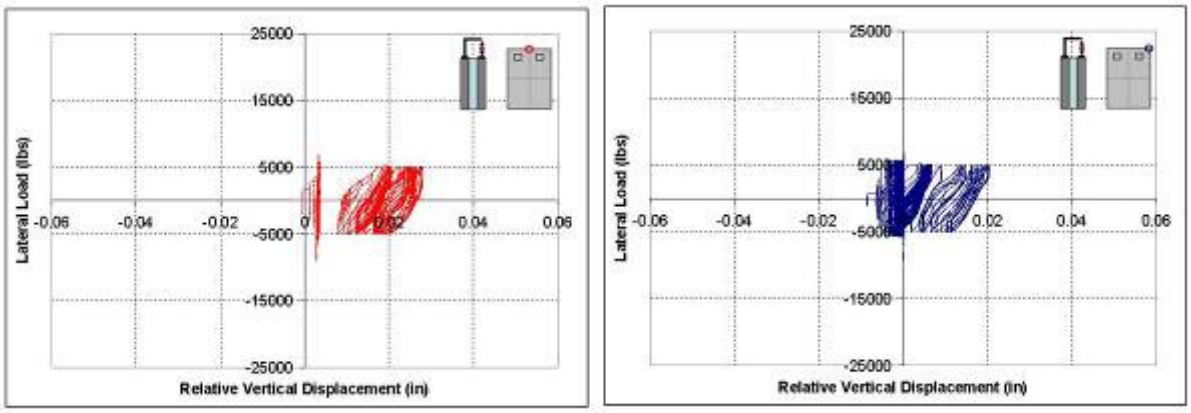

(a) (b)

Figure 3-54: Relative vertical displacement of XPS 4

The measurements at 7/8 of the panel height showed the wythes compressed towards each other with the application of the factored gravity loads while the mid height of the panel experienced minimal separation due to these loads. With the application of lateral loads, the measured values showed that the panel compressed during leeward forces and separated during windward forces. While mid-height exhibited a linear behavior throughout testing, the measurements at 7/8 panel height showed a non-linear behavior at the end of the cyclic loading regimen. With increased lateral load cycles, the top of the panel experienced nearly 0.02 inches of degradation while the mid height of the panel showed little degradation throughout the fatigue regimen as shown in Figure 3-55 (a) and (b), respectively.

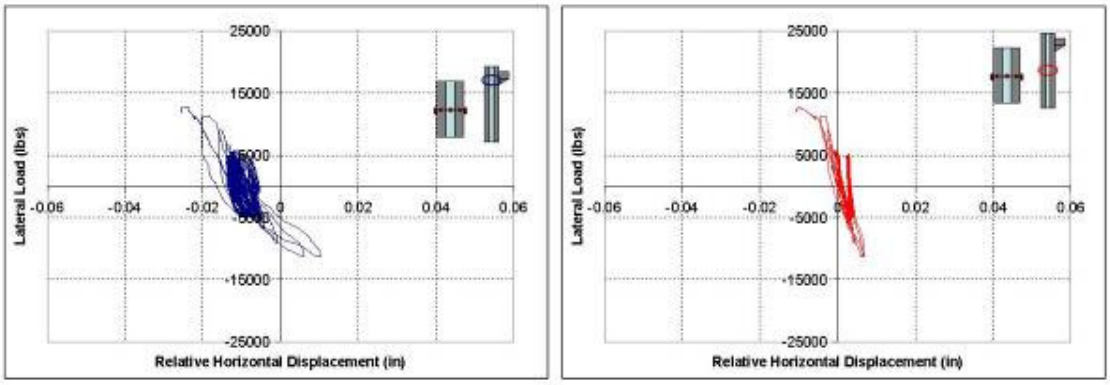

(a) (b)

Figure 3-55: Relative horizontal displacement of XPS 4

3.8 SURFACE STRAINS OF CONCRETE

Concrete surface strains were measured at the inner and outer panel surfaces for all tests. All measured strains during testing were only in the order of a few hundreds of microstrain. The designation "I" denotes inner wythe strain measurements while the designation "O" denotes the outer wythe strain measurements. Instruments were labeled as 1, 2, and 3 corresponding to the instrument located 6 inches, 3 feet, and 5.5 feet from the edge of the panel, respectively.

Test results indicated that the slopes of the load versus surface strain of the inner and outer faces are similar in magnitude and opposite in direction. The measured strain at zero lateral load is due to the effect of the applied compression axial load.

3.8.1 EPS Panels

Surface strain behavior was similar for both EPS foam core panels. The inner wythe panels experienced compressive strains while the outer wythe experienced tensile strains under the effect of applied factored gravity loads. This behavioral trend continued throughout the fatigue cycles. Both EPS panels experienced strain degradation throughout the lateral load cycles as shown in Figure 3-56 and Figure 3-57. The measured values suggest some errors of reading the "outer 2" and "inner 1" strains of panel EPS 1; however, the trend of the data was consistent with other strain instruments.

During the application of the lateral leeward and windward forces, the strain increased and decreased in linear relationship to a load of approximately 15 kips. The measured tensile strains at this level were 433 and 213 microstrain for EPS 1 and EPS 2, respectively. At this load level, tensile cracks were observed for both panels.

Based on an assumed linear elastic behavior of the concrete and an elastic modulus of $57000\sqrt{f_c}$ /2, the measured strain is within the uncracked tensile strain limit of $10\sqrt{f_c}$.

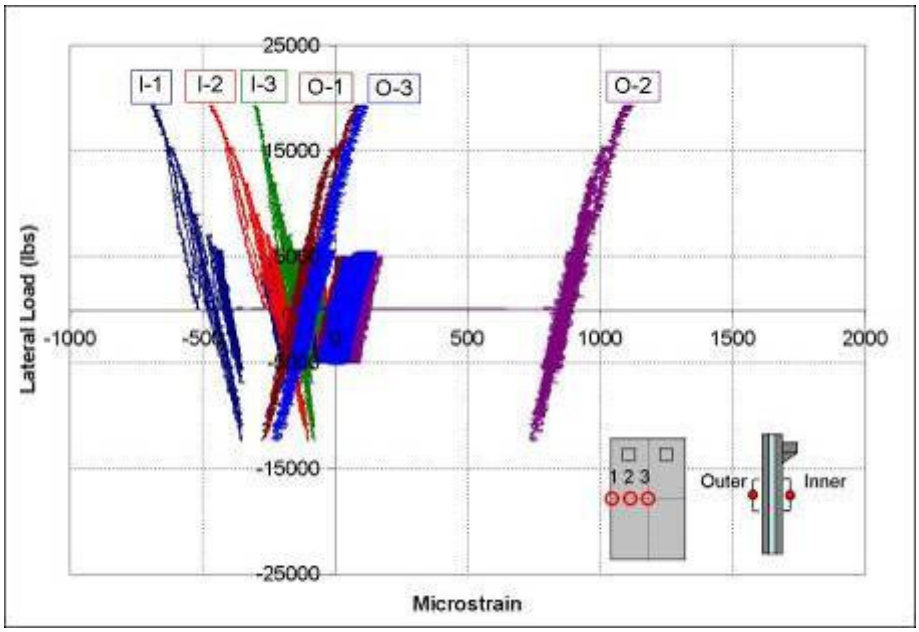

Figure 3-56: Face strains of EPS 1

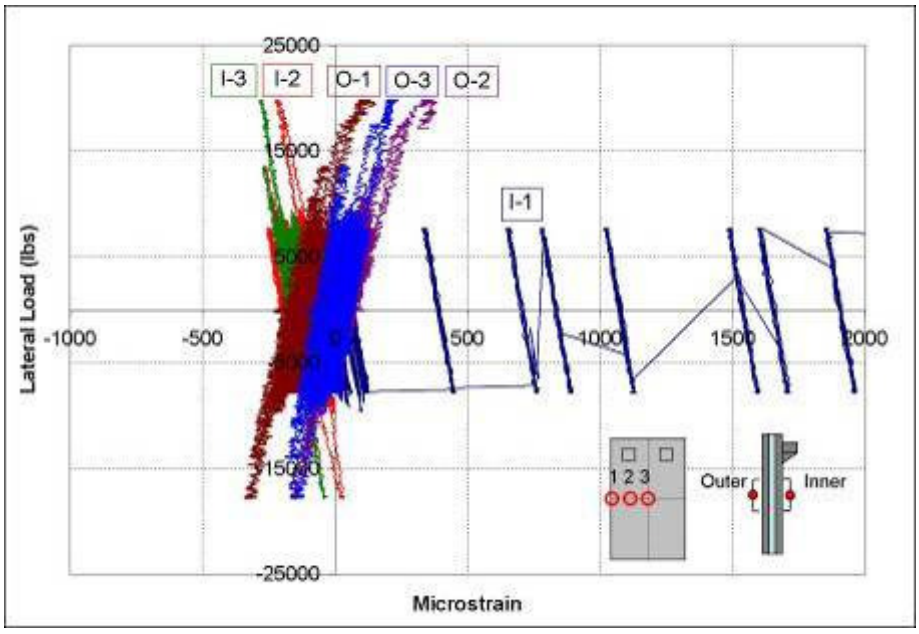

Figure 3-57: Face strain of EPS 2

3.8.2 XPS Panels

Measured surface strain data of the XPS panels showed that the inner wythe experienced compressive strains while the outer wythe experienced tensile strains throughout the loading sequence. Panels XPS 1, XPS 2 and XPS 3 experienced significant strain degradation

throughout the lateral load cycles while panel XPS 4 experienced considerably less degradation as shown in Figure 3-58 through Figure 3-61. Shift of the reading of the strain gauge I-1 suggest possible error of the instrument, however, the trend of the data was consistent with other strain instruments.

In general, the measured load strain relationship for all tested panels were linear up to a lateral load level of 15 kips with the exception of panel XPS 3 which failed at a much lower load level. Measured strains for all tested panels were within the elastic range of the concrete in tension.

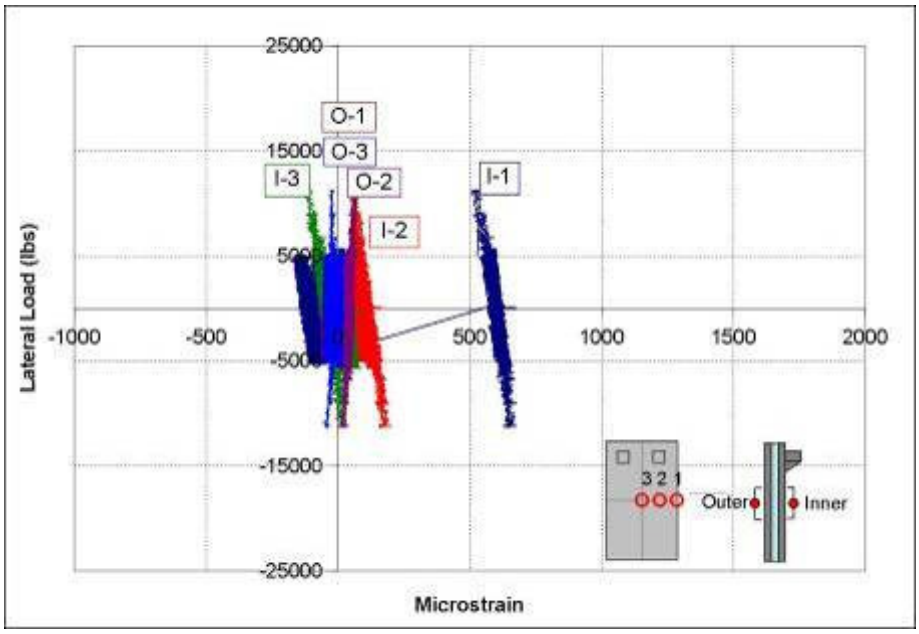

Figure 3-58: Face strains of XPS 1

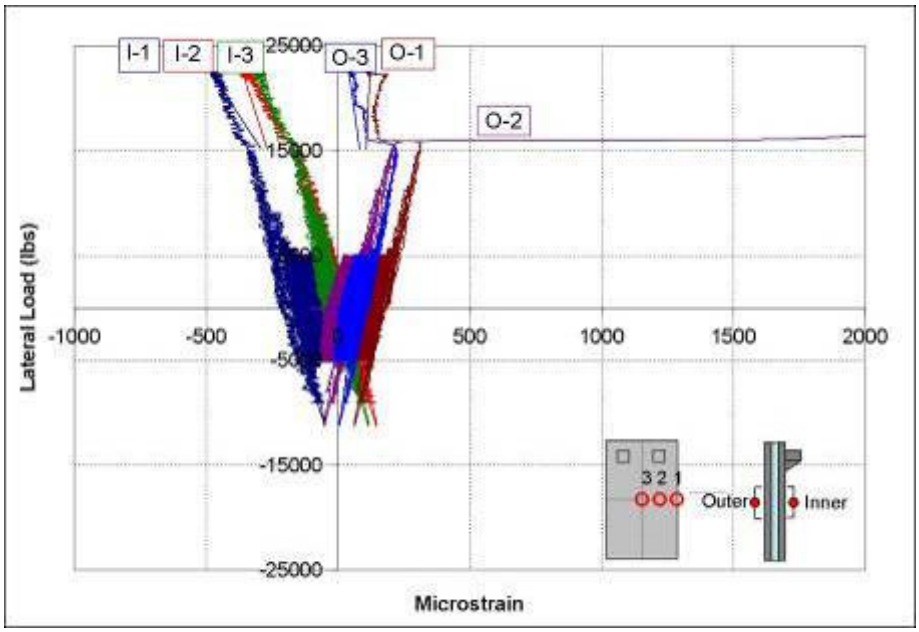

Figure 3-59: Face strain of XPS 2

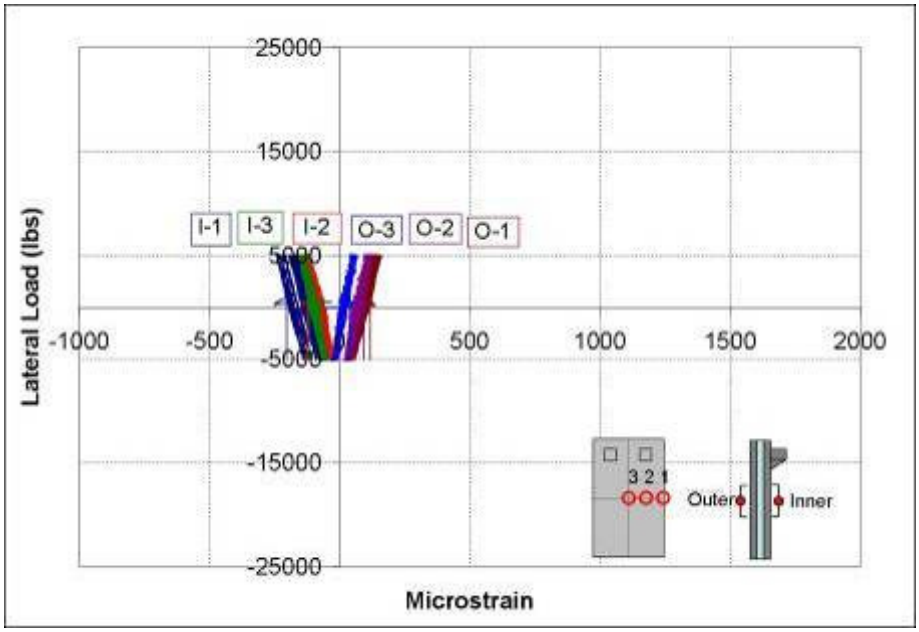

Figure 3-60: Face strain of XPS 3

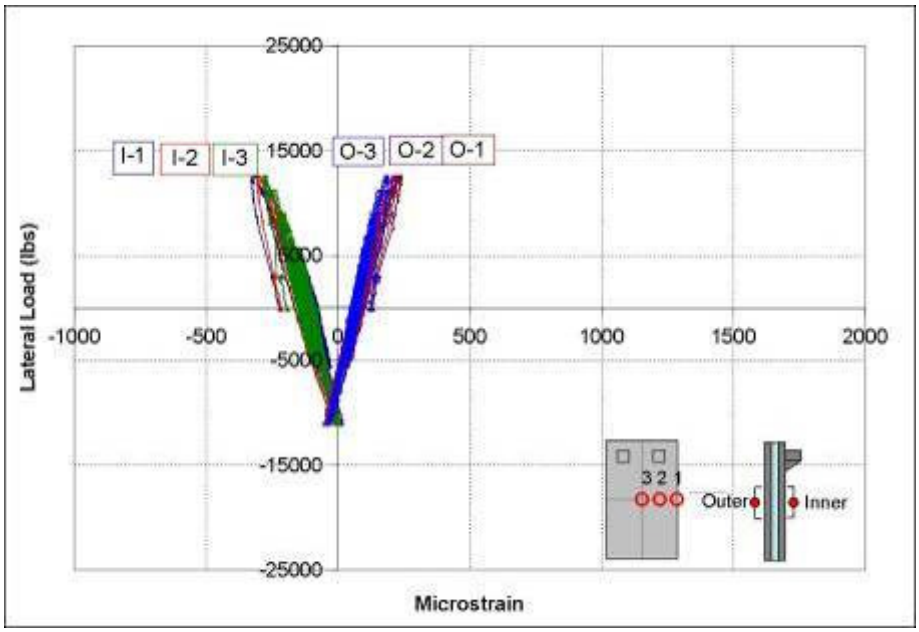

Figure 3-61: Face strain of XPS 4

3.9 STRAIN ACROSS THE PANEL THICKNESS AT MID-HEIGHT

Four strain gauges were used to measure the strain across the thickness of the panel at quarter-height, mid-height and 7/8-height as shown in Figure 3-62 (a), (b) and (c), respectively. The measured strains were used to establish strain profiles across the panel thickness. It should be noted that the measured strain at the quarter-height of the panel were very small and in the order of magnitude of the accuracy range of the strain gauges used, therefore they were not used to draw a definite conclusion regarding to the composite action. The measurements at mid-height and 7/8 of the panel height were larger in magnitude due to a higher moment region and therefore were used to study the composite action presented in this section. Quarter-height strain data is presented in APPENDIX A, Figure 7-7 through Figure 7-18.

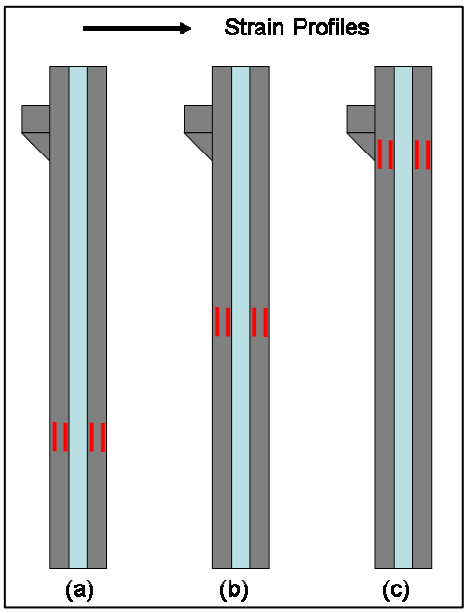

Figure 3-62: Strain Profile Orientations

3.9.1 Panel EPS 1

The measured strains across the panel thickness of EPS 1 at mid-height are shown in Figure 3-63. Maximum compressive strain occurred along the inner wythe and the maximum tension strain along the outer wythe. An initial compressive strain was measured across the panel thickness due to the application of the gravity load. Throughout the lateral load cycles, panel degradation was observed, evident by increasing the measured strain across the panel.

Based on the measured strain at mid-height of the panel, the strain profile across the section was established after the application of the axial load, ultimate design load and failure load, as shown in Figure 3-64 (a), (b) and (c), respectively. The strain profile indicates that the neutral axis is located closer to the elastic centroid of the cross-section than the elastic centroid if each individual wythe which indicates a high level of composite action. The strain profile also indicates that the inner wythe carried a majority of the axial load while the wythes resisted bending moments due to the eccentric location of the applied axial load and the lateral loads.

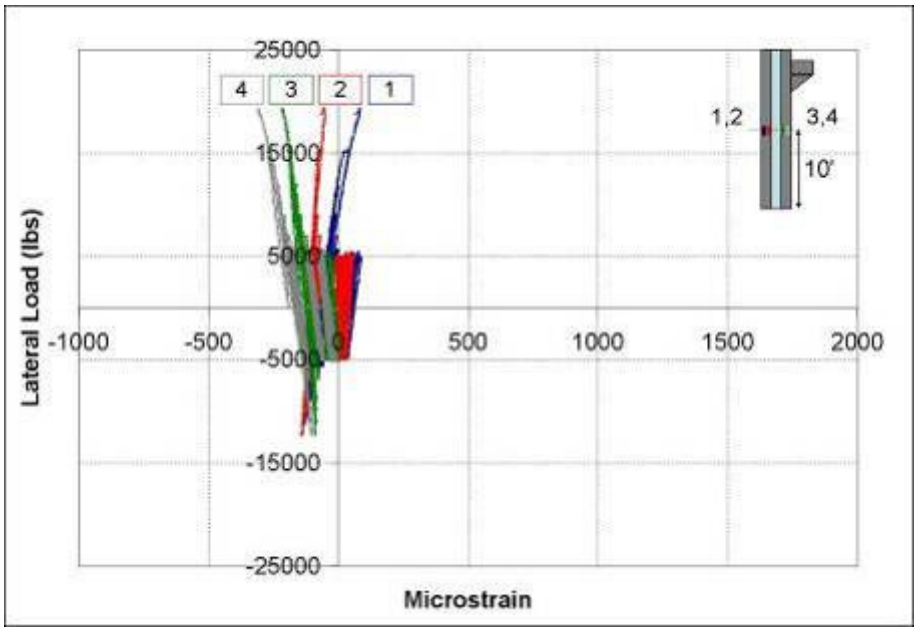

Figure 3-63: Mid-height side strain gauges of EPS 1

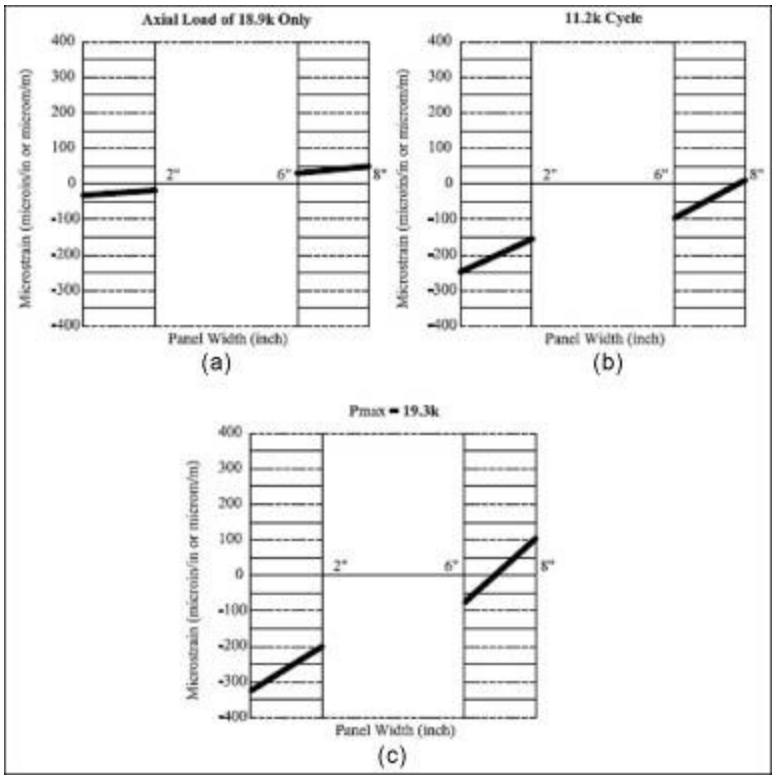

Figure 3-64: Mid-height side strain profile of EPS 1

3.9.2 Panel EPS 2

Pane ESP 2 exhibited nearly the same strain behavior as panel EPS 1. The inner wythe exhibited the maximum compressive strain while the outer wythe exhibited the maximum tension strain as shown in Figure 3-65. Strain profiles were established for the same load levels as panel EPS 1 and exhibited the same linear strain profile with the neutral axis location near the composite elastic centroid of the cross-section which indicates a highly composite section as shown in Figure 3-66 (a), (b) and (c), respectively.

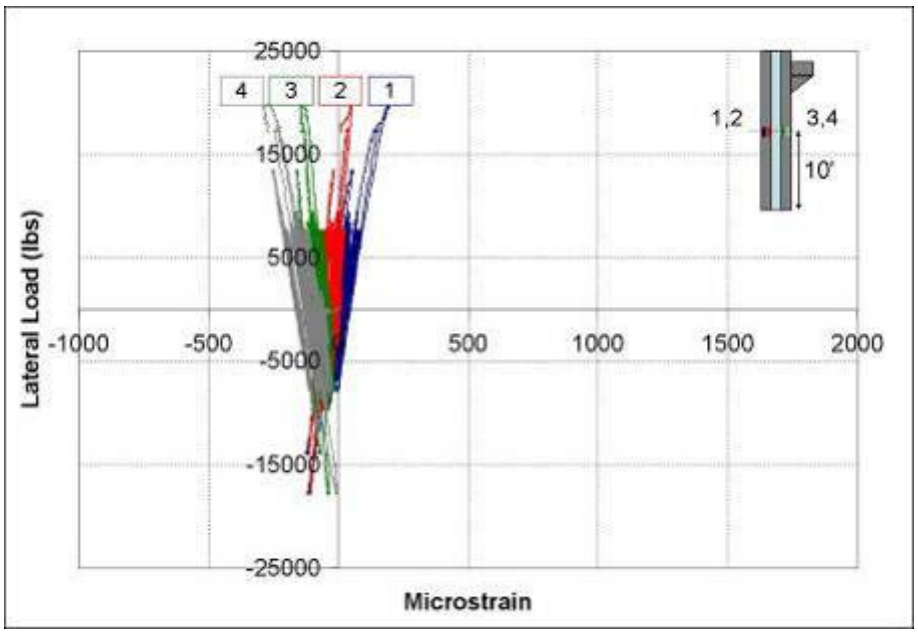

Figure 3-65: Mid-height side strain gauges of EPS 2

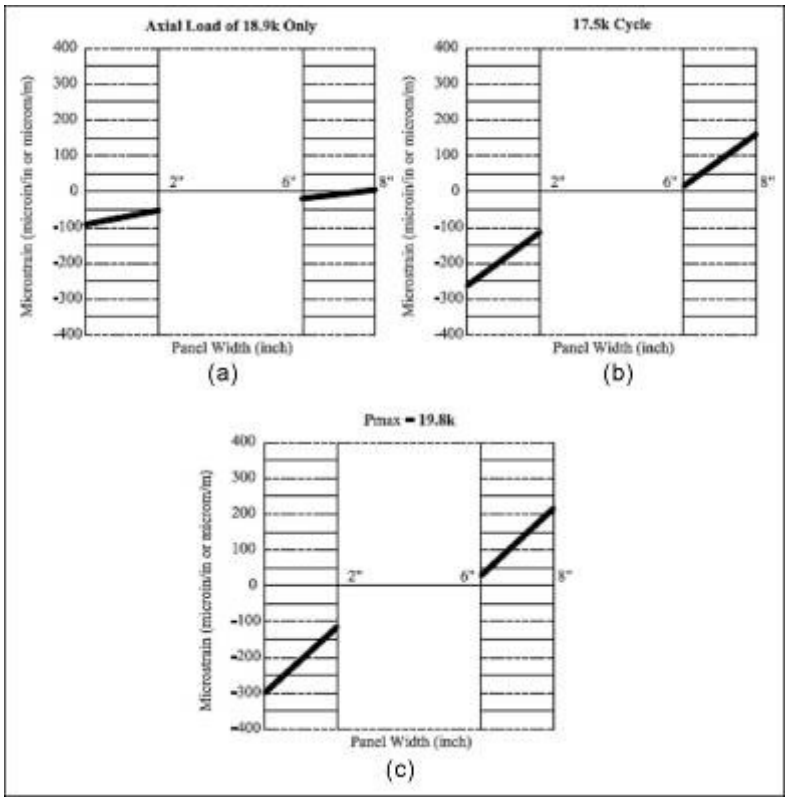

Figure 3-66: Mid-height side strain profile of EPS 2

3.9.3 Panel XPS 1

Panel XPS 1 exhibited almost constant compressive strain distributed across the inner wythe and almost constant tension strain across the outer wythe during leeward forces as shown in Figure 3-67. This behavior reversed during windward forces. Strain profiles established due to the application of the gravity load and at failure load, shown in Figure 3-68 (a) and (b), respectively shows equal but with opposite sign convention in the outer and inner wythes. This behavior is believed to reflect a highly composite action of the inner and outer wythes in carrying the applied load.

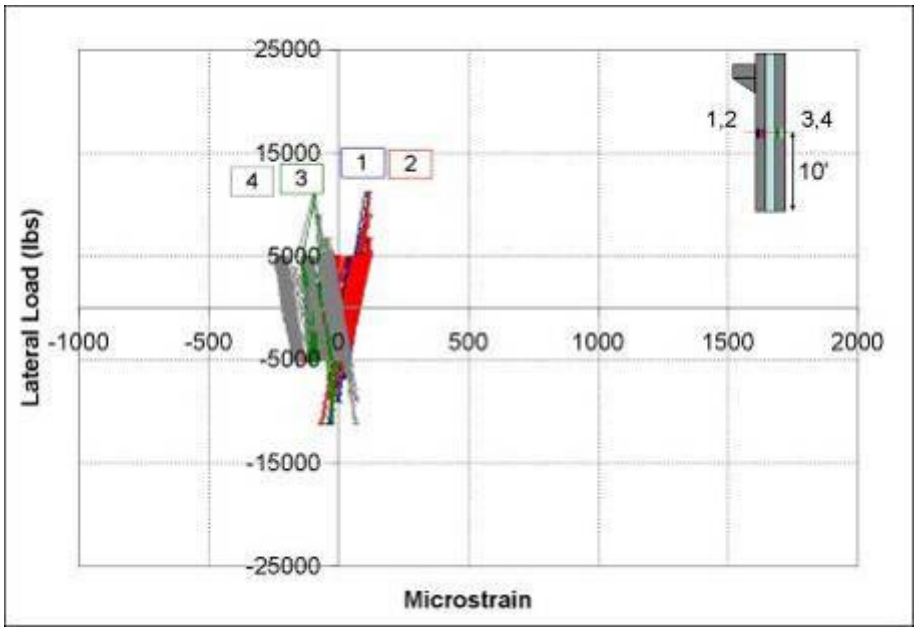

Figure 3-67: Mid-height side strain gauges of XPS 1

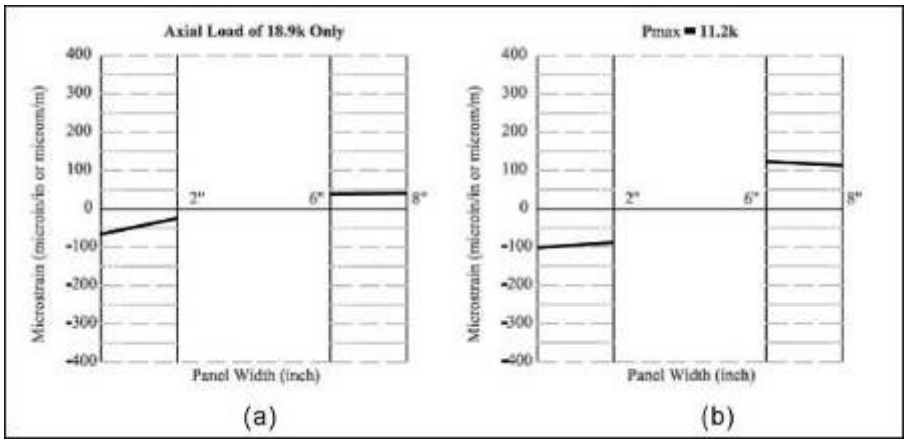

Figure 3-68: Mid-height side strain profile of XPS 1

3.9.4 Panel XPS 2

The measured strains for panel XPS 2 indicate that each wythe act independently in carrying the applied load. The measured strain of the inner surface of each wythe were in compression while the outer surface of each wythe were in tension as shown in Figure 3-69. The established strain profiles immediately after the application of the axial load, at ultimate design load and prior to failure load are shown in Figure 3-70 (a), (b) and (c), respectively. The strain profile for each wythe was independent of the neutral axis located within the

thickness of each wythe. The strain profile after application of the axial load only indicates that a majority of the axial load was resisted by the inner wythe while the bending moment due to the eccentrically applied axial load and the lateral loads were resisted by each wythe independently proportional to their individual stiffness. As lateral load was applied, the slope of the strain profile for each wythe increased equally showing that each wythe resisted the applied bending moments with respect to their individual stiffness resulting in similar curvature of both wythes.

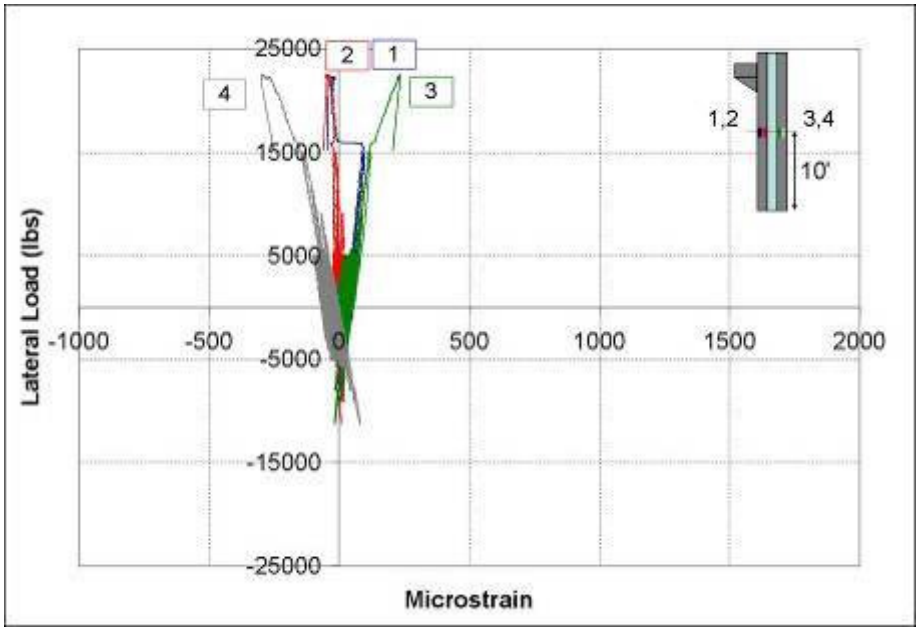

Figure 3-69: Mid-height side strain gauges of XPS 2

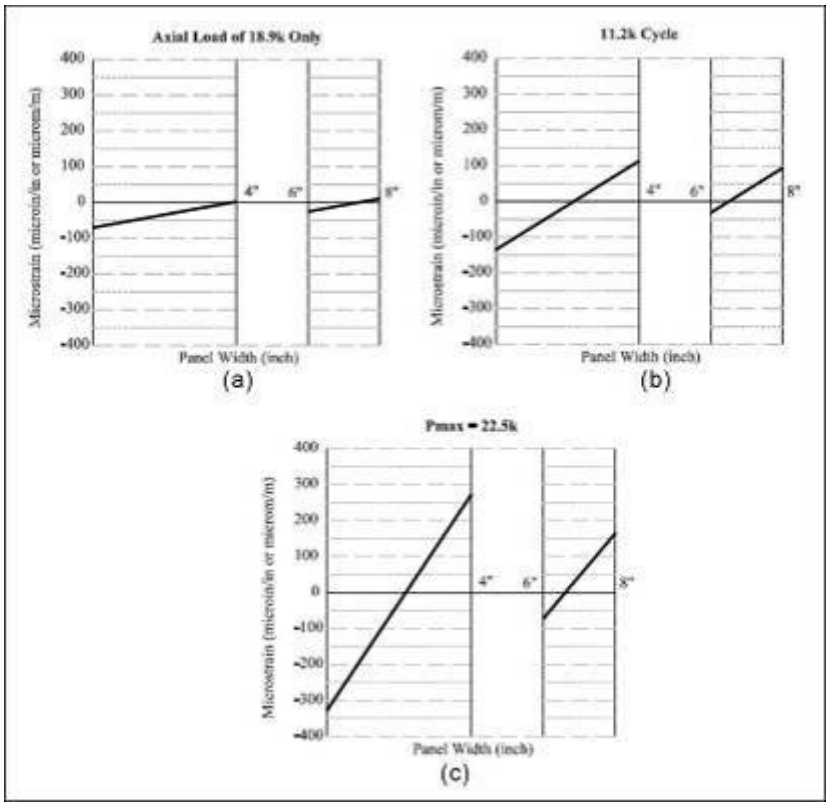

Figure 3-70: Mid-height side strain profile of XPS 2

3.9.5 Panel XPS 3

Strain measurements across the panel thickness at mid-height are shown in Figure 3-71. Panel XPS 3 experienced maximum compressive strain along the inner panel surface. The strain varied linearly across the panel section with a maximum tensile strain along the outer panel surface as shown in Figure 3-71. Critical strain profiles were established after the application of the axial load and after 1005 cycles of the 5 kip lateral load as shown in Figure 3-72 (a) and (b), respectively. It was observed that the inner wythe experienced a greater compressive strain than the outer wythe due to the application of the axial load. With the application of the lateral load, the slope of the strain across each wythe increased in the same order of magnitude as shown in Figure 3-72. Initially, the strain profile showed minimal discontinuity across the panel width indicating some level of composite action. As the lateral

load cycles increased, the discontinuity increased evident by shifting of the neutral axis towards the elastic centroid of each wythe. This behavior reflected definite degradation of the composite action of the panel.

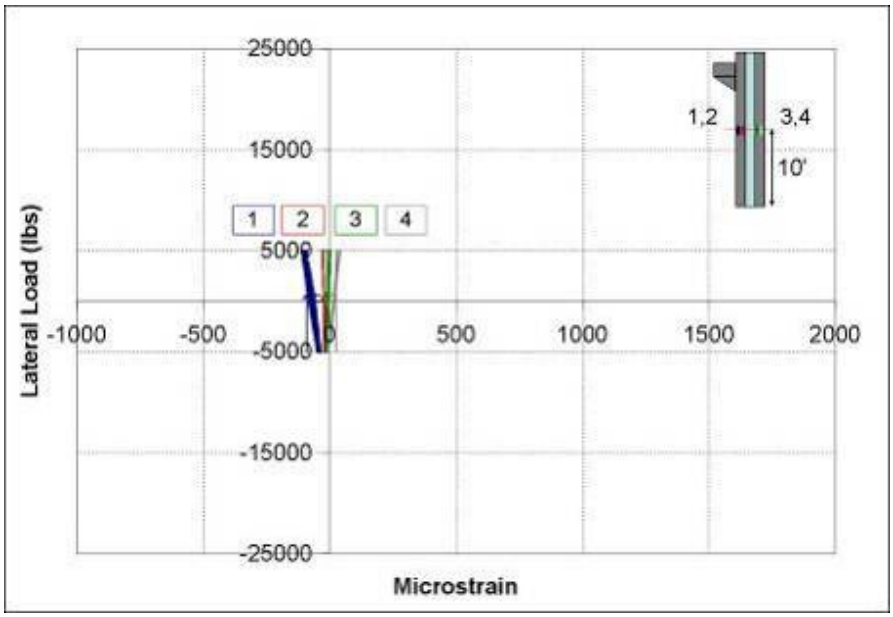

Figure 3-71: Mid-height side strain gauges of XPS 3

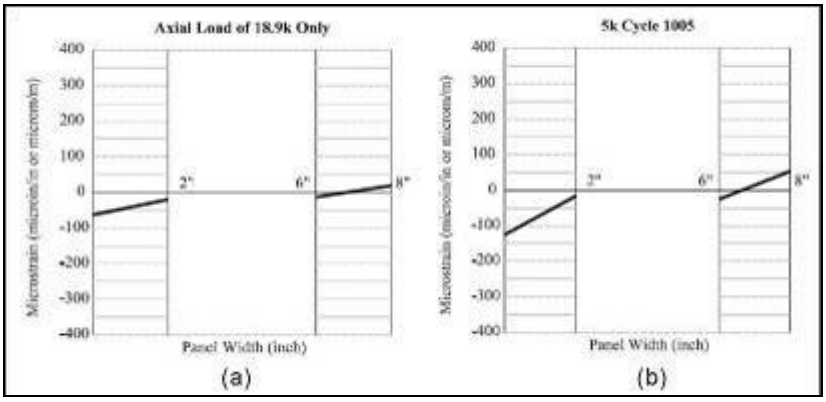

Figure 3-72: Mid-height side strain profile of XPS 3

3.9.6 Panel XPS 4

Strain across panel XPS 4 thickness showed linear strain transition from inner to outer panel surfaces. The inner wythe experienced the maximum compressive strain while the outer wythe experienced the maximum tensile strain as shown in Figure 3-73. The strain profiles established after application of the axial load, at ultimate design load and prior to

failure load, as shown in Figure 3-74 (a), (b) and (c) respectively, showed that the inner wythe was subjected to higher compressive force than the outer wythe. This behavior suggests that the inner wythe resisted more axial load than the outer wythe. Initially, the panel exhibited a single neutral axis; however, as the lateral load was increased, two neutral axes were developed and were located close to the elastic centroid of each respective wythe as shown in Figure 3-74. This behavior indicates that the panel initially behaved in composite action; however, that composite action was degraded with increasing the applied lateral load. Observation of the strain profile after application of the axial load only shows that the inner wythe resisted a larger portion of the axial load while the bending moments due to applied lateral loads was resisted equally by each wythe individually. As lateral load was increased, the slope of the strain profile increased equally for each wythe showing that each wythe resisted applied bending moments proportional to their individual stiffness.

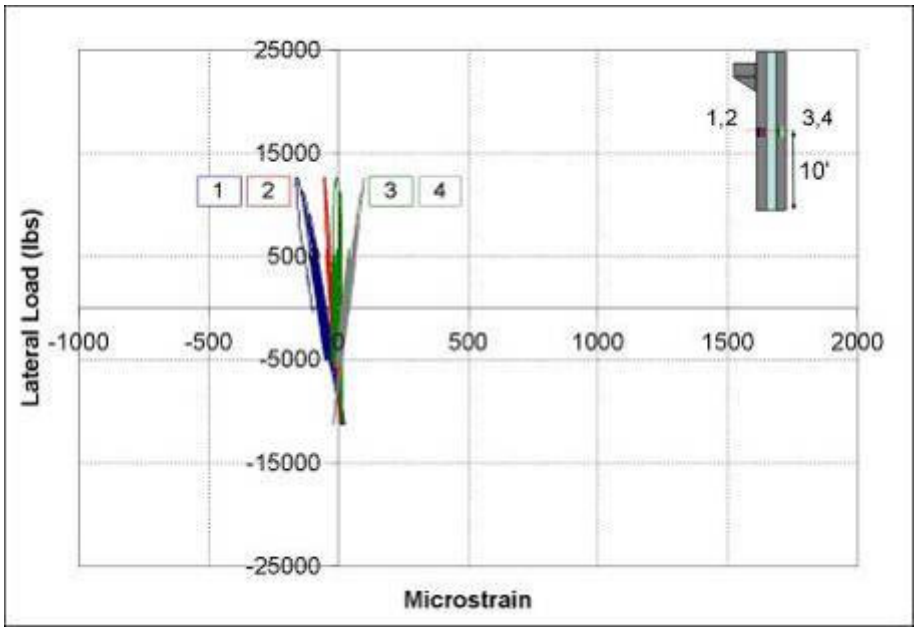

Figure 3-73: Mid-height side strain gauges of XPS 4

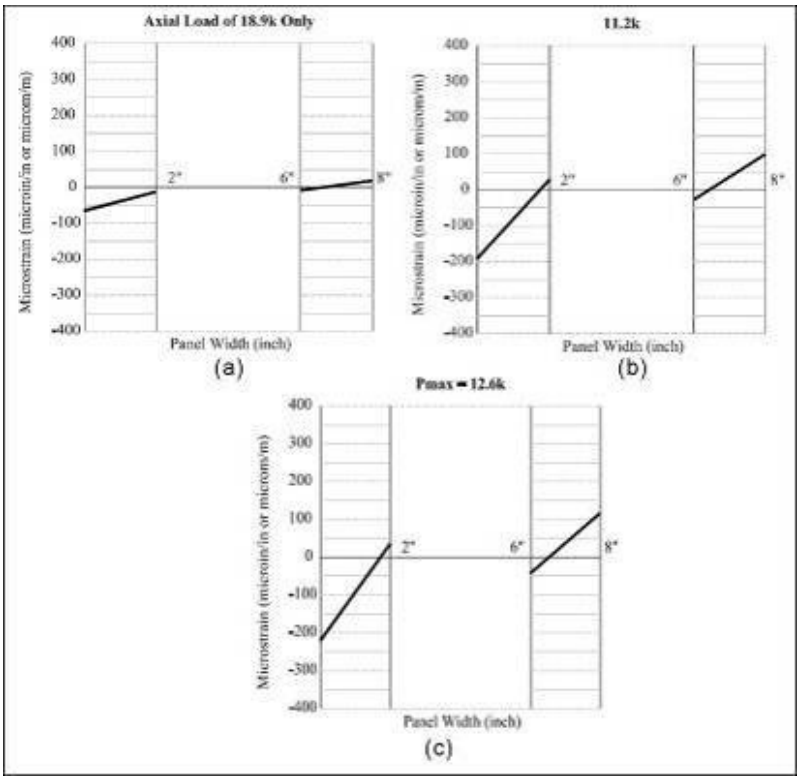

Figure 3-74: Mid-height side strain profile of XPS 4

3.10 STRAIN ACROSS THE PANEL THICKNESS AT 7/8-HEIGHT

In order to exemplify the strain behavior along the height of the panels, strain profiles were measured at 7/8 of the panel height for panel XPS 3 and XPS 4.

3.10.1 Panel XPS 3

Strain measurements across the panel thickness at 7/8 of the panel height are shown in Figure 3-75. Maximum compressive strain occurred along the inner surface of each wythe while the maximum tension strain occurred along the outer surface of each wythe. This profile indicates that each wythe acted independently under flexural stresses. The strain profile due to axial load only and after completion of 1005 lateral load cycles of 5 kips is shown in Figure 3-76 (a) and (b), respectively. The measured profiles suggest that initially the inner wythe experienced compressive strain higher than the outer wythe due to the

applied axial compressive load. This behavior reflects that the inner wythe resisted more axial load than the outer wythe. The slope of the strain profile across each wythe were similar throughout the entire loading regimen. Slope of the strain profile in each wythe increased with an increase the number of cycles. The strain profile indicates that there was two independent neutral axes for each wythe throughout testing. This behavior suggests that the two wythes share the applied lateral load independently. Shift of the neutral axis of the inner wythe suggest that the panel experienced degradation of the partial composite action during the fatigue regimen. Observation of the strain profiles shows that a majority of the axial load was resisted by the inner wythe while the bending moment was resisted by each wythe individually with respect to their individual stiffness, similar to the behavior at mid-height.

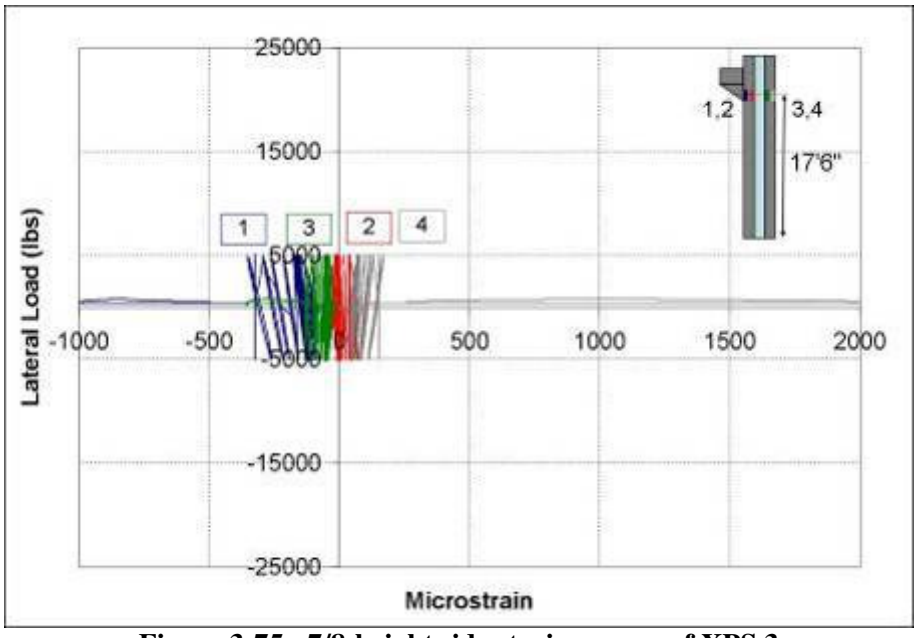

Figure 3-75: 7/8-height side strain gauges of XPS 3

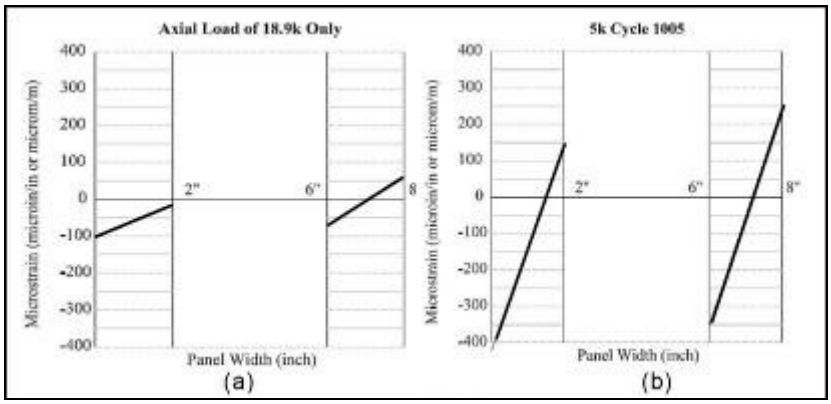

Figure 3-76: 7/8-height side strain profile of XPS 3

3.10.2 Panel XPS 4

Panel XPS 4 exhibited nearly the same behavior as XPS 3. XPS 4, however, sustained the entire loading regimen. Strain measurements across the panel thickness at 7/8 of the panel height are shown in Figure 3-77. Strain profiles for XPS 4 were established immediately after the application of the axial load, ultimate design load cycle and prior to the failure load as shown in Figure 3-78 (a), (b) and (c), respectively. Similar to XPS 3, the strain profile suggest that a majority of the axial load was carried by the inner wythe while the two wythes shared the bending moment due to the eccentricity of the axial load. The strain profile for all the load cases shown in Figure 3-78 indicate clearly that both wythes carried the applied moment due to the applied lateral load and the eccentricity of the axial load independently and a majority of the axial load was carried by the inner wythe. Similar to mid-height behavior, the axial load was resisted by the inner wythe while the bending moment was resisted by each wythe individually.

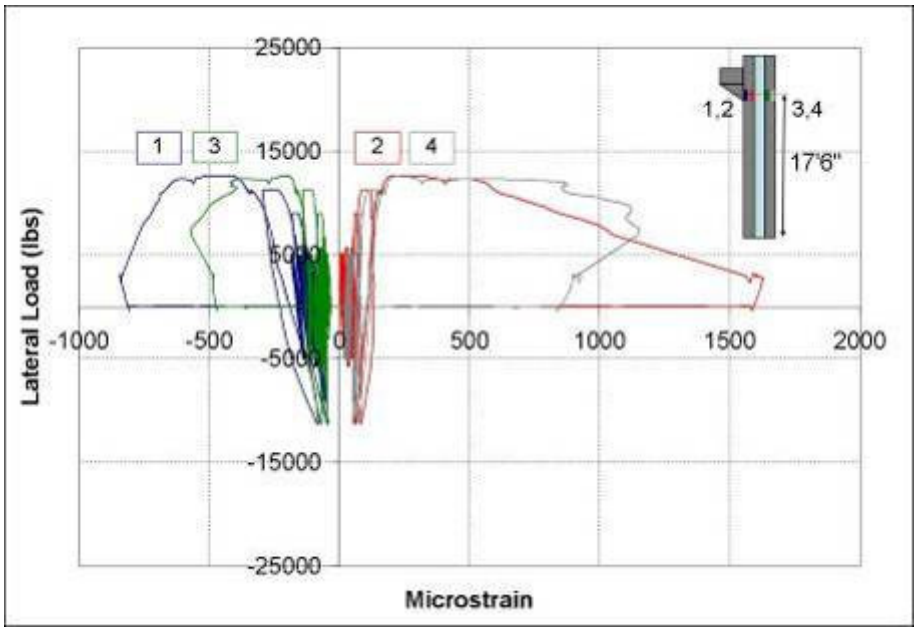

Figure 3-77: 7/8-height side strain gauges of XPS 4

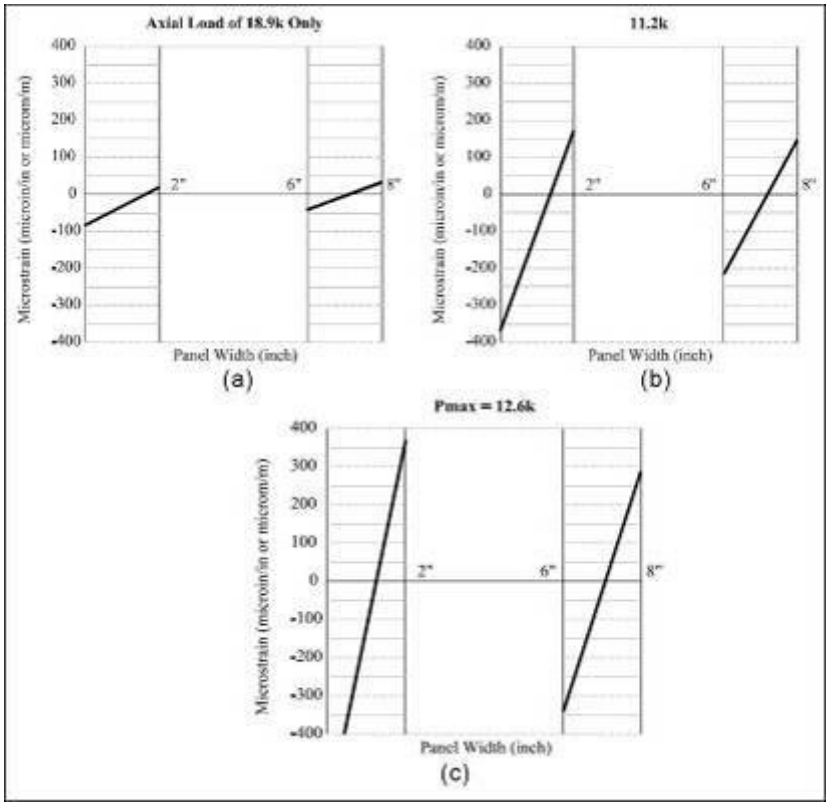

Figure 3-78: 7/8-height side strain profile of XPS 4

3.11 AS-BUILT CONDITIONS

Upon delivery of panels XPS 1 and XPS 2, it was noticed that the foam and the outer wythe were separated by approximately 7/16 inch at various locations as shown in Figure 3-79. It was also noticed that the steel wire mesh of the outer wythe was periodically separated from the concrete and was located between the foam and the inner surface of the outer wythe.

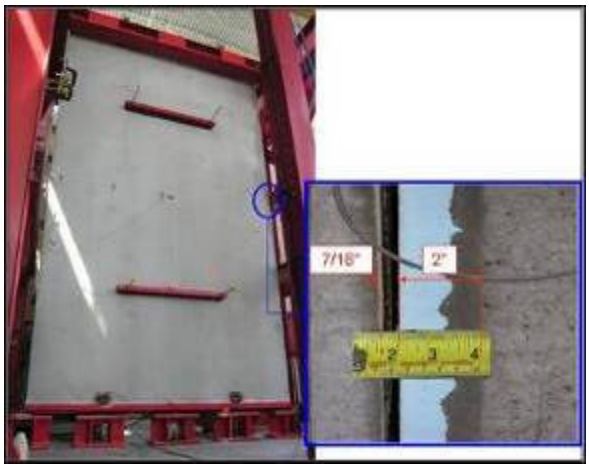

Figure 3-79: Gap between insulation and outer wythe for XPS 1 and XPS 2 panels

3.11.1 Panel XPS 1

After cutting the panel into eight pieces along the width, it was found that there were solid concrete blocks connecting the two concrete wythes around each of the lifting hooks, as shown in Figure 3-80. The solid concrete blocks measured 18 inches by 18 inches. Additional solid blocks 6 inches by 6 inches were found around the four rod locations at the quarter-height along with two 16 inches wide by 24 inches high solid zones at the top lifting hooks. As-built locations of the C-Grid and solid blocks are sketched and compared to design drawings in Figure 3-81 (a) and (b), respectively.

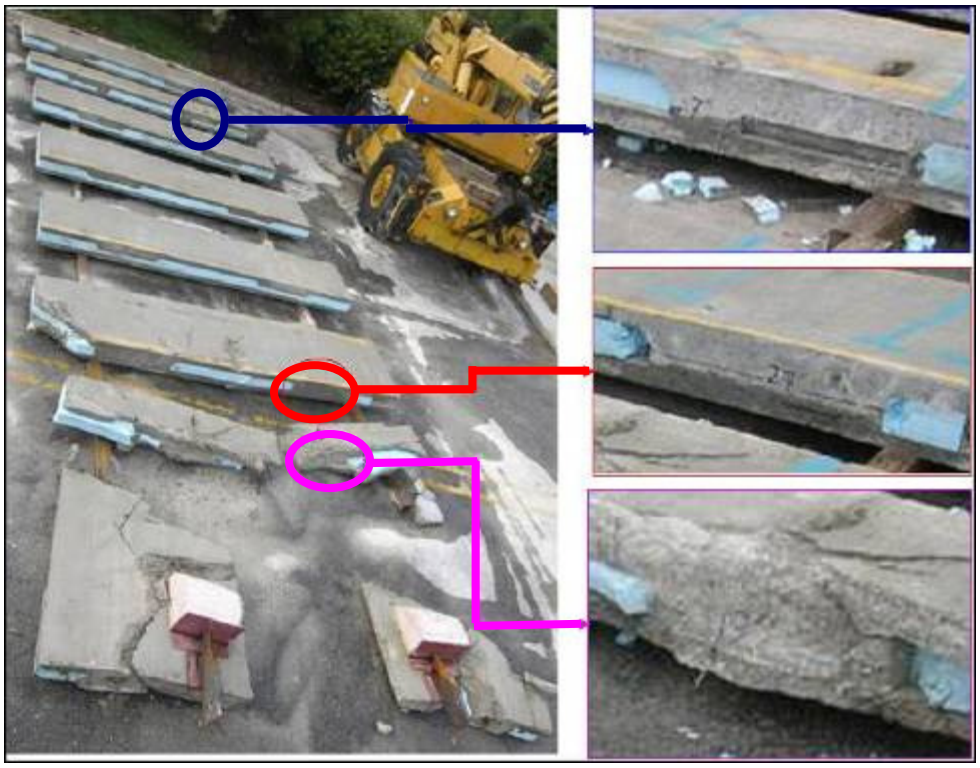

Figure 3-80: Solid zones of panel XPS 1

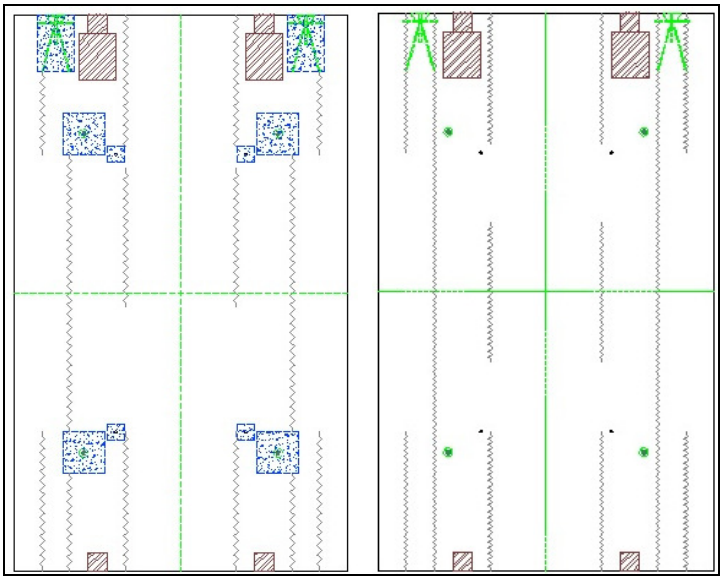

(a) As-built (b) Design

Figure 3-81: Shear grid and solid zone locations for XPS 1

Comparing Figure 3-81 indicate:

1. The two continuous C-GRID stopped 5 feet from the top of the panel. This resulted in the presence of only 4 grids instead of 6 along the top quarter of the panel.

2. The inner C-Grid sections located at the center of the panel height were shifted up by 2 feet.

3.11.2 Panel XPS 2

Following the same procedure, XPS 2 panel was cut into nine pieces as shown in Figure 3-82. By inspection of the panel, two solid concrete zones, 16 inches by 3 inches were located at the top lifting hooks. It was also noted that instead of providing separate grid for the inner center strips, the inner bottom strips were extended as shown in Figure 3-83 (b); therefore, the C-Grid was not centered within the panel as indicated in Figure 3-83 (a).

Figure 3-82: Investigation of panel XPS 2

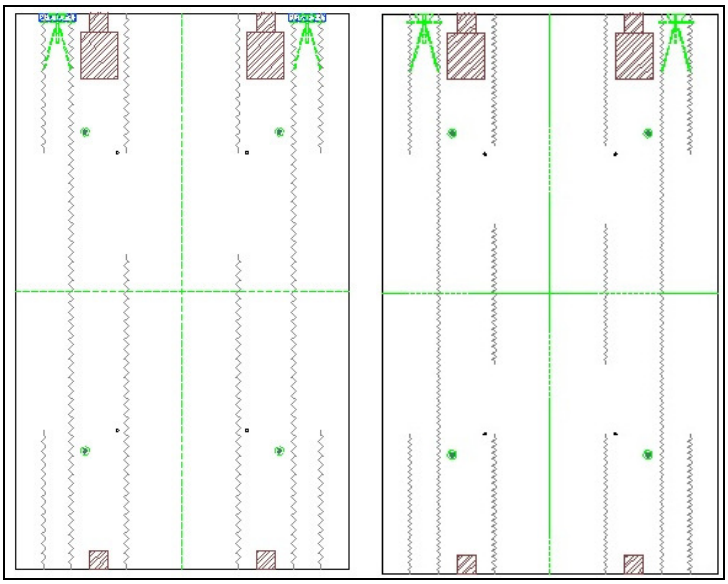

(a) (b)

Figure 3-83: Shear grid and solid zone locations for XPS 2

Bond of the foam to the concrete surface was also inspected. It was noticed that the concrete wythes would easily separate and the foam would pull off by hand as shown in Figure 3-84.

Figure 3-84: Separation of the concrete wythes for XPS 2

Bond of the outer wythe was also considerably less than that of the inner wythe due to the presence of several voids on the concrete surface. The size of the voids ranged between 1/8" to 3" in diameter and approximately 1/4" in depth. It was also noted that the inner wythe surface was very smooth as shown in Figure 3-85 (a) and (b) for the inner surface of the inner and outer wythes respectively.

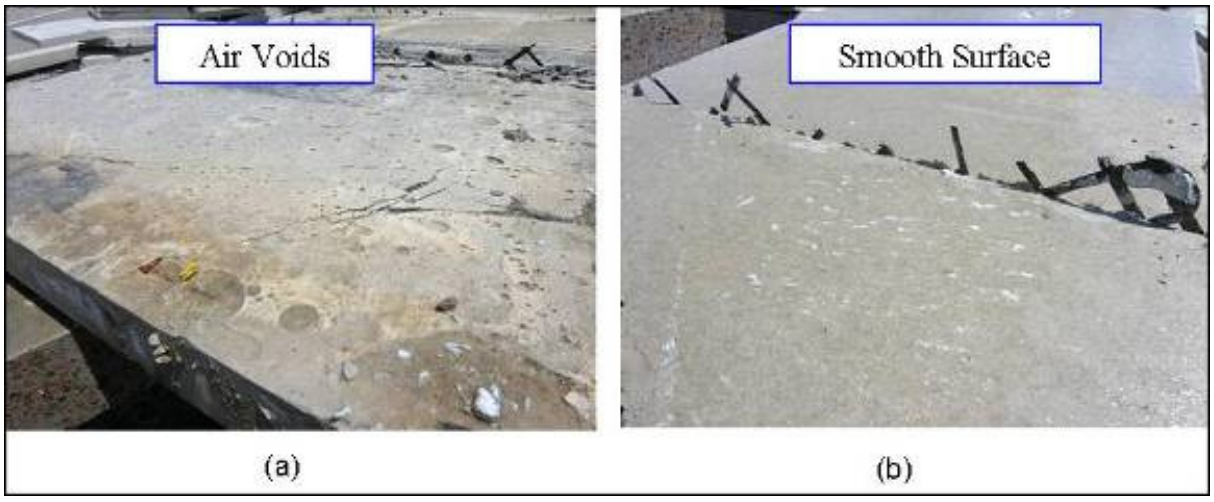

Figure 3-85: Interior surface conditions of XPS 2

4 ANALYSIS AND DISCUSSION

4.1 INTRODUCTION

This chapter deals with the evaluation of the behavior and the degree of composite action achieved for the tested concrete sandwich wall panels. The level of composite action is evaluated under deflection criterion.

The level of composite action is evaluated based on the measured deflections corresponding to the applied compressive axial loads, the first lateral load cycle and after the completion of the entire fatigue cyclic loading condition. The predicted deflection, including the secondary effects due to the applied axial loads, follow the design procedure outlined in the *State-of-the-Art of Precast/Prestressed Sandwich Wall Panels* report published by PCI (1997).

4.2 ANALYTICAL MODEL

The following assumptions are used in the analytical modeling presented in this thesis. The assumptions address the loading condition, cracking of the concrete and performance of the panel core under fully composite and fully non-composite behavior. The assumptions are:

1. The applied axial load is uniformly distributed across the panel width
2. The applied lateral load is uniformly distributed across the panel width
3. The panel does not have initial deflections before applying loads
4. Branson's effective moment of inertia adequately represents the behavior of the panel after cracking
5. Fully composite action implies infinite shear stiffness of the panel core
6. Fully non-composite action implies there is no shear stiffness connecting the two concrete wythes

The objective of the analytical phase is to quantify the percent composite action of the tested panels. The percent composite action can be evaluating using two methods. The first

method compares the experimental value to the fully composite and fully non-composite value. This comparative approach was first introduced by Pessiki and Mlynarczyk (2003) where they compared the elastic moments of inertia. The tested panels conducted by Pessiki and Mlynarczyk (2003) were subjected to lateral forces only, and the panels were not subjected to axial loads; therefore, there is no P-δ effect. In this study, the secondary P-δ effect was added due to the presence of the applied axial compressive load. Determination of the deflection due to secondary effects is an iterative procedure; therefore evaluation of the experimental moment of inertia for a panel subjected to axial loads is a complex process. According to the classical theory for pure bending, the moment of inertia and the associated deflections are proportional. Therefore, it is proposed to evaluate the percent composite action of the tested panels by comparing the measured lateral deflections rather than the moments of inertia.

For the purpose of this thesis, it is proposed to determine the percentage of composite action, κ, based on the measured lateral deflection, Δ_{exp}, the fully non-composite deflection, Δ_{nc}, and the fully composite deflection, Δ_c, using the following equation.

$$\kappa = \frac{\Delta_{\exp} - \Delta_{nc}}{\Delta_c - \Delta_{nc}} \qquad \textbf{Equation 4-1}$$

A graphical representation of Equation 4-1 is shown in Figure 4-1.

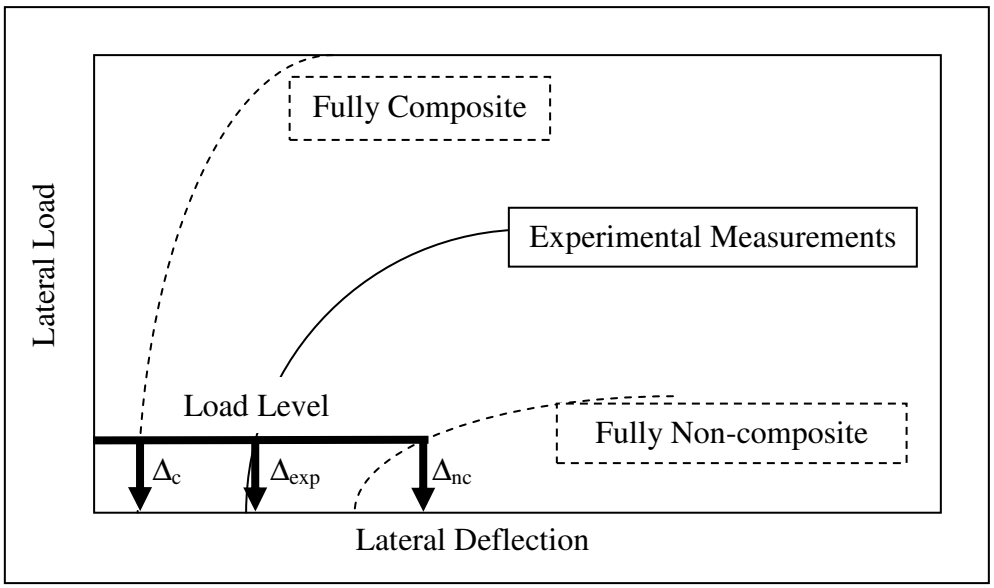

Figure 4-1: Percent composite action

The second method used to evaluate the percent composite action is to compare the measured lateral deflection, Δ_{exp}, to the fully composite deflection, Δ_c, using the following equation.

$$\kappa = \frac{\Delta_{exp}}{\Delta_c} \qquad \textbf{Equation 4-2}$$

Equation 4-2 depicts the magnitude of deflection greater than that of a fully composite behavior. This relationship corresponds to the shearing deformation each panel experienced.

4.3 PERCENT COMPOSITE ACTION BASED ON DEFLECTION CRITERION

In order to develop the percent composite action with respect to deflection criterion, it is required to determine the deflections of the fully composite and fully non-composite behavior under the same loading condition. In this case, the deflection was calculated at mid-height of the panel to match the measured deflections for all tested panels.

The modulus of elasticity of the concrete used for both EPS panels is based on the values provided by the precast company which is half the values estimated by ACI 318-05. The

significant reduction of the modulus is due to the type of gravel used by the producer of the two EPS panels tested in this program. This modulus was verified by laboratory tests conducted by the precaster.

To generalize calculations of the cross-section properties for all tested panels, the geometry of a typical cross-section of the tested panels is shown in general format in Figure 4-2.

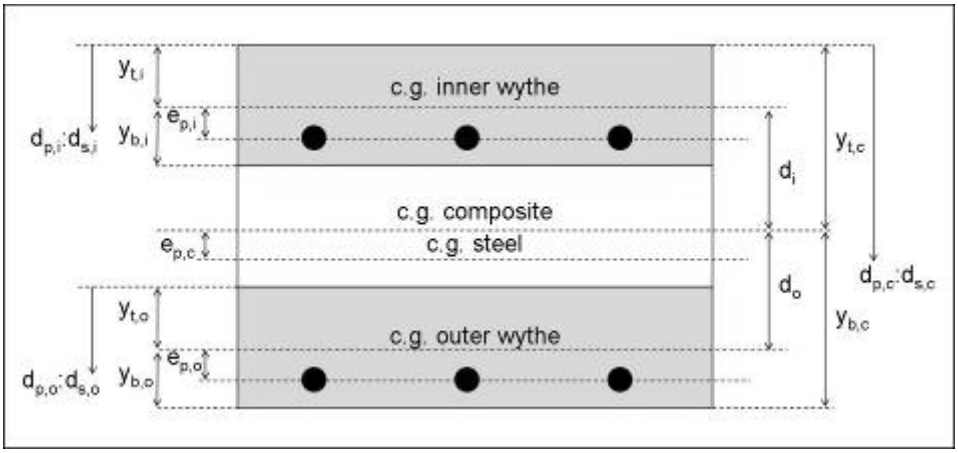

Figure 4-2: Cross-sectional dimensions

The applied gravity and lateral loads are also shown in general format for all panels in Figure 4-3.

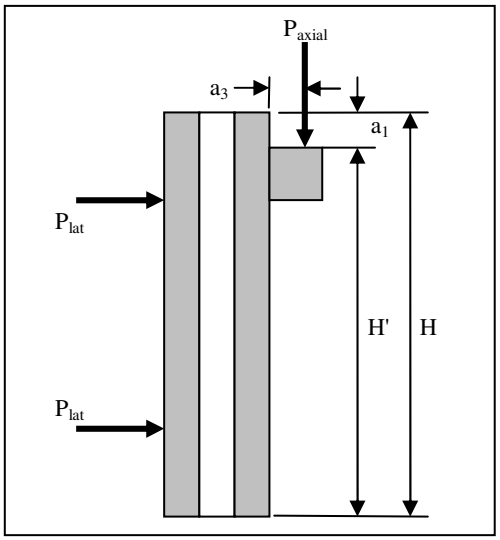

Figure 4-3: Applied load dimensions

4.3.1 Deflections of Fully Composite Behavior

To develop the theoretical deflections for fully composite behavior, load deflection curves were calculated for each panel at lateral load intervals of 1 kip up to a lateral load of 60 kips. Throughout the analysis, an applied axial compressive load of 37.8 kips is assumed to be applied on the corbels which simulates the typical testing sequence. The analysis assumes that the moment due to the eccentric location of the applied axial load is resisted by the entire composite section of the panel. Therefore, the eccentricity will be taken from the elastic centroid of the composite section to the location of the applied axial load. Based on the calculated cracked moment of inertia and the gross moment of inertia, the effective moment of inertia at any given loading condition can be evaluated using Branson's equation as specified in ACI 318-05. It should be noted that the calculation is based on an assumed modulus of rupture of the concrete of $10\sqrt{f_c'}$ as estimated by Losch (2005) and Mehta et. al. (2006), where f_c' is the concrete strength on the day of testing.

The lateral deflections due to the applied moment can be calculated using the effective moment of inertia and the modulus of elasticity either reported by the producer or estimated based on the measured compressive concrete strength on the day of testing. An initial lateral deflection is assumed, then the secondary lateral deflection is evaluated. The lateral deflection is adjusted and the secondary lateral deflection is re-evaluated. This process is repeated until convergence of the total lateral deflection. This process can be repeated for lateral load increments of 1 kip up to a total lateral load of 60 kips.

4.3.2 Deflections of Fully Non-composite Behavior

The non-composite behavior of the panels assumes that both concrete wythes resist the total applied moment due to the lateral loads relative to their individual stiffness. Therefore, the moment resisted by each wythe, M_i or M_o, can be determined as a ratio of the total applied moment, M, relative to the inertia, $I_{nc,i}$ and $I_{nc,o}$ as shown in the following equation.

$$M_i = \frac{I_{nc,i}}{I_{nc}} M$$
$$M_o = \frac{I_{nc,o}}{I_{nc}} M$$

Equation 4-3

Since there is no rigid shear connection between the two concrete wythes, the applied axial load is assumed to be resisted entirely by the inner wythe only. However, the moment due to the eccentricity of the applied axial load, measured from the axial load to the elastic centroid of the inner wythe, will be carried by the two wythes relative to their moment of inertia.

After distribution of the applied moment, the cracking moment and effective moment of inertia can be evaluated for each wythe. The non-composite effective moment of inertia is then extracted by summing the effective moment of inertia of each individual wythe. The lateral deflections and secondary P-δ deflections can then be evaluated in a similar fashion to fully composite behavior.

Each load level requires reevaluation of the moment distribution between the wythes, the effective moment of inertia and the lateral deflections. A load deflection curve was created by following this procedure at every 1 kip lateral load interval to a total lateral load of 60 kips.

A summary of the analytical procedures is described in detail in APPENDIX B.

4.3.3 Results

Several factors have a significant effect on the fully composite and fully non-composite load deflection curves. The concrete strength has a significant effect on both the fully composite and fully non-composite behavior. As shown in Figure 4-4, panel XPS 1 exhibited a noticeably higher cracking strength in comparison to panels XPS 3 and 4 due to its higher concrete strength. Panels EPS 1 and EPS 2 show that the modulus of elasticity has a significant effect on both the composite and non-composite behavior. Increasing the panel configuration from a 4-2-2 to a 2-4-2, similar to panel XPS 2 in comparison to panel XPS 3, significantly increases the non-composite stiffness but does not greatly affect the composite stiffness as shown in Figure 4-4.

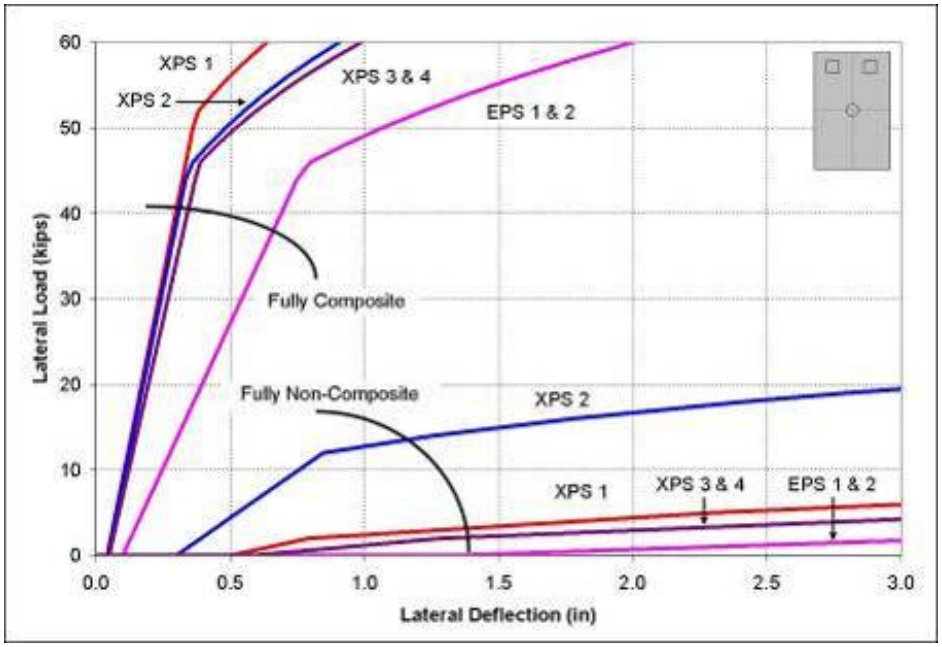

Figure 4-4: Theoretical boundary curves

Characteristics of the tested panels can be defined by comparing the measured behavior to their appropriate theoretical limits. The first lateral load cycle and failure load cycle were

compared to the theoretical boundaries for each panel. Both EPS panels exhibited similar load deflection behavior resulting in similar composite action characteristics. Both panels exhibited an initial stiffness and axial load deflection similar to that of a fully composite panel as shown by the 5 kip lateral load cycle in Figure 4-5. Panel EPS 2 exhibited an initial deflection less than that of the fully composite behavior. Throughout the fatigue regimen, significant deflection degradation was observed for both EPS panels while the elastic stiffness remained similar throughout testing. The fully non-composite deflections were large in magnitude and significantly greater at service load than the scale provided in Figure 4-5. Non-composite deflections are very large due to the large secondary deflections each wythe experiences under the effect of the axial load.

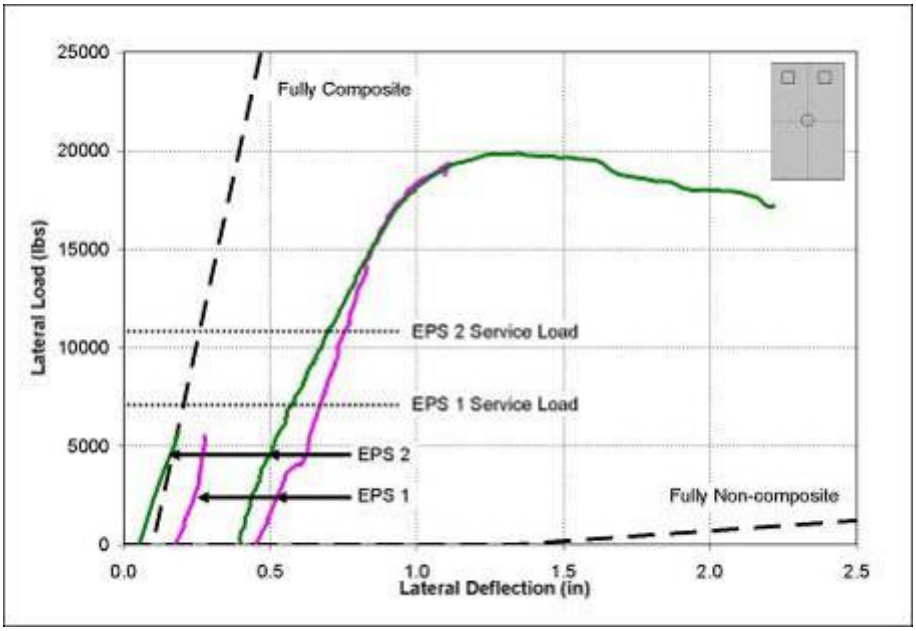

Figure 4-5: Experimental EPS failure cycle

Panel XPS 1 exhibited a highly composite behavior before and after the fatigue regimen as shown in Figure 4-6. Both the deflection and stiffness was similar to the fully composite behavior and minimal degradation was observed throughout testing.

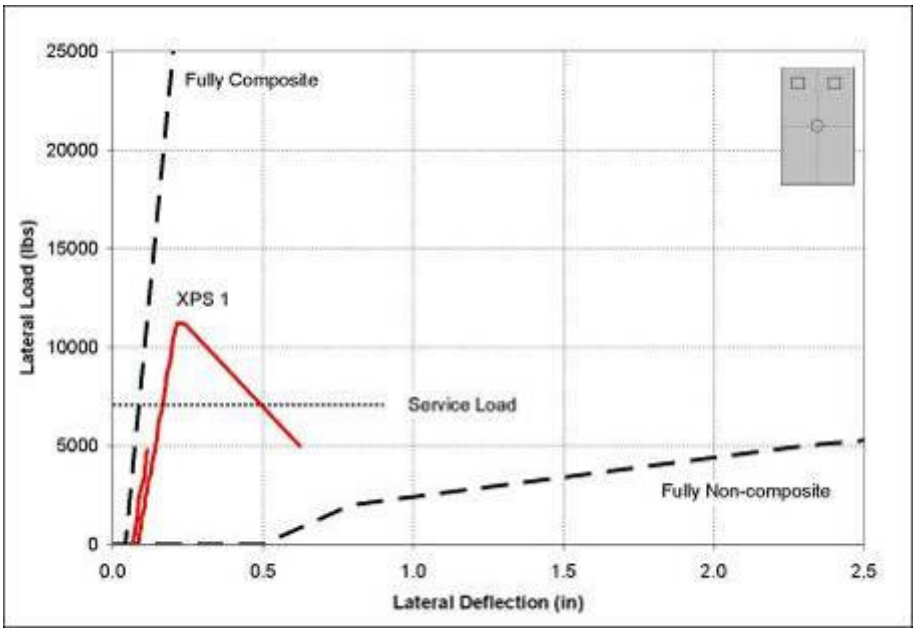

Figure 4-6: Experimental XPS 1 failure cycle

Panel XPS 2 exhibited significantly reduced stiffness in comparison to panel XPS 1 despite the additional concrete area. Initially, the deflection due to the gravity loads was closer to composite than non-composite behavior; however, at the end of the fatigue regimen, the experimental deflection measurements were significantly closer to fully non-composite than fully composite behavior. Deflection due to the applied axial load prior to failure was considerably higher, but diverged with an increase in lateral load. The experimental cracking load occurred at approximately 15 kips which was similar in magnitude to the fully non-composite cracking load of the inner wythe which occurred at approximately 12 kips as shown in Figure 4-7.

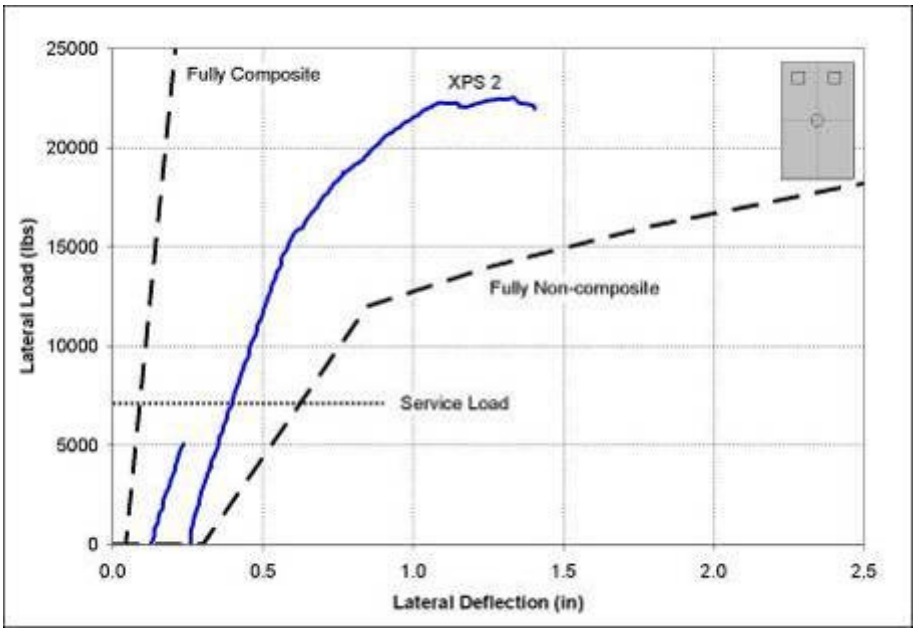

Figure 4-7: Experimental XPS 2 failure cycle

The only difference between XPS 3 and XPS 4 is the amount of the C-GRID used, and both panels have similar fully composite and fully non-composite predictions. Panel XPS 4 exhibited stiffness considerably larger than fully non-composite behavior; however, it is slightly less than that of a fully composite behavior as shown in Figure 4-8. Lateral deflections due to the eccentrically applied axial load experienced significant degradation throughout the fatigue regimen. Panel XPS 3 exhibited significantly more deflection degradation than panel XPS 4. Initially, the deflection due to axial load was approximately half way between that of fully composite and fully non-composite behavior. Deflections due to the applied axial load experienced significant degradation throughout the subsequent fatigue cycles. Lateral deflection due to the eccentrically applied axial load prior to failure was greater than that predicted for non-composite behavior indicating significant reduction in the percent composite action. XPS 3 experienced softening throughout the lateral load fatigue cycles but still remained substantially stiffer than fully non-composite behavior.

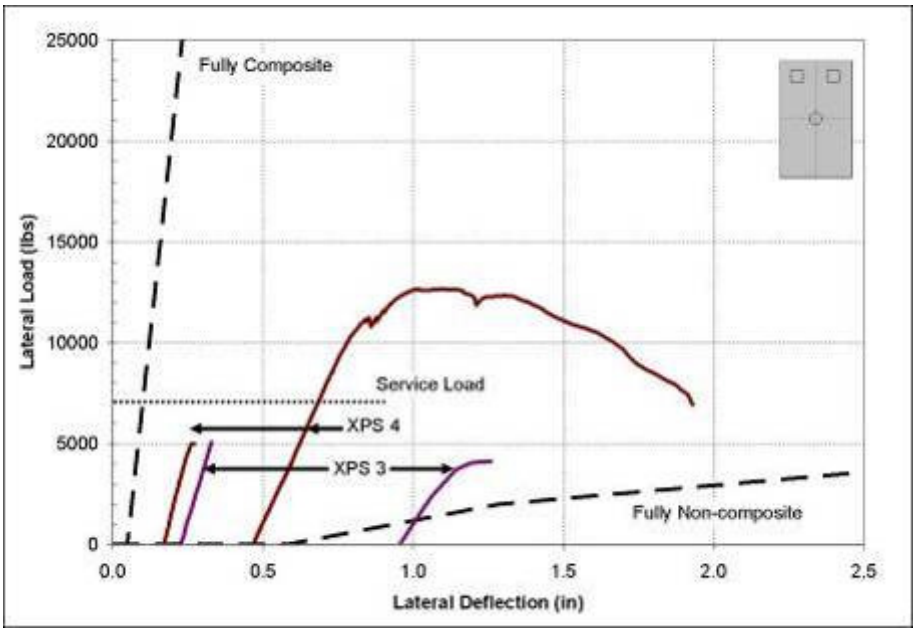

Figure 4-8: Experimental XPS 3 and 4 failure cycle

The percent composite action can be evaluated by two methods. The first method compares the experimental behavior to both the fully composite and fully non-composite behavior. The percent composite action is evaluated at the application of the applied axial load, the first 5 kip lateral load cycle with applied factored gravity loads and service load condition. These results are summarized in Table 4-1.

Table 4-1: Percent composite action associated with each tested panel

Panel	Percent Composite Action at Axial Load	Percent Composite Action at 1st 5k Cycle	Percent Composite Action at Service Load
EPS 1	100%	99%	98%
EPS 2	100%	100%	99%
XPS 1	95%	98%	98%
XPS 2	62%	64%	39%
XPS 3	78%	94%	N/A
XPS 4	83%	95%	90%

The second method compares the experimental behavior to only the fully composite behavior. The values in Table 4-2 represent the magnitude of the experimental deflection

with respect to the fully composite deflections at the respective load levels. For example, a 2.0 composite action indicates that the experimental deflection was twice that of the fully composite deflection. These comparisons are given in Table 4-2.

Table 4-2: Experimental deflections with respect to fully composite deflections

Panel	Experimental/Composite Deflection at Axial Load	Experimental/Composite Deflection at 1st 5k Cycle	Experimental/Composite Deflection at Service Load
EPS 1	1.01	1.48	3.14
EPS 2	0.64	1.06	2.79
XPS 1	1.57	1.52	1.92
XPS 2	3.29	3.12	4.57
XPS 3	3.42	3.69	N/A
XPS 4	2.84	3.05	6.72

A detailed summary of all analytical calculations are shown in APPENDIX C.

4.4 ANALYSIS OF THE TEST RESULTS

Comparing the analytical results to experimental values indicates that a panel containing an EPS foam core exhibits superior percent composite action than an unprepared XPS foam panel with the same configuration and C-GRID layout. The enhanced behavior of an EPS panel in comparison to an XPS panel is attributed to the increased bond strength between the foam and the concrete, as exhibited by panel EPS 1 and EPS 2 in comparison to XPS 3.

The percent composite action can also be significantly enhanced by providing solid concrete zones between the concrete wythes to resist shear as shown with panel XPS 1. Alternatively, providing additional C-GRID increases the percent composite action and overall panel behavior as shown by panel XPS 4 in comparison to panel XPS 3. Providing additional C-GRID is not as structurally efficient as providing solid concrete zones as demonstrated by panel XPS 4 in comparison to panel XPS 1. Another optimization technique includes increasing the wythe thickness. By providing a 4-2-2 panel configuration

in comparison to a 2-4-2 panel configuration, the percent composite action can be significantly increased as demonstrated by panel XPS 2 in comparison to panel XPS 3.

4.5 DESIGN PROCEDURES

A design approach is proposed detailing the selection of longitudinal steel and shear transfer reinforcement for a given panel geometry, foam core and shear transfer mechanism. Design of precast concrete sandwich panels can be performed as follows:

1. Conduct a structural analysis to determine the applied loads.
2. Determine the panel configuration, wythe and core thicknesses, type of foam and the type of shear transfer mechanisms. These characteristics may be iterated to determine optimum design. Note that the panel slenderness should not exceed 200 as specified by ACI 533.
3. Determine if panel is to be designed as fully composite or fully non-composite during service. This behavior will be used throughout the design procedures.
4. Calculate the composite or non-composite section properties shown in Figure 4-9 and Figure 4-10.
5. Determine composite or non-composite panel deflection due to service loads at the panel height of maximum moment. Lateral deflections are to include initial bows as specified by ACI 533. Slenderness effects are to be included as specified by ACI 318-05 section 14.8 or another second order analysis.

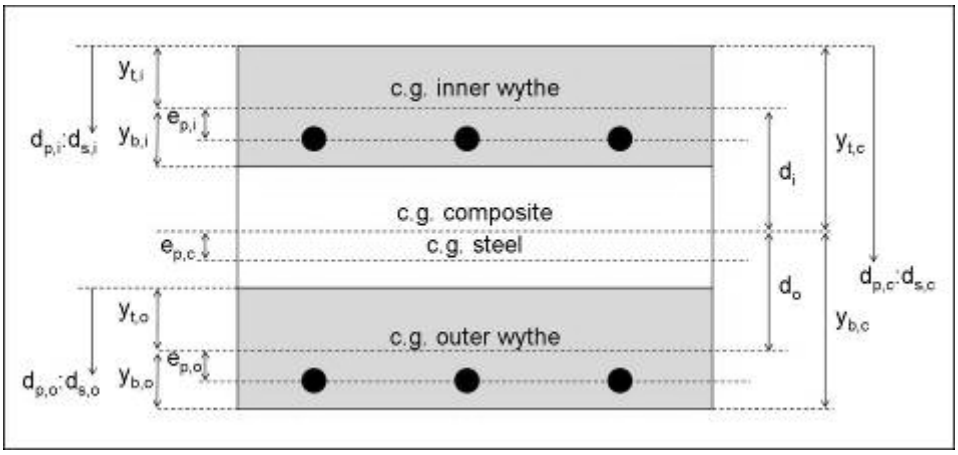

Figure 4-9: Cross-section parameters

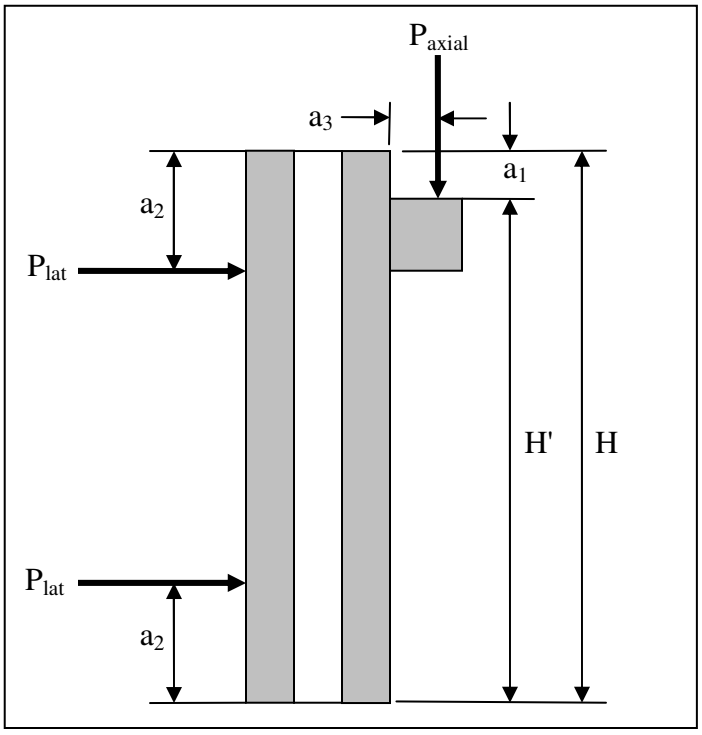

Figure 4-10: Loading parameters

6. Evaluate the critical moments and shears due to the applied loads including eccentricity effects as specified by ACI 318-05 section 14.8.3. Maximum moments due to stripping, handling and erecting should also be considered.
7. Design flexural reinforcement for fully composite or fully non-composite behavior in accordance to ACI 318-05 and PCI Design Handbook. If the panel is load bearing,

then an interaction diagram will be necessary for design. If stripping or handling controls the design, than the tension should not be greater than $5\sqrt{f_{c,28}'}$. If erection controls the design, than the tension rupture should not be greater than $5\sqrt{f_{ci}'}$. Prestressing should be equal between the two wythes.

8. Ensure minimum reinforcement requirements are met in accordance to ACI 318-05 section 18.11.1.
9. Calculate service load lateral deflections for fully composite or fully non-composite at the expected height of maximum deflection including shear deformation. Lateral deflections are to include initial bows as specified by ACI 533. Slenderness effects are to be included as specified by ACI 318-05 section 14.8 or another second order analysis. Lateral deflections should satisfy deflection limits specified by ACI 533 Table 2.5.2.
10. Design the shear transfer mechanism to sustain ultimate panel shears. Shear flow capacities of the shear transfer mechanism have to exceed the shear flows induced due to the applied loads. Shear flow capacities of the shear transfer mechanism have to be provided by the shear transfer mechanism supplier or structural tests must be performed to develop these values.

5 SUMMARY AND CONCLUSIONS

5.1 SUMMARY

Precast prestressed concrete insulated sandwich wall panels are typically used for the construction of building envelopes. Wall panels consist of two outer layers of concrete separated by a layer of foam insulation. Panels can serve to carry gravity loads from floors or roofs, to resist normal or transverse lateral loads caused by wind, to insulate a structure and to provide interior and exterior finished wall surfaces.

Recently, there is an attempt to utilize a carbon-fiber shear connection grid to join the two concrete wythes in order to achieve the structural efficiency of the panel while avoiding the thermal bridges created by traditional means of shear transfer. Connecting concrete wythes with carbon grid, which has a very low thermal conductivity, allows a panel to develop composite structural action without developing thermal bridges, thus maintaining the insulating value of the panel.

To quantify the structural behavior of concrete sandwich panels reinforced with C-GRID, six precast prestressed concrete sandwich wall panels were tested using four different parameters believed to affect the structural behavior. The testing variables included solid concrete zones through the foam core, different shear reinforcement ratios using C-GRID, wythe thicknesses and type of foam core material. Five of the tested panels were a 2-4-2 configuration with two internal pilasters. Two panels used expanded polystyrene (EPS) foam and three panels used expanded polystyrene (XPS) foam. One panel had a 4-2-2 confirmation and XPS foam. Five panels were reinforced with 90 linear feet of C-GRID as a shear transfer mechanism in comparison with the exception of one panel reinforced 120

linear feet of C-GRID. One panel also contained several solid concrete zones as an additional shear transfer mechanism. Each panel consisted of two outer layers of prestressed concrete, with a welded wire mesh centered in each wythe.

Panels were tested in a vertical position between two steel frames that allowed the simultaneous application of gravity and lateral loads. Vertical loads were applied to simulate the effects of a double-tee roof deck and associated live load. Reverse cyclical lateral loads were applied to simulate the effects of a 120 MPH or 150 MPH wind over a 50 year service life. Following the fatigue regimen, panels were laterally loaded up to failure.

Evaluation of experimental data indicates that the foam core has a significant impact on the composite action. Panels with EPS foam exhibited the highest failure lateral loads of all 2-4-2 panel configurations. The EPS panels in comparison to the XPS panels had a rougher foam surface and enhanced bond behavior that significantly improves the composite behavior. An XPS foam core panel with a 4-2-2 configuration exhibited a higher failure load than the EPS panels; however, this was contributed to the increased wythe thicknesses of the 4-2-2 configuration.

An XPS foam core panel with solid concrete zones connecting the concrete wythes exhibited the highest panel stiffness while an XPS foam core panel with a 2-4-2 configuration and the same shear reinforcement ratio as used in the EPS panels exhibited the lowest panel stiffness. The XPS foam core panel with a 2-4-2 configuration with the same shear reinforcement ratio as the EPS panels exhibited insufficient shear grid to sustain the proposed loading sequence. An increase in panel stiffness was observed by increasing the shear reinforcement; however, the stiffness was lower than elements with solid concrete

zones. This comparison confirms that the shear transfer mechanism greatly affects the panel core stiffness, thus influencing the overall panel stiffness for a given panel configuration. Increasing the panel configuration from a 2-4-2 to a 4-2-2 increases the panel stiffness due to a higher moment of inertia.

An analytical analysis was performed by comparing the experimentally measured lateral deflections at mid-height of the panel to fully composite and fully non-composite lateral deflections. Analytical comparisons indicated that both EPS panels exhibited 100% composite action with respect to lateral deflections. XPS panels with the same panel configuration and C-GRID failed prior to reaching service load. The percent composite action with respect to service deflections increased to nearly 40% by increasing the panel configuration from a 2-4-2 to a 4-2-2. Increasing the C-GRID quantity from 90 linear feet to 120 linear feet for a 2-4-2 XPS panel increased the percent composite action with respect to service deflection to approximately 90%. Providing solid concrete zones resulted in the highest structurally efficient XPS panel exhibiting a 98% composite action.

5.2 CONCULSIONS

Several conclusions were developed based on experimental observation and analytical comparisons.

1. EPS foam exhibits improved bond characteristics in comparison XPS foam due to the rougher surface texture of EPS foam

2. Panels with EPS foam cores require less C-GRID than XPS foam core panels due to their enhanced bond strength of EPS foam

3. EPS foam core panels exhibited enhanced behavior with respect to strength, deflection and percent composite action in comparison to XPS foam core panels

4. A 4-2-2 panel configuration exhibited increased flexural capacity and percent composite action in comparison to a 2-4-2 panel configuration with the same foam core and shear resistance

5. Panel degradation decreases with higher shear transfer resistance

6. Insufficient shear transfer resistance results in low percent composite action and a premature flexural failure due to C-GRID rupture

7. Increased shear transfer resistance results in stiffer panel behavior and reduced panel degradation

5.3 RECOMMENDATIONS

Several recommendations were introduced.

1. Develop degradation factor of C-GRID through fatigue cycles

2. Develop concrete modulus of elasticity relationship in comparison to number of fatigue cycles

3. Develop the strength to C-GRID reinforcement ratio relationship

4. Investigate the failure mode to corbel location relationship

6 BIBLIOGRAPHY

"2030 Cement Consumption to Reach 183 Million Annual Metric Tons." GoStructural. 03 Mar. 2008. 28 Mar. 2008 <http://www.gostructural.com/article.asp?id=2691>.

"C-GRID Specifications" Altus Group. 2006. 3 July 2008 <http://www.altusprecast.com/components/content_manager_v03/view_web_site/htdocs/menu_ps.asp?NodeId=-1135603282&Group_ID=1137682951&Parent_ID=-1>.

"Plastic Foams for Concrete Homes." PCA. 2008. 18 Mar. 2008 <http://www.cement.org/homes/brief04.asp>.

ACI Committee 318. Building Code Requirements for Structural Concrete (ACI 318-05). Farmington Hills, MI: American Concrete Institute, 2005.

ACI Concrete Institute 533. Guide for Precast Concrete Wall Panels (ACI 533-93). Farmington Hills, MI: American Concrete Institute, 2004.

American Society of Civil Engineers (ASCE). Minimal Design Loads for Buildings and Other Structures (SEI/ASCE 7-02). Reston, VA: ASCE, 2003.

ASTM C579, ASTM C579-07: Standard Specification fro Rigid, Cellular Polystyrene Thermal Insulation. *Annual Book of ASTM Standards*, American Society of Testing and Materials, West Conshohocken, PA, 2007.

Benayoune, A, A A. Abdule Samad, D N. Trikha, A A. Abang Ali, and S.H.M. Ellinna. "Flexural Behaviour of Pre-Cast Concrete Sandwich Composite Panel - Experimental and Theoretical Investigations." Elsevier 22 (2008): 580-592.

Bush, T.D., and G.L. Stine. "Flexural Behavior of Composite Prestressed Sandwich Panels." PCI JOURNAL 39.2 (1994): 112-121.

Christian, J, and J Kosny. "Home Energy." Home Energy Magazine Online November/December 1999. 26 Feb. 2008. <http://www.homeenergy.org/archive/hem.dis.anl.gov/eehem/99/991110.html>.

Dow Chemical Company. "EPS Claims Crumble When Truth is Exposed." Advertisement. 18 Mar. 2008. <http://www.dow.com/PublishedLiterature/dh_0067/0901b803800675f2.pdf?filepath=/PublishToInternet/InternetDOWCOM/styrofoam/pdfs/noreg/179-06147&fromPage=BasicSearch>.

Gleich, H. "New Carbon Fiber Reinforcement Advances Sandwich Wall Panels." STRUCTURE Magazine April (2007): 61-63.

Hau, E. Wind Turbines: Fundamental, Technologies, Application, Economics. New York: Springer-Verlag Berlin Heidelberg, 2000. 455-458.

Hibbeler, R.C. Mechanics of Materials. 5th ed. New Jersey: Prentice Hall, 2003.

Horvath, J S. "Expanded Polystyrene (EPS) Geofoam: an Introduction to Material Behavior." Geotextiles and Geomembranes 13 (1994): 263-280.

Lee, Byoung-Jun, and Stephen Pessiki. "Design and Analysis of Precast, Prestressed Concrete Three-Wythe Sandwich Wall Panels." PCI JOURNAL 52.4 (2007): 70-83.

Lee, Byoung-Jun, and Stephen Pessiki. "Experimental Evaluation of Precast, Prestressed Concrete, Three-Wythe Sandwich Wall Panels." PCI JOURNAL 53 (2008): 95-115.

Losch, Edward. "Precast/Prestressed Concrete Sandwich Walls." STRUCTURE Magazine April (2005): 16-20.

Manwell, J F., J G. McGowan, and A L. Rogers. Wind Energy Explained: Theory, Design, and Application. John Wiley and Sons, 2002. 56-60.

Mehta, P. Kumar, and Paulo J. M. Monteiro. Concrete: Microstructure, Properties, and Materials. 3rd ed. New York: McGraw-Hill, 1993.

PCI Committee On Precast Sandwich Wall Panels. "State-of-the-Art of Precast/Prestressed Sandwich Wall Panels." PCI JOURNAL 42.2 (1997): 3-61.

PCI Committee On Precast Sandwich Wall Panels. "State-of-the-Art of Precast/Prestressed Sandwich Wall Panels." PCI JOURNAL 42.3 (1997): 3-61.

Pessiki, Stephen, and Alexandar Mlynarczyk. "Experimental Evaluation of Composite Behavior of Precast Concrete Sandwich Wall Panels." PCI JOURNAL: 48.2 (2003).

Precast/Prestressed Concrete Institute. PCI Industry Handbook. 6th ed. Chicago: 2004.

Salmon, David C., Amin Einea, Maher K. Tadros, and Todd D. Culp. "Full Scale Testing of Precast Concrete Sandwich Panels." ACI STRUCTURAL JOURNAL 94.4 (1997): 354-362.

Xu, Y L. "Determination of Wind-Induced Fatigue Loading on Roof Cladding." Journal of Engineering Mechanics 121.9 (1995): 956-963.

7 APPENDIX A

DETAILED TEST DATA

7.1 LATERAL DEFLECTIONS

7.1.1 Panel EPS 1

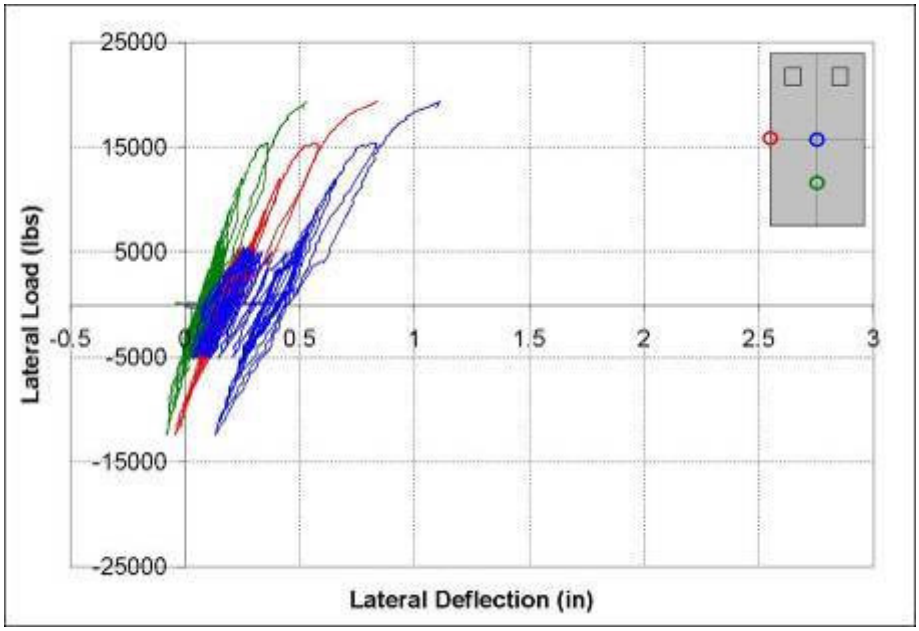

Figure 7-1: Lateral displacements of EPS 1

7.1.2 Panel EPS 2

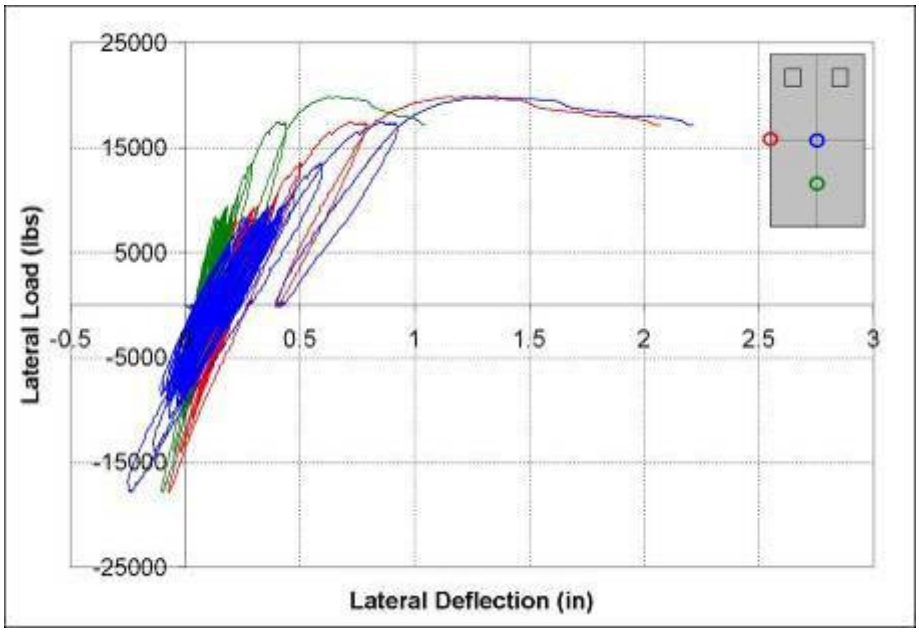

Figure 7-2: Lateral displacement of EPS 2

7.1.3 Panel XPS 1

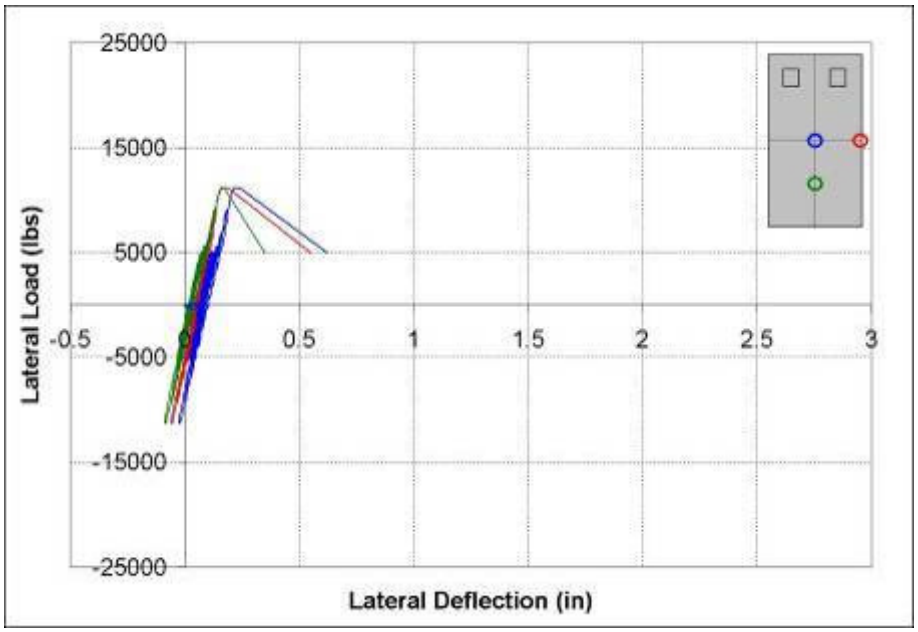

Figure 7-3: Lateral displacements of XPS 1

7.1.4 Panel XPS 2

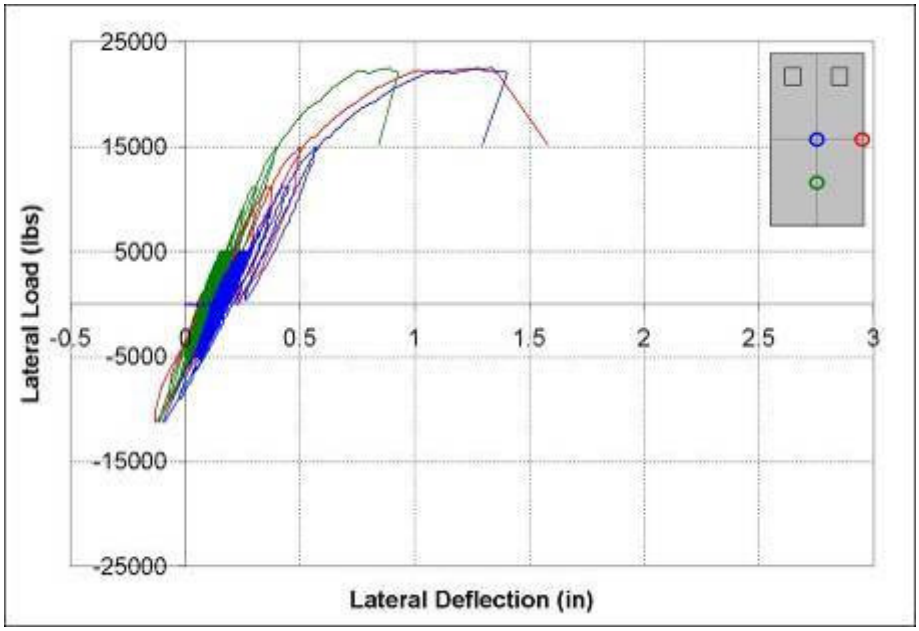

Figure 7-4: Lateral displacement of XPS 2

7.1.5 Panel XPS 3

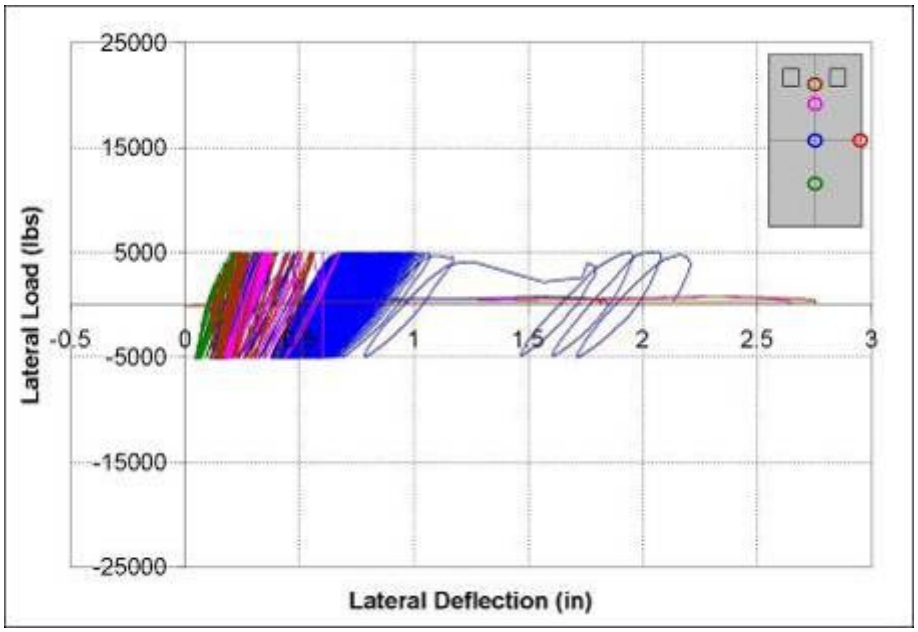

Figure 7-5: Lateral displacement of XPS 3

7.1.6 Panel XPS 4

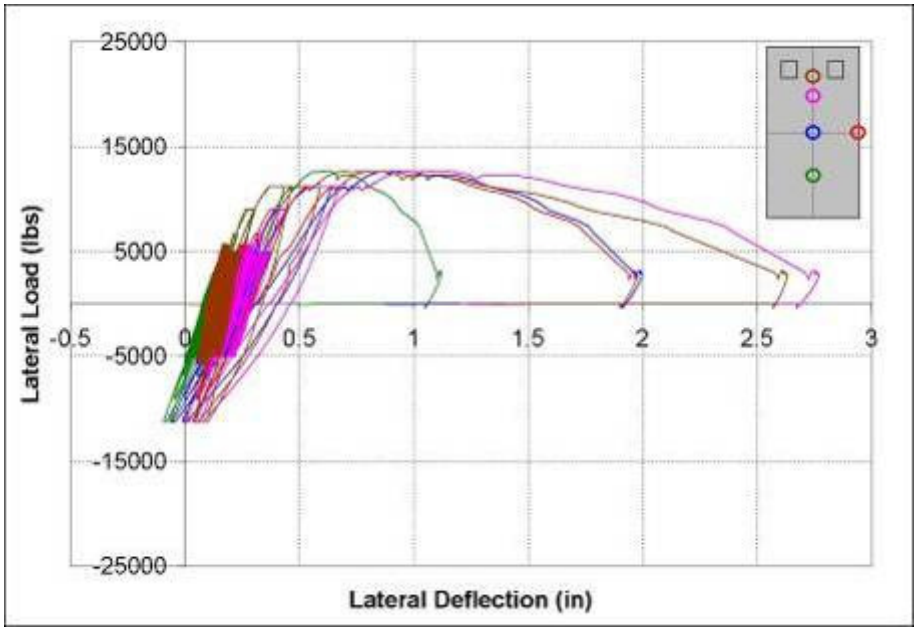

Figure 7-6: Lateral displacement of XPS 4

7.2 PANEL SIDE STRAIN MEASUREMENTS AT QUARTER-HEIGHT

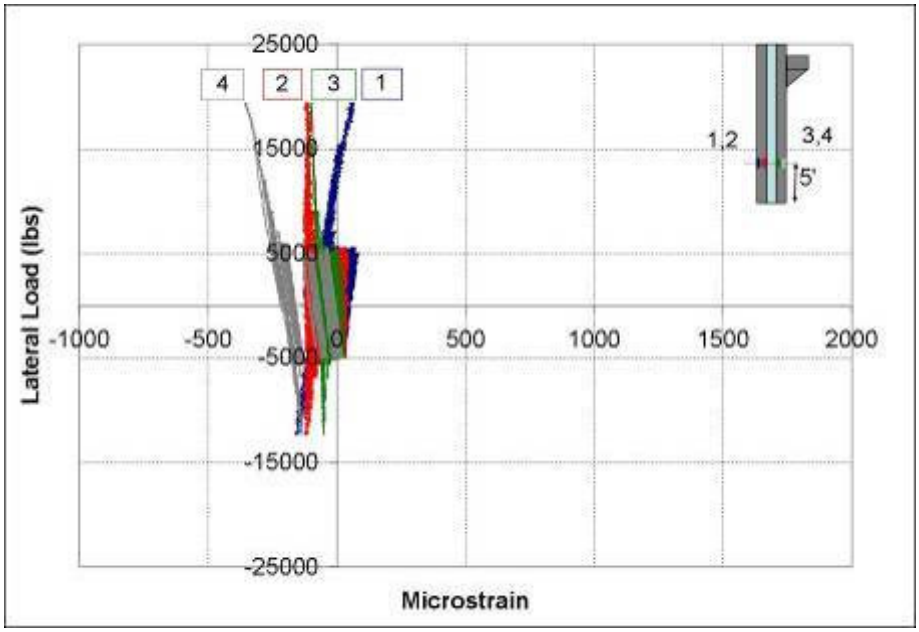

Figure 7-7: Quarter-height side strain gauges of EPS 1

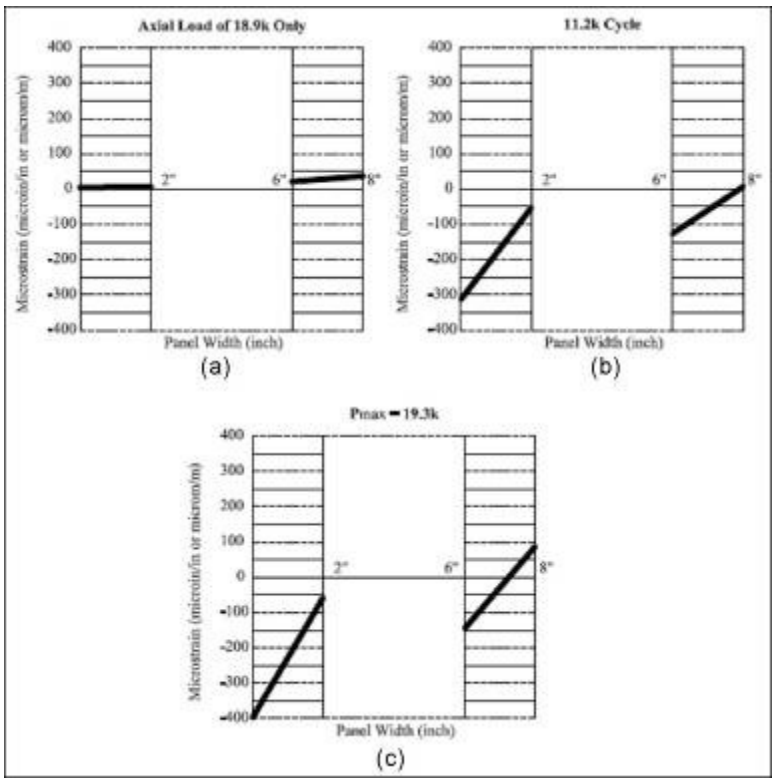

Figure 7-8: Quarter-height side strain profile of EPS 1
(a) Axial load only (b) Ultimate load (c) Failure load

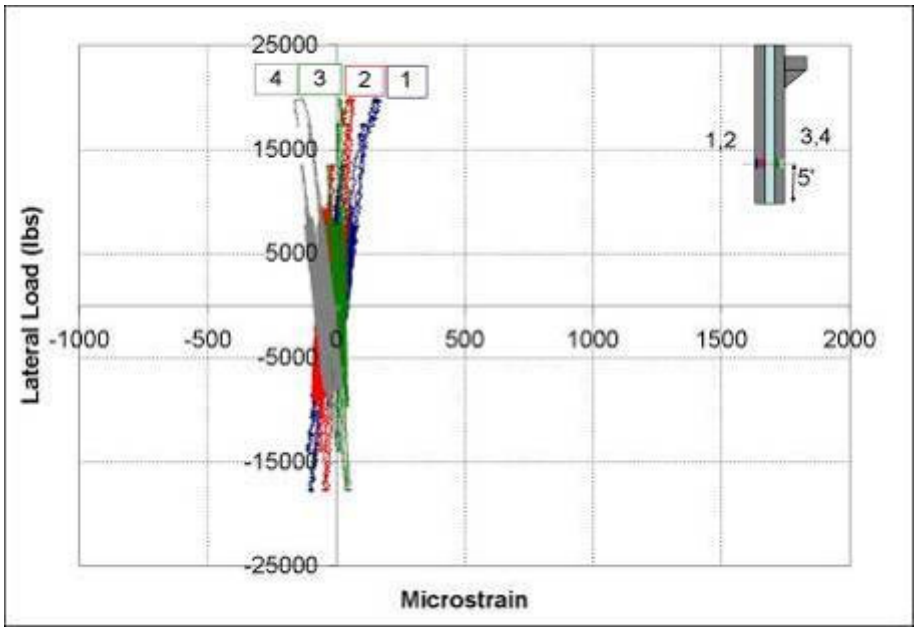

Figure 7-9: Quarter-height side strain gauges of EPS 2

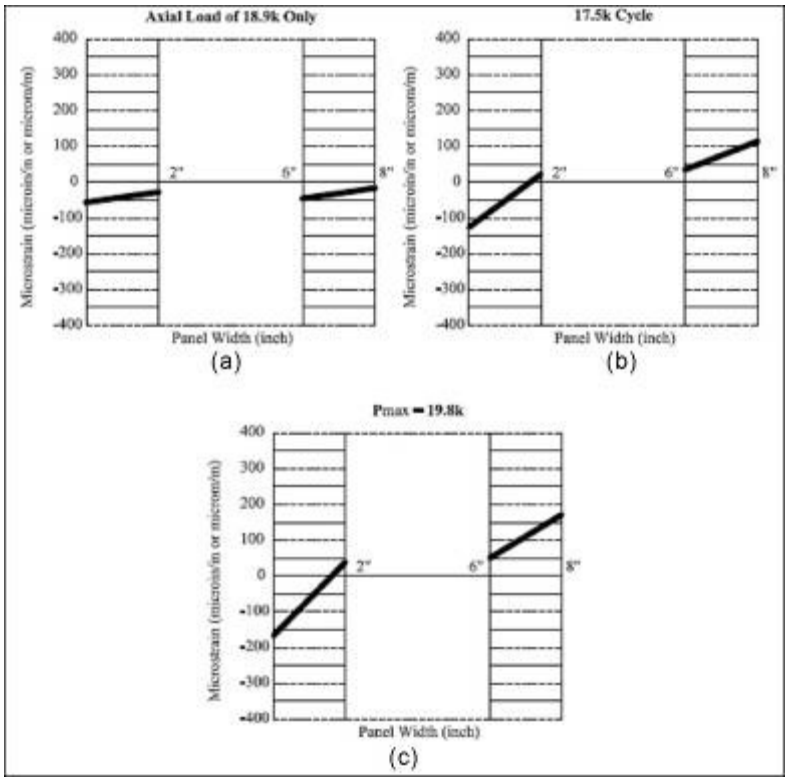

Figure 7-10: Quarter-height side strain profile of EPS 2
(a) Axial load only (b) Ultimate load (c) Failure load

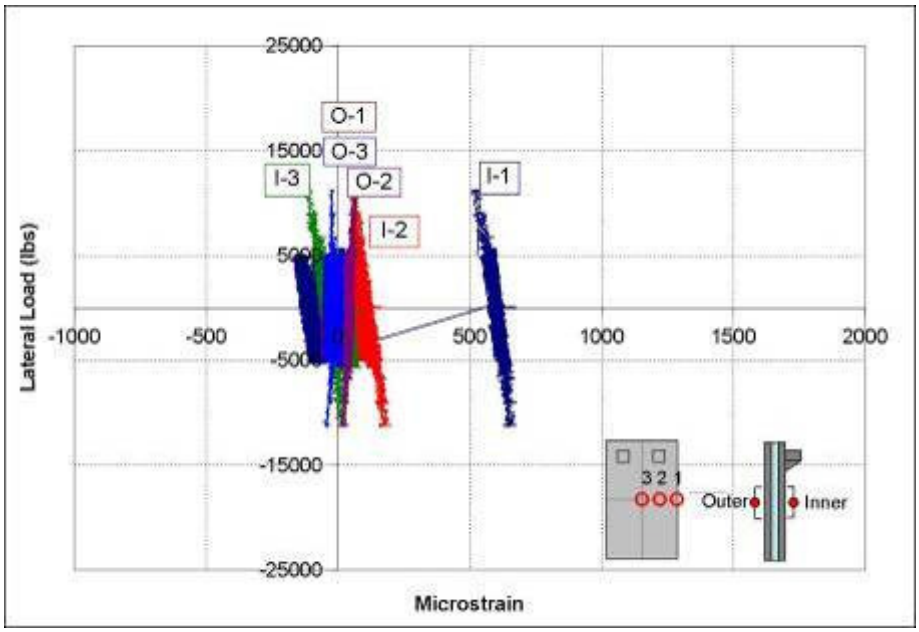

Figure 7-11: Quarter-height side strain gauges of XPS 1

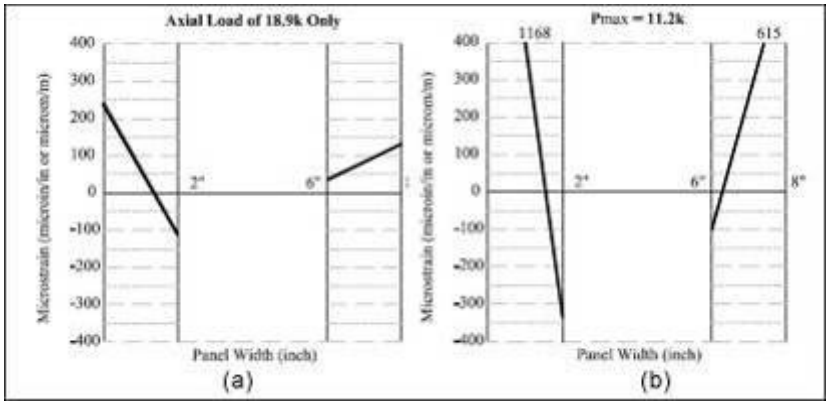

Figure 7-12: Quarter-height side strain gauges of XPS 1
(a)Axial load only (b) Ultimate and failure load

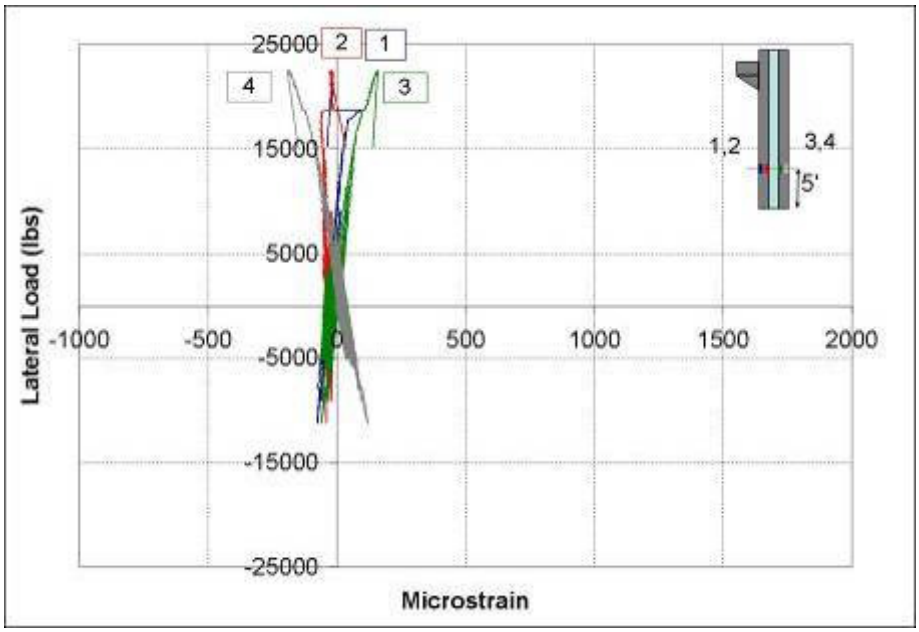

Figure 7-13: Quarter-height side strain gauges of XPS 2

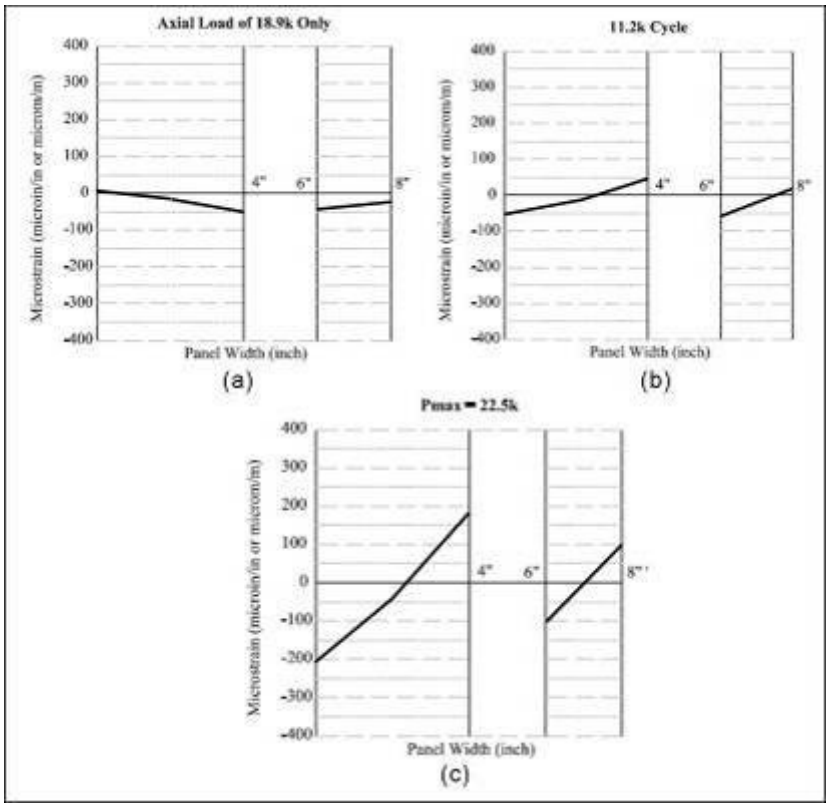

Figure 7-14: Quarter-height side strain profile of XPS 2
(a) Axial load only (b) Ultimate load (c) Failure load

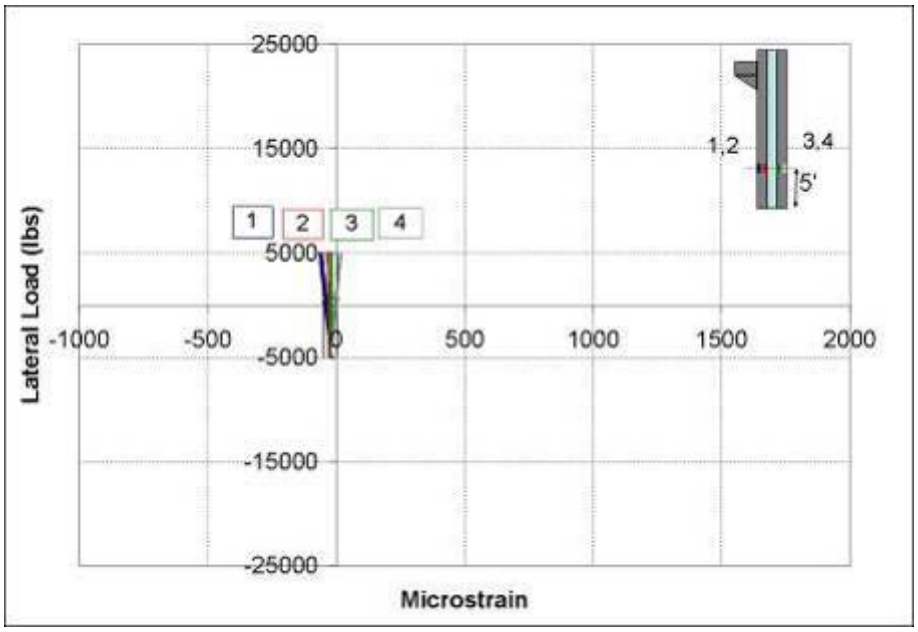

Figure 7-15: Quarter-height side strain gauges of XPS 3

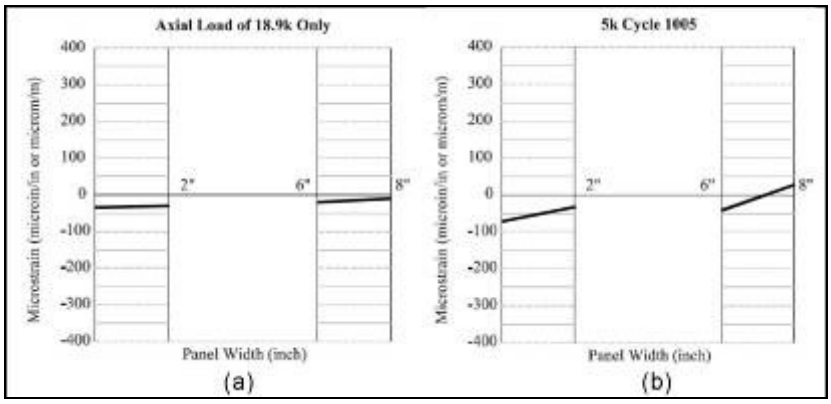

Figure 7-16: Quarter-height side strain profile of XPS 3
(a) Axial load only (b) Cycle 1282 of 5k cycles

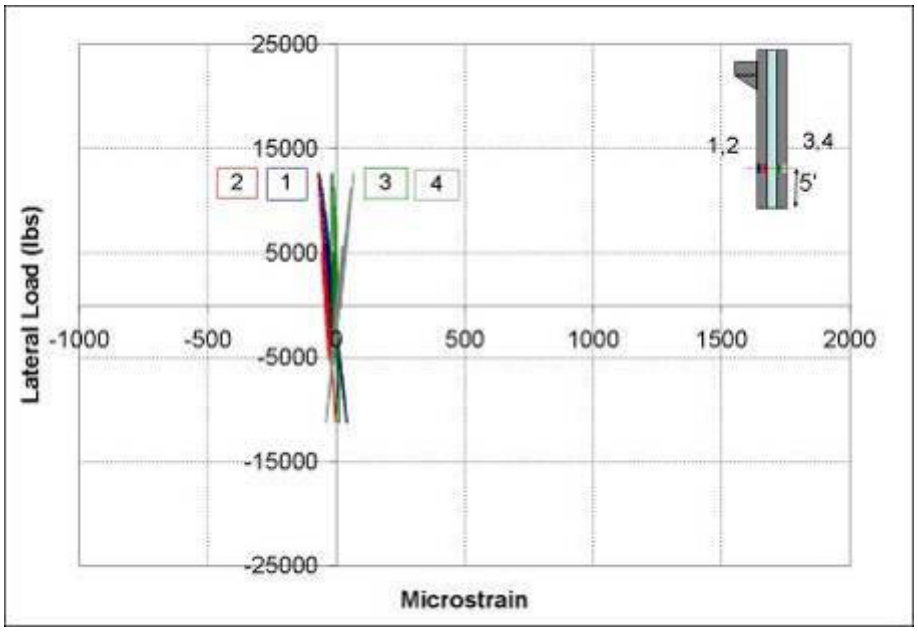

Figure 7-17: Quarter-height side strain gauges of XPS 4

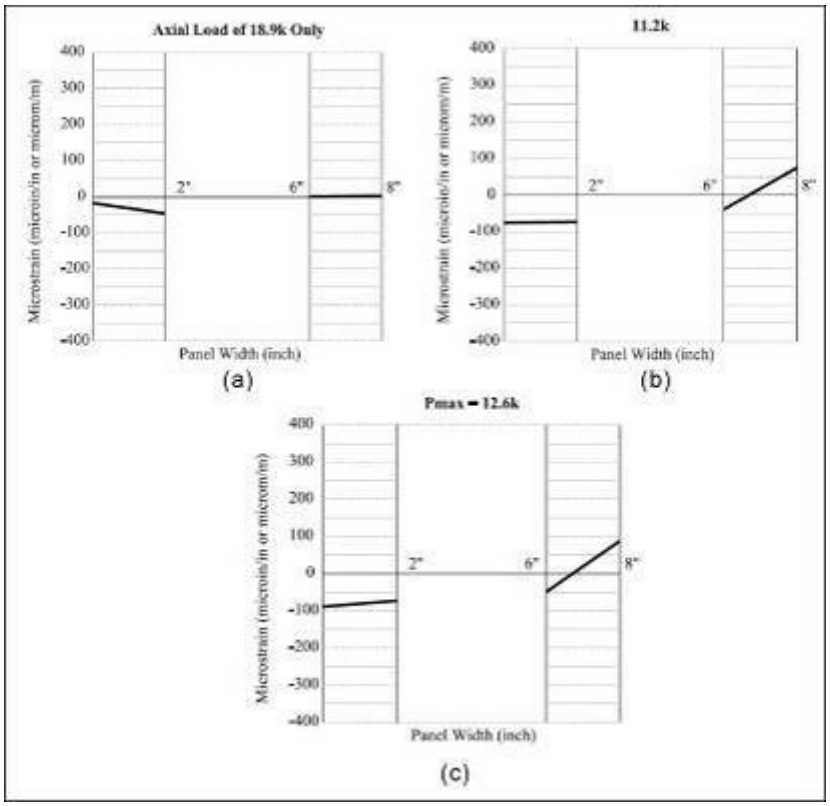

Figure 7-18: Quarter-height side strain profile of XPS 4
(a) Axial load only (b) Ultimate load (c) Failure load

8 APPENDIX B

ANALYTICAL STEPS

1. Calculate concrete strength at day of testing

$$f_{cm}(t) = f_{c28}\left(\frac{t}{4+0.85t}\right)$$

Where $f_{cm}(t)$ is the strength of interest, f_{c28} is 28 day concrete strength and t is time in days (Mehta .1993).

2. Extract dimensions from cross-section
   a. Width, b (in)
   b. Height to axial load, H' (in)
   c. Total height, H (in)
   d. Thickness, t (in)
   e. Inner wythe area, $A_{c,i}$ (in^2)
   f. Outer wythe area, $A_{c,o}$ (in^2)
   g. Inner wythe top extreme fiber, $y_{t,i}$ (in)
   h. Inner wythe bottom extreme fiber, $y_{b,i}$ (in)
   i. Outer wythe top and bottom extreme fiber, $y_{t,o} = y_{b,o}$ (in)
   j. Composite bottom extreme fiber, $y_{b,c}$ (in)
   k. Composite top extreme fiber, $y_{t,c}$ (in)
   l. Composite centroid to inner wythe centroid, d_i (in)
   m. Composite centroid to outer wythe centroid, d_o (in)
   n. Top of panel to top of corbel, a_1 (in)
   o. Top of panel to lateral load, a_2 (in)
   p. Inner wythe surface to axial load, a_3 (in)
   q. Top of panel to height of interest, x_1 (in)
   r. Bottom of panel to height of interest, x (in)

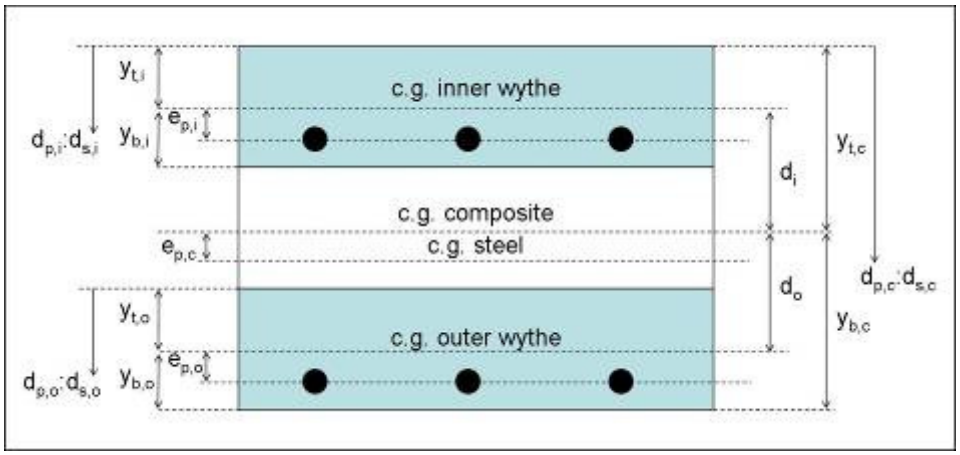

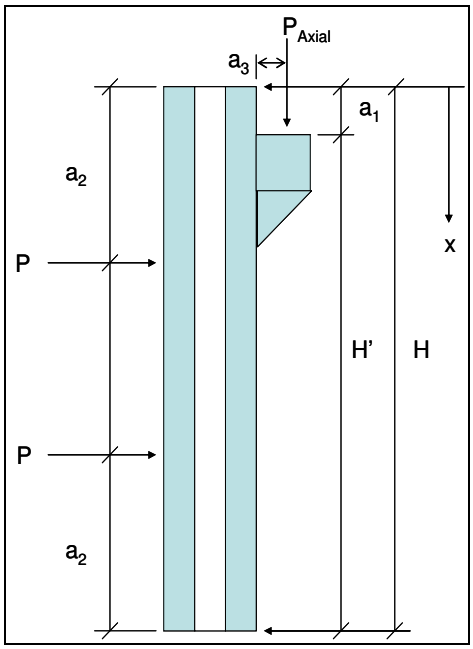

3. Calculate section properties
   a. Inner wythe area, $A_{c,i}$ (in^2)
   b. Outer wythe area, $A_{c,o}$ (in^2)
   c. Total concrete area, A_c (in^2)
      $A_c=A_{c,i}+A_{c,o}$
   d. Inner wythe Moment of Inertia, $I_{nc,i}$ (in^4)
   e. Outer wythe Moment of Inertia, $I_{nc,o}$ (in^4)
   f. Composite Moment of Inertia, I_c (in^4)
      $$I_c = \left(I_{nc,i} + A_{c,i}d_i^{\,2}\right) + \left(I_{nc,o} + A_{c,o}d_o^{\,2}\right)$$
   g. Inner wythe ratio of Moment of Inertia, %I
      $$\%I = \frac{I_{nc,i}}{I_{nc,i} + I_{nc,o}}$$
   h. Outer wythe ratio of Moment of Inertia, %O
      $$\%O = \frac{I_{nc,o}}{I_{nc,i} + I_{nc,o}}$$
4. Determine prestressing properties
   a. Prestressing area, $A_{p,c}$ (both wythes) (in^2)
   b. Prestressing area inner wythe, $A_{p,i}$ (in^2)
   c. Prestressing area outer wythe, $A_{p,o}$ (in^2)
   d. Composite prestressing depth, $d_{p,c}$ (in)
   e. Composite prestressing eccentricity, $e_{p,c}$ (in)
   f. Inner wythe prestressing depth, $d_{p,i}$ (in)
   g. Inner wythe prestressing eccentricity, $e_{p,i}$ (in)
   h. Outer wythe prestressing depth, $d_{p,o}$ (in)
   i. Outer wythe prestressing eccentricity, $e_{p,o}$ (in)

j. Prestressing modulus, E_p (ksi)
k. Strand yield strength, f_{py} (ksi)
l. Strand ultimate strength, f_{pu} (ksi)
m. Initial prestressing, f_{pi}/f_{pu}
n. Initial prestressing strength, f_{pi} (ksi)

$$f_{pi} = \frac{f_{pi}}{f_{pu}} f_{pu}$$

o. Initial composite prestressing force, $P_{i,c}$ (kip)

$$P_{i,c} = f_{pi} A_{pc}$$

p. Initial inner wythe prestressing force, $P_{i,i}$ (kip)

$$P_{i,i} = f_{pi} A_{p,i}$$

q. Initial outer wythe prestressing force, $P_{i,o}$ (kip)

$$P_{i,o} = f_{pi} A_{p,o}$$

r. Prestressing losses
    i. Determine
        1. time to testing, t_{relax} (hours)
        2. time to set, t_{set} (hours)
        3. Relative humidity, RH (%)
        4. Volume concrete, V (in^3)
        5. Specimen surface area, S (in^2)
        6. Volume/surface area, V/S (in)
        7. Shrinkage coefficient, k_{sh}
        8. Creep coefficient, k_{cr}
    ii. Stage 1: stress transfer
        1. Steel relaxation

$$\Delta f_{pR} = f_{pi} \frac{\log(t_{set})}{10} \left(\frac{f_{pi}}{f_{py}} + 0.55 \right)$$

        2. Elastic shortening

$$\Delta f_{pES} = n_i f_{pES}$$

$$f_{pES} = average(f_{pES,i}, f_{pES,o})$$

$$f_{pES,i} = -\frac{P_{e,i}}{A_c} - \frac{P_{e,i}\left(d_i - e_{p,i}\right)^2}{I_c} + \frac{P_{e,o}\left(d_i - e_{p,i}\right)\left(d_o + e_{p,o}\right)}{I_c} - \frac{P_{axial}}{A_c}$$

$$f_{pES,o} = -\frac{P_{e,o}}{A_c} - \frac{P_{e,o}\left(d_o + e_{p,o}\right)^2}{I_c} + \frac{P_{e,i}\left(d_i - e_{p,i}\right)\left(d_o + e_{p,o}\right)}{I_c} - \frac{P_{axial}}{A_c}$$

$$n_i = \frac{E_{ps}}{E_{ci}}$$

    iii. Stage 2 & 3: time of test
        1. Shrinkage losses

$$\Delta f_{pSH} = 8.2x10^{-6} k_{sh} E_{ps} \left(1 - 0.06V/S\right)(100 - RH)$$

2. Steel relaxation

$$\Delta f_{pR} = f_{pi} \frac{\log(t_{test}) - \log(t_{set})}{10} \left(\frac{f_{pi}}{f_{py}} + 0.55 \right)$$

3. Creep losses

$$\Delta f_{pCR} = n k_{cr} \left(f_{cs} - f_{csd} \right)$$

$$f_{csd} = 0 \Rightarrow NO\ superimposed\ dead\ load$$

$$f_{cs} = average(f_{pES,i}, f_{pES,o})$$

$$n = \frac{E_{ps}}{E_c}$$

iv. Calculate losses

$$losses = 1 - \frac{f_{pi} - \Delta f_{pR} - \Delta f_{pES} - \Delta f_{pSH} - \Delta f_{pR} - \Delta f_{pCR}}{f_{pi}}$$

$$R = 1 - losses$$

s. Effective composite prestressing force, $P_{e,c}$ (kip)
$$P_{e,c} = P_{i,c} R$$

t. Effective inner wythe prestressing force, $P_{e,i}$ (kip)
$$P_{e,i} = P_{i,i} R$$

u. Effective outer wythe prestressing force, $P_{e,o}$ (kip)
$$P_{e,o} = P_{i,o} R$$

5. Determine mild steel properties
   a. Steel area for both wythes, $A_{s,c}$ (in^2)
   b. Steel area per wythe, $A_{s,nc}$ (in^2)
   c. Steel modulus, E_s (ksi)
   d. Fully composite steel depth, $d_{s,c}$ (in)
   e. Inner wythe steel depth, $d_{s,i}$ (in)
   f. Outer wythe steel depth, $d_{s,o}$ (in)
   g. Steel yield strength, f_{sy} (ksi)
6. Determine concrete properties
   a. Concrete unit weight, γ_c (pcf)
   b. Initial concrete strength, f_{ci} (ksi)
   c. Initial concrete modulus, E_{ci} (ksi)
   $$E_{ci} = 57\sqrt{f_{ci}}$$
   d. Concrete strength, f_c (ksi)
   e. Concrete modulus, E_c (ksi)
   $$E_c = 57\sqrt{f_c}$$
   f. Initial modular ratio, n_i
   g. Modular ratio, n

h. Maximum concrete strain, ε_{cu} (in/in)
i. Tension modulus constant, $XX\sqrt{f_c}$
j. Tension modulus, f_r (ksi)
k. Neutral axis depth constant, β_1

$$\beta_1 = 0.85 < 0.85 - \frac{f'_c - 4000}{1000} 0.05 \le 0.65$$

Values in psi

7. Evaluate loads
   a. Composite axial load, P_{axial} (kip)
   b. Inner wythe axial load, $P_{axial,i}$ (kip)
   c. Outer wythe axial load, $P_{axial,o}$ (kip)
   d. Composite axial load eccentricity, $e_{a,c}$ (in)

$$e_{a,c} = a_3 + y_{t,c}$$

   e. Inner wythe axial load eccentricity, $e_{a,i}$ (in)

$$e_{a,i} = a_3 + y_{t,i}$$

   f. Outer wythe axial load eccentricity, $e_{a,o}$ (in)

$$e_{a,o} = a_3 + y_{t,o}$$

   g. Composite axial load moment, $M_{e,c}$ (kip-in)

$$M_{e,c} = P_{axial} e_{a,c}$$

   h. Inner wythe axial load moment, $M_{e,i}$ (kip-in)

$$M_{e,i} = P_{axial} e_{a,i}$$

   i. Outer wythe axial load moment, $M_{e,o}$ (kip-in)

$$M_{e,o} = P_{axial} e_{a,o}$$

8. Determine cracking properties
   a. Composite cracking moment, $M_{cr,c}$ (kip-in)

$$M_{cr,c} = \frac{I_c}{y_{b,c}} \left(f_r + \frac{P_{e,c}}{A_c} + \frac{P_{axial}}{A_c} + \frac{P_{e,c} e_{p,c}}{I_c} y_{b,c} \right)$$

   b. Inner wythe cracking moment, $M_{cr,i}$ (kip-in)

$$M_{cr,i} = \frac{I_{nc,i}}{y_{b,i}} \left(f_r + \frac{P_{e,i}}{A_{c,i}} + \frac{P_{axial,i}}{A_{c,i}} + \frac{P_{e,i} e_{p,i}}{I_{nc,o}} y_{b,i} \right)$$

   c. Outer wythe cracking moment, $M_{cr,o}$ (kip-in)

$$M_{cr,o} = \frac{I_{nc,o}}{y_{b,o}} \left(f_r + \frac{P_{e,o}}{A_{c,o}} + \frac{P_{axial,o}}{A_{c,o}} + \frac{P_{e,o} e_{p,o}}{I_{nc,o}} y_{b,o} \right)$$

   d. Composite cracking moment of inertia, $I_{cr,c}$ (in^4)

$$I_{cr,c} = \frac{bx^3}{3} + \left(n_s A_{s,nc} + n_p A_{p,i}\right)(d_1 - x)^2 + \left(n_s A_{s,nc} + n_p A_{p,o}\right)(d_2 - x)^2$$

$$x = \sqrt{\frac{c}{a} + \left(\frac{b}{2a}\right)^2} - \frac{b}{2a}$$

$$a = \frac{b}{2} \quad b = width$$

$$b = 2n_s A_{s,nc} + n_p \left(A_{p,i} + A_{p,o}\right)$$

$$c = n_s A_{s,nc} \left(d_1 + d_2\right) + n_p \left(A_{p,i} d_1 + A_{p,o} d_2\right)$$

e. Inner wythe cracking moment of inertia, $I_{cr,i}$ (in^4)

$$I_{cr,i} = \frac{bx^3}{3} + \left(n_s A_{s,nc} + n_p A_{p,i}\right)(d_1 - x)^2$$

$$x = \sqrt{\frac{c}{a} + \left(\frac{b}{2a}\right)^2} - \frac{b}{2a}$$

$$a = \frac{b}{2} \quad b = width$$

$$b = 2n_s A_{s,nc} + n_p \left(A_{p,i}\right)$$

$$c = n_s A_{s,nc} \left(d_1\right) + n_p \left(A_{p,i} d_1\right)$$

f. Outer wythe cracking moment of inertia, $I_{cr,o}$ (in^4)

$$I_{cr,o} = \frac{bx^3}{3} + \left(n_s A_{s,nc} + n_p A_{p,o}\right)(d_3 - x)^2$$

$$x = \sqrt{\frac{c}{a} + \left(\frac{b}{2a}\right)^2} - \frac{b}{2a}$$

$$a = \frac{b}{2} \quad b = width$$

$$b = 2n_s A_{s,nc} + n_p \left(A_{p,o}\right)$$

$$c = n_s A_{s,nc} \left(d_3\right) + n_p \left(A_{p,o} d_3\right)$$

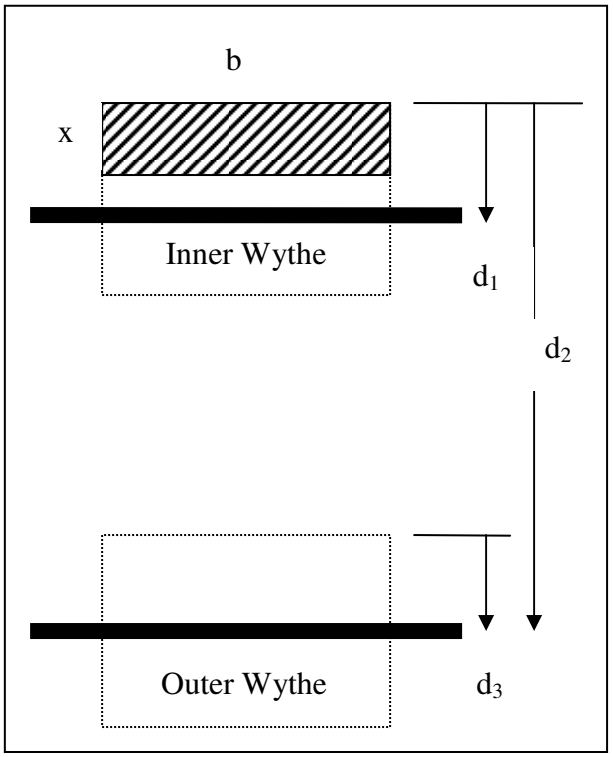

9. Calculate deflections
   a. Composite behavior
      i. Find applied moment, M_a (kip-in)

$$M_a = \frac{M_{e,c} H' x_1}{H^2} + P_{lat} a_2$$

      ii. Find effective moment of inertia, I_e (in^4)

$$I_e = \left(\frac{M_{cr,c}}{M_a}\right)^3 I_c + \left[1 - \left(\frac{M_{cr,c}}{M_a}\right)^3\right] I_{cr,c} \le I_c$$

      iii. Calculate $I_e E_c$ ($kip\text{-}in^2$)
      iv. Determine deflection due to applied moment, Δ_{app} (in)

$$\Delta_{app} = \frac{P_{lat} a_2}{6 E_c I_e}\left(3Hx - 3x^2 - a_2^{\,2}\right) - \frac{M_{e,c}}{6 E_c I_e}\left[3\left(a_1^{\,2} + x^2\right) - \frac{x^3}{H} - \left(2H + \frac{3a_1^{\,2}}{H}\right)x\right]$$

      v. Determine deflection due to P-δ, $\Delta_{P\text{-}\delta}$ (in)

$$\Delta_{P-\delta} = \frac{P_{axial,c} H^2}{8 E_c I_e} e_i$$

      vi. Iterate second order deflection until convergence

$$e_1 = \Delta_{app}$$

$$\Delta_1 = \Delta_{P-\delta} e_1$$

$$e_2 = \Delta_{app} + \Delta_1$$

$$\Delta_2 = \Delta_{P-\delta} e_2$$

b. Non-composite behavior

i. Find applied moment, M_a (kip-in)

$$M_{a,i} = \frac{M_{e,i} H' x_1}{H^2} + \%I * P_{lat} a_2$$

$$M_{a,o} = \frac{M_{e,o} H' x_1}{H^2} + \%O * P_{lat} a_2$$

ii. Find effective moment of inertia, I_e (in^4)

$$I_{e,i} = \left(\frac{M_{cr,i}}{M_{a,i}}\right)^3 I_{c,i} + \left[1 - \left(\frac{M_{cr,i}}{M_{a,i}}\right)^3\right] I_{cr,i} \le I_{nc,i}$$

$$I_{e,o} = \left(\frac{M_{cr,o}}{M_{a,o}}\right)^3 I_{c,o} + \left[1 - \left(\frac{M_{cr,o}}{M_{a,o}}\right)^3\right] I_{cr,o} \le I_{nc,o}$$

$$I_e = I_{e,i} + I_{e,o}$$

iii. Calculate $I_e E_c$ (kip-in^2)

iv. Determine deflection due to applied moment, Δ_{app} (in)

$$\Delta_{app} = \frac{P_{lat} a_2}{6 E_c I_e}\left(3Hx - 3x^2 - a_2{}^2\right) - \frac{M_{e,i}}{6 E_c I_e}\left[3\left(a_1{}^2 + x^2\right) - \frac{x^3}{H} - \left(2H + \frac{3a_1{}^2}{H}\right)x\right]$$

v. Determine deflection due to P-δ, $\Delta_{P\text{-}\delta}$ (in)

$$\Delta_{P-\delta} = \frac{P_{axial} H^2}{8 E_c I_e} e_i$$

vi. Iterate second order deflection until convergence

$$e_1 = \Delta_{app}$$

$$\Delta_1 = \Delta_{P-\delta} e_1$$

$$e_2 = \Delta_{app} + \Delta_1$$

$$\Delta_2 = \Delta_{P-\delta} e_2$$

10. Calculate percent composite action, κ (2 methods)

$$\kappa_1 = \frac{\Delta_{\exp} - \Delta_{nc}}{\Delta_c - \Delta_{nc}}$$

$$\kappa_2 = \frac{\Delta_{\exp}}{\Delta_c}$$

9 APPENDIX C

ANALYTICAL CALCULATIONS

9.1 EPS 1 CALCULATIONS

9.1.1 Input

PRECAST PRESTRESSED CONCRETE SANDWICH WALL PANEL DATA INPUT				
Input and Properties:				
Dimensions	Width	b	12	ft
	Width	b	144	in
	Height to axial load	H'	19	ft
	Height to axial load	H'	228	in
	Total height	H	20	ft
	Total height	H	240	in
	Inner wythe thickness	t_1	2.67	in
	Outer wythe thickness	t_2	2.00	in
	Insulation thickness	t_3	3.33	in
	Total thickness	t	8.00	in
	Composite top extreme fiber	$y_{t,c}$	3.86	in
	Composite bottom extreme fiber	$y_{b,c}$	4.14	in
	Inner wythe top extreme fiber	$y_{t,i}$	1.50	in
	Inner wythe bottom extreme fiber	$y_{b,i}$	2.50	in
	Outer wythe top extreme fiber	$y_{t,o}$	1.00	in
	Outer wythe bottom extreme fiber	$y_{b,o}$	1.00	in
	Composite centroid to inner centroid	d_i	2.36	in
	Composite centroid to outer centroid	d_o	3.14	in
	Top panel to top corbel	a_1	12	in
	End of panel to lateral load	a_2	60	in
	Bottom panel to measured lateral deflection	x_1	120	in
	Top panel to measured lateral delfection	x	120	in
	Bottom panel to maximum moment	x_2	180	in
	Top panel to maximum moment	x_3	60	in
Section properties	Inner wythe area	$A_{c,i}$	384	in^2
	Outer wythe area	$A_{c,o}$	288	in^2
	Concrete area	A_c	672	in^2
	Fully composite MOI	I_c	5493	in^4
	Inner wythe MOI	$I_{nc,i}$	416	in^4
	Outer wythe MOI	$I_{nc,o}$	96	in^4
	Fully noncomposite MOI	I_{nc}	512	in^4
	Inner wythe stiffness	I	81.3%	
	Outer wythe stiffness	O	18.8%	
Prestress properties	Prestressed area both wythes	$A_{p,c}$	0.85	in^2
	Prestressed area inner wythe	$A_{p,i}$	0.425	in^2
	Prestressed area outer wythe	$A_{p,o}$	0.425	in^3
	Fully composite prestressing depth	$d_{p,c}$	4.00	in
	Fully composite prestressing eccentricity	$e_{p,c}$	0.14	in

Prestress properties	Inner wythe prestressing depth	$d_{p,i}$	1.00	in
	Inner wythe prestressing eccentricity	$e_{p,i}$	-0.50	in
	Outer wythe prestressing depth	$d_{p,o}$	1.00	in
	Outer wythe prestressing eccentricity	$e_{p,o}$	0.00	in
	Prestressing modulus	E_{ps}	28500	ksi
	Strand yield strength	f_{py}	243	ksi
	Strand ultimate strength	f_{pu}	270	ksi
	Yield/Ultimate	f_{pi}/f_{pu}	0.75	
	Initial prestressing strength	f_{pi}	202.5	ksi
	Initial compsote prestressing force	$P_{i,c}$	172	kip
	Initial inner wythe prestressing force	$P_{i,i}$	86	kip
	Initial outer wythe prestressing force	$P_{i,o}$	86	kip
	1-losses	R	85%	
	Effective compsote prestressing force	$P_{e,c}$	146	kip
	Effective inner wythe prestressing force	$P_{e,i}$	73	kip
	Effective inner wythe prestressing force	$P_{e,o}$	73	kip
	Time to testing	t_{relac}	2184	hrs
	Time to set	t_{set}	16	hrs
	Relative humidity	RH	70	%
	Volume of concrete	V	161395	in^3
	Specimen surface area	S	140544	in^2
	Volume/surface area	V/S	1.14836	in
	Friction loss coefficient	k	0	
	Shrinkage coefficient	ksh	1	
	Creep coeficient	kcr	2	
	Anchorage Seating	Δ_A	0	in
	Friction coefficient	μ	0	
	Wobble coefficient	α	0	

Note: Percent composite action and deflections calculated at mid-height

Note: Moment capacities and ultimate load calculated at 3/4-height

Mild steel properties	Steel area both wythes	$A_{s,c}$	0.3296	in^2
	Steel area each wythe	$A_{s,nc}$	0.1648	in^2
	Steel modulus	E_s	29000	ksi
	Fully composite steel depth	$d_{s,c}$	4.00	in
	Inner wythe steel depth	d_{si}	1.00	in
	Outer wythe steel depth	$d_{s,o}$	1.00	in
	Strand yield strength	f_{sy}	65	ksi
Concrete properties	Concrete unit weight	γ_c	145	pcf
	Initial concrete strength	f'_{ci}	3.5	psi
	Initial concrete modulus	E_{ci}	1686	ksi
	Concrete strength	f'_c	7.63	ksi
	Concrete modulus	E_c	2489	ksi
	Maximum concrete strain	ε_{cu}	0.003	in/in
	Tension modulus constant	$K\sqrt{f'_c}=$	10.0	
	Tension modulus	$f_r=$	0.873	ksi
	NA depth constant	β_1	0.6685	
	Initial prestressed modular ratio	n_i	16.903	
	Prestressed modular ratio	n	11.448	
Safety factors	Flexural phi factor	ϕ_f	0.9	
	Shear phi factor	ϕ_v	0.85	
Loads	Composite axial load	P_{axial}	37.8	kip
	Inner wythe axial load	$P_{axial,i}$	37.8	kip
	Outer wythe axial load	$P_{axial,o}$	0.0	kip
	Wythe surface to axial load	a_3	6	in
	Composite axial load eccentricity	$e_{a,c}$	9.86	in
	Inner wythe axial load eccentricity	$e_{a,i}$	7.50	in
	Outer wythe axial load eccentricity	$e_{a,o}$	13.00	in
	Composite axial load moment	$M_{e,c}$	373	kip-in
	Inner wythe axial load moment	$M_{e,i}$	284	kip-in
	Outer wythe axial load moment	$M_{e,o}$	0	kip-in
Cracking properties	Composite cracking moment	$M_{cr,c}$	1543	kip-in
	Inner wythe cracking moment	$M_{cr,i}$	157	kip-in
	Outer wythe cracking moment	$M_{cr,o}$	108	kip-in
	Composite cracking MOI	$I_{cr,c}$	286	in^4
	Inner wythe cracking MOI	$I_{cr,i}$	4.6	in^4
	Outer wythe cracking MOI	$I_{cr,o}$	4.6	in^4
Deflection	Initial bow	e_i	0	in

9.1.2 Prestressing Losses

PRECAST PRESTRESSED CONCRETE SANDWICH WALL PANEL DATA INPUT

Stage 0: Jacking

Anchorage Seating Losses			Friction Losses		
Δf_{pA} =	0	ksi	Δf_{pF} =	0	ksi
Stage 0 Loss =	0	ksi			
f_{pi} =	202.5	kip			

Stage I: Stress Transfer

Steel Relaxation Losses

t_1 =	0	hrs
t_2 =	16	hrs
f_{pi} =	203	ksi
Δf_{pR} =	6.9	ksi

Elastic Shortening Losses

Ass. Δf_{pES} =	3.02	ksi			
f_{pi} =	193	ksi			
P_{ti} =	82	kip	P_{axial} =	37.8	kip
P_{to} =	82	kip			

Elastic Shortening

M_b =	0	kip-ft
M_b =	0	kip-in
$f_{pES,i}$ =	-0.166	ksi
$f_{pES,o}$ =	-0.191	ksi
$\Delta f_{pES,i}$ =	2.81	ksi
$\Delta f_{pES,o}$ =	3.23	ksi
Difference =	0.00	
Stage I Loss =	9.93	ksi
f_{pi} =	193	kip

Stage II: Transfer to Placement of Superimposed Dead Load

Creep Losses

M_{SD} =	0	kip-ft
M_{SD} =	0	kip-in
$f_{cs,I}$ =	0.166	ksi
f_{csd} =	0.000	ksi
f_{csd} =	0.000	ksi
Δf_{pCR} =	**3.80**	**ksi**

Shrinkage Losses

Δf_{pSH} =	**6.53**	**ksi**

Steel Relaxatinn Losses

t_1 =	16	hrs
t_2 =	2184	hrs
f_{pI} =	193	ksi
Δf_{pR} =	**9.97**	**ksi**

Stress Increase Due to Loading

Δf_{SD} =	**0.00**	**ksi**

Stage II Loss =	**20.3**	**ksi**
f_{pi} =	**172**	**kip**

Total Losses =	**20**	**ksi**
f_{pe} =	**172**	**ksi**
P_e =	**146**	**kip**
R =	**85%**	
Losses =	**15%**	

9.1.3 Cracked Moment of Inertia

INFORCED CONCRETE SANDWICH WALL PANEL CRACKED MOMENT OF INERTIA

$x<d_i$			$x \geq d_i$			Outer wythe		
b =	144	in	b =	144	in	b =	144	n
d_o =	7	in	d_o =	7	in	d_o =	na	n
d_i =	1	in	d_i =	1	in	d_i =	1	n
t_1 =	2.67	in	t_1 =	2.67	in	t_1 =	2.67	n
A_s =	0.1648	/wythe [in^2]	A_s =	0.1648	/wythe [in^2]	A_s =	0.1648	/wythe [in^2]
A_{ps} =	0.425	Inner wythe [in^2]	A_{ps} =	0.425	Inner wythe [in^2]	A_{ps} =	0.425	nner wythe [in^2
A_{ps} =	0.425	Outer wythe [in^2]	A_{ps} =	0.425	Outer wythe [in^2]	A_{ps} =	0.425	Outer wythe [in
E_s =	29000000	psi	E_s =	29000000	psi	E_s =	29000000	si
E_{ps} =	28500000	psi	E_{ps} =	28500000	psi	E_{ps} =	28500000	si
E_c =	2489471	psi	E_c =	2489471.33	psi	E_c =	2489471.33	si
n_s =	11.649		n_s =	11.649		n_s =	11.649	
n_{ps} =	11.448		n_{ps} =	11.448		n_{ps} =	11.448	

Composite			Composite			Outer Non-Composite		
a =	72		a =	72		a =	72	
b =	13.571		b =	6.785		b =	6.785	
c =	54.282		c =	47.497		c =	6.785	
x =	0.779	in	x =	0.766	in	x =	0.263	n
	-0.968	in		-0.861	in		-0.353	n
I_{comp} =	285.6	in^4	I_{comp} =	285.3	in^4	$I_{non\text{-}comp/wythe}$ =	4.6	n^4

Inner Non-Composite		
a =	72	
b =	6.785	
c =	6.785	
x =	0.263	in
	-0.358	in
mp/wythe =	4.6	in^4

9.1.4 Composite Deflection

REINFORCED CONCRETE SANDWICH WALL PANEL COMPOSITE DEFELCTION

P_{axial}	$P_{lateral}$	$2P_{lateral}$	M_a	I_{eff}	EI	Δ_{app}	Δ_{P-D}/e_i	e_1
kip	kip	kip	kip-in	in^4	$kip-in^2$	in	in/in	in
37.8	0	0	177	5493	13674578	0.097	0.020	0.097
37.8	1	2	237	5493	13674578	0.126	0.020	0.126
37.8	2.5	5	327	5493	13674578	0.170	0.020	0.170
37.8	3.5	7	387	5493	13674578	0.198	0.020	0.198
37.8	4	8	417	5493	13674578	0.213	0.020	0.213
37.8	5.45	10.9	504	5493	13674578	0.255	0.020	0.255
37.8	6	12	537	5493	13674578	0.271	0.020	0.271
37.8	7	14	597	5493	13674578	0.300	0.020	0.300
37.8	8	16	657	5493	13674578	0.329	0.020	0.329
37.8	9	18	717	5493	13674578	0.358	0.020	0.358
37.8	9.5	19	747	5493	13674578	0.372	0.020	0.372
37.8	11	22	837	5493	13674578	0.416	0.020	0.416
37.8	12	24	897	5493	13674578	0.445	0.020	0.445
37.8	13	26	957	5493	13674578	0.474	0.020	0.474
37.8	14	28	1017	5493	13674578	0.503	0.020	0.503
37.8	14.8	29.6	1065	5493	13674578	0.526	0.020	0.526
37.8	16	32	1137	5493	13674578	0.560	0.020	0.560
37.8	17	34	1197	5493	13674578	0.589	0.020	0.589
37.8	18	36	1257	5493	13674578	0.618	0.020	0.618
37.8	19	38	1317	5493	13674578	0.647	0.020	0.647
37.8	20	40	1377	5493	13674578	0.676	0.020	0.676
37.8	21	42	1437	5493	13674578	0.705	0.020	0.705
37.8	22	44	1497	5493	13674578	0.734	0.020	0.734
37.8	23	46	1557	5353	13326049	0.763	0.020	0.763
37.8	24	48	1617	4810	11973272	0.905	0.023	0.905
37.8	25	50	1677	4341	10807203	1.039	0.025	1.039
37.8	26	52	1737	3935	9796712	1.187	0.028	1.187
37.8	27	54	1797	3582	8916693	1.348	0.031	1.348
37.8	28	56	1857	3272	8146751	1.524	0.033	1.524
37.8	29	58	1917	3001	7470199	1.715	0.036	1.715
37.8	30	60	1977	2761	6873296	1.922	0.040	1.922

Δ_1	e_2	Δ_2	error	e_3	Δ_3	error	e_4	Δ_4
in	in	in	%	in	in	%	in	in
0.002	0.099	0.002	1.99%	0.099	0.002	0.04%	0.099	0.002
0.003	0.129	0.003	1.99%	0.129	0.003	0.04%	0.129	0.003
0.003	0.173	0.003	1.99%	0.173	0.003	0.04%	0.173	0.003
0.004	0.202	0.004	1.99%	0.203	0.004	0.04%	0.203	0.004
0.004	0.217	0.004	1.99%	0.217	0.004	0.04%	0.217	0.004
0.005	0.260	0.005	1.99%	0.260	0.005	0.04%	0.260	0.005
0.005	0.276	0.005	1.99%	0.276	0.006	0.04%	0.276	0.006
0.006	0.306	0.006	1.99%	0.306	0.006	0.04%	0.306	0.006
0.007	0.335	0.007	1.99%	0.335	0.007	0.04%	0.335	0.007
0.007	0.365	0.007	1.99%	0.365	0.007	0.04%	0.365	0.007
0.007	0.380	0.008	1.99%	0.380	0.008	0.04%	0.380	0.008
0.008	0.424	0.008	1.99%	0.424	0.008	0.04%	0.424	0.008
0.009	0.453	0.009	1.99%	0.454	0.009	0.04%	0.454	0.009
0.009	0.483	0.010	1.99%	0.483	0.010	0.04%	0.483	0.010
0.010	0.513	0.010	1.99%	0.513	0.010	0.04%	0.513	0.010
0.010	0.536	0.011	1.99%	0.536	0.011	0.04%	0.536	0.011
0.011	0.572	0.011	1.99%	0.572	0.011	0.04%	0.572	0.011
0.012	0.601	0.012	1.99%	0.601	0.012	0.04%	0.601	0.012
0.012	0.631	0.013	1.99%	0.631	0.013	0.04%	0.631	0.013
0.013	0.660	0.013	1.99%	0.660	0.013	0.04%	0.661	0.013
0.013	0.690	0.014	1.99%	0.690	0.014	0.04%	0.690	0.014
0.014	0.719	0.014	1.99%	0.720	0.014	0.04%	0.720	0.014
0.015	0.749	0.015	1.99%	0.749	0.015	0.04%	0.749	0.015
0.016	0.799	0.016	2.04%	0.799	0.016	0.04%	0.799	0.016
0.021	0.925	0.021	2.27%	0.926	0.021	0.05%	0.926	0.021
0.026	1.065	0.027	2.52%	1.066	0.027	0.06%	1.066	0.027
0.033	1.220	0.034	2.78%	1.220	0.034	0.08%	1.220	0.034
0.041	1.389	0.042	3.05%	1.390	0.042	0.09%	1.391	0.042
0.051	1.575	0.053	3.34%	1.577	0.053	0.11%	1.577	0.053
0.062	1.778	0.065	3.64%	1.780	0.065	0.13%	1.780	0.065
0.076	1.998	0.079	3.96%	2.001	0.079	0.15%	2.001	0.079

9.1.5 Non-composite Deflection

REINFORCED CONCRETE SANDWICH WALL PANEL NON-COMPOSITE DEFELCTION

P_{axial}	$P_{lateral}$	$2P_{lateral}$	M_3	$M_{3,I}$	$M_{3,O}$	$I_{eff,I}$	$I_{eff,O}$	I_{eff}	EI
kip	kip	kip	kip-in	kip-in	kip-in	in^4	in^4	in^4	$kip-in^2$
37.8	0	0	177	135	0	416	96	512	1274609
37.8	1	2	237	183	11	262	96	358	890183
37.8	2.5	5	327	257	28	98	96	194	484173
37.8	3.5	7	387	305	39	60	96	156	389089
37.8	4	8	417	330	45	49	96	145	360531
37.8	5.45	10.9	504	400	61	29	96	125	311862
37.8	6	12	537	427	68	25	96	121	300988
37.8	7	14	597	476	79	19	96	115	286963
37.8	8	16	657	525	90	16	96	112	277673
37.8	9	18	717	573	101	13	96	109	271277
37.8	9.5	19	747	598	107	12	96	108	268819
37.8	11	22	837	671	124	10	66	76	188188
37.8	12	24	897	720	135	9	52	61	150690
37.8	13	26	957	768	146	8	42	50	123738
37.8	14	28	1017	817	158	7	34	42	103864
37.8	14.8	29.6	1065	856	167	7	30	37	91567
37.8	16	32	1137	915	180	7	24	31	77385
37.8	17	34	1197	963	191	6	21	27	68405
37.8	18	36	1257	1012	203	6	19	25	61290
37.8	19	38	1317	1061	214	6	16	22	55581
37.8	20	40	1377	1110	225	6	15	20	50945
37.8	21	42	1437	1158	236	6	13	19	47143
37.8	22	44	1497	1207	248	5	12	18	43994
37.8	23	46	1557	1256	259	5	11	17	41364
37.8	24	48	1617	1305	270	5	10	16	39150
37.8	25	50	1677	1353	281	5	10	15	37274
37.8	26	52	1737	1402	293	5	9	14	35672
37.8	27	54	1797	1451	304	5	9	14	34297
37.8	28	56	1857	1500	315	5	8	13	33110
37.8	29	58	1917	1548	326	5	8	13	32079
37.8	30	60	1977	1597	338	5	8	13	31180

Δ_{app}	Δ_{P-D}/e	e_1	Δ_1	e_2	Δ_2	error	e_3	Δ_3
in	in/in	in	in	in	in	%	in	in
1.042	0.214	1.042	0.223	1.265	0.270	21.35%	1.312	0.280
1.937	0.306	1.937	0.592	2.529	0.773	30.57%	2.710	0.829
4.788	0.562	4.788	2.692	7.480	4.204	56.21%	8.993	5.055
6.976	0.699	6.976	4.880	11.856	8.293	69.95%	15.269	10.680
8.078	0.755	8.078	6.098	14.176	10.701	75.49%	18.779	14.176
11.180	0.873	11.180	9.756	20.936	18.271	87.27%	29.451	25.701
12.307	0.904	12.307	11.128	23.436	21.191	90.42%	3.3E+01	3.0E+01
14.289	0.948	14.289	13.552	27.840	26.404	94.84%	4.1E+01	3.9E+01
16.193	0.980	16.193	15.871	32.064	31.428	98.01%	4.8E+01	4.7E+01
18.034	1.003	18.034	18.093	36.128	36.245	100.33%	5.4E+01	5.4E+01
18.936	1.012	18.936	19.171	38.107	38.581	101.24%	5.8E+01	5.8E+01
30.206	1.446	30.206	43.684	73.889	106.859	144.62%	1.4E+02	2.0E+02
40.350	1.806	40.350	72.875	113.225	204.495	180.61%	2.4E+02	4.4E+02
52.339	2.199	52.339	115.120	167.459	368.324	219.95%	4.2E+02	9.3E+02
66.166	2.620	66.166	173.379	239.545	627.691	262.03%	6.9E+02	1.8E+03
78.512	2.972	78.512	233.356	311.868	926.946	297.22%	1.0E+03	3.0E+03
99.041	3.517	99.041	348.323	447.364	1573.358	351.69%	1.7E+03	5.9E+03
117.833	3.979	117.833	468.818	586.651	2334.092	397.87%	2.5E+03	9.8E+03
137.972	4.441	137.972	612.665	750.637	3333.209	444.05%	3.5E+03	1.5E+04
159.270	4.897	159.270	779.889	939.159	4598.742	489.67%	4.8E+03	2.3E+04
181.534	5.342	181.534	969.788	1151.322	6150.572	534.22%	6.3E+03	3.4E+04
204.576	5.773	204.576	1181.036	1385.612	7999.252	577.31%	8.2E+03	4.7E+04
228.220	6.186	228.220	1411.834	1640.054	10145.839	618.63%	1.0E+04	6.4E+04
252.304	6.580	252.304	1660.059	1912.362	12582.592	657.96%	1.3E+04	8.4E+04
276.685	6.952	276.685	1923.414	2200.099	15294.307	695.16%	1.6E+04	1.1E+05
301.240	7.302	301.240	2199.557	2500.797	18259.996	730.17%	1.9E+04	1.4E+05
325.867	7.630	325.867	2486.200	2812.067	21454.672	762.95%	2.2E+04	1.7E+05
350.478	7.935	350.478	2781.188	3131.667	24851.046	793.54%	2.5E+04	2.0E+05
375.007	8.220	375.007	3082.547	3457.555	28421.005	822.00%	2.9E+04	2.4E+05
399.399	8.484	399.399	3388.514	3787.912	32136.799	848.40%	3.3E+04	2.8E+05
423.612	8.729	423.612	3697.544	4121.156	35971.946	872.86%	3.6E+04	3.2E+05

error	e_4	Δ_4	error	e_5	Δ_5	error	e_6	Δ_6
%	in	in	%	in	in	%	in	in
3.76%	1.322	0.282	0.77%	1.324	0.283	0.16%	1.325	0.283
7.16%	2.766	0.846	2.04%	2.783	0.851	0.61%	2.788	0.852
20.23%	9.843	5.533	9.46%	10.321	5.802	4.86%	10.590	5.953
28.79%	17.657	12.350	15.64%	19.327	13.519	9.46%	20.495	14.336
32.47%	22.254	16.799	18.50%	24.877	18.779	11.79%	26.857	20.274
40.67%	36.881	32.186	25.23%	43.366	37.845	17.58%	49.025	42.784
42.94%	4.3E+01	3.9E+01	27.16%	5.1E+01	4.6E+01	19.31%	5.8E+01	5.3E+01
46.17%	5.3E+01	5.0E+01	29.95%	6.4E+01	6.1E+01	21.86%	7.5E+01	7.2E+01
48.52%	6.3E+01	6.2E+01	32.02%	7.8E+01	7.6E+01	23.77%	9.2E+01	9.1E+01
50.24%	7.2E+01	7.3E+01	33.55%	9.1E+01	9.1E+01	25.20%	1.1E+02	1.1E+02
50.93%	7.7E+01	7.8E+01	34.17%	9.7E+01	9.8E+01	25.78%	1.2E+02	1.2E+02
85.50%	2.3E+02	3.3E+02	66.66%	3.6E+02	5.2E+02	57.84%	5.5E+02	8.0E+02
116.25%	4.8E+02	8.7E+02	97.09%	9.1E+02	1.6E+03	88.97%	1.7E+03	3.0E+03
151.20%	9.8E+02	2.2E+03	132.39%	2.2E+03	4.8E+03	125.30%	4.9E+03	1.1E+04
189.66%	1.9E+03	4.9E+03	171.57%	5.0E+03	1.3E+04	165.55%	1.3E+04	3.5E+04
222.40%	3.1E+03	9.1E+03	205.03%	9.2E+03	2.7E+04	199.78%	2.7E+04	8.1E+04
273.83%	6.0E+03	2.1E+04	257.62%	2.1E+04	7.4E+04	253.35%	7.4E+04	2.6E+05
317.95%	9.9E+03	3.9E+04	302.67%	3.9E+04	1.6E+05	299.06%	1.6E+05	6.2E+05
362.43%	1.6E+04	6.9E+04	348.03%	6.9E+04	3.1E+05	344.94%	3.1E+05	1.4E+06
406.62%	2.3E+04	1.1E+05	393.01%	1.2E+05	5.6E+05	390.34%	5.6E+05	2.8E+06
449.99%	3.4E+04	1.8E+05	437.09%	1.8E+05	9.7E+05	434.75%	9.7E+05	5.2E+06
492.07%	4.8E+04	2.7E+05	479.80%	2.7E+05	1.6E+06	477.74%	1.6E+06	9.2E+06
532.54%	6.4E+04	4.0E+05	520.83%	4.0E+05	2.5E+06	518.98%	2.5E+06	1.5E+07
571.15%	8.5E+04	5.6E+05	559.93%	5.6E+05	3.7E+06	558.26%	3.7E+06	2.4E+07
607.74%	1.1E+05	7.5E+05	596.94%	7.5E+05	5.2E+06	595.42%	5.2E+06	3.6E+07
642.21%	1.4E+05	9.9E+05	631.79%	9.9E+05	7.2E+06	630.39%	7.2E+06	5.3E+07
674.54%	1.7E+05	1.3E+06	664.45%	1.3E+06	9.7E+06	663.15%	9.7E+06	7.4E+07
704.73%	2.0E+05	1.6E+06	694.93%	1.6E+06	1.3E+07	693.72%	1.3E+07	1.0E+08
732.84%	2.4E+05	1.9E+06	723.30%	1.9E+06	1.6E+07	722.16%	1.6E+07	1.3E+08
758.95%	2.8E+05	2.3E+06	749.63%	2.3E+06	2.0E+07	748.55%	2.0E+07	1.7E+08
783.14%	3.2E+05	2.8E+06	774.02%	2.8E+06	2.4E+07	772.99%	2.4E+07	2.1E+08

error	e_7	Δ_7	error	e_8	Δ_8	error	e_9
%	in	in	%	in	in	%	in
0.03%	1.325	0.283	0.01%	1.325	0.283	0.00%	1.325
0.19%	2.789	0.853	0.06%	2.790	0.853	0.02%	2.790
2.60%	10.741	6.038	1.43%	10.826	6.085	0.79%	10.874
6.04%	21.312	14.907	3.99%	21.883	15.307	2.68%	22.283
7.96%	28.352	21.403	5.57%	29.481	22.254	3.98%	30.332
13.05%	53.963	47.094	10.07%	58.273	50.855	7.99%	62.035
14.64%	6.5E+01	5.9E+01	11.55%	7.1E+01	6.4E+01	9.36%	7.7E+01
17.01%	8.6E+01	8.1E+01	13.79%	9.6E+01	9.1E+01	11.49%	1.1E+02
18.82%	1.1E+02	1.0E+02	15.53%	1.2E+02	1.2E+02	13.17%	1.3E+02
20.20%	1.3E+02	1.3E+02	16.86%	1.5E+02	1.5E+02	14.47%	1.6E+02
20.75%	1.4E+02	1.4E+02	17.40%	1.6E+02	1.6E+02	15.00%	1.8E+02
53.00%	8.3E+02	1.2E+03	50.10%	1.2E+03	1.8E+03	48.27%	1.8E+03
85.03%	3.1E+03	5.6E+03	83.00%	5.6E+03	1.0E+04	81.92%	1.0E+04
122.33%	1.1E+04	2.4E+04	121.02%	2.4E+04	5.2E+04	120.43%	5.3E+04
163.36%	3.5E+04	9.1E+04	162.54%	9.1E+04	2.4E+05	162.23%	2.4E+05
198.08%	8.2E+04	2.4E+05	197.51%	2.4E+05	7.2E+05	197.32%	7.2E+05
252.16%	2.6E+05	9.2E+05	251.83%	9.2E+05	3.2E+06	251.73%	3.2E+06
298.17%	6.2E+05	2.5E+06	297.94%	2.5E+06	9.9E+06	297.89%	9.9E+06
344.25%	1.4E+06	6.1E+06	344.10%	6.1E+06	2.7E+07	344.06%	2.7E+07
389.80%	2.8E+06	1.4E+07	389.69%	1.4E+07	6.6E+07	389.67%	6.6E+07
434.32%	5.2E+06	2.8E+07	434.24%	2.8E+07	1.5E+08	434.22%	1.5E+08
477.38%	9.2E+06	5.3E+07	477.32%	5.3E+07	3.1E+08	477.31%	3.1E+08
518.69%	1.5E+07	9.4E+07	518.64%	9.4E+07	5.8E+08	518.63%	5.8E+08
558.01%	2.4E+07	1.6E+08	557.97%	1.6E+08	1.0E+09	557.96%	1.0E+09
595.20%	3.6E+07	2.5E+08	595.17%	2.5E+08	1.8E+09	595.17%	1.8E+09
630.20%	5.3E+07	3.9E+08	630.17%	3.9E+08	2.8E+09	630.17%	2.8E+09
662.98%	7.4E+07	5.6E+08	662.95%	5.6E+08	4.3E+09	662.95%	4.3E+09
693.56%	1.0E+08	7.9E+08	693.54%	7.9E+08	6.3E+09	693.54%	6.3E+09
722.02%	1.3E+08	1.1E+09	722.00%	1.1E+09	8.9E+09	722.00%	8.9E+09
748.42%	1.7E+08	1.4E+09	748.41%	1.4E+09	1.2E+10	748.40%	1.2E+10
772.88%	2.1E+08	1.8E+09	772.86%	1.8E+09	1.6E+10	772.86%	1.6E+10

Δ_9	error	e_{10}	Δ_{10}	error
in	%	in	in	%
0.283	0.00%	1.325	0.283	0.00%
0.853	0.01%	2.790	0.853	0.00%
6.112	0.44%	10.900	6.127	0.25%
15.587	1.83%	22.563	15.782	1.25%
22.898	2.89%	30.975	23.383	2.12%
54.137	6.45%	65.317	57.002	5.29%
6.9E+01	7.74%	8.2E+01	7.4E+01	6.49%
1.0E+02	9.78%	1.1E+02	1.1E+02	8.45%
1.3E+02	11.41%	1.5E+02	1.5E+02	10.04%
1.6E+02	12.68%	1.8E+02	1.8E+02	11.29%
1.8E+02	13.21%	2.0E+02	2.0E+02	11.81%
2.6E+03	47.08%	2.6E+03	3.8E+03	46.29%
1.8E+04	81.33%	1.8E+04	3.3E+04	81.00%
1.2E+05	120.17%	1.2E+05	2.5E+05	120.05%
6.2E+05	162.11%	6.2E+05	1.6E+06	162.06%
2.1E+06	197.26%	2.1E+06	6.4E+06	197.23%
1.1E+07	251.71%	1.1E+07	4.0E+07	251.70%
3.9E+07	297.87%	3.9E+07	1.6E+08	297.87%
1.2E+08	344.05%	1.2E+08	5.3E+08	344.05%
3.2E+08	389.67%	3.2E+08	1.6E+09	389.67%
7.9E+08	434.22%	7.9E+08	4.2E+09	434.22%
1.8E+09	477.31%	1.8E+09	1.0E+10	477.31%
3.6E+09	518.63%	3.6E+09	2.2E+10	518.63%
6.9E+09	557.96%	6.9E+09	4.5E+10	557.96%
1.2E+10	595.16%	1.2E+10	8.5E+10	595.16%
2.1E+10	630.17%	2.1E+10	1.5E+11	630.17%
3.3E+10	662.95%	3.3E+10	2.5E+11	662.95%
5.0E+10	693.54%	5.0E+10	4.0E+11	693.54%
7.3E+10	722.00%	7.3E+10	6.0E+11	722.00%
1.0E+11	748.40%	1.0E+11	8.7E+11	748.40%
1.4E+11	772.86%	1.4E+11	1.2E+12	772.86%

9.1.6 Deflection Percent Composite Action

REINFORCED CONCRETE SANDWICH WALL PANEL PERCENT COMPOSITE ACTION

P_{max} =	19.8	kip	Axial Load deflection:	0.1	in
P_y =	15	kip	1st 5k deflection:	0.256	in
Δ_y =	0.845	in	%PCA Axial Load:	99.9%	
Δ_i =	0.456	in	%PCA 1st 5k:	99.2%	
n =	6.0				
E =	50				
Elastic stiffness =	39	ksi			

	Service Load	Deflection
Lat Id	7	0
	7	20

		Composite	Non-Composite	Test Data		Pessiki
Axial Load	Lat. Load	Deflection	Deflection	Lat. Load	Deflection	%PCA
kip	kip	in	in	kip	in	%
0	0.0	0	0	0.0	0.000	0%
37.8	0.0	0.099	1.325	0.0	0.456	71%
37.8	2.0	0.129	2.790	2.0	0.508	86%
37.8	5.0	0.173	10.900	5.0	0.586	96%
37.8	7.0	0.203	22.563	7.0	0.638	98.1%
37.8	8.0	0.217	30.975	8.0	0.663	99%
37.8	10.9	0.260	65.317	10.9	0.739	99.3%
37.8	12.0	0.276	81.546	12.0	0.767	99%
37.8	14.0	0.306	113.893	14.0	0.819	100%
37.8	16.0	0.335	148.201	16.0	0.883	100%
37.8	18.0	0.365	183.008	18.0	0.983	100%
37.8	19.0	0.380	200.309	19.0	1.059	100%
37.8	22.0	0.424	2.6E+03			
37.8	24.0	0.454	1.8E+04			
37.8	26.0	0.483	1.2E+05			
37.8	28.0	0.513	6.2E+05			
37.8	29.6	0.536	2.1E+06			
37.8	32.0	0.572	1.1E+07			
37.8	34.0	0.601	3.9E+07			
37.8	36.0	0.631	1.2E+08			
37.8	38.0	0.661	3.2E+08			
37.8	40.0	0.690	7.9E+08			
37.8	42.0	0.720	1.8E+09			
37.8	44.0	0.749	3.6E+09			
37.8	46.0	0.799	6.9E+09			
37.8	48.0	0.926	1.2E+10			
37.8	50.0	1.066	2.1E+10			
37.8	52.0	1.220	3.3E+10			
37.8	54.0	1.391	5.0E+10			
37.8	56.0	1.577	7.3E+10			
37.8	58.0	1.780	1.0E+11			
37.8	60.0	2.001	1.4E+11			

9.2 EPS 2 CALCULATIONS

9.2.1 Input

PRECAST PRESTRESSED CONCRETE SANDWICH WALL PANEL DATA INPUT

Input and Properties:

Dimensions	Width	b	12	ft
	Width	b	144	in
	Height to axial load	H'	19	ft
	Height to axial load	H'	228	in
	Total height	H	20	ft
	Total height	H	240	in
	Inner wythe thickness	t_1	2.67	in
	Outer wythe thickness	t_2	2.00	in
	Insulation thickness	t_3	3.33	in
	Total thickness	t	8.00	in
	Composite top extreme fiber	$y_{t,c}$	3.86	in
	Composite bottom extreme fiber	$y_{b,c}$	4.14	in
	Inner wythe top extreme fiber	$y_{t,i}$	1.50	in
	Inner wythe bottom extreme fiber	$y_{b,i}$	2.50	in
	Outer wythe top extreme fiber	$y_{t,o}$	1.00	in
	Outer wythe bottom extreme fiber	$y_{b,o}$	1.00	in
	Composite centroid to inner centroid	d_i	2.36	in
	Composite centroid to outer centroid	d_o	3.14	in
	Top panel to top corbel	a_1	12	in
	End of panel to lateral load	a_2	60	in
	Bottom panel to measured lateral deflection	x_1	120	in
	Top panel to measured lateral delfection	x	120	in
	Bottom panel to maximum moment	x_2	180	in
	Top panel to maximum moment	x_3	60	in
Section properties	Inner wythe area	$A_{c,i}$	384	in^2
	Outer wythe area	$A_{c,o}$	288	in^2
	Concrete area	A_c	672	in^2
	Fully composite MOI	I_c	5493	in^4
	Inner wythe MOI	$I_{nc,i}$	416	in^4
	Outer wythe MOI	$I_{nc,o}$	96	in^4
	Fully noncomposite MOI	I_{nc}	512	in^4
	Inner wythe stiffness	%I	81.3%	
	Outer wythe stiffness	%O	18.8%	
Prestress properties	Prestressed area both wythes	$A_{p,c}$	0.85	in^2
	Prestressed area inner wythe	$A_{p,i}$	0.425	in^2
	Prestressed area outer wythe	$A_{p,o}$	0.425	in^2
	Fully composite prestressing depth	$d_{p,c}$	4.00	in
	Fully composite prestressing eccentricity	$e_{p,c}$	0.14	in

Prestress properties	Inner wythe prestressing depth	$d_{p,i}$	1.00	in
	Inner wythe prestressing eccentricity	$e_{p,i}$	-0.50	in
	Outer wythe prestressing depth	$d_{p,o}$	1.00	in
	Outer wythe prestressing eccentricity	$e_{p,o}$	0.00	in
	Prestressing modulus	E_{ps}	28500	ksi
	Strand yield strength	f_{py}	243	ksi
	Strand ultimate strength	f_{pu}	270	ksi
	Yield/Ultimate	f_{pi}/f_{pu}	0.75	
	Initial prestressing strength	f_{pi}	202.5	ksi
	Initial compsote prestressing force	$P_{i,c}$	172	kip
	Initial inner wythe prestressing force	$P_{i,i}$	86	kip
	Initial outer wythe prestressing force	$P_{i,o}$	86	kip
	1-losses	R	85%	
	Effective compsote prestressing force	$P_{e,o}$	146	kip
	Effective inner wythe prestressing force	$P_{e,i}$	73	kip
	Effective inner wythe prestressing force	$P_{e,o}$	73	kip
	Time to testing	t_{relax}	2184	hrs
	Time to set	t_{set}	16	hrs
	Relative humidity	RH	70	%
	Volume of concrete	V	161395	in^3
	Specimen surface area	S	140544	in^2
	Volume/surface area	V/S	1.14836	in
	Friction loss coefficient	k	0	
	Shrinkage coefficient	ksh	1	
	Creep coeficient	kcr	2	
	Anchorage Seating	Δ_A	0	in
	Friction coefficient	μ	0	
	Wobble coefficient	α	0	

Note: Percent composite action and deflections calculated at mid-height

Note: Moment capacities and ultimate load calculated at3/4-height

Mild steel properties	Steel area both wythes	$A_{s,c}$	0.3296	in^2
	Steel area each wythe	$A_{s,nc}$	0.1648	in^2
	Steel modulus	E_s	29000	ksi
	Fully composite steel depth	$d_{s,c}$	4.00	in
	Inner wythe steel depth	$d_{s,i}$	1.00	in
	Outer wythe steel depth	$d_{s,o}$	1.00	in
	Strand yield strength	f_{sy}	65	ksi
Concrete properties	Concrete unit weight	γ_c	145	pcf
	Initial concrete strength	f'_{ci}	3.5	psi
	Initial concrete modulus	E_{ci}	1686	ksi
	Concrete strength	f'_c	7.67	ksi
	Concrete modulus	E_c	2496	ksi
	Maximum concrete strain	ε_{cu}	0.003	in/in
	Tension modulus constant	$K\sqrt{f'_c}=$	10.0	
	Tension modulus	$f_r=$	0.876	ksi
	NA depth constant	β_1	0.6665	
	Initial prestressed modular ratio	n_i	16.903	
	Prestressed modular ratio	n	11.418	
Safety factors	Flexural phi factor	ϕ_f	0.9	
	Shear phi factor	ϕ_v	0.85	
Loads	Composite axial load	P_{axial}	37.8	kip
	Inner wythe axial load	$P_{axial,i}$	37.8	kip
	Outer wythe axial load	$P_{axial,o}$	0.0	kip
	Wythe surface to axial load	a_3	6	in
	Composite axial load eccentricity	$e_{a,c}$	9.86	in
	Inner wythe axial load eccentricity	$e_{a,i}$	7.50	in
	Outer wythe axial load eccentricity	$e_{a,o}$	13.00	in
	Composite axial load moment	$M_{e,c}$	373	kip-in
	Inner wythe axial load moment	$M_{e,i}$	284	kip-in
	Outer wythe axial load moment	$M_{e,o}$	0	kip-in
Cracking properties	Composite cracking moment	$M_{cr,c}$	1546	kip-in
	Inner wythe cracking moment	$M_{cr,i}$	157	kip-in
	Outer wythe cracking moment	$M_{cr,o}$	108	kip-in
	Composite cracking MOI	$I_{cr,c}$	285	in^4
	Inner wythe cracking MOI	$I_{cr,i}$	4.5	in^4
	Outer wythe cracking MOI	$I_{cr,o}$	4.5	in^4
Deflection	Initial bow	e_i	0	in

9.2.2 Prestressing Losses

PRECAST PRESTRESSED CONCRETE SANDWICH WALL PANEL DATA INPUT

Stage 0: Jacking

Anchorage Seating Losses			**Friction Losses**		
Δf_{pA} =	**0**	**ksi**	**Δf_{pF} =**	**0**	**ksi**
Stage 0 Loss =	**0**	**ksi**			
f_{pi} =	**202.5**	**kip**			

Stage I: Stress Transfer

Steel Relaxation Losses

t_1 =	0	hrs
t_2 =	16	hrs
f_{pi} =	203	ksi
Δf_{pR} =	**6.9**	**ksi**

Elastic Shortening Losses

Ass. Δf_{pES} =	3.02	ksi			
f_{pi} =	193	ksi			
$P_{i,i}$ =	82	kip	$P_{axial,i}$ =	37.8	kip
$P_{i,o}$ =	82	kip			

Elastic Shortening

M_D =	0	kip-ft
M_D =	0	kip-in
$f_{pES,i}$ =	-0.166	ksi
$f_{pES,o}$ =	-0.191	ksi
$\Delta f_{pES,i}$ =	**2.81**	**ksi**
$\Delta f_{pES,o}$ =	**3.23**	**ksi**
Difference =	0.00	
Stage I Loss =	**9.93**	**ksi**
f_{pi} =	**193**	**kip**

Stage II: Transfer to Placement of Superimposed Dead Load

Creep Losses

M_{SD} =	0	kip-ft
M_{SD} =	0	kip-in
f_{csi} =	0.166	ksi
f_{csd} =	0.000	ksi
f_{csd} =	0.000	ksi
Δf_{pCR} =	**3.79**	**ksi**

Shrinkage Losses

Δf_{pSH} =	**6.53**	**ksi**

Steel Relaxation Losses

t_1 =	16	hrs
t_2 =	2184	hrs
f_{pi} =	193	ksi
Δf_{pR} =	**9.97**	**ksi**

Stress Increase Due to Loading

Δf_{SD} =	**0.00**	**ksi**

Stage II Loss =	**20.3**	**ksi**
f_{pi} =	**172**	**kip**

Total Losses =	**20**	**ksi**
f_{pe} =	**172**	**ksi**
P_e =	**146**	**kip**
R =	**85%**	
Losses =	**15%**	

9.2.3 Cracked Moment of Inertia

REINFORCED CONCRETE SANDWICH WALL PANEL CRACKED MOMENT OF INERTIA

x<d1			x≥d1			Outer wythe		
b =	144	in	b =	144	in	b =	144	in
do =	7	in	do =	7	in	do =	na	in
d1 =	'	in	d1 =	1	in	d1 =	1	in
t1 =	2.67	in	t1 =	2.67	in	t1 =	2.67	in
As =	0.1648	Awythe [in²]	As =	0.1648	Awythe [in²]	As =	0.1648	Awythe [in²]
Aps =	0.425	Inner wythe [in²]	Aps =	0.425	Inner wythe [in²]	Aps =	0.425	Inner wythe [in²]
Aps =	0.425	Outer wythe [in²]	Aps =	0.425	Outer wythe [in²]	Aps =	0.425	Outer wythe [in²]
Es =	29000000	psi	Es =	29000000	psi	Es =	29000000	psi
Epr =	28500000	psi	Epr =	28500000	psi	Epr =	28500000	psi
Ec =	2495900	psi	Ec =	2495900.20	psi	Ec =	2495900.20	psi
ns =	11.619		ns =	11.619		ns =	11.619	
nps =	11.418		nps =	11.418		nps =	11.418	

Composite			Composite			Outer Non-Composite		
a =	72		a =	72		a =	72	
b =	13.535		b =	6.768		b =	6.768	
c =	54.140		c =	47.373		c =	6.768	
x =	0.778	in	x =	0.766	in	x =	0.253	in
	-0.968	in		-0.360	in		-0.357	in
I_{comp} =	284.9	in⁴	I_{comp} =	284.6	in⁴	$I_{non\text{-}comp\,wythe}$ =	4.5	in⁴

Inner Non-Composite		
a =	72	
b =	6.768	
c =	6.768	
x =	0.263	in
	-0.357	in
$I_{non\text{-}comp\,wythe}$ =	4.5	in⁴

9.2.4 Composite Deflection

REINFORCED CONCRETE SANDWICH WALL PANEL COMPOSITE DEFELCTION

P_{axial}	$P_{lateral}$	$2P_{lateral}$	M_a	I_{eff}	EI	Δ_{app}	Δ_{p-D}/e_i	e_t
kip	kip	kip	kip-in	in^4	$kip-in^2$	in	in/in	in
37.8	0	0	177	5493	13710375	0.097	0.020	0.097
37.8	1	2	237	5493	13710375	0.126	0.020	0.126
37.8	2.5	5	327	5493	13710375	0.169	0.020	0.169
37.8	3.5	7	387	5493	13710375	0.198	0.020	0.198
37.8	4	8	417	5493	13710375	0.212	0.020	0.212
37.8	5.45	10.9	504	5493	13710375	0.254	0.020	0.254
37.8	6	12	537	5493	13710375	0.270	0.020	0.270
37.8	7	14	597	5493	13710375	0.299	0.020	0.299
37.8	8	16	657	5493	13710375	0.328	0.020	0.328
37.8	9	18	717	5493	13710375	0.357	0.020	0.357
37.8	9.5	19	747	5493	13710375	0.371	0.020	0.371
37.8	11	22	837	5493	13710375	0.415	0.020	0.415
37.8	12	24	897	5493	13710375	0.443	0.020	0.443
37.8	13	26	957	5493	13710375	0.472	0.020	0.472
37.8	14	28	1017	5493	13710375	0.501	0.020	0.501
37.8	14.8	29.6	1065	5493	13710375	0.524	0.020	0.524
37.8	16	32	1137	5493	13710375	0.559	0.020	0.559
37.8	17	34	1197	5493	13710375	0.588	0.020	0.588
37.8	18	36	1257	5493	13710375	0.617	0.020	0.617
37.8	19	38	1317	5493	13710375	0.646	0.020	0.646
37.8	20	40	1377	5493	13710375	0.675	0.020	0.675
37.8	21	42	1437	5493	13710375	0.703	0.020	0.703
37.8	22	44	1497	5493	13710375	0.732	0.020	0.732
37.8	23	46	1557	5363	13436095	0.777	0.020	0.777
37.8	24	48	1617	4836	12071532	0.897	0.023	0.897
37.8	25	50	1677	4365	10895306	1.031	0.025	1.031
37.8	26	52	1737	3957	9876011	1.177	0.028	1.177
37.8	27	54	1797	3601	8988326	1.337	0.030	1.337
37.8	28	56	1857	3290	8211677	1.512	0.033	1.512
37.8	29	58	1917	3017	7529231	1.702	0.036	1.702
37.8	30	60	1977	2775	6927127	1.907	0.039	1.907

Δ_1	e_2	Δ_2	error	e_3	Δ_3	error	e_4	Δ_4
in	in	in	%	in	in	%	in	in
0.002	0.099	0.002	1.99%	0.099	0.002	0.04%	0.099	0.002
0.002	0.128	0.003	1.99%	0.128	0.003	0.04%	0.128	0.003
0.003	0.172	0.003	1.99%	0.173	0.003	0.04%	0.173	0.003
0.004	0.202	0.004	1.99%	0.202	0.004	0.04%	0.202	0.004
0.004	0.217	0.004	1.99%	0.217	0.004	0.04%	0.217	0.004
0.005	0.259	0.005	1.99%	0.259	0.005	0.04%	0.259	0.005
0.005	0.276	0.005	1.99%	0.276	0.005	0.04%	0.276	0.005
0.006	0.305	0.006	1.99%	0.305	0.006	0.04%	0.305	0.006
0.007	0.334	0.007	1.99%	0.335	0.007	0.04%	0.335	0.007
0.007	0.364	0.007	1.99%	0.364	0.007	0.04%	0.364	0.007
0.007	0.379	0.008	1.99%	0.379	0.008	0.04%	0.379	0.008
0.008	0.423	0.008	1.99%	0.423	0.008	0.04%	0.423	0.008
0.009	0.452	0.009	1.99%	0.452	0.009	0.04%	0.452	0.009
0.009	0.482	0.010	1.99%	0.482	0.010	0.04%	0.482	0.010
0.010	0.511	0.010	1.99%	0.511	0.010	0.04%	0.511	0.010
0.010	0.535	0.011	1.99%	0.535	0.011	0.04%	0.535	0.011
0.011	0.570	0.011	1.99%	0.570	0.011	0.04%	0.570	0.011
0.012	0.600	0.012	1.99%	0.600	0.012	0.04%	0.600	0.012
0.012	0.629	0.012	1.99%	0.629	0.012	0.04%	0.629	0.012
0.013	0.658	0.013	1.99%	0.659	0.013	0.04%	0.659	0.013
0.013	0.688	0.014	1.99%	0.688	0.014	0.04%	0.688	0.014
0.014	0.717	0.014	1.99%	0.718	0.014	0.04%	0.718	0.014
0.015	0.747	0.015	1.99%	0.747	0.015	0.04%	0.747	0.015
0.016	0.792	0.016	2.03%	0.793	0.016	0.04%	0.793	0.016
0.020	0.918	0.021	2.25%	0.918	0.021	0.05%	0.918	0.021
0.026	1.056	0.026	2.50%	1.057	0.026	0.06%	1.057	0.026
0.032	1.209	0.033	2.76%	1.210	0.033	0.07%	1.210	0.033
0.040	1.378	0.042	3.03%	1.379	0.042	0.09%	1.379	0.042
0.050	1.562	0.052	3.31%	1.564	0.052	0.11%	1.564	0.052
0.062	1.763	0.064	3.61%	1.765	0.064	0.13%	1.765	0.064
0.075	1.982	0.078	3.93%	1.985	0.078	0.15%	1.985	0.078

9.2.5 Non-composite Deflection

REINFORCED CONCRETE SANDWICH WALL PANEL NON-COMPOSITE DEFELCTION

P_{axial}	$P_{lateral}$	$2P_{lateral}$	M_s	$M_{s,l}$	$M_{s,o}$	$I_{eff,i}$	$I_{eff,o}$	I_{eff}	EI
kip	kip	kip	kip-in	kip-in	kip-in	in^4	in^4	in^4	$kip\text{-}in^2$
37.8	0	0	177	135	0	416	96	512	1277946
37.8	1	2	237	183	11	263	96	359	897183
37.8	2.5	5	327	257	28	99	96	195	487132
37.8	3.5	7	387	305	39	61	96	157	391101
37.8	4	8	417	330	45	49	96	145	362259
37.8	5.45	10.9	504	400	61	29	96	125	313105
37.8	6	12	537	427	68	25	96	121	302124
37.8	7	14	597	476	79	19	96	115	287959
37.8	8	16	657	525	90	16	96	112	278577
37.8	9	18	717	573	101	13	96	109	272117
37.8	9.5	19	747	598	107	12	96	108	269634
37.8	11	22	837	671	124	10	66	76	189683
37.8	12	24	897	720	135	9	52	61	151849
37.8	13	26	957	768	146	8	42	50	124655
37.8	14	28	1017	817	158	7	34	42	104604
37.8	14.8	29.6	1065	856	167	7	30	37	92197
37.8	16	32	1137	915	180	7	25	31	77888
37.8	17	34	1197	963	191	6	21	28	68827
37.8	18	36	1257	1012	203	6	19	25	61648
37.8	19	38	1317	1061	214	6	17	22	55888
37.8	20	40	1377	1110	225	6	15	21	51211
37.8	21	42	1437	1158	236	6	13	19	47374
37.8	22	44	1497	1207	248	5	12	18	44197
37.8	23	46	1557	1256	259	5	11	17	41543
37.8	24	48	1617	1305	270	5	10	16	39310
37.8	25	50	1677	1353	281	5	10	15	37416
37.8	26	52	1737	1402	293	5	9	14	35800
37.8	27	54	1797	1451	304	5	9	14	34413
37.8	28	56	1857	1500	315	5	8	13	33215
37.8	29	58	1917	1548	326	5	8	13	32175
37.8	30	60	1977	1597	338	5	8	13	31268

Δ_{app}	Δ_{P-D}/e	e_1	Δ_1	e_2	Δ_2	error	e_3	Δ_3
in	in/in	in	in	in	in	%	in	in
1.039	0.213	1.039	0.221	1.261	0.269	21.30%	1.308	0.279
1.922	0.303	1.922	0.583	2.505	0.760	30.33%	2.682	0.814
4.759	0.559	4.759	2.659	7.418	4.144	55.87%	8.904	4.974
6.940	0.696	6.940	4.830	11.770	8.190	69.59%	15.131	10.529
8.039	0.751	8.039	6.040	14.079	10.578	75.13%	18.617	13.987
11.135	0.869	11.135	9.679	20.814	18.093	86.92%	29.228	25.406
12.261	0.901	1.2E+01	1.1E+01	2.3E+01	2.1E+01	90.08%	3.3E+01	3.0E+01
14.239	0.945	1.4E+01	1.3E+01	2.8E+01	2.6E+01	94.51%	4.0E+01	3.8E+01
16.140	0.977	1.6E+01	1.6E+01	3.2E+01	3.1E+01	97.70%	4.7E+01	4.6E+01
17.979	1.000	1.8E+01	1.8E+01	3.6E+01	3.6E+01	100.02%	5.4E+01	5.4E+01
18.879	1.009	1.9E+01	1.9E+01	3.8E+01	3.8E+01	100.94%	5.7E+01	5.8E+01
29.968	1.435	3.0E+01	4.3E+01	7.3E+01	1.0E+02	143.48%	1.3E+02	1.9E+02
40.042	1.792	4.0E+01	7.2E+01	1.1E+02	2.0E+02	179.23%	2.4E+02	4.3E+02
51.954	2.183	5.2E+01	1.1E+02	1.7E+02	3.6E+02	218.33%	4.1E+02	9.0E+02
65.699	2.602	6.6E+01	1.7E+02	2.4E+02	6.2E+02	260.18%	6.8E+02	1.8E+03
77.976	2.952	7.8E+01	2.3E+02	3.1E+02	9.1E+02	295.19%	9.9E+02	2.9E+03
98.403	3.494	9.8E+01	3.4E+02	4.4E+02	1.5E+03	349.43%	1.6E+03	5.7E+03
117.111	3.954	1.2E+02	4.6E+02	5.8E+02	2.3E+03	395.43%	2.4E+03	9.5E+03
137.171	4.415	1.4E+02	6.1E+02	7.4E+02	3.3E+03	441.47%	3.4E+03	1.5E+04
158.395	4.870	1.6E+02	7.7E+02	9.3E+02	4.5E+03	486.98%	4.7E+03	2.3E+04
180.594	5.315	1.8E+02	9.6E+02	1.1E+03	6.1E+03	531.45%	6.2E+03	3.3E+04
203.578	5.745	2.0E+02	1.2E+03	1.4E+03	7.9E+03	574.49%	8.1E+03	4.6E+04
227.173	6.158	2.3E+02	1.4E+03	1.6E+03	1.0E+04	615.79%	1.0E+04	6.3E+04
251.215	6.551	2.5E+02	1.6E+03	1.9E+03	1.2E+04	655.12%	1.3E+04	8.3E+04
275.563	6.923	2.8E+02	1.9E+03	2.2E+03	1.5E+04	692.35%	1.5E+04	1.1E+05
300.093	7.274	3.0E+02	2.2E+03	2.5E+03	1.8E+04	727.39%	1.8E+04	1.3E+05
324.701	7.602	3.2E+02	2.5E+03	2.8E+03	2.1E+04	760.22%	2.2E+04	1.6E+05
349.300	7.909	3.5E+02	2.8E+03	3.1E+03	2.5E+04	790.87%	2.5E+04	2.0E+05
373.821	8.194	3.7E+02	3.1E+03	3.4E+03	2.8E+04	819.40%	2.9E+04	2.3E+05
398.209	8.459	4.0E+02	3.4E+03	3.8E+03	3.2E+04	845.88%	3.2E+04	2.7E+05
422.423	8.704	4.2E+02	3.7E+03	4.1E+03	3.6E+04	870.41%	3.6E+04	3.1E+05

error	e_4	Δ_4	error	e_5	Δ_5	error	e_6	Δ_6
%	in	in	%	in	in	%	in	in
3.74%	1.318	0.281	0.77%	1.320	0.281	0.16%	1.321	0.281
7.06%	2.735	0.830	2.00%	2.752	0.835	0.59%	2.757	0.836
20.03%	9.734	5.438	9.32%	10.197	5.697	4.76%	10.456	5.842
28.55%	17.469	12.157	15.46%	19.097	13.289	9.32%	20.229	14.077
32.23%	22.026	16.548	18.31%	24.587	18.472	11.63%	26.511	19.918
40.42%	36.541	31.762	25.02%	42.898	37.288	17.40%	48.423	42.091
42.69%	4.2E+01	3.8E+01	26.95%	5.0E+01	4.5E+01	19.12%	5.8E+01	5.2E+01
45.92%	5.2E+01	5.0E+01	29.74%	6.4E+01	6.0E+01	21.67%	7.5E+01	7.0E+01
48.28%	6.2E+01	6.1E+01	31.81%	7.7E+01	7.5E+01	23.58%	9.1E+01	8.9E+01
50.01%	7.2E+01	7.2E+01	33.34%	9.0E+01	9.0E+01	25.01%	1.1E+02	1.1E+02
50.70%	7.7E+01	7.7E+01	33.96%	9.6E+01	9.7E+01	25.59%	1.2E+02	1.2E+02
84.55%	2.2E+02	3.2E+02	65.74%	3.5E+02	5.0E+02	56.91%	5.3E+02	7.6E+02
115.04%	4.7E+02	8.4E+02	95.88%	8.8E+02	1.6E+03	87.73%	1.6E+03	2.9E+03
149.74%	9.5E+02	2.1E+03	130.91%	2.1E+03	4.7E+03	123.78%	4.7E+03	1.0E+04
187.95%	1.8E+03	4.8E+03	169.82%	4.8E+03	1.3E+04	163.76%	1.3E+04	3.3E+04
220.50%	3.0E+03	8.8E+03	203.09%	8.9E+03	2.6E+04	197.80%	2.6E+04	7.8E+04
271.68%	5.8E+03	2.0E+04	255.41%	2.1E+04	7.2E+04	251.11%	7.2E+04	2.5E+05
315.61%	9.7E+03	3.8E+04	300.29%	3.8E+04	1.5E+05	296.64%	1.5E+05	6.0E+05
359.94%	1.5E+04	6.7E+04	345.49%	6.7E+04	3.0E+05	342.37%	3.0E+05	1.3E+06
404.01%	2.3E+04	1.1E+05	390.36%	1.1E+05	5.5E+05	387.67%	5.5E+05	2.7E+06
447.29%	3.3E+04	1.8E+05	434.35%	1.8E+05	9.4E+05	431.99%	9.4E+05	5.0E+06
489.32%	4.7E+04	2.7E+05	477.01%	2.7E+05	1.5E+06	474.93%	1.5E+06	8.9E+06
529.76%	6.3E+04	3.9E+05	518.01%	3.9E+05	2.4E+06	516.15%	2.4E+06	1.5E+07
568.36%	8.3E+04	5.5E+05	557.10%	5.5E+05	3.6E+06	555.42%	3.6E+06	2.3E+07
604.97%	1.1E+05	7.4E+05	594.14%	7.4E+05	5.1E+06	592.60%	5.1E+06	3.5E+07
639.47%	1.3E+05	9.7E+05	629.02%	9.7E+05	7.1E+06	627.61%	7.1E+06	5.2E+07
671.85%	1.6E+05	1.2E+06	661.73%	1.2E+06	9.5E+06	660.42%	9.5E+06	7.2E+07
702.10%	2.0E+05	1.6E+06	692.27%	1.6E+06	1.2E+07	691.05%	1.2E+07	9.8E+07
730.27%	2.3E+05	1.9E+06	720.71%	1.9E+06	1.6E+07	719.56%	1.6E+07	1.3E+08
756.45%	2.7E+05	2.3E+06	747.11%	2.3E+06	2.0E+07	746.02%	2.0E+07	1.7E+08
780.72%	3.1E+05	2.7E+06	771.58%	2.7E+06	2.4E+07	770.55%	2.4E+07	2.1E+08

error	e_7	Δ_7	error	e_8	Δ_8	error	e_9
%	in	in	%	in	in	%	in
0.03%	1.321	0.281	0.01%	1.321	0.281	0.00%	1.321
0.18%	2.758	0.837	0.05%	2.759	0.837	0.02%	2.759
2.54%	10.601	5.923	1.38%	10.682	5.968	0.76%	10.727
5.93%	21.017	14.626	3.90%	21.566	15.007	2.61%	21.948
7.83%	27.957	21.004	5.45%	29.043	21.820	3.88%	29.859
12.88%	53.226	46.266	9.92%	57.401	49.895	7.84%	61.030
14.46%	6.4E+01	5.8E+01	11.38%	7.0E+01	6.3E+01	9.21%	7.5E+01
16.83%	8.5E+01	8.0E+01	13.62%	9.4E+01	8.9E+01	11.33%	1.0E+02
18.64%	1.1E+02	1.0E+02	15.35%	1.2E+02	1.2E+02	13.00%	1.3E+02
20.01%	1.3E+02	1.3E+02	16.68%	1.4E+02	1.4E+02	14.29%	1.6E+02
20.57%	1.4E+02	1.4E+02	17.22%	1.6E+02	1.6E+02	14.83%	1.8E+02
52.04%	7.9E+02	1.1E+03	49.11%	1.2E+03	1.7E+03	47.26%	1.7E+03
83.76%	3.0E+03	5.3E+03	81.70%	5.3E+03	9.6E+03	80.59%	9.6E+03
120.76%	1.0E+04	2.3E+04	119.43%	2.3E+04	4.9E+04	118.83%	4.9E+04
161.54%	3.3E+04	8.6E+04	160.70%	8.6E+04	2.2E+05	160.38%	2.2E+05
196.07%	7.8E+04	2.3E+05	195.49%	2.3E+05	6.8E+05	195.29%	6.8E+05
249.91%	2.5E+05	8.8E+05	249.56%	8.8E+05	3.1E+06	249.47%	3.1E+06
295.73%	6.0E+05	2.4E+06	295.51%	2.4E+06	9.4E+06	295.45%	9.4E+06
341.68%	1.3E+06	5.8E+06	341.52%	5.8E+06	2.6E+07	341.48%	2.6E+07
387.12%	2.7E+06	1.3E+07	387.01%	1.3E+07	6.3E+07	386.98%	6.3E+07
431.55%	5.0E+06	2.7E+07	431.47%	2.7E+07	1.4E+08	431.46%	1.4E+08
474.57%	8.9E+06	5.1E+07	474.51%	5.1E+07	2.9E+08	474.49%	2.9E+08
515.85%	1.5E+07	9.1E+07	515.80%	9.1E+07	5.6E+08	515.79%	5.6E+08
555.17%	2.3E+07	1.5E+08	555.13%	1.5E+08	1.0E+09	555.12%	1.0E+09
592.38%	3.5E+07	2.5E+08	592.35%	2.5E+08	1.7E+09	592.35%	1.7E+09
627.42%	5.2E+07	3.7E+08	627.39%	3.7E+08	2.7E+09	627.39%	2.7E+09
660.25%	7.2E+07	5.5E+08	660.22%	5.5E+08	4.2E+09	660.22%	4.2E+09
690.89%	9.8E+07	7.7E+08	690.87%	7.7E+08	6.1E+09	690.87%	6.1E+09
719.42%	1.3E+08	1.1E+09	719.40%	1.1E+09	8.7E+09	719.40%	8.7E+09
745.89%	1.7E+08	1.4E+09	745.88%	1.4E+09	1.2E+10	745.88%	1.2E+10
770.43%	2.1E+08	1.8E+09	770.41%	1.8E+09	1.6E+10	770.41%	1.6E+10

Δ_9	error	e_{10}	Δ_{10}	error
in	%	in	in	%
0.281	0.00%	1.321	0.281	0.00%
0.837	0.00%	2.759	0.837	0.00%
5.993	0.42%	10.752	6.007	0.24%
15.273	1.77%	22.213	15.458	1.21%
22.433	2.81%	30.472	22.893	2.05%
53.049	6.32%	64.184	55.791	5.17%
6.8E+01	7.59%	8.0E+01	7.2E+01	6.36%
9.8E+01	9.62%	1.1E+02	1.1E+02	8.29%
1.3E+02	11.24%	1.5E+02	1.4E+02	9.87%
1.6E+02	12.51%	1.8E+02	1.8E+02	11.12%
1.8E+02	13.03%	2.0E+02	2.0E+02	11.64%
2.4E+03	46.05%	2.5E+03	3.6E+03	45.24%
1.7E+04	79.98%	1.7E+04	3.1E+04	79.65%
1.1E+05	118.56%	1.1E+05	2.4E+05	118.44%
5.8E+05	160.26%	5.8E+05	1.5E+06	160.21%
2.0E+06	195.23%	2.0E+06	5.9E+06	195.21%
1.1E+07	249.44%	1.1E+07	3.7E+07	249.43%
3.7E+07	295.43%	3.7E+07	1.5E+08	295.43%
1.1E+08	341.47%	1.1E+08	5.0E+08	341.47%
3.1E+08	386.98%	3.1E+08	1.5E+09	386.98%
7.5E+08	431.45%	7.5E+08	4.0E+09	431.45%
1.7E+09	474.49%	1.7E+09	9.7E+09	474.49%
3.5E+09	515.79%	3.5E+09	2.1E+10	515.79%
6.6E+09	555.12%	6.6E+09	4.3E+10	555.12%
1.2E+10	592.35%	1.2E+10	8.2E+10	592.35%
2.0E+10	627.39%	2.0E+10	1.4E+11	627.39%
3.2E+10	660.22%	3.2E+10	2.4E+11	660.22%
4.8E+10	690.87%	4.8E+10	3.8E+11	690.87%
7.1E+10	719.40%	7.1E+10	5.8E+11	719.40%
1.0E+11	745.88%	1.0E+11	8.5E+11	745.88%
1.4E+11	770.41%	1.4E+11	1.2E+12	770.41%

9.2.6 Deflection Percent Composite Action

REINFORCED CONCRETE SANDWICH WALL PANEL PERCENT COMPOSITE ACTION

P_{max} =	19.8	kip	Axial Load deflection:	0.062	in
P_y =	15	kip	1st 5k deflection:	0.184	in
Δ_y =	0.845	in	%PCA Axial Load:	103.0%	
Δ_i =	0.395	in	%PCA 1st 5k:	99.9%	
n =	6.0				
E =	43				
Elastic stiffness =	33	ksi			

	Service Load	Deflection
Lat Id	10.9	0
	10.9	20

		Composite	Non-Composite	Test Data		Pessiki
Axial Load	Lat. Load	Deflection	Deflection	Lat. Load	Deflection	%PCA
kip	kip	in	in	kip	in	%
0	0.0	0	0	0.0	0.000	0%
37.8	0.0	0.099	1.321	0.0	0.395	76%
37.8	2.0	0.128	2.759	2.0	0.455	88%
37.8	5.0	0.173	10.752	5.0	0.545	96%
37.8	7.0	0.202	22.213	7.0	0.605	98.2%
37.8	8.0	0.217	30.472	8.0	0.635	99%
37.8	10.9	0.259	64.184	10.9	0.722	99.3%
37.8	12.0	0.276	80.125	12.0	0.755	99%
37.8	14.0	0.305	111.917	14.0	0.815	100%
37.8	16.0	0.335	145.661	16.0	0.892	100%
37.8	18.0	0.364	179.916	18.0	1.008	100%
37.8	19.0	0.379	196.947	19.0	1.096	100%
37.8	22.0	0.423	2.5E+03			
37.8	24.0	0.452	1.7E+04			
37.8	26.0	0.482	1.1E+05			
37.8	28.0	0.511	5.8E+05			
37.8	29.6	0.535	2.0E+06			
37.8	32.0	0.570	1.1E+07			
37.8	34.0	0.600	3.7E+07			
37.8	36.0	0.629	1.1E+08			
37.8	38.0	0.659	3.1E+08			
37.8	40.0	0.688	7.5E+08			
37.8	42.0	0.718	1.7E+09			
37.8	44.0	0.747	3.5E+09			
37.8	46.0	0.793	6.6E+09			
37.8	48.0	0.918	1.2E+10			
37.8	50.0	1.057	2.0E+10			
37.8	52.0	1.210	3.2E+10			
37.8	54.0	1.379	4.8E+10			
37.8	56.0	1.564	7.1E+10			
37.8	58.0	1.765	1.0E+11			
37.8	60.0	1.985	1.4E+11			

9.3 XPS 1 CALCULATIONS

9.3.1 Input

PRECAST PRESTRESSED CONCRETE SANDWICH WALL PANEL DATA INPUT

Input and Properties:

Dimensions	Width	b	12	ft
	Width	b	144	in
	Height to axial load	H'	19	ft
	Height to axial load	H'	228	in
	Total height	H	20	ft
	Total height	H	240	in
	Inner wythe thickness	t_1	2.67	in
	Outer wythe thickness	t_2	2.00	in
	Insulation thickness	t_3	3.33	in
	Total thickness	t	8.00	in
	Composite top extreme fiber	$y_{t,c}$	3.86	in
	Composite bottom extreme fiber	$y_{b,c}$	4.14	in
	Inner wythe top extreme fiber	$y_{t,i}$	1.50	in
	Inner wythe bottom extreme fiber	$y_{b,i}$	2.50	in
	Outer wythe top extreme fiber	$y_{t,o}$	1.00	in
	Outer wythe bottom extreme fiber	$y_{b,o}$	1.00	in
	Composite centroid to inner centroid	d_i	2.36	in
	Composite centroid to outer centroid	d_o	3.14	in
	Top panel to top corbe	a_1	12	in
	End of panel to lateral load	a_2	60	in
	Bottom panel to measured lateral deflection	x_1	120	in
	Top panel to measured lateral deflection	x	120	in
	Bottom panel to maximum moment	x_2	180	in
	Top panel to maximum moment	x_3	60	in
Section properties	Inner wythe area	$A_{c,i}$	334	in^2
	Outer wythe area	$A_{c,o}$	238	in^2
	Concrete area	A_c	672	in^2
	Fully composite MOI	I_c	5490	in^4
	Inner wythe MOI	$I_{nc,i}$	416	in^4
	Outer wythe MOI	$I_{nc,o}$	96	in^4
	Fully noncomposite MOI	I_{nc}	512	in^4
	Inner wythe stiffness	%I	81.3%	
	Outer wythe stiffness	%O	18.8%	
Prestress properties	Prestressed area both wythes	$A_{p,c}$	0.85	in^2
	Prestressed area inner wythe	$A_{p,i}$	0.425	in^2
	Prestressed area outer wythe	$A_{p,o}$	0.425	in^2
	Fully composite prestressing depth	$d_{p,c}$	4.00	in
	Fully composite prestressing eccentricity	$e_{p,c}$	0.14	in

Prestress properties	Inner wythe prestressing depth	$d_{p,i}$	1.00	in
	Inner wythe prestressing eccentricity	$e_{p,i}$	-0.50	in
	Outer wythe prestressing depth	$d_{p,o}$	1.00	in
	Outer wythe prestressing eccentricity	$e_{p,o}$	0.00	in
	Prestressing modulus	E_{ps}	28500	ksi
	Strand yield strength	f_{py}	243	ksi
	Strand ultimate strength	f_{pu}	270	ksi
	Yield/Ultimate	f_{pi}/f_{pu}	0.75	
	Initial prestressing strength	f_{pi}	202.5	ksi
	Initial compsote prestressing force	$P_{i,c}$	172	kip
	Initial inner wythe prestressing force	$P_{i,i}$	86	kip
	Initial outer wythe prestressing force	$P_{i,o}$	86	kip
	1-losses	R	87%	
	Effective compsote prestressing force	$P_{e,o}$	149	kip
	Effective inner wythe prestressing force	$P_{e,i}$	75	kip
	Effective inner wythe prestressing force	$P_{e,o}$	75	kip
	Time to testing	t_{relax}	2184	hrs
	Time to set	t_{set}	16	hrs
	Relative humidity	RH	70	%
	Volume of concrete	V	161395	in^3
	Specimen surface area	S	140544	in^2
	Volume/surface area	V/S	1.14836	in
	Friction loss coefficient	k	0	
	Shrinkage coefficient	ksh	1	
	Creep coeficient	kcr	2	
	Anchorage Seating	Δ_A	0	in
	Friction coefficient	μ	0	
	Wobble coefficient	α	0	

Note: Percent composite action and deflections calculated at mid-height

Note: Moment capacities and ultimate load calculated at 3/4-height

Mild steel properties	Steel area both wythes	$A_{s,c}$	0.3296	in^2
	Steel area each wythe	$A_{s,nc}$	0.1648	in^2
	Steel modulus	E_s	29000	ksi
	Fully composite steel depth	$d_{s,c}$	4.00	in
	Inner wythe steel depth	$d_{s,i}$	1.00	in
	Outer wythe steel depth	$d_{s,o}$	1.00	in
	Strand yield strength	f_{sy}	65	ksi
Concrete properties	Concrete unit weight	γ_c	145	pcf
	Initial concrete strength	f'_{ci}	3.5	psi
	Initial concrete modulus	E_{ci}	3372	ksi
	Concrete strength	f'_c	10.08	ksi
	Concrete modulus	E_c	5723	ksi
	Maximum concrete strain	ε_{cu}	0.003	in/in
	Tension modulus constant	$K\sqrt{f'_c}=$	10.0	
	Tension modulus	$f_r=$	1.004	ksi
	NA depth constant	β_1	0.65	
	Initial prestressed modular ratio	n_i	8.452	
	Prestressed modular ratio	n	4.980	
Safety factors	Flexural phi factor	ϕ_f	0.9	
	Shear phi factor	ϕ_v	0.85	
Loads	Composite axial load	P_{axial}	37.8	kip
	Inner wythe axial load	$P_{axial,i}$	37.8	kip
	Outer wythe axial load	$P_{axial,o}$	0.0	kip
	Wythe surface to axial load	a_3	6	in
	Composite axial load eccentricity	$e_{a,c}$	9.86	in
	Inner wythe axial load eccentricity	$e_{a,i}$	7.50	in
	Outer wythe axial load eccentricity	$e_{a,o}$	13.00	in
	Composite axial load moment	$M_{e,c}$	373	kip-in
	Inner wythe axial load moment	$M_{e,i}$	284	kip-in
	Outer wythe axial load moment	$M_{e,o}$	0	kip-in
Cracking properties	Composite cracking moment	$M_{cr,c}$	1722	kip-in
	Inner wythe cracking moment	$M_{cr,i}$	178	kip-in
	Outer wythe cracking moment	$M_{cr,o}$	121	kip-in
	Composite cracking MOI	$I_{cr,c}$	131	in^4
	Inner wythe cracking MOI	$I_{cr,i}$	2.3	in^4
	Outer wythe cracking MOI	$I_{cr,o}$	2.3	in^4
Deflection	Initial bow	e_i	0	in

9.3.2 Prestressing Losses

PRECAST PRESTRESSED CONCRETE SANDWICH WALL PANEL DATA INPUT

Stage 0: Jacking

Anchorage Seating Losses

Δf_{pA} = 0 ksi

Friction Losses

Δf_{pF} = 0 ksi

Stage 0 Loss = 0 ksi

f_{pi} = 202.5 kip

Stage I: Stress Transfer

Steel Relaxation Losses

t_1 = 0 hrs

t_2 = 16 hrs

f_{pi} = 203 ksi

Δf_{pR} = **6.9** ksi

Elastic Shortening Losses

Ass. Δf_{pES} = 1.52 ksi

f_{pi} = 194 ksi

$P_{i,i}$ = 82 kip $P_{axial,i}$ = 37.8 kip

$P_{i,o}$ 82 kip

Elastic Shortening

M_D = 0 kip-ft

M_D = 0 kip-in

$f_{pES,i}$ = -0.167 ksi

$f_{pES,o}$ = -0.192 ksi

$\Delta f_{pES,i}$ = **1.41** ksi

$\Delta f_{pES,o}$ = **1.62** ksi

Difference = 0.00

Stage I Loss = **8.43** ksi

f_{pi} = **194** kip

Stage II: Transfer to Placement of Superimposed Dead Load

Creep Losses

M_{SD} =	0	kip-ft
M_{SD} =	0	kip-in
f_{csi} =	0.167	ksi
f_{csd} =	0.000	ksi
f_{csd} =	0.000	ksi
Δf_{pCR} =	**1.66**	**ksi**

Shrinkage Losses

Δf_{pSH} =	**6.53**	**ksi**

Steel Relaxation Losses

t_1 =	16	hrs
t_2 =	2184	hrs
f_{pi} =	194	ksi
Δf_{pR} =	**10.30**	**ksi**

Stress Increase Due to Loading

Δf_{SD} =	**0.00**	**ksi**

Stage II Loss =	**18.5**	**ksi**
f_{ci} =	**176**	**kip**

Total Losses =	**18**	**ksi**
f_{pe} =	**176**	**ksi**
P_{eff} =	**149**	**kip**
R =	**87%**	
Losses =	**13%**	

9.3.3 Cracked Moment of Inertia

REINFORCED CONCRETE SANDWICH WALL PANEL CRACKED MOMENT OF INERTIA

x<d₁

h =	144	in
d_o =	7	in
d_1 =	1	in
t_1 =	2.67	in
A_s =	0.1648	/wythe [in^2]
A_{ps} =	0.425	Inner wythe [in^2]
A_{ps} =	0.425	Outer wythe [in^2]
E_s =	29000000	ps
E_{ps} =	28500000	ps
E_c =	5722755	ps
n_s =	5.067	
n_{ps} =	4.980	

Composite

a =	72	
b =	5.903	
c =	23.613	
x =	0.533	in
	-0.615	in
I_{comp} =	131.4	in^4

Inner Non-Composite

a =	72	
b =	2.952	
c =	2.952	
x =	0.183	in
	-0.224	in
$I_{non\text{-}comp/wythe}$ =	2.3	in^4

x≥d₁

h =	144	in
d_o =	7	in
d_1 =	1	in
t_1 =	2.67	in
A_s =	0.1648	/wythe [in^2]
A_{ps} =	0.425	Inner wythe [in^2]
A_{ps} =	0.425	Outer wythe [in^2]
E_s =	29000000	psi
E_{ps} =	28500000	psi
E_c =	5722754.58	psi
n_s =	5.067	
n_{ps} =	4.980	

Composite

a =	72	
b =	2.952	
c =	20.652	
x =	0.516	in
	-0.557	in
I_{comp} =	130.7	in^4

Outer wythe

h =	144	in
d_o =	na	in
d =	1	in
t_1 =	2.67	in
A_s =	0.1648	/wythe [in^2]
A_{ps} =	0.425	Inner wythe [in^2]
A_{ps} =	0.425	Outer wythe [in^2]
E_s =	29000000	psi
E_{ps} =	28500000	psi
E_c =	5722754.58	psi
n_s =	5.067	
n_{ps} =	4.980	

Outer Non-Composite

a =	72	
b =	2.952	
c =	2.952	
x =	0.183	in
	-0.224	in
$I_{non\text{-}comp/wythe}$ =	2.3	in^4

9.3.4 Composite Deflection

REINFORCED CONCRETE SANDWICH WALL PANEL COMPOSITE DEFELCTION

P_{axial}	$P_{lateral}$	$2P_{lateral}$	M_a	I_{eff}	EI	Δ_{app}	Δ_{p-D}/e_i	e_t
kip	kip	kip	kip-in	in^4	$kip-in^2$	in	in/in	in
37.8	0	0	177	5493	31434888	0.042	0.009	0.042
37.8	1	2	237	5493	31434888	0.055	0.009	0.055
37.8	2.5	5	327	5493	31434888	0.074	0.009	0.074
37.8	3.5	7	387	5493	31434888	0.086	0.009	0.086
37.8	4	8	417	5493	31434888	0.093	0.009	0.093
37.8	5.45	10.9	504	5493	31434888	0.111	0.009	0.111
37.8	6	12	537	5493	31434888	0.118	0.009	0.118
37.8	7	14	597	5493	31434888	0.130	0.009	0.130
37.8	8	16	657	5493	31434888	0.143	0.009	0.143
37.8	9	18	717	5493	31434888	0.156	0.009	0.156
37.8	9.5	19	747	5493	31434888	0.162	0.009	0.162
37.8	11	22	837	5493	31434888	0.181	0.009	0.181
37.8	12	24	897	5493	31434888	0.193	0.009	0.193
37.8	13	26	957	5493	31434888	0.206	0.009	0.206
37.8	14	28	1017	5493	31434888	0.219	0.009	0.219
37.8	14.8	29.6	1065	5493	31434888	0.229	0.009	0.229
37.8	16	32	1137	5493	31434888	0.244	0.009	0.244
37.8	17	34	1197	5493	31434888	0.256	0.009	0.256
37.8	18	36	1257	5493	31434888	0.269	0.009	0.269
37.8	19	38	1317	5493	31434888	0.282	0.009	0.282
37.8	20	40	1377	5493	31434888	0.294	0.009	0.294
37.8	21	42	1437	5493	31434888	0.307	0.009	0.307
37.8	22	44	1497	5493	31434888	0.319	0.009	0.319
37.8	23	46	1557	5493	31434888	0.332	0.009	0.332
37.8	24	48	1617	5493	31434888	0.345	0.009	0.345
37.8	25	50	1677	5493	31434888	0.357	0.009	0.357
37.8	26	52	1737	5355	30646602	0.379	0.009	0.379
37.8	27	54	1797	4849	27751050	0.433	0.010	0.433
37.8	28	56	1857	4407	25217686	0.492	0.011	0.492
37.8	29	58	1917	4018	22991605	0.557	0.012	0.557
37.8	30	60	1977	3674	21027596	0.628	0.013	0.628

Δ_1	e_2	Δ_2	error	e_3	Δ_3	error	e_4	Δ_4
in	in	in	%	in	in	%	in	in
0.000	0.043	0.000	0.87%	0.043	0.000	0.01%	0.043	0.000
0.000	0.055	0.000	0.87%	0.055	0.000	0.01%	0.055	0.000
0.001	0.074	0.001	0.87%	0.074	0.001	0.01%	0.074	0.001
0.001	0.087	0.001	0.87%	0.087	0.001	0.01%	0.087	0.001
0.001	0.093	0.001	0.87%	0.093	0.001	0.01%	0.093	0.001
0.001	0.112	0.001	0.87%	0.112	0.001	0.01%	0.112	0.001
0.001	0.119	0.001	0.87%	0.119	0.001	0.01%	0.119	0.001
0.001	0.132	0.001	0.87%	0.132	0.001	0.01%	0.132	0.001
0.001	0.144	0.001	0.87%	0.144	0.001	0.01%	0.144	0.001
0.001	0.157	0.001	0.87%	0.157	0.001	0.01%	0.157	0.001
0.001	0.163	0.001	0.87%	0.163	0.001	0.01%	0.163	0.001
0.002	0.182	0.002	0.87%	0.182	0.002	0.01%	0.182	0.002
0.002	0.195	0.002	0.87%	0.195	0.002	0.01%	0.195	0.002
0.002	0.208	0.002	0.87%	0.208	0.002	0.01%	0.208	0.002
0.002	0.221	0.002	0.87%	0.221	0.002	0.01%	0.221	0.002
0.002	0.231	0.002	0.87%	0.231	0.002	0.01%	0.231	0.002
0.002	0.246	0.002	0.87%	0.246	0.002	0.01%	0.246	0.002
0.002	0.259	0.002	0.87%	0.259	0.002	0.01%	0.259	0.002
0.002	0.271	0.002	0.87%	0.271	0.002	0.01%	0.271	0.002
0.002	0.284	0.002	0.87%	0.284	0.002	0.01%	0.284	0.002
0.003	0.297	0.003	0.87%	0.297	0.003	0.01%	0.297	0.003
0.003	0.309	0.003	0.87%	0.309	0.003	0.01%	0.309	0.003
0.003	0.322	0.003	0.87%	0.322	0.003	0.01%	0.322	0.003
0.003	0.335	0.003	0.87%	0.335	0.003	0.01%	0.335	0.003
0.003	0.348	0.003	0.87%	0.348	0.003	0.01%	0.348	0.003
0.003	0.360	0.003	0.87%	0.360	0.003	0.01%	0.360	0.003
0.003	0.383	0.003	0.89%	0.383	0.003	0.01%	0.383	0.003
0.004	0.437	0.004	0.98%	0.437	0.004	0.01%	0.437	0.004
0.005	0.498	0.005	1.08%	0.498	0.005	0.01%	0.498	0.005
0.007	0.564	0.007	1.18%	0.564	0.007	0.01%	0.564	0.007
0.008	0.636	0.008	1.29%	0.636	0.008	0.02%	0.636	0.008

9.3.5 Non-composite Deflection

REINFORCED CONCRETE SANDWICH WALL PANEL NON-COMPOSITE DEFELCTION

P_{axial}	$P_{lateral}$	$2P_{lateral}$	M_s	$M_{s,l}$	$M_{s,o}$	$I_{eff,i}$	$I_{eff,o}$	I_{eff}	EI
kip	kip	kip	kip-in	kip-in	kip-in	in^4	in^4	in^4	$kip\text{-}in^2$
37.8	0	0	177	135	0	416	96	512	2930050
37.8	1	2	237	183	11	383	96	479	2741502
37.8	2.5	5	327	257	28	141	96	237	1358728
37.8	3.5	7	387	305	39	85	96	181	1034894
37.8	4	8	417	330	45	68	96	164	937633
37.8	5.45	10.9	504	400	61	39	96	135	771878
37.8	6	12	537	427	68	32	96	128	734846
37.8	7	14	597	476	79	24	96	120	687080
37.8	8	16	657	525	90	19	96	115	655440
37.8	9	18	717	573	101	15	96	111	633657
37.8	9.5	19	747	598	107	13	96	109	625284
37.8	11	22	837	671	124	10	90	100	575097
37.8	12	24	897	720	135	9	70	79	450706
37.8	13	26	957	768	146	7	56	63	361286
37.8	14	28	1017	817	158	7	45	52	295346
37.8	14.8	29.6	1065	856	167	6	38	44	254541
37.8	16	32	1137	915	180	5	31	36	207477
37.8	17	34	1197	963	191	5	26	31	177672
37.8	18	36	1257	1012	203	5	22	27	154058
37.8	19	38	1317	1061	214	4	19	24	135107
37.8	20	40	1377	1110	225	4	17	21	119720
37.8	21	42	1437	1158	236	4	15	19	107096
37.8	22	44	1497	1207	248	4	13	17	96642
37.8	23	46	1557	1256	259	3	12	15	87911
37.8	24	48	1617	1305	270	3	11	14	80561
37.8	25	50	1677	1353	281	3	10	13	74329
37.8	26	52	1737	1402	293	3	9	12	69011
37.8	27	54	1797	1451	304	3	8	11	64445
37.8	28	56	1857	1500	315	3	8	11	60502
37.8	29	58	1917	1548	326	3	7	10	57080
37.8	30	60	1977	1597	338	3	7	9	54095

Δ_{app}	Δ_{P-D}/e	e_1	Δ_1	e_2	Δ_2	error	e_3	Δ_3
in	in/in	in	in	in	in	%	in	in
0.453	0.093	0.453	0.042	0.495	0.046	9.29%	0.499	0.046
0.629	0.099	0.629	0.062	0.691	0.069	9.93%	0.698	0.069
1.706	0.200	1.706	0.342	2.048	0.410	20.03%	2.116	0.424
2.623	0.263	2.623	0.690	3.313	0.871	26.30%	3.494	0.919
3.106	0.290	3.106	0.902	4.008	1.163	29.03%	4.269	1.239
4.517	0.353	4.517	1.593	6.110	2.154	35.26%	6.671	2.352
5.041	0.370	5.0E+00	1.9E+00	6.9E+00	2.6E+00	37.04%	7.6E+00	2.8E+00
5.968	0.396	6.0E+00	2.4E+00	8.3E+00	3.3E+00	39.61%	9.3E+00	3.7E+00
6.860	0.415	6.9E+00	2.8E+00	9.7E+00	4.0E+00	41.52%	1.1E+01	4.5E+00
7.721	0.430	7.7E+00	3.3E+00	1.1E+01	4.7E+00	42.95%	1.2E+01	5.4E+00
8.141	0.435	8.1E+00	3.5E+00	1.2E+01	5.1E+00	43.53%	1.3E+01	5.8E+00
9.884	0.473	9.9E+00	4.7E+00	1.5E+01	6.9E+00	47.32%	1.7E+01	7.9E+00
13.491	0.604	1.3E+01	8.1E+00	2.2E+01	1.3E+01	60.39%	2.7E+01	1.6E+01
17.926	0.753	1.8E+01	1.4E+01	3.1E+01	2.4E+01	75.33%	4.2E+01	3.1E+01
23.269	0.921	2.3E+01	2.1E+01	4.5E+01	4.1E+01	92.15%	6.4E+01	5.9E+01
28.243	1.069	2.8E+01	3.0E+01	5.8E+01	6.2E+01	106.92%	9.1E+01	9.7E+01
36.941	1.312	3.7E+01	4.8E+01	8.5E+01	1.1E+02	131.18%	1.5E+02	2.0E+02
45.366	1.532	4.5E+01	6.9E+01	1.1E+02	1.8E+02	153.18%	2.2E+02	3.4E+02
54.890	1.767	5.5E+01	9.7E+01	1.5E+02	2.7E+02	176.66%	3.2E+02	5.7E+02
65.521	2.014	6.6E+01	1.3E+02	2.0E+02	4.0E+02	201.44%	4.6E+02	9.3E+02
77.250	2.273	7.7E+01	1.8E+02	2.5E+02	5.7E+02	227.33%	6.5E+02	1.5E+03
90.053	2.541	9.0E+01	2.3E+02	3.2E+02	8.1E+02	254.13%	9.0E+02	2.3E+03
103.892	2.816	1.0E+02	2.9E+02	4.0E+02	1.1E+03	281.62%	1.2E+03	3.4E+03
118.715	3.096	1.2E+02	3.7E+02	4.9E+02	1.5E+03	309.59%	1.6E+03	5.0E+03
134.461	3.378	1.3E+02	4.5E+02	5.9E+02	2.0E+03	337.83%	2.1E+03	7.2E+03
151.062	3.662	1.5E+02	5.5E+02	7.0E+02	2.6E+03	366.15%	2.7E+03	1.0E+04
168.441	3.944	1.7E+02	6.6E+02	8.3E+02	3.3E+03	394.37%	3.5E+03	1.4E+04
186.521	4.223	1.9E+02	7.9E+02	9.7E+02	4.1E+03	422.31%	4.3E+03	1.8E+04
205.222	4.498	2.1E+02	9.2E+02	1.1E+03	5.1E+03	449.84%	5.3E+03	2.4E+04
224.464	4.768	2.2E+02	1.1E+03	1.3E+03	6.2E+03	476.81%	6.4E+03	3.1E+04
244.170	5.031	2.4E+02	1.2E+03	1.5E+03	7.4E+03	503.12%	7.7E+03	3.9E+04

error	e_4	Δ_4	error	e_5	Δ_5	error	e_6	Δ_6
%	in	in	%	in	in	%	in	in
0.79%	0.500	0.046	0.07%	0.500	0.046	0.01%	0.500	0.046
0.90%	0.698	0.069	0.09%	0.698	0.069	0.01%	0.698	0.069
3.34%	2.130	0.427	0.65%	2.133	0.427	0.13%	2.133	0.427
5.48%	3.542	0.931	1.37%	3.554	0.935	0.35%	3.558	0.936
6.53%	4.345	1.261	1.78%	4.367	1.268	0.51%	4.374	1.270
9.19%	6.869	2.422	2.97%	6.939	2.447	1.02%	6.964	2.455
10.01%	7.9E+00	2.9E+00	3.37%	8.0E+00	2.9E+00	1.21%	8.0E+00	3.0E+00
11.24%	9.6E+00	3.8E+00	4.00%	9.8E+00	3.9E+00	1.52%	9.8E+00	3.9E+00
12.18%	1.1E+01	4.7E+00	4.51%	1.2E+01	4.8E+00	1.79%	1.2E+01	4.8E+00
12.90%	1.3E+01	5.6E+00	4.91%	1.3E+01	5.7E+00	2.01%	1.3E+01	5.8E+00
13.20%	1.4E+01	6.0E+00	5.08%	1.4E+01	6.2E+00	2.10%	1.4E+01	6.2E+00
15.20%	1.8E+01	8.4E+00	6.24%	1.8E+01	8.7E+00	2.78%	1.9E+01	8.8E+00
22.74%	3.0E+01	1.8E+01	11.19%	3.1E+01	1.9E+01	6.07%	3.2E+01	2.0E+01
32.37%	4.9E+01	3.7E+01	18.42%	5.5E+01	4.1E+01	11.72%	5.9E+01	4.5E+01
44.19%	8.3E+01	7.6E+01	28.24%	9.9E+01	9.2E+01	20.29%	1.1E+02	1.1E+02
55.25%	1.3E+02	1.3E+02	38.05%	1.6E+02	1.7E+02	29.47%	2.0E+02	2.2E+02
74.43%	2.3E+02	3.0E+02	55.97%	3.4E+02	4.5E+02	47.08%	4.9E+02	6.4E+02
92.68%	3.8E+02	5.9E+02	73.68%	6.3E+02	9.7E+02	64.98%	1.0E+03	1.6E+03
112.81%	6.3E+02	1.1E+03	93.65%	1.2E+03	2.1E+03	85.43%	2.1E+03	3.7E+03
134.61%	1.0E+03	2.0E+03	115.58%	2.1E+03	4.2E+03	108.00%	4.3E+03	8.6E+03
157.88%	1.6E+03	3.5E+03	139.18%	3.6E+03	8.2E+03	132.28%	8.3E+03	1.9E+04
182.36%	2.4E+03	6.0E+03	164.13%	6.1E+03	1.6E+04	157.91%	1.6E+04	4.0E+04
207.82%	3.5E+03	1.0E+04	190.13%	1.0E+04	2.8E+04	184.55%	2.8E+04	8.0E+04
234.00%	5.1E+03	1.6E+04	216.90%	1.6E+04	5.0E+04	211.89%	5.0E+04	1.5E+05
260.67%	7.3E+03	2.5E+04	244.16%	2.5E+04	8.4E+04	239.67%	8.4E+04	2.8E+05
287.61%	1.0E+04	3.7E+04	271.69%	3.7E+04	1.4E+05	267.64%	1.4E+05	5.0E+05
314.60%	1.4E+04	5.4E+04	299.25%	5.5E+04	2.2E+05	295.59%	2.2E+05	8.5E+05
341.46%	1.8E+04	7.7E+04	326.65%	7.8E+04	3.3E+05	323.33%	3.3E+05	1.4E+06
368.02%	2.4E+04	1.1E+05	353.72%	1.1E+05	4.9E+05	350.69%	4.9E+05	2.2E+06
394.14%	3.1E+04	1.5E+05	380.31%	1.5E+05	7.0E+05	377.54%	7.0E+05	3.3E+06
419.70%	3.9E+04	1.9E+05	406.31%	2.0E+05	9.8E+05	403.75%	9.8E+05	4.9E+06

error	e_7	Δ_7	error	e_8	Δ_8	error	e_9
%	in	in	%	in	in	%	in
0.00%	0.500	0.046	0.00%	0.500	0.046	0.00%	0.500
0.00%	0.698	0.069	0.00%	0.698	0.069	0.00%	0.698
0.03%	2.134	0.427	0.01%	2.134	0.427	0.00%	2.134
0.09%	3.558	0.936	0.02%	3.559	0.936	0.01%	3.559
0.15%	4.376	1.270	0.04%	4.376	1.270	0.01%	4.376
0.35%	6.972	2.458	0.12%	6.975	2.459	0.04%	6.976
0.44%	8.0E+00	3.0E+00	0.16%	8.0E+00	3.0E+00	0.06%	8.0E+00
0.59%	9.9E+00	3.9E+00	0.23%	9.9E+00	3.9E+00	0.09%	9.9E+00
0.73%	1.2E+01	4.9E+00	0.30%	1.2E+01	4.9E+00	0.12%	1.2E+01
0.85%	1.3E+01	5.8E+00	0.36%	1.4E+01	5.8E+00	0.15%	1.4E+01
0.90%	1.4E+01	6.3E+00	0.39%	1.4E+01	6.3E+00	0.17%	1.4E+01
1.28%	1.9E+01	8.8E+00	0.60%	1.9E+01	8.9E+00	0.28%	1.9E+01
3.46%	3.3E+01	2.0E+01	2.02%	3.3E+01	2.0E+01	1.19%	3.4E+01
7.90%	6.3E+01	4.7E+01	5.52%	6.5E+01	4.9E+01	3.94%	6.7E+01
15.55%	1.3E+02	1.2E+02	12.40%	1.4E+02	1.3E+02	10.16%	1.5E+02
24.34%	2.4E+02	2.6E+02	20.93%	2.9E+02	3.1E+02	18.50%	3.4E+02
41.99%	6.7E+02	8.8E+02	38.79%	9.2E+02	1.2E+03	36.66%	1.2E+03
60.34%	1.6E+03	2.5E+03	57.64%	2.5E+03	3.8E+03	56.01%	3.9E+03
81.39%	3.8E+03	6.7E+03	79.27%	6.7E+03	1.2E+04	78.11%	1.2E+04
104.59%	8.6E+03	1.7E+04	102.98%	1.7E+04	3.5E+04	102.20%	3.5E+04
129.46%	1.9E+04	4.3E+04	128.26%	4.3E+04	9.8E+04	127.74%	9.8E+04
155.59%	4.0E+04	1.0E+05	154.70%	1.0E+05	2.6E+05	154.35%	2.6E+05
182.65%	8.0E+04	2.3E+05	181.98%	2.3E+05	6.4E+05	181.74%	6.4E+05
210.33%	1.5E+05	4.8E+05	209.82%	4.8E+05	1.5E+06	209.66%	1.5E+06
238.37%	2.8E+05	9.6E+05	237.99%	9.6E+05	3.2E+06	237.88%	3.2E+06
266.56%	5.0E+05	1.8E+06	266.26%	1.8E+06	6.7E+06	266.18%	6.7E+06
294.68%	8.5E+05	3.3E+06	294.45%	3.3E+06	1.3E+07	294.39%	1.3E+07
322.55%	1.4E+06	5.9E+06	322.37%	5.9E+06	2.5E+07	322.33%	2.5E+07
350.03%	2.2E+06	9.8E+06	349.88%	9.8E+06	4.4E+07	349.85%	4.4E+07
376.96%	3.3E+06	1.6E+07	376.84%	1.6E+07	7.6E+07	376.81%	7.6E+07
403.24%	4.9E+06	2.5E+07	403.14%	2.5E+07	1.3E+08	403.12%	1.3E+08

Δ_9	error	e_{10}	Δ_{10}	error
in	%	in	in	%
0.046	0.00%	0.500	0.046	0.00%
0.069	0.00%	0.698	0.069	0.00%
0.427	0.00%	2.134	0.427	0.00%
0.936	0.00%	3.559	0.936	0.00%
1.270	0.00%	4.376	1.270	0.00%
2.460	0.02%	6.977	2.460	0.01%
3.0E+00	0.02%	8.0E+00	3.0E+00	0.01%
3.9E+00	0.04%	9.9E+00	3.9E+00	0.01%
4.9E+00	0.05%	1.2E+01	4.9E+00	0.02%
5.8E+00	0.07%	1.4E+01	5.8E+00	0.03%
6.3E+00	0.07%	1.4E+01	6.3E+00	0.03%
8.9E+00	0.13%	1.9E+01	8.9E+00	0.06%
2.0E+01	0.71%	3.4E+01	2.0E+01	0.43%
5.0E+01	2.85%	6.8E+01	5.2E+01	2.09%
1.4E+02	8.50%	1.7E+02	1.5E+02	7.22%
3.6E+02	16.70%	3.9E+02	4.2E+02	15.30%
1.6E+03	35.19%	1.7E+03	2.2E+03	34.15%
5.9E+03	55.00%	6.0E+03	9.2E+03	54.35%
2.1E+04	77.48%	2.1E+04	3.7E+04	77.12%
7.1E+04	101.82%	7.1E+04	1.4E+05	101.63%
2.2E+05	127.51%	2.2E+05	5.1E+05	127.41%
6.6E+05	154.22%	6.6E+05	1.7E+06	154.16%
1.8E+06	181.66%	1.8E+06	5.1E+06	181.63%
4.6E+06	209.61%	4.6E+06	1.4E+07	209.59%
1.1E+07	237.85%	1.1E+07	3.7E+07	237.84%
2.5E+07	266.16%	2.5E+07	9.0E+07	266.16%
5.2E+07	294.38%	5.2E+07	2.1E+08	294.37%
1.0E+08	322.32%	1.0E+08	4.4E+08	322.32%
2.0E+08	349.84%	2.0E+08	9.0E+08	349.84%
3.6E+08	376.81%	3.6E+08	1.7E+09	376.81%
6.3E+08	403.12%	6.3E+08	3.2E+09	403.12%

9.3.6 Deflection Percent Composite Action

REINFORCED CONCRETE SANDWICH WALL PANEL PERCENT COMPOSITE ACTION

P_{max} =	11.2	kip	Axial Load deflection:	0.0675	in
P_y =	11.2	kip	1st 5k deflection:	0.1125	in
Δ_y =	0.215	in	%PCA Axial Load:	94.6%	
Δ_i =	0.0865	in	%PCA 1st 5k:	98.1%	
n =	0.0				
E =	0				
Elastic stiffness =	87	ksi			

	Service Load	Deflection
Lat Id	7	0
	7	20

		Composite	Non-Composite	Test Data		Pessiki
Axial Load	Lat. Load	Deflection	Deflection	Lat. Load	Deflection	%PCA
kip	kip	in	in	kip	in	%
0	0.0	0	0	0.0	0.000	0%
37.8	0.0	0.043	0.500	0.0	0.087	90%
37.8	2.0	0.055	0.698	2.0	0.109	92%
37.8	5.0	0.074	2.134	5.0	0.144	97%
37.8	7.0	0.087	3.559	7.0	0.167	97.7%
37.8	8.0	0.093	4.376	8.0	0.178	98%
37.8	10.9	0.112	6.977	10.9	0.212	98.5%
37.8	12.0	0.119	8.0E+00			
37.8	14.0	0.132	9.9E+00			
37.8	16.0	0.144	1.2E+01			
37.8	18.0	0.157	1.4E+01			
37.8	19.0	0.163	1.4E+01			
37.8	22.0	0.182	1.9E+01			
37.8	24.0	0.195	3.4E+01			
37.8	26.0	0.208	6.8E+01			
37.8	28.0	0.221	1.7E+02			
37.8	29.6	0.231	3.9E+02			
37.8	32.0	0.246	1.7E+03			
37.8	34.0	0.259	6.0E+03			
37.8	36.0	0.271	2.1E+04			
37.8	38.0	0.284	7.1E+04			
37.8	40.0	0.297	2.2E+05			
37.8	42.0	0.309	6.6E+05			
37.8	44.0	0.322	1.8E+06			
37.8	46.0	0.335	4.6E+06			
37.8	48.0	0.348	1.1E+07			
37.8	50.0	0.360	2.5E+07			
37.8	52.0	0.383	5.2E+07			
37.8	54.0	0.437	1.0E+08			
37.8	56.0	0.498	2.0E+08			
37.8	58.0	0.564	3.6E+08			
37.8	60.0	0.636	6.3E+08			

9.4 XPS 2 CALCULATIONS

9.4.1 Input

PRECAST PRESTRESSED CONCRETE SANDWICH WALL PANEL DATA INPUT

Input and Properties:

Dimensions	Width	b	12	ft
	Width	b	144	in
	Height to axial load	H'	19	ft
	Height to axial load	H'	228	in
	Total height	H	20	ft
	Total height	H	240	in
	Inner wythe thickness	t_1	4.00	in
	Outer wythe thickness	t_2	2.00	in
	Insulation thickness	t_3	2.00	in
	Total thickness	t	8.00	in
	Composite top extreme fiber	$y_{t,c}$	3.67	in
	Composite bottom extreme fiber	$y_{b,c}$	4.33	in
	Inner wythe top extreme fiber	$y_{t,i}$	2.00	in
	Inner wythe bottom extreme fiber	$y_{b,i}$	2.00	in
	Outer wythe top extreme fiber	$y_{t,o}$	1.00	in
	Outer wythe bottom extreme fiber	$y_{b,o}$	1.00	in
	Composite centroid to inner centroid	d_i	1.67	in
	Composite centroid to outer centroid	d_o	3.33	in
	Top panel to top corbe	a_1	12	in
	End of panel to lateral load	a_2	60	in
	Bottom panel to measured lateral deflection	x_1	120	in
	Top panel to measured lateral deflection	x	120	in
	Bottom panel to maximum moment	x_2	130	in
	Top panel to maximum moment	x_0	60	in
Section properties	Inner wythe area	$A_{c,i}$	576	in^2
	Outer wythe area	$A_{c,o}$	288	in^2
	Concrete area	A_c	864	in^2
	Fully composite MOI	I_c	5604	in^4
	Inner wythe MOI	$I_{nc,i}$	768	in^4
	Outer wythe MOI	$I_{nc,o}$	96	in^4
	Fully noncomposite MOI	I_{nc}	864	in^4
	Inner wythe stiffness	%I	86.9%	
	Outer wythe stiffness	%O	11.1%	
Prestress properties	Prestressed area both wythes	$A_{p,c}$	0.85	in^2
	Prestressed area inner wythe	$A_{p,i}$	0.765	in^2
	Prestressed area outer wythe	$A_{p,o}$	0.425	in^2
	Fully composite prestressing depth	$d_{p,c}$	4.50	in
	Fully composite prestressing eccentricity	$e_{p,c}$	0.83	in

Prestress properties	Inner wythe prestressing depth	$d_{p,i}$	2.00	in
	Inner wythe prestressing eccentricity	$e_{p,i}$	0.00	in
	Outer wythe prestressing depth	$d_{p,o}$	1.00	in
	Outer wythe prestressing eccentricity	$e_{p,o}$	0.00	in
	Prestressing modulus	E_{ps}	28500	ksi
	Strand yield strength	f_{py}	243	ksi
	Strand ultimate strength	f_{pu}	270	ksi
	Yield/Ultimate	f_{pi}/f_{pu}	0.75	
	Initial prestressing strength	f_{pi}	202.5	ksi
	Initial compsote prestressing force	$P_{i,c}$	172	kip
	Initial inner wythe prestressing force	$P_{i,i}$	155	kip
	Initial outer wythe prestressing force	$P_{i,o}$	86	kip
	1-losses	R	86%	
	Effective compsote prestressing force	$P_{e,o}$	149	kip
	Effective inner wythe prestressing force	$P_{e,i}$	134	kip
	Effective inner wythe prestressing force	$P_{e,o}$	74	kip
	Time to testing	t_{relax}	2184	hrs
	Time to set	t_{set}	16	hrs
	Relative humidity	RH	70	%
	Volume of concrete	V	207360	in^3
	Specimen surface area	S	147456	in^2
	Volume/surface area	V/S	1.40625	in
	Friction loss coefficient	k	0	
	Shrinkage coefficient	ksh	1	
	Creep coeficient	kcr	2	
	Anchorage Seating	Δ_A	0	in
	Friction coefficient	μ	0	
	Wobble coefficient	α	0	

Note: Percent composite action and deflections calculated at mid-height

Note: Moment capacities and ultimate load calculated at 3/4-height

Mild steel properties	Steel area both wythes	$A_{s,c}$	0.3296	in^2
	Steel area each wythe	$A_{s,nc}$	0.1648	in^2
	Steel modulus	E_s	29000	ksi
	Fully composite steel depth	$d_{s,c}$	4.00	in
	Inner wythe steel depth	$d_{s,i}$	2.00	in
	Outer wythe steel depth	$d_{s,o}$	1.00	in
	Strand yield strength	f_{sy}	65	ksi
Concrete properties	Concrete unit weight	γ_c	145	pcf
	Initial concrete strength	f'_{ci}	3.5	psi
	Initial concrete modulus	E_{ci}	3372	ksi
	Concrete strength	f'_c	8.79	ksi
	Concrete modulus	E_c	5344	ksi
	Maximum concrete strain	ε_{cu}	0.003	in/in
	Tension modulus constant	$K\sqrt{f'_c}$ =	10.0	
	Tension modulus	f_r =	0.938	ksi
	NA depth constant	β_1	0.65	
	Initial prestressed modular ratio	n_i	8.452	
	Prestressed modular ratio	n	5.333	
Safety factors	Flexural phi factor	ϕ_f	0.9	
	Shear phi factor	ϕ_v	0.85	
Loads	Composite axial load	P_{axial}	37.8	kip
	Inner wythe axial load	$P_{axial,i}$	37.8	kip
	Outer wythe axial load	$P_{axial,o}$	0.0	kip
	Wythe surface to axial load	a_3	6	in
	Composite axial load eccentricity	$e_{a,c}$	9.67	in
	Inner wythe axial load eccentricity	$e_{a,i}$	8.00	in
	Outer wythe axial load eccentricity	$e_{a,o}$	13.00	in
	Composite axial load moment	$M_{e,c}$	366	kip-in
	Inner wythe axial load moment	$M_{e,i}$	302	kip-in
	Outer wythe axial load moment	$M_{e,o}$	0	kip-in
Cracking properties	Composite cracking moment	$M_{cr,c}$	1533	kip-in
	Inner wythe cracking moment	$M_{cr,i}$	474	kip-in
	Outer wythe cracking moment	$M_{cr,o}$	115	kip-in
	Composite cracking MOI	$I_{cr,c}$	224	in^4
	Inner wythe cracking MOI	$I_{cr,i}$	15.6	in^4
	Outer wythe cracking MOI	$I_{cr,o}$	2.4	in^4
Deflection	Initial bow	e_i	0	in

9.4.2 Prestressing Losses

PRECAST PRESTRESSED CONCRETE SANDWICH WALL PANEL DATA INPUT

Stage 0: Jacking

Anchorage Seating Losses			**Friction Losses**		
Δf_{pA} =	**0**	**ksi**	**Δf_{pF} =**	**0**	**ksi**
Stage 0 Loss =	**0**	**ksi**			
f_{pi} =	**202.5**	**kip**			

Stage I: Stress Transfer

Steel Relaxation Losses

t_1 =	0	hrs
t_2 =	16	hrs
f_{pi} =	203	ksi
Δf_{pR} =	**6.9**	**ksi**

Elastic Shortening Losses

Ass. Δf_{pES} =	1.85	ksi			
f_{pi} =	194	ksi			
$P_{i,i}$ =	148	kip	$P_{axial,i}$ =	37.8	kip
$P_{i,o}$ =	82	kip			

Elastic Shortening

M_D =	0	kip-ft
M_D =	0	kip-in
$f_{pES,i}$ =	-0.207	ksi
$f_{pES,o}$ =	-0.231	ksi
$\Delta f_{pES,i}$ =	**1.75**	**ksi**
$\Delta f_{pES,o}$ =	**1.95**	**ksi**
Difference =	0.00	
Stage I Loss =	**8.76**	**ksi**
f_{pi} =	**194**	**kip**

Stage II: Transfer to Placement of Superimposed Dead Load

Creep Losses

M_{SD} =	0	kip-ft
M_{SD} =	0	kip-in
f_{csi} =	0.207	ksi
f_{csd} =	0.000	ksi
f_{csd} =	0.000	ksi
Δf_{pCR} =	2.21	ksi

Shrinkage Losses

Δf_{pSH} =	6.42	ksi

Steel Relaxation Losses

t_1 =	16	hrs
t_2 =	2184	hrs
f_{pi} =	194	ksi
Δf_{pR} =	10.23	ksi

Stress Increase Due to Loading

Δf_{SD} =	0.00	ksi

Stage II Loss =	18.9	ksi
f_{pi} =	175	kip

Total Losses =	19	ksi
f_{pe} =	175	ksi
P_e =	149	kip
R =	86%	
Losses =	14%	

9.4.3 Cracked Moment of Inertia

REINFORCED CONCRETE SANDWICH WALL PANEL CRACKED MOMENT OF INERTIA

x<d₁

h =	144	in
d_o =	7	in
d_1 =	2	in
t_1 =	4	in
A_s =	0.1648	/wythe [in^2]
A_{ps} =	0.765	Inner wythe [in^2]
A_{ps} =	0.425	Outer wythe [in^2]
E_s =	29000000	ps
E_{ps} =	28500000	ps
E_c =	5344034.99	ps
n_s =	5.427	
n_{ps} =	5.333	

Composite

a =	72	
b =	8.136	
c =	32.074	
x =	0.613	in
	-0.726	in
I_{comp} =	223.5	in^4

Inner Non-Composite

a =	72	
b =	4.974	
c =	9.948	
x =	0.339	in
	-0.408	in
$I_{non\text{-}comp/wythe}$ =	15.6	in^4

x≥d₁

h =	144	in
d_o =	7	in
d_1 =	2	in
t_1 =	4	in
A_s =	0.1648	/wythe [in^2]
A_{ps} =	0.765	Inner wythe [in^2]
A_{ps} =	0.425	Outer wythe [in^2]
E_s =	29000000	psi
E_{ps} =	28500000	psi
E_c =	5344034.99	psi
n_s =	5.427	
n_{ps} =	5.333	

Composite

a =	72	
b =	8.161	
c =	34.619	
x =	0.674	in
	-0.718	in
I_{comp} =	213.8	in^4

Outer wythe

h =	144	in
d_o =	na	in
d =	1	in
t_1 =	4	in
A_s =	0.1648	/wythe [in^2]
A_{ps} =	0.765	Inner wythe [in^2]
A_{ps} =	0.425	Outer wythe [in^2]
E_s =	29000000	psi
E_{ps} =	28500000	psi
E_c =	5344034.99	psi
n_s =	5.427	
n_{ps} =	5.333	

Outer Non-Composite

a =	72	
b =	3.161	
c =	3.161	
x =	0.189	in
	-0.233	in
$I_{non\text{-}comp/wythe}$ =	2.4	in^4

9.4.4 Composite Deflection

REINFORCED CONCRETE SANDWICH WALL PANEL COMPOSITE DEFELCTION

P_{axial}	$P_{lateral}$	$2P_{lateral}$	M_a	I_{eff}	EI	Δ_{app}	Δ_{p-D}/e_i	e_t
kip	kip	kip	kip-in	in^4	$kip-in^2$	in	in/in	in
37.8	0	0	174	5664	30268665	0.043	0.009	0.043
37.8	1	2	234	5664	30268665	0.056	0.009	0.056
37.8	2.5	5	324	5664	30268665	0.076	0.009	0.076
37.8	3.5	7	384	5664	30268665	0.089	0.009	0.089
37.8	4	8	414	5664	30268665	0.095	0.009	0.095
37.8	5.45	10.9	501	5664	30268665	0.114	0.009	0.114
37.8	6	12	534	5664	30268665	0.122	0.009	0.122
37.8	7	14	594	5664	30268665	0.135	0.009	0.135
37.8	8	16	654	5664	30268665	0.148	0.009	0.148
37.8	9	18	714	5664	30268665	0.161	0.009	0.161
37.8	9.5	19	744	5664	30268665	0.167	0.009	0.167
37.8	11	22	834	5664	30268665	0.187	0.009	0.187
37.8	12	24	894	5664	30268665	0.200	0.009	0.200
37.8	13	26	954	5664	30268665	0.213	0.009	0.213
37.8	14	28	1014	5664	30268665	0.226	0.009	0.226
37.8	14.8	29.6	1062	5664	30268665	0.237	0.009	0.237
37.8	16	32	1134	5664	30268665	0.252	0.009	0.252
37.8	17	34	1194	5664	30268665	0.265	0.009	0.265
37.8	18	36	1254	5664	30268665	0.279	0.009	0.279
37.8	19	38	1314	5664	30268665	0.292	0.009	0.292
37.8	20	40	1374	5664	30268665	0.305	0.009	0.305
37.8	21	42	1434	5664	30268665	0.318	0.009	0.318
37.8	22	44	1494	5664	30268665	0.331	0.009	0.331
37.8	23	46	1554	5448	29112599	0.358	0.009	0.358
37.8	24	48	1614	4886	26112702	0.414	0.010	0.414
37.8	25	50	1674	4403	23527660	0.476	0.012	0.476
37.8	26	52	1734	3984	21288170	0.545	0.013	0.545
37.8	27	54	1794	3619	19338369	0.620	0.014	0.620
37.8	28	56	1854	3300	17632892	0.703	0.015	0.703
37.8	29	58	1914	3019	16134638	0.793	0.017	0.793
37.8	30	60	1974	2772	14813065	0.890	0.018	0.890

Δ_1	e_2	Δ_2	error	e_3	Δ_3	error	e_4	Δ_4
in	in	in	%	in	in	%	in	in
0.000	0.043	0.000	0.90%	0.043	0.000	0.01%	0.043	0.000
0.001	0.057	0.001	0.90%	0.057	0.001	0.01%	0.057	0.001
0.001	0.076	0.001	0.90%	0.076	0.001	0.01%	0.076	0.001
0.001	0.090	0.001	0.90%	0.090	0.001	0.01%	0.090	0.001
0.001	0.096	0.001	0.90%	0.096	0.001	0.01%	0.096	0.001
0.001	0.115	0.001	0.90%	0.115	0.001	0.01%	0.115	0.001
0.001	0.123	0.001	0.90%	0.123	0.001	0.01%	0.123	0.001
0.001	0.136	0.001	0.90%	0.136	0.001	0.01%	0.136	0.001
0.001	0.149	0.001	0.90%	0.149	0.001	0.01%	0.149	0.001
0.001	0.162	0.001	0.90%	0.162	0.001	0.01%	0.162	0.001
0.002	0.169	0.002	0.90%	0.169	0.002	0.01%	0.169	0.002
0.002	0.189	0.002	0.90%	0.189	0.002	0.01%	0.189	0.002
0.002	0.202	0.002	0.90%	0.202	0.002	0.01%	0.202	0.002
0.002	0.215	0.002	0.90%	0.215	0.002	0.01%	0.215	0.002
0.002	0.228	0.002	0.90%	0.228	0.002	0.01%	0.228	0.002
0.002	0.239	0.002	0.90%	0.239	0.002	0.01%	0.239	0.002
0.002	0.255	0.002	0.90%	0.255	0.002	0.01%	0.255	0.002
0.002	0.268	0.002	0.90%	0.268	0.002	0.01%	0.268	0.002
0.003	0.281	0.003	0.90%	0.281	0.003	0.01%	0.281	0.003
0.003	0.294	0.003	0.90%	0.294	0.003	0.01%	0.294	0.003
0.003	0.307	0.003	0.90%	0.307	0.003	0.01%	0.307	0.003
0.003	0.321	0.003	0.90%	0.321	0.003	0.01%	0.321	0.003
0.003	0.334	0.003	0.90%	0.334	0.003	0.01%	0.334	0.003
0.003	0.361	0.003	0.93%	0.361	0.003	0.01%	0.361	0.003
0.004	0.418	0.004	1.04%	0.418	0.004	0.01%	0.418	0.004
0.006	0.482	0.006	1.16%	0.482	0.006	0.01%	0.482	0.006
0.007	0.552	0.007	1.28%	0.552	0.007	0.02%	0.552	0.007
0.009	0.629	0.009	1.41%	0.629	0.009	0.02%	0.629	0.009
0.011	0.714	0.011	1.54%	0.714	0.011	0.02%	0.714	0.011
0.013	0.806	0.014	1.69%	0.806	0.014	0.03%	0.806	0.014
0.016	0.906	0.017	1.84%	0.907	0.017	0.03%	0.907	0.017

9.4.5 Non-composite Deflection

REINFORCED CONCRETE SANDWICH WALL PANEL NON-COMPOSITE DEFELCTION

P_{axial}	$P_{lateral}$	$2P_{lateral}$	M_s	$M_{s,l}$	$M_{s,o}$	$I_{eff,l}$	$I_{eff,o}$	I_{eff}	EI
kip	kip	kip	kip-in	kip-in	kip-in	in^4	in^4	in^4	$kip\text{-}in^2$
37.8	0	0	174	144	0	768	96	864	4617246
37.8	1	2	234	197	7	768	96	864	4617246
37.8	2.5	5	324	277	17	768	96	864	4617246
37.8	3.5	7	384	330	23	768	96	864	4617246
37.8	4	8	414	357	27	768	96	864	4617246
37.8	5.45	10.9	501	434	36	768	96	864	4617246
37.8	6	12	534	464	40	768	96	864	4617246
37.8	7	14	594	517	47	597	96	693	3703570
37.8	8	16	654	570	53	449	96	545	2910819
37.8	9	18	714	624	60	347	96	443	2366358
37.8	9.5	19	744	650	63	308	96	404	2157422
37.8	11	22	834	730	73	222	96	318	1698555
37.8	12	24	894	784	80	183	96	279	1488482
37.8	13	26	954	837	87	153	96	249	1328576
37.8	14	28	1014	890	93	129	96	225	1204712
37.8	14.8	29.6	1062	933	99	115	96	211	1125007
37.8	16	32	1134	997	107	97	96	193	1029594
37.8	17	34	1194	1050	113	85	96	181	966891
37.8	18	36	1254	1104	120	75	84	160	853241
37.8	19	38	1314	1157	127	67	72	140	745543
37.8	20	40	1374	1210	133	61	62	123	657408
37.8	21	42	1434	1264	140	55	54	109	584576
37.8	22	44	1494	1317	147	51	47	98	523855
37.8	23	46	1554	1370	153	47	42	88	472823
37.8	24	48	1614	1424	160	43	37	80	429617
37.8	25	50	1674	1477	167	41	33	74	392790
37.8	26	52	1734	1530	173	38	30	68	361203
37.8	27	54	1794	1584	180	36	27	62	333956
37.8	28	56	1854	1637	187	34	24	58	310326
37.8	29	58	1914	1690	193	32	22	54	289732
37.8	30	60	1974	1744	200	31	20	51	271700

Δ_{app}	Δ_{P-D}/e	e_1	Δ_1	e_2	Δ_2	error	e_3	Δ_3
in	in/in	in	in	in	in	%	in	in
0.282	0.059	0.282	0.017	0.299	0.018	5.89%	0.300	0.018
0.368	0.059	0.368	0.022	0.390	0.023	5.89%	0.391	0.023
0.497	0.059	0.497	0.029	0.526	0.031	5.89%	0.528	0.031
0.582	0.059	0.582	0.034	0.617	0.036	5.89%	0.619	0.036
0.625	0.059	0.625	0.037	0.662	0.039	5.89%	0.664	0.039
0.750	0.059	0.750	0.044	0.794	0.047	5.89%	0.796	0.047
0.797	0.059	8.0E-01	4.7E-02	8.4E-01	5.0E-02	5.89%	8.5E-01	5.0E-02
1.100	0.073	1.1E+00	8.1E-02	1.2E+00	8.7E-02	7.35%	1.2E+00	8.7E-02
1.536	0.093	1.5E+00	1.4E-01	1.7E+00	1.6E-01	9.35%	1.7E+00	1.6E-01
2.057	0.115	2.1E+00	2.4E-01	2.3E+00	2.6E-01	11.50%	2.3E+00	2.7E-01
2.348	0.126	2.3E+00	3.0E-01	2.6E+00	3.3E-01	12.62%	2.7E+00	3.4E-01
3.331	0.160	3.3E+00	5.3E-01	3.9E+00	6.2E-01	16.02%	4.0E+00	6.3E-01
4.068	0.183	4.1E+00	7.4E-01	4.8E+00	8.8E-01	18.28%	4.9E+00	9.0E-01
4.855	0.205	4.9E+00	9.9E-01	5.9E+00	1.2E+00	20.49%	6.1E+00	1.2E+00
5.683	0.226	5.7E+00	1.3E+00	7.0E+00	1.6E+00	22.59%	7.3E+00	1.6E+00
6.368	0.242	6.4E+00	1.5E+00	7.9E+00	1.9E+00	24.19%	8.3E+00	2.0E+00
7.419	0.264	7.4E+00	2.0E+00	9.4E+00	2.5E+00	26.43%	9.9E+00	2.6E+00
8.310	0.281	8.3E+00	2.3E+00	1.1E+01	3.0E+00	28.15%	1.1E+01	3.2E+00
9.881	0.319	9.9E+00	3.2E+00	1.3E+01	4.2E+00	31.90%	1.4E+01	4.5E+00
11.839	0.365	1.2E+01	4.3E+00	1.6E+01	5.9E+00	36.50%	1.8E+01	6.5E+00
14.029	0.414	1.4E+01	5.8E+00	2.0E+01	8.2E+00	41.40%	2.2E+01	9.2E+00
16.454	0.466	1.6E+01	7.7E+00	2.4E+01	1.1E+01	46.56%	2.8E+01	1.3E+01
19.117	0.520	1.9E+01	9.9E+00	2.9E+01	1.5E+01	51.95%	3.4E+01	1.8E+01
22.018	0.576	2.2E+01	1.3E+01	3.5E+01	2.0E+01	57.56%	4.2E+01	2.4E+01
25.154	0.633	2.5E+01	1.6E+01	4.1E+01	2.6E+01	63.35%	5.1E+01	3.2E+01
28.521	0.693	2.9E+01	2.0E+01	4.8E+01	3.3E+01	69.29%	6.2E+01	4.3E+01
32.111	0.753	3.2E+01	2.4E+01	5.6E+01	4.2E+01	75.35%	7.5E+01	5.6E+01
35.917	0.815	3.6E+01	2.9E+01	6.5E+01	5.3E+01	81.50%	8.9E+01	7.3E+01
39.928	0.877	4.0E+01	3.5E+01	7.5E+01	6.6E+01	87.70%	1.1E+02	9.3E+01
44.133	0.939	4.4E+01	4.1E+01	8.6E+01	8.0E+01	93.94%	1.2E+02	1.2E+02
48.519	1.002	4.9E+01	4.9E+01	9.7E+01	9.7E+01	100.17%	1.5E+02	1.5E+02

error	e_4	Δ_4	error	e_5	Δ_5	error	e_6	Δ_6
%	in	in	%	in	in	%	in	in
0.33%	0.300	0.018	0.02%	0.300	0.018	0.00%	0.300	0.018
0.33%	0.391	0.023	0.02%	0.391	0.023	0.00%	0.391	0.023
0.33%	0.528	0.031	0.02%	0.528	0.031	0.00%	0.528	0.031
0.33%	0.619	0.036	0.02%	0.619	0.036	0.00%	0.619	0.036
0.33%	0.664	0.039	0.02%	0.664	0.039	0.00%	0.664	0.039
0.33%	0.797	0.047	0.02%	0.797	0.047	0.00%	0.797	0.047
0.33%	8.5E-01	5.0E-02	0.02%	8.5E-01	5.0E-02	0.00%	8.5E-01	5.0E-02
0.50%	1.2E+00	8.7E-02	0.04%	1.2E+00	8.7E-02	0.00%	1.2E+00	8.7E-02
0.80%	1.7E+00	1.6E-01	0.07%	1.7E+00	1.6E-01	0.01%	1.7E+00	1.6E-01
1.19%	2.3E+00	2.7E-01	0.13%	2.3E+00	2.7E-01	0.02%	2.3E+00	2.7E-01
1.41%	2.7E+00	3.4E-01	0.18%	2.7E+00	3.4E-01	0.02%	2.7E+00	3.4E-01
2.21%	4.0E+00	6.4E-01	0.35%	4.0E+00	6.4E-01	0.06%	4.0E+00	6.4E-01
2.83%	5.0E+00	9.1E-01	0.50%	5.0E+00	9.1E-01	0.09%	5.0E+00	9.1E-01
3.48%	6.1E+00	1.2E+00	0.69%	6.1E+00	1.3E+00	0.14%	6.1E+00	1.3E+00
4.16%	7.3E+00	1.7E+00	0.90%	7.3E+00	1.7E+00	0.20%	7.3E+00	1.7E+00
4.71%	8.4E+00	2.0E+00	1.09%	8.4E+00	2.0E+00	0.26%	8.4E+00	2.0E+00
5.53%	1.0E+01	2.7E+00	1.38%	1.0E+01	2.7E+00	0.36%	1.0E+01	2.7E+00
6.18%	1.1E+01	3.2E+00	1.64%	1.2E+01	3.2E+00	0.45%	1.2E+01	3.3E+00
7.71%	1.4E+01	4.6E+00	2.28%	1.4E+01	4.6E+00	0.71%	1.4E+01	4.6E+00
9.76%	1.8E+01	6.7E+00	3.25%	1.9E+01	6.8E+00	1.15%	1.9E+01	6.8E+00
12.12%	2.3E+01	9.6E+00	4.48%	2.4E+01	9.8E+00	1.77%	2.4E+01	9.9E+00
14.79%	2.9E+01	1.4E+01	6.00%	3.0E+01	1.4E+01	2.63%	3.0E+01	1.4E+01
17.76%	3.7E+01	1.9E+01	7.84%	3.8E+01	2.0E+01	3.78%	3.9E+01	2.0E+01
21.03%	4.6E+01	2.7E+01	10.00%	4.9E+01	2.8E+01	5.23%	5.0E+01	2.9E+01
24.57%	5.8E+01	3.6E+01	12.49%	6.2E+01	3.9E+01	7.04%	6.4E+01	4.1E+01
28.36%	7.1E+01	5.0E+01	15.31%	7.8E+01	5.4E+01	9.20%	8.3E+01	5.7E+01
32.38%	8.8E+01	6.7E+01	18.43%	9.9E+01	7.4E+01	11.73%	1.1E+02	8.0E+01
36.59%	1.1E+02	8.8E+01	21.83%	1.2E+02	1.0E+02	14.60%	1.4E+02	1.1E+02
40.98%	1.3E+02	1.2E+02	25.49%	1.6E+02	1.4E+02	17.82%	1.8E+02	1.6E+02
45.50%	1.6E+02	1.5E+02	29.37%	2.0E+02	1.8E+02	21.33%	2.3E+02	2.1E+02
50.13%	1.9E+02	1.9E+02	33.45%	2.4E+02	2.4E+02	25.11%	2.9E+02	2.9E+02

error	e_7	Δ_7	error	e_8	Δ_8	error	e_9
%	in	in	%	in	in	%	in
0.00%	0.300	0.018	0.00%	0.300	0.018	0.00%	0.300
0.00%	0.391	0.023	0.00%	0.391	0.023	0.00%	0.391
0.00%	0.528	0.031	0.00%	0.528	0.031	0.00%	0.528
0.00%	0.619	0.036	0.00%	0.619	0.036	0.00%	0.619
0.00%	0.664	0.039	0.00%	0.664	0.039	0.00%	0.664
0.00%	0.797	0.047	0.00%	0.797	0.047	0.00%	0.797
0.00%	8.5E-01	5.0E-02	0.00%	8.5E-01	5.0E-02	0.00%	8.5E-01
0.00%	1.2E+00	8.7E-02	0.00%	1.2E+00	8.7E-02	0.00%	1.2E+00
0.00%	1.7E+00	1.6E-01	0.00%	1.7E+00	1.6E-01	0.00%	1.7E+00
0.00%	2.3E+00	2.7E-01	0.00%	2.3E+00	2.7E-01	0.00%	2.3E+00
0.00%	2.7E+00	3.4E-01	0.00%	2.7E+00	3.4E-01	0.00%	2.7E+00
0.01%	4.0E+00	6.4E-01	0.00%	4.0E+00	6.4E-01	0.00%	4.0E+00
0.02%	5.0E+00	9.1E-01	0.00%	5.0E+00	9.1E-01	0.00%	5.0E+00
0.03%	6.1E+00	1.3E+00	0.01%	6.1E+00	1.3E+00	0.00%	6.1E+00
0.05%	7.3E+00	1.7E+00	0.01%	7.3E+00	1.7E+00	0.00%	7.3E+00
0.06%	8.4E+00	2.0E+00	0.02%	8.4E+00	2.0E+00	0.00%	8.4E+00
0.10%	1.0E+01	2.7E+00	0.03%	1.0E+01	2.7E+00	0.01%	1.0E+01
0.13%	1.2E+01	3.3E+00	0.04%	1.2E+01	3.3E+00	0.01%	1.2E+01
0.23%	1.5E+01	4.6E+00	0.07%	1.5E+01	4.6E+00	0.02%	1.5E+01
0.41%	1.9E+01	6.8E+00	0.15%	1.9E+01	6.8E+00	0.05%	1.9E+01
0.72%	2.4E+01	9.9E+00	0.30%	2.4E+01	9.9E+00	0.12%	2.4E+01
1.20%	3.1E+01	1.4E+01	0.55%	3.1E+01	1.4E+01	0.25%	3.1E+01
1.89%	3.9E+01	2.0E+01	0.96%	4.0E+01	2.1E+01	0.50%	4.0E+01
2.86%	5.1E+01	2.9E+01	1.60%	5.1E+01	3.0E+01	0.91%	5.2E+01
4.16%	6.6E+01	4.2E+01	2.53%	6.7E+01	4.2E+01	1.56%	6.8E+01
5.84%	8.6E+01	5.9E+01	3.82%	8.8E+01	6.1E+01	2.55%	8.9E+01
7.91%	1.1E+02	8.5E+01	5.52%	1.2E+02	8.8E+01	3.94%	1.2E+02
10.39%	1.5E+02	1.2E+02	7.67%	1.6E+02	1.3E+02	5.80%	1.6E+02
13.26%	2.0E+02	1.7E+02	10.27%	2.1E+02	1.9E+02	8.17%	2.3E+02
16.51%	2.6E+02	2.4E+02	13.31%	2.9E+02	2.7E+02	11.04%	3.1E+02
20.10%	3.4E+02	3.4E+02	16.77%	3.9E+02	3.9E+02	14.38%	4.4E+02

Δ_9	error	e_{10}	Δ_{10}	error
in	%	in	in	%
0.018	0.00%	0.300	0.018	0.00%
0.023	0.00%	0.391	0.023	0.00%
0.031	0.00%	0.528	0.031	0.00%
0.036	0.00%	0.619	0.036	0.00%
0.039	0.00%	0.664	0.039	0.00%
0.047	0.00%	0.797	0.047	0.00%
5.0E-02	0.00%	8.5E-01	5.0E-02	0.00%
8.7E-02	0.00%	1.2E+00	8.7E-02	0.00%
1.6E-01	0.00%	1.7E+00	1.6E-01	0.00%
2.7E-01	0.00%	2.3E+00	2.7E-01	0.00%
3.4E-01	0.00%	2.7E+00	3.4E-01	0.00%
6.4E-01	0.00%	4.0E+00	6.4E-01	0.00%
9.1E-01	0.00%	5.0E+00	9.1E-01	0.00%
1.3E+00	0.00%	6.1E+00	1.3E+00	0.00%
1.7E+00	0.00%	7.3E+00	1.7E+00	0.00%
2.0E+00	0.00%	8.4E+00	2.0E+00	0.00%
2.7E+00	0.00%	1.0E+01	2.7E+00	0.00%
3.3E+00	0.00%	1.2E+01	3.3E+00	0.00%
4.6E+00	0.01%	1.5E+01	4.6E+00	0.00%
6.8E+00	0.02%	1.9E+01	6.8E+00	0.01%
9.9E+00	0.05%	2.4E+01	9.9E+00	0.02%
1.4E+01	0.12%	3.1E+01	1.4E+01	0.05%
2.1E+01	0.26%	4.0E+01	2.1E+01	0.13%
3.0E+01	0.52%	5.2E+01	3.0E+01	0.30%
4.3E+01	0.98%	6.8E+01	4.3E+01	0.61%
6.2E+01	1.72%	9.1E+01	6.3E+01	1.17%
9.0E+01	2.86%	1.2E+02	9.2E+01	2.09%
1.3E+02	4.47%	1.7E+02	1.4E+02	3.49%
2.0E+02	6.62%	2.4E+02	2.1E+02	5.45%
2.9E+02	9.34%	3.4E+02	3.2E+02	8.02%
4.4E+02	12.60%	4.9E+02	4.9E+02	11.21%

9.4.6 Deflection Percent Composite Action

REINFORCED CONCRETE SANDWICH WALL PANEL PERCENT COMPOSITE ACTION

P_{max} =	22.5	kip	Axial Load deflection:	0.1415	in
P_y =	15	kip	1st 5k deflection:	0.237	in
Δ_y =	0.583	in	%PCA Axial Load:	61.7%	
Δ_i =	0.2595	in	%PCA 1st 5k:	64.4%	
n =	5.5				
E =	65				
Elastic stiffness =	46	ksi			

	Service Load	Deflection
Lat Id	7	0
	7	20

		Composite	Non-Composite	Test Data		Pessiki
Axial Load	Lat. Load	Deflection	Deflection	Lat. Load	Deflection	%PCA
kip	kip	in	in	kip	in	%
0	0.0	0	0	0.0	0.000	0%
37.8	0.0	0.043	0.300	0.0	0.260	16%
37.8	2.0	0.057	0.391	2.0	0.303	26%
37.8	5.0	0.076	0.528	5.0	0.367	36%
37.8	7.0	0.090	0.619	7.0	0.411	39.3%
37.8	8.0	0.096	0.664	8.0	0.432	41%
37.8	10.9	0.115	0.797	10.9	0.495	44.3%
37.8	12.0	0.123	0.847	12.0	0.519	45%
37.8	14.0	0.136	1.187	14.0	0.562	59%
37.8	16.0	0.149	1.694	16.0	0.632	69%
37.8	18.0	0.162	2.324	18.0	0.714	74%
37.8	19.0	0.169	2.686	19.0	0.774	76%
37.8	22.0	0.189	3.967	22.0	1.060	77%
37.8	24.0	0.202	5.0E+00			
37.8	26.0	0.215	6.1E+00			
37.8	28.0	0.228	7.3E+00			
37.8	29.6	0.239	8.4E+00			
37.8	32.0	0.255	1.0E+01			
37.8	34.0	0.268	1.2E+01			
37.8	36.0	0.281	1.5E+01			
37.8	38.0	0.294	1.9E+01			
37.8	40.0	0.307	2.4E+01			
37.8	42.0	0.321	3.1E+01			
37.8	44.0	0.334	4.0E+01			
37.8	46.0	0.361	5.2E+01			
37.8	48.0	0.418	6.8E+01			
37.8	50.0	0.482	9.1E+01			
37.8	52.0	0.552	1.2E+02			
37.8	54.0	0.629	1.7E+02			
37.8	56.0	0.714	2.4E+02			
37.8	58.0	0.806	3.4E+02			
37.8	60.0	0.907	4.9E+02			

9.5 XPS 3 CALCULATIONS

9.5.1 Input

PRECAST PRESTRESSED CONCRETE SANDWICH WALL PANEL DATA INPUT

Input and Properties:

Dimensions	Width	b	12	ft
	Width	b	144	in
	Height to axial load	H'	19	ft
	Height to axial load	H'	228	in
	Total height	H	20	ft
	Total height	H	240	in
	Inner wythe thickness	t_1	2.67	in
	Outer wythe thickness	t_2	2.00	in
	Insulation thickness	t_3	3.33	in
	Total thickness	t	8.00	in
	Composite top extreme fiber	$y_{t,c}$	3.86	in
	Composite bottom extreme fiber	$y_{b,c}$	4.14	in
	Inner wythe top extreme fiber	$y_{t,i}$	1.50	in
	Inner wythe bottom extreme fiber	$y_{b,i}$	2.50	in
	Outer wythe top extreme fiber	$y_{t,o}$	1.00	in
	Outer wythe bottom extreme fiber	$y_{b,o}$	1.00	in
	Composite centroid to inner centroid	d_i	2.36	in
	Composite centroid to outer centroid	d_o	3.14	in
	Top panel to top corbe	a_1	12	in
	End of panel to lateral load	a_2	60	in
	Bottom panel to measured lateral deflection	x_1	120	in
	Top panel to measured lateral deflection	x	120	in
	Bottom panel to maximum moment	x_2	180	in
	Top panel to maximum moment	x_0	60	in
Section properties	Inner wythe area	$A_{c,i}$	334	in^2
	Outer wythe area	$A_{c,o}$	238	in^2
	Concrete area	A_c	672	in^2
	Fully composite MOI	I_c	5490	in^4
	Inner wythe MOI	$I_{nc,i}$	416	in^4
	Outer wythe MOI	$I_{nc,o}$	96	in^4
	Fully noncomposite MOI	I_{nc}	512	in^4
	Inner wythe stiffness	%I	81.3%	
	Outer wythe stiffness	%O	18.8%	
Prestress properties	Prestressed area both wythes	$A_{p,c}$	0.85	in^2
	Prestressed area inner wythe	$A_{p,i}$	0.425	in^2
	Prestressed area outer wythe	$A_{p,o}$	0.425	in^2
	Fully composite prestressing depth	$d_{p,c}$	4.00	in
	Fully composite prestressing eccentricity	$e_{p,c}$	0.14	in

Prestress properties	Inner wythe prestressing depth	$d_{p,i}$	1.00	in
	Inner wythe prestressing eccentricity	$e_{p,i}$	-0.50	in
	Outer wythe prestressing depth	$d_{p,o}$	1.00	in
	Outer wythe prestressing eccentricity	$e_{p,o}$	0.00	in
	Prestressing modulus	E_{ps}	28500	ksi
	Strand yield strength	f_{py}	243	ksi
	Strand ultimate strength	f_{pu}	270	ksi
	Yield/Ultimate	f_{pi}/f_{pu}	0.75	
	Initial prestressing strength	f_{pi}	202.5	ksi
	Initial compsote prestressing force	$P_{i,c}$	172	kip
	Initial inner wythe prestressing force	$P_{i,i}$	86	kip
	Initial outer wythe prestressing force	$P_{i,o}$	86	kip
	1-losses	R	87%	
	Effective compsote prestressing force	$P_{e,o}$	149	kip
	Effective inner wythe prestressing force	$P_{e,i}$	75	kip
	Effective inner wythe prestressing force	$P_{e,o}$	75	kip
	Time to testing	t_{relax}	2184	hrs
	Time to set	t_{set}	16	hrs
	Relative humidity	RH	70	%
	Volume of concrete	V	161395	in^3
	Specimen surface area	S	140544	in^2
	Volume/surface area	V/S	1.14836	in
	Friction loss coefficient	k	0	
	Shrinkage coefficient	ksh	1	
	Creep coeficient	kcr	2	
	Anchorage Seating	Δ_A	0	in
	Friction coefficient	μ	0	
	Wobble coefficient	α	0	

Note: Percent composite action and deflections calculated at mid-height

Note: Moment capacities and ultimate load calculated at 3/4-height

Mild steel properties	Steel area both wythes	$A_{s,c}$	0.3296	in^2
	Steel area each wythe	$A_{s,nc}$	0.1648	in^2
	Steel modulus	E_s	29000	ksi
	Fully composite steel depth	$d_{s,c}$	4.00	in
	Inner wythe steel depth	$d_{s,i}$	1.00	in
	Outer wythe steel depth	$d_{s,o}$	1.00	in
	Strand yield strength	f_{sy}	65	ksi
Concrete properties	Concrete unit weight	γ_c	145	pcf
	Initial concrete strength	f'_{ci}	3.5	psi
	Initial concrete modulus	E_{ci}	3372	ksi
	Concrete strength	f'_c	7.67	ksi
	Concrete modulus	E_c	4992	ksi
	Maximum concrete strain	ε_{cu}	0.003	in/in
	Tension modulus constant	$K\sqrt{f'_c}=$	10.0	
	Tension modulus	$f_r=$	0.876	ksi
	NA depth constant	β_1	0.6665	
	Initial prestressed modular ratio	n_i	8.4515	
	Prestressed modular ratio	n	5.7092	
Safety factors	Flexural phi factor	ϕ_f	0.9	
	Shear phi factor	ϕ_v	0.85	
Loads	Composite axial load	P_{axial}	37.8	kip
	Inner wythe axial load	$P_{axial,i}$	37.8	kip
	Outer wythe axial load	$P_{axial,o}$	0.0	kip
	Wythe surface to axial load	a_3	6	in
	Composite axial load eccentricity	$e_{a,c}$	9.86	in
	Inner wythe axial load eccentricity	$e_{a,i}$	7.50	in
	Outer wythe axial load eccentricity	$e_{a,o}$	13.00	in
	Composite axial load moment	$M_{e,c}$	373	kip-in
	Inner wythe axial load moment	$M_{e,i}$	284	kip-in
	Outer wythe axial load moment	$M_{e,o}$	0	kip-in
Cracking properties	Composite cracking moment	$M_{cr,c}$	1551	kip-in
	Inner wythe cracking moment	$M_{cr,i}$	157	kip-in
	Outer wythe cracking moment	$M_{cr,o}$	109	kip-in
	Composite cracking MOI	$I_{cr,c}$	149	in^4
	Inner wythe cracking MOI	$I_{cr,i}$	2.5	in^4
	Outer wythe cracking MOI	$I_{cr,o}$	2.5	in^4
Deflection	Initial bow	e_i	0	in

9.5.2 Prestressing Losses

PRECAST PRESTRESSED CONCRETE SANDWICH WALL PANEL DATA INPUT

Stage 0: Jacking

Anchorage Seating Losses			**Friction Losses**		
Δf_{pA} =	**0**	**ksi**	**Δf_{pF} =**	**0**	**ksi**
Stage 0 Loss =	**0**	**ksi**			
f_{pi} =	**202.5**	**kip**			

Stage I: Stress Transfer

Steel Relaxation Losses

t_1 =	0	hrs
t_2 =	16	hrs
f_{pi} =	203	ksi
Δf_{pR} =	**6.9**	**ksi**

Elastic Shortening Losses

Ass. Δf_{pES} =	1.52	ksi			
f_{pi} =	194	ksi			
$P_{i,i}$ =	82	kip	$P_{axial,i}$ =	37.8	kip
$P_{i,o}$ =	82	kip			

Elastic Shortening

M_D =	0	kip-ft
M_D =	0	kip-in
$f_{pES,i}$ =	-0.167	ksi
$f_{pES,o}$ =	-0.192	ksi
$\Delta f_{pES,i}$ =	**1.41**	**ksi**
$\Delta f_{pES,o}$ =	**1.62**	**ksi**
Difference =	0.00	
Stage I Loss =	**8.43**	**ksi**
f_{pi} =	**194**	**kip**

Stage II: Transfer to Placement of Superimposed Dead Load

Creep Losses

M_{SD} =	0	kip-ft
M_{SD} =	0	kip-in
f_{csi} =	0.167	ksi
f_{csd} =	0.000	ksi
f_{csd} =	0.000	ksi
Δf_{pCR} =	**1.91**	**ksi**

Shrinkage Losses

Δf_{pSH} =	**6.53**	**ksi**

Steel Relaxation Losses

t_1 =	16	hrs
t_2 =	2184	hrs
f_{pi} =	194	ksi
Δf_{pR} =	**10.30**	**ksi**

Stress Increase Due to Loading

Δf_{SD} =	**0.00**	**ksi**

Stage II Loss =	**18.7**	**ksi**
f_{pi} =	**175**	**kip**

Total Losses =	**19**	**ksi**
f_{pe} =	**175**	**ksi**
P_e =	**149**	**kip**
R =	**87%**	
Losses =	**13%**	

9.5.3 Cracked Moment of Inertia

REINFORCED CONCRETE SANDWICH WALL PANEL CRACKED MOMENT OF INERTIA

$x<d_1$			$x \geq d_1$			Outer wythe		
b =	144	in	b =	144	in	b =	144	in
d_o =	7	in	d_o =	7	in	d_o =	na	in
d_1 =	1	in	d_1 =	1	in	d =	1	in
t_2 =	2.67	in	t_1 =	2.67	in	t_1 =	2.67	in
A_s =	0.1648	Awythe [in^2]	A_s =	0.1648	Awythe [in^2]	A_s =	0.1648	Awythe [in^2]
A_{ps} =	0.425	Inner wythe [in^2]	A_{ps} =	0.425	Inner wythe [in^2]	A_{ps} =	0.425	Inner wythe [in^2]
A_{ps} =	0.425	Outer wythe [in^2]	A_{ps} =	0.425	Outer wythe [in^2]	A_{ps} =	0.425	Outer wythe [in^2]
E_s =	29000000	psi	E_s =	29000000	psi	E_s =	29000000	psi
E_{ps} =	28500000	psi	E_{ps} =	28500000	psi	E_{ps} =	28500000	psi
E_c =	4991977	psi	E_c =	4991976.56	psi	E_c =	4991976.56	psi
n_s =	5.809		n_s =	5.809		n_s =	5.809	
n_{ps} =	5.709		n_{ps} =	5.709		n_{ps} =	5.709	

Composite			Composite			Outer Wythe Non-Composite		
a =	72		a =	72		a =	72	
b =	6.768		b =	3.384		b =	3.384	
c =	27.070		c =	23.636		c =	3.384	
x =	0.568	in	x =	0.551	in	x =	0.195	in
	-0.662	in		-0.598	in		-0.242	in
I_{comp} =	149.4	in^4	I_{comp} =	148.8	in^4	$I_{non\text{-}comp\ wythe}$ =	2.5	in^4

Inner Wythe Non-Composite		
a =	72	
b =	3.384	
c =	3.384	
x =	0.195	in
	-0.242	in
$I_{non\text{-}comp\ wythe}$ =	2.5	in^4

9.5.4 Composite Deflection

REINFORCED CONCRETE SANDWICH WALL PANEL COMPOSITE DEFELCTION

P_{axial}	$P_{lateral}$	$2P_{lateral}$	M_a	I_{eff}	EI	Δ_{app}	Δ_{p-D}/e_i	e_t
kip	kip	kip	kip-in	in^4	$kip-in^2$	in	in/in	in
37.8	0	0	177	5493	27420751	0.048	0.010	0.048
37.8	1	2	237	5493	27420751	0.063	0.010	0.063
37.8	2.5	5	327	5493	27420751	0.085	0.010	0.085
37.8	3.5	7	387	5493	27420751	0.099	0.010	0.099
37.8	4	8	417	5493	27420751	0.106	0.010	0.106
37.8	5.45	10.9	504	5493	27420751	0.127	0.010	0.127
37.8	6	12	537	5493	27420751	0.135	0.010	0.135
37.8	7	14	597	5493	27420751	0.150	0.010	0.150
37.8	8	16	657	5493	27420751	0.164	0.010	0.164
37.8	9	18	717	5493	27420751	0.178	0.010	0.178
37.8	9.5	19	747	5493	27420751	0.186	0.010	0.186
37.8	11	22	837	5493	27420751	0.207	0.010	0.207
37.8	12	24	897	5493	27420751	0.222	0.010	0.222
37.8	13	26	957	5493	27420751	0.236	0.010	0.236
37.8	14	28	1017	5493	27420751	0.251	0.010	0.251
37.8	14.8	29.6	1065	5493	27420751	0.262	0.010	0.262
37.8	16	32	1137	5493	27420751	0.280	0.010	0.280
37.8	17	34	1197	5493	27420751	0.294	0.010	0.294
37.8	18	36	1257	5493	27420751	0.308	0.010	0.308
37.8	19	38	1317	5493	27420751	0.323	0.010	0.323
37.8	20	40	1377	5493	27420751	0.337	0.010	0.337
37.8	21	42	1437	5493	27420751	0.352	0.010	0.352
37.8	22	44	1497	5493	27420751	0.366	0.010	0.366
37.8	23	46	1557	5436	27136692	0.385	0.010	0.385
37.8	24	48	1617	4869	24306660	0.446	0.011	0.446
37.8	25	50	1677	4380	21867226	0.513	0.012	0.513
37.8	26	52	1737	3957	19753262	0.588	0.014	0.588
37.8	27	54	1797	3588	17912249	0.671	0.015	0.671
37.8	28	56	1857	3266	16301518	0.762	0.017	0.762
37.8	29	58	1917	2982	14886159	0.861	0.018	0.861
37.8	30	60	1977	2732	13637428	0.969	0.020	0.969

Δ_1	e_2	Δ_2	error	e_3	Δ_3	error	e_4	Δ_4
in	in	in	%	in	in	%	in	in
0.000	0.049	0.000	0.99%	0.049	0.000	0.01%	0.049	0.000
0.001	0.064	0.001	0.99%	0.064	0.001	0.01%	0.064	0.001
0.001	0.085	0.001	0.99%	0.085	0.001	0.01%	0.085	0.001
0.001	0.100	0.001	0.99%	0.100	0.001	0.01%	0.100	0.001
0.001	0.107	0.001	0.99%	0.107	0.001	0.01%	0.107	0.001
0.001	0.128	0.001	0.99%	0.128	0.001	0.01%	0.128	0.001
0.001	0.136	0.001	0.99%	0.136	0.001	0.01%	0.136	0.001
0.001	0.151	0.001	0.99%	0.151	0.001	0.01%	0.151	0.001
0.002	0.166	0.002	0.99%	0.166	0.002	0.01%	0.166	0.002
0.002	0.180	0.002	0.99%	0.180	0.002	0.01%	0.180	0.002
0.002	0.187	0.002	0.99%	0.187	0.002	0.01%	0.187	0.002
0.002	0.209	0.002	0.99%	0.209	0.002	0.01%	0.209	0.002
0.002	0.224	0.002	0.99%	0.224	0.002	0.01%	0.224	0.002
0.002	0.239	0.002	0.99%	0.239	0.002	0.01%	0.239	0.002
0.002	0.253	0.003	0.99%	0.253	0.003	0.01%	0.253	0.003
0.003	0.265	0.003	0.99%	0.265	0.003	0.01%	0.265	0.003
0.003	0.282	0.003	0.99%	0.282	0.003	0.01%	0.282	0.003
0.003	0.297	0.003	0.99%	0.297	0.003	0.01%	0.297	0.003
0.003	0.311	0.003	0.99%	0.311	0.003	0.01%	0.311	0.003
0.003	0.326	0.003	0.99%	0.326	0.003	0.01%	0.326	0.003
0.003	0.341	0.003	0.99%	0.341	0.003	0.01%	0.341	0.003
0.003	0.355	0.004	0.99%	0.355	0.004	0.01%	0.355	0.004
0.004	0.370	0.004	0.99%	0.370	0.004	0.01%	0.370	0.004
0.004	0.388	0.004	1.00%	0.388	0.004	0.01%	0.388	0.004
0.005	0.451	0.005	1.12%	0.451	0.005	0.01%	0.451	0.005
0.006	0.520	0.006	1.24%	0.520	0.006	0.02%	0.520	0.006
0.008	0.597	0.008	1.38%	0.597	0.008	0.02%	0.597	0.008
0.010	0.681	0.010	1.52%	0.681	0.010	0.02%	0.681	0.010
0.013	0.774	0.013	1.67%	0.775	0.013	0.03%	0.775	0.013
0.016	0.876	0.016	1.83%	0.877	0.016	0.03%	0.877	0.016
0.019	0.988	0.020	2.00%	0.988	0.020	0.04%	0.988	0.020

9.5.5 Non-composite Deflection

REINFORCED CONCRETE SANDWICH WALL PANEL NON-COMPOSITE DEFELCTION

P_{axial}	$P_{lateral}$	$2P_{lateral}$	M_s	$M_{s,i}$	$M_{s,o}$	$I_{eff,i}$	$I_{eff,o}$	I_{eff}	EI
kip	kip	kip	kip-in	kip-in	kip-in	in^4	in^4	in^4	$kip\text{-}in^2$
37.8	0	0	177	135	0	416	96	512	2555892
37.8	1	2	237	183	11	262	96	358	1788503
37.8	2.5	5	327	257	28	97	96	193	965784
37.8	3.5	7	387	305	39	59	96	155	773110
37.8	4	8	417	330	45	47	96	143	715242
37.8	5.45	10.9	504	400	61	28	96	124	616621
37.8	6	12	537	427	68	23	96	119	594588
37.8	7	14	597	476	79	17	96	113	566168
37.8	8	16	657	525	90	14	96	110	547343
37.8	9	18	717	573	101	11	96	107	534383
37.8	9.5	19	747	598	107	10	96	106	529401
37.8	11	22	837	671	124	8	66	74	369978
37.8	12	24	897	720	135	7	52	58	291882
37.8	13	26	957	768	146	6	41	47	235756
37.8	14	28	1017	817	158	5	33	39	194375
37.8	14.8	29.6	1065	856	167	5	29	34	168773
37.8	16	32	1137	915	180	5	23	28	139248
37.8	17	34	1197	963	191	4	20	24	120554
37.8	18	36	1257	1012	203	4	17	21	105745
37.8	19	38	1317	1061	214	4	15	19	93862
37.8	20	40	1377	1110	225	4	13	17	84215
37.8	21	42	1437	1158	236	4	12	15	76301
37.8	22	44	1497	1207	248	3	11	14	69749
37.8	23	46	1557	1256	259	3	10	13	64276
37.8	24	48	1617	1305	270	3	9	12	59670
37.8	25	50	1677	1353	281	3	8	11	55765
37.8	26	52	1737	1402	293	3	7	11	52433
37.8	27	54	1797	1451	304	3	7	10	49572
37.8	28	56	1857	1500	315	3	6	9	47101
37.8	29	58	1917	1548	326	3	6	9	44957
37.8	30	60	1977	1597	338	3	6	9	43088

Δ_{app}	Δ_{P-D}/e_0	e_1	Δ_1	e_2	Δ_2	error	e_3	Δ_3
in	in/in	in	in	in	in	%	in	in
0.520	0.106	0.520	0.055	0.575	0.061	10.65%	0.581	0.062
0.964	0.152	0.964	0.147	1.111	0.169	15.22%	1.133	0.172
2.400	0.282	2.400	0.676	3.077	0.867	28.18%	3.268	0.921
3.511	0.352	3.511	1.236	4.747	1.671	35.20%	5.182	1.824
4.072	0.381	4.072	1.549	5.621	2.139	38.05%	6.211	2.363
5.654	0.441	5.654	2.496	8.150	3.597	44.14%	9.251	4.083
6.230	0.458	6.2E+00	2.9E+00	9.1E+00	4.2E+00	45.77%	1.0E+01	4.8E+00
7.242	0.481	7.2E+00	3.5E+00	1.1E+01	5.2E+00	48.07%	1.2E+01	6.0E+00
8.215	0.497	8.2E+00	4.1E+00	1.2E+01	6.1E+00	49.72%	1.4E+01	7.1E+00
9.155	0.509	9.2E+00	4.7E+00	1.4E+01	7.0E+00	50.93%	1.6E+01	8.2E+00
9.615	0.514	9.6E+00	4.9E+00	1.5E+01	7.5E+00	51.41%	1.7E+01	8.8E+00
15.364	0.736	1.5E+01	1.1E+01	2.7E+01	2.0E+01	73.56%	3.5E+01	2.6E+01
20.831	0.932	2.1E+01	1.9E+01	4.0E+01	3.8E+01	93.24%	5.8E+01	5.4E+01
27.471	1.154	2.7E+01	3.2E+01	5.9E+01	6.8E+01	115.44%	9.6E+01	1.1E+02
35.356	1.400	3.5E+01	5.0E+01	8.5E+01	1.2E+02	140.02%	1.5E+02	2.2E+02
42.596	1.613	4.3E+01	6.9E+01	1.1E+02	1.8E+02	161.26%	2.2E+02	3.6E+02
55.041	1.954	5.5E+01	1.1E+02	1.6E+02	3.2E+02	195.45%	3.7E+02	7.3E+02
66.861	2.258	6.7E+01	1.5E+02	2.2E+02	4.9E+02	225.76%	5.6E+02	1.3E+03
79.969	2.574	8.0E+01	2.1E+02	2.9E+02	7.4E+02	257.37%	8.2E+02	2.1E+03
94.312	2.900	9.4E+01	2.7E+02	3.7E+02	1.1E+03	289.96%	1.2E+03	3.4E+03
109.818	3.232	1.1E+02	3.5E+02	4.6E+02	1.5E+03	323.17%	1.6E+03	5.2E+03
126.398	3.567	1.3E+02	4.5E+02	5.8E+02	2.1E+03	356.69%	2.2E+03	7.8E+03
143.950	3.902	1.4E+02	5.6E+02	7.1E+02	2.8E+03	390.20%	2.9E+03	1.1E+04
162.367	4.234	1.6E+02	6.9E+02	8.5E+02	3.6E+03	423.42%	3.8E+03	1.6E+04
181.538	4.561	1.8E+02	8.3E+02	1.0E+03	4.6E+03	456.11%	4.8E+03	2.2E+04
201.351	4.880	2.0E+02	9.8E+02	1.2E+03	5.8E+03	488.05%	6.0E+03	2.9E+04
221.701	5.191	2.2E+02	1.2E+03	1.4E+03	7.1E+03	519.07%	7.3E+03	3.8E+04
242.485	5.490	2.4E+02	1.3E+03	1.6E+03	8.6E+03	549.02%	8.9E+03	4.9E+04
263.609	5.778	2.6E+02	1.5E+03	1.8E+03	1.0E+04	577.82%	1.1E+04	6.1E+04
284.988	6.054	2.8E+02	1.7E+03	2.0E+03	1.2E+04	605.37%	1.2E+04	7.5E+04
306.546	6.316	3.1E+02	1.9E+03	2.2E+03	1.4E+04	631.64%	1.4E+04	9.1E+04

error	e_4	Δ_4	error	e_5	Δ_5	error	e_6	Δ_6
%	in	in	%	in	in	%	in	in
1.02%	0.582	0.062	0.11%	0.582	0.062	0.01%	0.582	0.062
2.01%	1.137	0.173	0.30%	1.137	0.173	0.05%	1.137	0.173
6.20%	3.321	0.936	1.64%	3.336	0.940	0.46%	3.341	0.941
9.17%	5.335	1.878	2.96%	5.389	1.897	1.01%	5.408	1.904
10.49%	6.435	2.449	3.61%	6.520	2.481	1.33%	6.553	2.493
13.52%	9.738	4.298	5.26%	9.952	4.393	2.20%	10.047	4.434
14.37%	1.1E+01	5.0E+00	5.75%	1.1E+01	5.2E+00	2.49%	1.1E+01	5.2E+00
15.61%	1.3E+01	6.3E+00	6.49%	1.4E+01	6.5E+00	2.93%	1.4E+01	6.6E+00
16.51%	1.5E+01	7.6E+00	7.05%	1.6E+01	7.9E+00	3.27%	1.6E+01	8.0E+00
17.19%	1.7E+01	8.9E+00	7.47%	1.8E+01	9.2E+00	3.54%	1.8E+01	9.3E+00
17.46%	1.8E+01	9.5E+00	7.64%	1.9E+01	9.8E+00	3.65%	1.9E+01	1.0E+01
31.18%	4.1E+01	3.0E+01	17.48%	4.6E+01	3.4E+01	10.95%	4.9E+01	3.6E+01
44.99%	7.5E+01	7.0E+01	28.93%	9.1E+01	8.5E+01	20.92%	1.1E+02	9.9E+01
61.86%	1.4E+02	1.6E+02	44.12%	1.9E+02	2.2E+02	35.34%	2.4E+02	2.8E+02
81.68%	2.5E+02	3.5E+02	62.95%	3.9E+02	5.4E+02	54.09%	5.8E+02	8.1E+02
99.53%	4.0E+02	6.5E+02	80.44%	6.9E+02	1.1E+03	71.89%	1.2E+03	1.9E+03
129.30%	7.8E+02	1.5E+03	110.21%	1.6E+03	3.1E+03	102.47%	3.2E+03	6.2E+03
156.46%	1.3E+03	3.0E+03	137.73%	3.1E+03	6.9E+03	130.79%	7.0E+03	1.6E+04
185.35%	2.2E+03	5.6E+03	167.18%	5.7E+03	1.5E+04	161.04%	1.5E+04	3.8E+04
215.60%	3.5E+03	1.0E+04	198.08%	1.0E+04	2.9E+04	192.68%	2.9E+04	8.5E+04
246.80%	5.3E+03	1.7E+04	229.99%	1.7E+04	5.6E+04	225.24%	5.6E+04	1.8E+05
278.59%	7.9E+03	2.8E+04	262.47%	2.8E+04	1.0E+05	258.29%	1.0E+05	3.6E+05
310.60%	1.1E+04	4.5E+04	295.17%	4.5E+04	1.7E+05	291.46%	1.8E+05	6.8E+05
342.53%	1.6E+04	6.8E+04	327.74%	6.8E+04	2.9E+05	324.43%	2.9E+05	1.2E+06
374.09%	2.2E+04	1.0E+05	359.90%	1.0E+05	4.6E+05	356.93%	4.6E+05	2.1E+06
405.05%	2.9E+04	1.4E+05	391.42%	1.4E+05	7.0E+05	388.73%	7.0E+05	3.4E+06
435.22%	3.8E+04	2.0E+05	422.09%	2.0E+05	1.0E+06	419.65%	1.0E+06	5.4E+06
464.43%	4.9E+04	2.7E+05	451.75%	2.7E+05	1.5E+06	449.52%	1.5E+06	8.1E+06
492.57%	6.1E+04	3.6E+05	480.31%	3.6E+05	2.1E+06	478.25%	2.1E+06	1.2E+07
519.55%	7.6E+04	4.6E+05	507.66%	4.6E+05	2.8E+06	505.75%	2.8E+06	1.7E+07
545.31%	9.2E+04	5.8E+05	533.76%	5.8E+05	3.7E+06	531.98%	3.7E+06	2.3E+07

error	e_7	Δ_7	error	e_8	Δ_8	error	e_9
%	in	in	%	in	in	%	in
0.00%	0.582	0.062	0.00%	0.582	0.062	0.00%	0.582
0.01%	1.137	0.173	0.00%	1.137	0.173	0.00%	1.137
0.13%	3.342	0.942	0.04%	3.342	0.942	0.01%	3.342
0.35%	5.415	1.906	0.12%	5.417	1.907	0.04%	5.418
0.50%	6.565	2.498	0.19%	6.570	2.500	0.07%	6.572
0.95%	10.089	4.453	0.42%	10.107	4.461	0.18%	10.115
1.11%	1.1E+01	5.2E+00	0.50%	1.1E+01	5.2E+00	0.23%	1.1E+01
1.37%	1.4E+01	6.7E+00	0.65%	1.4E+01	6.7E+00	0.31%	1.4E+01
1.58%	1.6E+01	8.1E+00	0.77%	1.6E+01	8.1E+00	0.38%	1.6E+01
1.74%	1.8E+01	9.4E+00	0.87%	1.9E+01	9.5E+00	0.44%	1.9E+01
1.81%	2.0E+01	1.0E+01	0.91%	2.0E+01	1.0E+01	0.47%	2.0E+01
7.26%	5.1E+01	3.8E+01	4.98%	5.3E+01	3.9E+01	3.49%	5.4E+01
16.13%	1.2E+02	1.1E+02	12.95%	1.3E+02	1.2E+02	10.69%	1.4E+02
30.14%	3.1E+02	3.6E+02	26.74%	3.8E+02	4.4E+02	24.36%	4.7E+02
49.15%	8.4E+02	1.2E+03	46.14%	1.2E+03	1.7E+03	44.21%	1.7E+03
67.44%	1.9E+03	3.1E+03	64.95%	3.1E+03	5.0E+03	63.50%	5.1E+03
98.92%	6.2E+03	1.2E+04	97.19%	1.2E+04	2.4E+04	96.33%	2.4E+04
127.94%	1.6E+04	3.6E+04	126.71%	3.6E+04	8.1E+04	126.18%	8.1E+04
158.78%	3.8E+04	9.8E+04	157.92%	9.8E+04	2.5E+05	157.58%	2.5E+05
190.89%	8.6E+04	2.5E+05	190.28%	2.5E+05	7.2E+05	190.07%	7.2E+05
223.81%	1.8E+05	5.9E+05	223.37%	5.9E+05	1.9E+06	223.23%	1.9E+06
257.14%	3.6E+05	1.3E+06	256.82%	1.3E+06	4.6E+06	256.73%	4.6E+06
290.52%	6.8E+05	2.7E+06	290.28%	2.7E+06	1.0E+07	290.22%	1.0E+07
323.66%	1.2E+06	5.2E+06	323.48%	5.2E+06	2.2E+07	323.44%	2.2E+07
356.29%	2.1E+06	9.5E+06	356.15%	9.5E+06	4.4E+07	356.12%	4.4E+07
388.19%	3.4E+06	1.7E+07	388.08%	1.7E+07	8.2E+07	388.06%	8.2E+07
419.18%	5.4E+06	2.8E+07	419.09%	2.8E+07	1.4E+08	419.07%	1.4E+08
449.11%	8.1E+06	4.5E+07	449.04%	4.5E+07	2.4E+08	449.03%	2.4E+08
477.89%	1.2E+07	6.9E+07	477.83%	6.9E+07	4.0E+08	477.82%	4.0E+08
505.43%	1.7E+07	1.0E+08	505.38%	1.0E+08	6.2E+08	505.37%	6.2E+08
531.70%	2.3E+07	1.5E+08	531.65%	1.5E+08	9.2E+08	531.64%	9.2E+08

Δ_9	error	e_{10}	Δ_{10}	error
in	%	in	in	%
0.062	0.00%	0.582	0.062	0.00%
0.173	0.00%	1.137	0.173	0.00%
0.942	0.00%	3.342	0.942	0.00%
1.907	0.02%	5.418	1.907	0.01%
2.501	0.03%	6.572	2.501	0.01%
4.465	0.08%	10.119	4.466	0.04%
5.3E+00	0.10%	1.1E+01	5.3E+00	0.05%
6.7E+00	0.15%	1.4E+01	6.7E+00	0.07%
8.1E+00	0.19%	1.6E+01	8.1E+00	0.09%
9.5E+00	0.22%	1.9E+01	9.5E+00	0.11%
1.0E+01	0.24%	2.0E+01	1.0E+01	0.12%
4.0E+01	2.48%	5.5E+01	4.1E+01	1.78%
1.3E+02	9.01%	1.6E+02	1.4E+02	7.71%
5.4E+02	22.61%	5.7E+02	6.6E+02	21.29%
2.4E+03	42.92%	2.5E+03	3.5E+03	42.05%
8.2E+03	62.63%	8.2E+03	1.3E+04	62.10%
4.7E+04	95.90%	4.7E+04	9.2E+04	95.68%
1.8E+05	125.94%	1.8E+05	4.1E+05	125.84%
6.5E+05	157.45%	6.5E+05	1.7E+06	157.40%
2.1E+06	190.00%	2.1E+06	6.0E+06	189.97%
6.1E+06	223.19%	6.1E+06	2.0E+07	223.18%
1.6E+07	256.70%	1.6E+07	5.9E+07	256.69%
4.1E+07	290.21%	4.1E+07	1.6E+08	290.20%
9.3E+07	323.43%	9.3E+07	3.9E+08	323.42%
2.0E+08	356.11%	2.0E+08	9.1E+08	356.11%
4.0E+08	388.05%	4.0E+08	1.9E+09	388.05%
7.5E+08	419.07%	7.5E+08	3.9E+09	419.07%
1.3E+09	449.03%	1.3E+09	7.4E+09	449.02%
2.3E+09	477.82%	2.3E+09	1.3E+10	477.82%
3.7E+09	505.37%	3.7E+09	2.3E+10	505.37%
5.8E+09	531.64%	5.8E+09	3.7E+10	531.64%

9.5.6 Deflection Percent Composite Action

REINFORCED CONCRETE SANDWICH WALL PANEL PERCENT COMPOSITE ACTION

P_{max} =	5.1	kip	Axial Load deflection:	0.1676	in
P_y =	5.1	kip	1st 5k deflection:	0.3136	in
Δ_y =	0.328	in	%PCA Axial Load:	77.7%	
Δ_i =	0.227	in	%PCA 1st 5k:	93.0%	
n =	0.0		~1282 5k Cycle deflection:	1.259	in
E =	0		%PCA ~1282 5k Cycle:	64.0%	
Elastic stiffness =	50	ksi			

	Service Load	Deflection
Lat Id	7	0
	7	20

		Composite	Non-Composite	Test Data		Pessiki
Axial Load	Lat. Load	Deflection	Deflection	Lat. Load	Deflection	%PCA
kip	kip	in	in	kip	in	%
0	0.0	0	0	0.0	0.000	0%
37.8	0.0	0.049	0.582	0.0	0.227	67%
37.8	2.0	0.064	1.137	2.0	0.267	81%
37.8	5.0	0.085	3.342	5.0	0.326	92.6%
37.8	7.0	0.100	5.4E+00			
37.8	8.0	0.107	6.6E+00			
37.8	10.9	0.128	1.0E+01			
37.8	12.0	0.136	1.1E+01			
37.8	14.0	0.151	1.4E+01			
37.8	16.0	0.166	1.6E+01			
37.8	18.0	0.180	1.9E+01			
37.8	19.0	0.187	2.0E+01			
37.8	22.0	0.209	5.5E+01			
37.8	24.0	0.224	1.6E+02			
37.8	26.0	0.239	5.7E+02			
37.8	28.0	0.253	2.5E+03			
37.8	29.6	0.265	8.2E+03			
37.8	32.0	0.282	4.7E+04			
37.8	34.0	0.297	1.8E+05			
37.8	36.0	0.311	6.5E+05			
37.8	38.0	0.326	2.1E+06			
37.8	40.0	0.341	6.1E+06			
37.8	42.0	0.355	1.6E+07			
37.8	44.0	0.370	4.1E+07			
37.8	46.0	0.388	9.3E+07			
37.8	48.0	0.451	2.0E+08			
37.8	50.0	0.520	4.0E+08			
37.8	52.0	0.597	7.5E+08			
37.8	54.0	0.681	1.3E+09			
37.8	56.0	0.775	2.3E+09			
37.8	58.0	0.877	3.7E+09			
37.8	60.0	0.988	5.8E+09			

Note: Experimental data corresponds to 1st 5k lateral load cycle

9.6 XPS 4 CALCULATIONS

9.6.1 Input

PRECAST PRESTRESSED CONCRETE SANDWICH WALL PANEL DATA INPUT

Input and Properties:

Dimensions	Width	b	12	ft
	Width	b	144	in
	Height to axial load	H'	19	ft
	Height to axial load	H'	228	in
	Total height	H	20	ft
	Total height	H	240	in
	Inner wythe thickness	t_1	2.67	in
	Outer wythe thickness	t_2	2.00	in
	Insulation thickness	t_3	3.33	in
	Total thickness	t	8.00	in
	Composite top extreme fiber	$y_{t,c}$	3.86	in
	Composite bottom extreme fiber	$y_{b,c}$	4.14	in
	Inner wythe top extreme fiber	$y_{t,i}$	1.50	in
	Inner wythe bottom extreme fiber	$y_{b,i}$	2.50	in
	Outer wythe top extreme fiber	$y_{t,o}$	1.00	in
	Outer wythe bottom extreme fiber	$y_{b,o}$	1.00	in
	Composite centroid to inner centroid	d_i	2.36	in
	Composite centroid to outer centroid	d_o	3.14	in
	Top panel to top corbe	a_1	12	in
	End of panel to lateral load	a_2	60	in
	Bottom panel to measured lateral deflection	x_1	120	in
	Top panel to measured lateral deflection	x	120	in
	Bottom panel to maximum moment	x_2	180	in
	Top panel to maximum moment	x_3	60	in
Section properties	Inner wythe area	$A_{c,i}$	334	in^2
	Outer wythe area	$A_{c,o}$	238	in^2
	Concrete area	A_c	672	in^2
	Fully composite MOI	I_c	5490	in^4
	Inner wythe MOI	$I_{nc,i}$	416	in^4
	Outer wythe MOI	$I_{nc,o}$	96	in^4
	Fully noncomposite MOI	I_{nc}	512	in^4
	Inner wythe stiffness	%I	81.3%	
	Outer wythe stiffness	%O	18.8%	
Prestress properties	Prestressed area both wythes	$A_{p,c}$	0.85	in^2
	Prestressed area inner wythe	$A_{p,i}$	0.425	in^2
	Prestressed area outer wythe	$A_{p,o}$	0.425	in^2
	Fully composite prestressing depth	$d_{p,c}$	4.00	in
	Fully composite prestressing eccentricity	$e_{p,c}$	0.14	in

Prestress properties	Inner wythe prestressing depth	$d_{p,i}$	1.00	in
	Inner wythe prestressing eccentricity	$e_{p,i}$	-0.50	in
	Outer wythe prestressing depth	$d_{p,o}$	1.00	in
	Outer wythe prestressing eccentricity	$e_{p,o}$	0.00	in
	Prestressing modulus	E_{ps}	28500	ksi
	Strand yield strength	f_{py}	243	ksi
	Strand ultimate strength	f_{pu}	270	ksi
	Yield/Ultimate	f_{pi}/f_{pu}	0.75	
	Initial prestressing strength	f_{pi}	202.5	ksi
	Initial compsote prestressing force	$P_{i,c}$	172	kip
	Initial inner wythe prestressing force	$P_{i,i}$	86	kip
	Initial outer wythe prestressing force	$P_{i,o}$	86	kip
	1-losses	R	87%	
	Effective compsote prestressing force	$P_{e,o}$	149	kip
	Effective inner wythe prestressing force	$P_{e,i}$	75	kip
	Effective inner wythe prestressing force	$P_{e,o}$	75	kip
	Time to testing	t_{relax}	2184	hrs
	Time to set	t_{set}	16	hrs
	Relative humidity	RH	70	%
	Volume of concrete	V	161395	in^3
	Specimen surface area	S	140544	in^2
	Volume/surface area	V/S	1.14836	in
	Friction loss coefficient	k	0	
	Shrinkage coefficient	ksh	1	
	Creep coeficient	kcr	2	
	Anchorage Seating	Δ_A	0	in
	Friction coefficient	μ	0	
	Wobble coefficient	α	0	

Note: Percent composite action and deflections calculated at mid-height

Note: Moment capacities and ultimate load calculated at 3/4-height

Mild steel properties	Steel area both wythes	$A_{s,c}$	0.3296	in^2
	Steel area each wythe	$A_{s,nc}$	0.1648	in^2
	Steel modulus	E_s	29000	ksi
	Fully composite steel depth	$d_{s,c}$	4.00	in
	Inner wythe steel depth	$d_{s,i}$	1.00	in
	Outer wythe steel depth	$d_{s,o}$	1.00	in
	Strand yield strength	f_{sy}	65	ksi
Concrete properties	Concrete unit weight	γ_c	145	pcf
	Initial concrete strength	f'_{ci}	3.5	psi
	Initial concrete modulus	E_{ci}	3372	ksi
	Concrete strength	f'_c	7.34	ksi
	Concrete modulus	E_c	4883	ksi
	Maximum concrete strain	ε_{cu}	0.003	in/in
	Tension modulus constant	$K\sqrt{f'_c}$ =	10.0	
	Tension modulus	f_r =	0.857	ksi
	NA depth constant	β_1	0.683	
	Initial prestressed modular ratio	n_i	8.4515	
	Prestressed modular ratio	n	5.8361	
Safety factors	Flexural phi factor	ϕ_f	0.9	
	Shear phi factor	ϕ_v	0.85	
Loads	Composite axial load	P_{axial}	37.8	kip
	Inner wythe axial load	$P_{axial,i}$	37.8	kip
	Outer wythe axial load	$P_{axial,o}$	0.0	kip
	Wythe surface to axial load	a_3	6	in
	Composite axial load eccentricity	$e_{a,c}$	9.86	in
	Inner wythe axial load eccentricity	$e_{a,i}$	7.50	in
	Outer wythe axial load eccentricity	$e_{a,o}$	13.00	in
	Composite axial load moment	$M_{e,c}$	373	kip-in
	Inner wythe axial load moment	$M_{e,i}$	284	kip-in
	Outer wythe axial load moment	$M_{e,o}$	0	kip-in
Cracking properties	Composite cracking moment	$M_{cr,c}$	1526	kip-in
	Inner wythe cracking moment	$M_{cr,i}$	154	kip-in
	Outer wythe cracking moment	$M_{cr,o}$	107	kip-in
	Composite cracking MOI	$I_{cr,c}$	153	in^4
	Inner wythe cracking MOI	$I_{cr,i}$	2.6	in^4
	Outer wythe cracking MOI	$I_{cr,o}$	2.6	in^4
Deflection	Initial bow	e_i	0	in

9.6.2 Prestressing Losses

PRECAST PRESTRESSED CONCRETE SANDWICH WALL PANEL DATA INPUT

Stage 0: Jacking

Anchorage Seating Losses

Δf_{pA} = 0 ksi

Friction Losses

Δf_{pF} = 0 ksi

Stage 0 Loss = 0 ksi

f_{pi} = 202.5 kip

Stage I: Stress Transfer

Steel Relaxation Losses

t_1 = 0 hrs

t_2 = 16 hrs

f_{pi} = 203 ksi

Δf_{pR} = 6.9 ksi

Elastic Shortening Losses

Ass. Δf_{pES} = 1.52 ksi

f_{pi} = 194 ksi

$P_{i,i}$ = 82 kip

$P_{i,o}$ = 82 kip

$P_{axial,i}$ = 37.8 kip

Elastic Shortening

M_D = 0 kip-ft

M_D = 0 kip-in

$f_{pES,i}$ = -0.167 ksi

$f_{pES,o}$ = -0.192 ksi

$\Delta f_{pES,i}$ = 1.41 ksi

$\Delta f_{pES,o}$ = 1.62 ksi

Difference = 0.00

Stage I Loss = 8.43 ksi

f_{pi} = 194 kip

Stage II: Transfer to Placement of Superimposed Dead Load

Creep Losses

M_{SD} =	0	kip-ft
M_{SD} =	0	kip-in
f_{csi} =	0.167	ksi
f_{csd} =	0.000	ksi
f_{csd} =	0.000	ksi
Δf_{pCR} =	**1.95**	**ksi**

Shrinkage Losses

Δf_{pSH} =	**6.53**	**ksi**

Steel Relaxation Losses

t_1 =	16	hrs
t_2 =	2184	hrs
f_{pi} =	194	ksi
Δf_{pR} =	**10.30**	**ksi**

Stress Increase Due to Loading

Δf_{SD} =	**0.00**	**ksi**

Stage II Loss =	**18.8**	**ksi**
f_{pi} =	**175**	**kip**

Total Losses =	**19**	**ksi**
f_{pe} =	**175**	**ksi**
P_e =	**149**	**kip**
R =	**87%**	
Losses =	**13%**	

9.6.3 Cracked Moment of Inertia

REINFORCED CONCRETE SANDWICH WALL PANEL CRACKED MOMENT OF INERTIA

$x<d_1$			$x \geq d_1$			Outer wythe		
b =	144	in	b =	144	in	b =	144	in
d_o =	7	in	d_o =	7	in	d_o =	na	in
d_1 =	1	in	d_1 =	1	in	d =	1	in
t_c =	2.67	in	t_1 =	2.67	in	t_1 =	2.67	in
A_s =	0.1648	Awythe [in^2]	A_s =	0.1648	Awythe [in^2]	A_s =	0.1648	Awythe [in^2]
A_{ps} =	0.425	Inner wythe [in^2]	A_{ps} =	0.425	Inner wythe [in^2]	A_{ps} =	0.425	Inner wythe [in^2]
A_{ps} =	0.425	Outer wythe [in^2]	A_{ps} =	0.425	Outer wythe [in^2]	A_{ps} =	0.425	Outer wythe [in^2]
E_s =	29000000	ps	E_s =	29000000	psi	E_s =	29000000	psi
E_{ps} =	28500000	ps	E_{ps} =	28500000	psi	E_{ps} =	28500000	psi
E_c =	4003407	ps	E_c =	4003406.6	psi	E_c =	4003406.6	psi
n_s =	5.938		n_s =	5.938		n_s =	5.938	
n_{ps} =	5.836		n_{ps} =	5.836		n_{ps} =	5.836	

Composite			Composite			Outer Wythe Non-Composite		
a =	72		a =	72		a =	72	
b =	6.918		b =	3.459		b =	3.459	
c =	27.672		c =	24.213		c =	3.459	
x =	0.574	in	x =	0.556	in	x =	0.196	in
	-0.670	in		-0.604	in		-0.245	in
I_{comp} =	152.5	in^4	I_{comp} =	151.9	in^4	$I_{non-comp/wythe}$ =	2.6	in^4

Inner Wythe Non-Composite

a =	72	
b =	3.459	
c =	3.459	
x =	0.196	in
	-0.245	in
$I_{non-comp/wythe}$ =	2.6	in^4

9.6.4 Composite Deflection

REINFORCED CONCRETE SANDWICH WALL PANEL COMPOSITE DEFELCTION

P_{axial}	$P_{lateral}$	$2P_{lateral}$	M_a	I_{eff}	EI	Δ_{app}	$\Delta_{p-\Delta}/e_i$	e_t
kip	kip	kip	kip-in	in^4	$kip-in^2$	in	in/in	in
37.8	0	0	177	5493	26824380	0.050	0.010	0.050
37.8	1	2	237	5493	26824380	0.064	0.010	0.064
37.8	2.5	5	327	5493	26824380	0.086	0.010	0.086
37.8	3.5	7	387	5493	26824380	0.101	0.010	0.101
37.8	4	8	417	5493	26824380	0.109	0.010	0.109
37.8	5.45	10.9	504	5493	26824380	0.130	0.010	0.130
37.8	6	12	537	5493	26824380	0.138	0.010	0.138
37.8	7	14	597	5493	26824380	0.153	0.010	0.153
37.8	8	16	657	5493	26824380	0.168	0.010	0.168
37.8	9	18	717	5493	26824380	0.182	0.010	0.182
37.8	9.5	19	747	5493	26824380	0.190	0.010	0.190
37.8	11	22	837	5493	26824380	0.212	0.010	0.212
37.8	12	24	897	5493	26824380	0.227	0.010	0.227
37.8	13	26	957	5493	26824380	0.241	0.010	0.241
37.8	14	28	1017	5493	26824380	0.256	0.010	0.256
37.8	14.8	29.6	1065	5493	26824380	0.268	0.010	0.268
37.8	16	32	1137	5493	26824380	0.286	0.010	0.286
37.8	17	34	1197	5493	26824380	0.300	0.010	0.300
37.8	18	36	1257	5493	26824380	0.315	0.010	0.315
37.8	19	38	1317	5493	26824380	0.330	0.010	0.330
37.8	20	40	1377	5493	26824380	0.345	0.010	0.345
37.8	21	42	1437	5493	26824380	0.360	0.010	0.360
37.8	22	44	1497	5493	26824380	0.374	0.010	0.374
37.8	23	46	1557	5101	25302568	0.412	0.011	0.412
37.8	24	48	1617	4642	22669115	0.478	0.012	0.478
37.8	25	50	1677	4177	20399128	0.550	0.013	0.550
37.8	26	52	1737	3774	18432004	0.631	0.015	0.631
37.8	27	54	1797	3424	16718871	0.719	0.016	0.719
37.8	28	56	1857	3117	15220024	0.816	0.018	0.816
37.8	29	58	1917	2847	13902980	0.922	0.020	0.922
37.8	30	60	1977	2609	12740988	1.037	0.021	1.037

Δ_1	e_2	Δ_2	error	e_3	Δ_3	error	e_4	Δ_4
in	in	in	%	in	in	%	in	in
0.001	0.050	0.001	1.01%	0.050	0.001	0.01%	0.050	0.001
0.001	0.065	0.001	1.01%	0.065	0.001	0.01%	0.065	0.001
0.001	0.087	0.001	1.01%	0.087	0.001	0.01%	0.087	0.001
0.001	0.102	0.001	1.01%	0.102	0.001	0.01%	0.102	0.001
0.001	0.110	0.001	1.01%	0.110	0.001	0.01%	0.110	0.001
0.001	0.131	0.001	1.01%	0.131	0.001	0.01%	0.131	0.001
0.001	0.139	0.001	1.01%	0.140	0.001	0.01%	0.140	0.001
0.002	0.154	0.002	1.01%	0.154	0.002	0.01%	0.154	0.002
0.002	0.169	0.002	1.01%	0.169	0.002	0.01%	0.169	0.002
0.002	0.184	0.002	1.01%	0.184	0.002	0.01%	0.184	0.002
0.002	0.192	0.002	1.01%	0.192	0.002	0.01%	0.192	0.002
0.002	0.214	0.002	1.01%	0.214	0.002	0.01%	0.214	0.002
0.002	0.229	0.002	1.01%	0.229	0.002	0.01%	0.229	0.002
0.002	0.244	0.002	1.01%	0.244	0.002	0.01%	0.244	0.002
0.003	0.259	0.003	1.01%	0.259	0.003	0.01%	0.259	0.003
0.003	0.271	0.003	1.01%	0.271	0.003	0.01%	0.271	0.003
0.003	0.289	0.003	1.01%	0.289	0.003	0.01%	0.289	0.003
0.003	0.304	0.003	1.01%	0.304	0.003	0.01%	0.304	0.003
0.003	0.318	0.003	1.01%	0.318	0.003	0.01%	0.318	0.003
0.003	0.333	0.003	1.01%	0.333	0.003	0.01%	0.333	0.003
0.003	0.348	0.004	1.01%	0.348	0.004	0.01%	0.348	0.004
0.004	0.363	0.004	1.01%	0.363	0.004	0.01%	0.363	0.004
0.004	0.378	0.004	1.01%	0.378	0.004	0.01%	0.378	0.004
0.004	0.417	0.004	1.08%	0.417	0.004	0.01%	0.417	0.004
0.006	0.484	0.006	1.20%	0.484	0.006	0.01%	0.484	0.006
0.007	0.558	0.007	1.33%	0.558	0.007	0.02%	0.558	0.007
0.009	0.640	0.009	1.48%	0.640	0.009	0.02%	0.640	0.009
0.012	0.731	0.012	1.63%	0.731	0.012	0.03%	0.731	0.012
0.015	0.830	0.015	1.79%	0.831	0.015	0.03%	0.831	0.015
0.018	0.940	0.018	1.96%	0.940	0.018	0.04%	0.940	0.018
0.022	1.059	0.023	2.14%	1.059	0.023	0.04%	1.059	0.023

9.6.5 Non-composite Deflection

REINFORCED CONCRETE SANDWICH WALL PANEL NON-COMPOSITE DEFELCTION

P_{axial}	$P_{lateral}$	$2P_{lateral}$	M_s	$M_{s,i}$	$M_{s,o}$	$I_{eff,i}$	$I_{eff,o}$	I_{eff}	EI
kip	kip	kip	kip-in	kip-in	kip-in	in^4	in^4	in^4	$kip\text{-}in^2$
37.8	0	0	177	135	0	416	96	512	2500304
37.8	1	2	237	183	11	247	96	343	1674494
37.8	2.5	5	327	257	28	92	96	188	917480
37.8	3.5	7	387	305	39	56	96	152	740194
37.8	4	8	417	330	45	45	96	141	686947
37.8	5.45	10.9	504	400	61	26	96	122	596203
37.8	6	12	537	427	68	22	96	118	575929
37.8	7	14	597	476	79	17	96	113	549779
37.8	8	16	657	525	90	13	96	109	532458
37.8	9	18	717	573	101	11	96	107	520533
37.8	9.5	19	747	598	107	10	96	106	515949
37.8	11	22	837	671	124	8	63	71	345255
37.8	12	24	897	720	135	7	49	56	272737
37.8	13	26	957	768	146	6	39	45	220621
37.8	14	28	1017	817	158	5	32	37	182199
37.8	14.8	29.6	1065	856	167	5	27	32	158427
37.8	16	32	1137	915	180	5	22	27	131014
37.8	17	34	1197	963	191	4	19	23	113658
37.8	18	36	1257	1012	203	4	16	20	99910
37.8	19	38	1317	1061	214	4	14	18	88877
37.8	20	40	1377	1110	225	4	13	16	79921
37.8	21	42	1437	1158	236	4	11	15	72575
37.8	22	44	1497	1207	248	3	10	14	66491
37.8	23	46	1557	1256	259	3	9	13	61411
37.8	24	48	1617	1305	270	3	8	12	57135
37.8	25	50	1677	1353	281	3	8	11	53510
37.8	26	52	1737	1402	293	3	7	10	50417
37.8	27	54	1797	1451	304	3	7	10	47761
37.8	28	56	1857	1500	315	3	6	9	45468
37.8	29	58	1917	1548	326	3	6	9	43478
37.8	30	60	1977	1597	338	3	6	9	41742

Δ_{app}	Δ_{P-D}/e	e_1	Δ_1	e_2	Δ_2	error	e_3	Δ_3
in	in/in	in	in	in	in	%	in	in
0.531	0.109	0.531	0.058	0.589	0.064	10.89%	0.595	0.065
1.030	0.163	1.030	0.167	1.197	0.195	16.25%	1.224	0.199
2.527	0.297	2.527	0.750	3.276	0.972	29.66%	3.499	1.038
3.667	0.368	3.667	1.348	5.015	1.844	36.77%	5.511	2.026
4.240	0.396	4.240	1.680	5.919	2.345	39.62%	6.585	2.609
5.848	0.456	5.848	2.669	8.517	3.888	45.65%	9.736	4.444
6.432	0.473	6.4E+00	3.0E+00	9.5E+00	4.5E+00	47.26%	1.1E+01	5.2E+00
7.458	0.495	7.5E+00	3.7E+00	1.1E+01	5.5E+00	49.50%	1.3E+01	6.4E+00
8.444	0.511	8.4E+00	4.3E+00	1.3E+01	6.5E+00	51.11%	1.5E+01	7.7E+00
9.399	0.523	9.4E+00	4.9E+00	1.4E+01	7.5E+00	52.28%	1.7E+01	8.8E+00
9.866	0.527	9.9E+00	5.2E+00	1.5E+01	7.9E+00	52.75%	1.8E+01	9.4E+00
16.464	0.788	1.6E+01	1.3E+01	2.9E+01	2.3E+01	78.83%	4.0E+01	3.1E+01
22.294	0.998	2.2E+01	2.2E+01	4.5E+01	4.4E+01	99.79%	6.7E+01	6.7E+01
29.355	1.234	2.9E+01	3.6E+01	6.6E+01	8.1E+01	123.36%	1.1E+02	1.4E+02
37.719	1.494	3.8E+01	5.6E+01	9.4E+01	1.4E+02	149.38%	1.8E+02	2.7E+02
45.378	1.718	4.5E+01	7.8E+01	1.2E+02	2.1E+02	171.79%	2.6E+02	4.4E+02
58.500	2.077	5.8E+01	1.2E+02	1.8E+02	3.7E+02	207.73%	4.3E+02	9.0E+02
70.917	2.395	7.1E+01	1.7E+02	2.4E+02	5.8E+02	239.45%	6.5E+02	1.6E+03
84.640	2.724	8.5E+01	2.3E+02	3.2E+02	8.6E+02	272.41%	9.4E+02	2.6E+03
99.602	3.062	1.0E+02	3.1E+02	4.0E+02	1.2E+03	306.22%	1.3E+03	4.1E+03
115.718	3.405	1.2E+02	3.9E+02	5.1E+02	1.7E+03	340.54%	1.9E+03	6.3E+03
132.889	3.750	1.3E+02	5.0E+02	6.3E+02	2.4E+03	375.01%	2.5E+03	9.4E+03
151.002	4.093	1.5E+02	6.2E+02	7.7E+02	3.1E+03	409.32%	3.3E+03	1.4E+04
169.942	4.432	1.7E+02	7.5E+02	9.2E+02	4.1E+03	443.18%	4.3E+03	1.9E+04
189.592	4.763	1.9E+02	9.0E+02	1.1E+03	5.2E+03	476.34%	5.4E+03	2.6E+04
209.836	5.086	2.1E+02	1.1E+03	1.3E+03	6.5E+03	508.61%	6.7E+03	3.4E+04
230.565	5.398	2.3E+02	1.2E+03	1.5E+03	8.0E+03	539.82%	8.2E+03	4.4E+04
251.677	5.698	2.5E+02	1.4E+03	1.7E+03	9.6E+03	569.84%	9.9E+03	5.6E+04
273.078	5.986	2.7E+02	1.6E+03	1.9E+03	1.1E+04	598.57%	1.2E+04	7.0E+04
294.686	6.260	2.9E+02	1.8E+03	2.1E+03	1.3E+04	625.97%	1.4E+04	8.6E+04
316.425	6.520	3.2E+02	2.1E+03	2.4E+03	1.6E+04	652.00%	1.6E+04	1.0E+05

error	e_4	Δ_4	error	e_5	Δ_5	error	e_6	Δ_6
%	in	in	%	in	in	%	in	in
1.07%	0.596	0.065	0.12%	0.596	0.065	0.01%	0.596	0.065
2.27%	1.229	0.200	0.36%	1.229	0.200	0.06%	1.230	0.200
6.79%	3.565	1.057	1.89%	3.584	1.063	0.55%	3.590	1.065
9.88%	5.693	2.093	3.31%	5.760	2.118	1.18%	5.785	2.127
11.24%	6.848	2.713	4.00%	6.953	2.755	1.53%	6.994	2.771
14.31%	10.292	4.698	5.71%	10.546	4.814	2.47%	10.662	4.867
15.16%	1.2E+01	5.5E+00	6.22%	1.2E+01	5.6E+00	2.77%	1.2E+01	5.7E+00
16.39%	1.4E+01	6.9E+00	6.97%	1.4E+01	7.1E+00	3.23%	1.5E+01	7.2E+00
17.29%	1.6E+01	8.2E+00	7.53%	1.7E+01	8.5E+00	3.58%	1.7E+01	8.7E+00
17.95%	1.8E+01	9.5E+00	7.96%	1.9E+01	9.9E+00	3.85%	1.9E+01	1.0E+01
18.22%	1.9E+01	1.0E+01	8.13%	2.0E+01	1.1E+01	3.97%	2.0E+01	1.1E+01
34.75%	4.8E+01	3.8E+01	20.33%	5.4E+01	4.3E+01	13.32%	5.9E+01	4.7E+01
49.84%	8.9E+01	8.9E+01	33.19%	1.1E+02	1.1E+02	24.87%	1.3E+02	1.3E+02
68.13%	1.7E+02	2.0E+02	49.99%	2.3E+02	2.9E+02	41.11%	3.2E+02	3.9E+02
89.48%	3.0E+02	4.5E+02	70.54%	4.9E+02	7.3E+02	61.79%	7.7E+02	1.2E+03
108.58%	4.9E+02	8.4E+02	89.43%	8.8E+02	1.5E+03	81.10%	1.6E+03	2.7E+03
140.23%	9.6E+02	2.0E+03	121.26%	2.0E+03	4.3E+03	113.85%	4.3E+03	9.0E+03
168.91%	1.6E+03	3.9E+03	150.41%	4.0E+03	9.5E+03	143.83%	9.5E+03	2.3E+04
199.26%	2.7E+03	7.2E+03	181.38%	7.3E+03	2.0E+04	175.60%	2.0E+04	5.5E+04
230.84%	4.2E+03	1.3E+04	213.66%	1.3E+04	4.0E+04	208.59%	4.0E+04	1.2E+05
263.24%	6.4E+03	2.2E+04	246.79%	2.2E+04	7.5E+04	242.34%	7.5E+04	2.6E+05
296.06%	9.5E+03	3.6E+04	280.32%	3.6E+04	1.3E+05	276.41%	1.3E+05	5.0E+05
328.95%	1.4E+04	5.6E+04	313.89%	5.6E+04	2.3E+05	310.42%	2.3E+05	9.4E+05
361.59%	1.9E+04	8.4E+04	347.17%	8.5E+04	3.7E+05	344.07%	3.8E+05	1.7E+06
393.70%	2.6E+04	1.2E+05	379.86%	1.2E+05	5.9E+05	377.08%	5.9E+05	2.8E+06
425.05%	3.4E+04	1.7E+05	411.74%	1.7E+05	8.9E+05	409.23%	8.9E+05	4.5E+06
455.45%	4.4E+04	2.4E+05	442.63%	2.4E+05	1.3E+06	440.34%	1.3E+06	7.0E+06
484.77%	5.6E+04	3.2E+05	472.39%	3.2E+05	1.8E+06	470.28%	1.8E+06	1.0E+07
512.89%	7.0E+04	4.2E+05	500.91%	4.2E+05	2.5E+06	498.96%	2.5E+06	1.5E+07
539.75%	8.6E+04	5.4E+05	528.13%	5.4E+05	3.4E+06	526.32%	3.4E+06	2.1E+07
565.30%	1.0E+05	6.8E+05	554.00%	6.8E+05	4.4E+06	552.31%	4.4E+06	2.9E+07

error	e_7	Δ_7	error	e_8	Δ_8	error	e_9
%	in	in	%	in	in	%	in
0.00%	0.596	0.065	0.00%	0.596	0.065	0.00%	0.596
0.01%	1.230	0.200	0.00%	1.230	0.200	0.00%	1.230
0.16%	3.592	1.065	0.05%	3.592	1.066	0.01%	3.592
0.43%	5.794	2.130	0.16%	5.797	2.132	0.06%	5.799
0.60%	7.011	2.777	0.23%	7.017	2.780	0.09%	7.020
1.10%	10.715	4.891	0.50%	10.739	4.902	0.23%	10.750
1.27%	1.2E+01	5.7E+00	0.59%	1.2E+01	5.7E+00	0.28%	1.2E+01
1.55%	1.5E+01	7.3E+00	0.75%	1.5E+01	7.3E+00	0.37%	1.5E+01
1.77%	1.7E+01	8.7E+00	0.89%	1.7E+01	8.8E+00	0.45%	1.7E+01
1.94%	1.9E+01	1.0E+01	1.00%	2.0E+01	1.0E+01	0.52%	2.0E+01
2.01%	2.1E+01	1.1E+01	1.04%	2.1E+01	1.1E+01	0.54%	2.1E+01
9.26%	6.3E+01	5.0E+01	6.68%	6.6E+01	5.2E+01	4.94%	6.9E+01
19.87%	1.6E+02	1.5E+02	16.54%	1.8E+02	1.8E+02	14.17%	2.0E+02
35.94%	4.2E+02	5.2E+02	32.62%	5.5E+02	6.8E+02	30.34%	7.1E+02
57.05%	1.2E+03	1.8E+03	54.26%	1.8E+03	2.7E+03	52.54%	2.8E+03
76.93%	2.7E+03	4.7E+03	74.69%	4.7E+03	8.1E+03	73.45%	8.2E+03
110.59%	9.0E+03	1.9E+04	109.09%	1.9E+04	3.9E+04	108.38%	3.9E+04
141.25%	2.3E+04	5.5E+04	140.20%	5.5E+04	1.3E+05	139.76%	1.3E+05
173.56%	5.5E+04	1.5E+05	172.83%	1.5E+05	4.1E+05	172.56%	4.1E+05
206.99%	1.2E+05	3.7E+05	206.47%	3.7E+05	1.1E+06	206.30%	1.1E+06
241.06%	2.6E+05	8.7E+05	240.69%	8.7E+05	3.0E+06	240.58%	3.0E+06
275.38%	5.0E+05	1.9E+06	275.11%	1.9E+06	7.1E+06	275.03%	7.1E+06
309.59%	9.4E+05	3.8E+06	309.38%	3.8E+06	1.6E+07	309.33%	1.6E+07
343.38%	1.7E+06	7.4E+06	343.22%	7.4E+06	3.3E+07	343.19%	3.3E+07
376.50%	2.8E+06	1.3E+07	376.38%	1.3E+07	6.4E+07	376.35%	6.4E+07
408.73%	4.5E+06	2.3E+07	408.64%	2.3E+07	1.2E+08	408.62%	1.2E+08
439.92%	7.0E+06	3.8E+07	439.84%	3.8E+07	2.0E+08	439.82%	2.0E+08
469.92%	1.0E+07	6.0E+07	469.85%	6.0E+07	3.4E+08	469.84%	3.4E+08
498.64%	1.5E+07	9.0E+07	498.59%	9.0E+07	5.4E+08	498.58%	5.4E+08
526.03%	2.1E+07	1.3E+08	525.98%	1.3E+08	8.3E+08	525.97%	8.3E+08
552.05%	2.9E+07	1.9E+08	552.01%	1.9E+08	1.2E+09	552.00%	1.2E+09

Δ_9	error	e_{10}	Δ_{10}	error
in	%	in	in	%
0.065	0.00%	0.596	0.065	0.00%
0.200	0.00%	1.230	0.200	0.00%
1.066	0.00%	3.593	1.066	0.00%
2.132	0.02%	5.799	2.132	0.01%
2.781	0.04%	7.021	2.781	0.01%
4.907	0.10%	10.755	4.910	0.05%
5.8E+00	0.13%	1.2E+01	5.8E+00	0.06%
7.3E+00	0.18%	1.5E+01	7.3E+00	0.09%
8.8E+00	0.23%	1.7E+01	8.8E+00	0.12%
1.0E+01	0.27%	2.0E+01	1.0E+01	0.14%
1.1E+01	0.28%	2.1E+01	1.1E+01	0.15%
5.4E+01	3.71%	7.1E+01	5.6E+01	2.82%
2.0E+02	12.38%	2.2E+02	2.2E+02	10.99%
8.7E+02	28.72%	9.0E+02	1.1E+03	27.52%
4.1E+03	51.45%	4.1E+03	6.2E+03	50.75%
1.4E+04	72.75%	1.4E+04	2.4E+04	72.34%
8.1E+04	108.04%	8.1E+04	1.7E+05	107.88%
3.2E+05	139.58%	3.2E+05	7.5E+05	139.51%
1.1E+06	172.46%	1.1E+06	3.0E+06	172.43%
3.5E+06	206.25%	3.5E+06	1.1E+07	206.23%
1.0E+07	240.55%	1.0E+07	3.4E+07	240.54%
2.7E+07	275.01%	2.7E+07	1.0E+08	275.01%
6.4E+07	309.32%	6.4E+07	2.6E+08	309.32%
1.4E+08	343.18%	1.4E+08	6.4E+08	343.18%
3.0E+08	376.35%	3.0E+08	1.4E+09	376.35%
5.9E+08	408.62%	5.9E+08	3.0E+09	408.61%
1.1E+09	439.82%	1.1E+09	5.9E+09	439.82%
1.9E+09	469.84%	1.9E+09	1.1E+10	469.84%
3.2E+09	498.57%	3.2E+09	1.9E+10	498.57%
5.2E+09	525.97%	5.2E+09	3.2E+10	525.97%
8.0E+09	552.00%	8.0E+09	5.2E+10	552.00%

9.6.6 Deflection Percent Composite Action

REINFORCED CONCRETE SANDWICH WALL PANEL PERCENT COMPOSITE ACTION

P_{max} =	12.6	kip	Axial Load deflection:	0.142	in
P_y =	10	kip	1st 5k deflection:	0.2651	in
Δ_y =	0.780	in	%PCA Axial Load:	83.2%	
Δ_i =	0.468	in	%PCA 1st 5k:	94.9%	
n =	9.0				
E =	40				
Elastic stiffness =	32	ksi			

	Service Load	Deflection
Lat Id	7	0
	7	20

		Composite	Non-Composite	Test Data		Pessiki
Axial Load	Lat. Load	Deflection	Deflection	Lat. Load	Deflection	%PCA
kip	kip	in	in	kip	in	%
0	0.0	0	0	0.0	0.000	0%
37.8	0.0	0.050	0.596	0.0	0.468	23%
37.8	2.0	0.065	1.230	2.0	0.530	60%
37.8	5.0	0.087	3.593	5.0	0.624	85%
37.8	7.0	0.102	5.799	7.0	0.686	89.7%
37.8	8.0	0.110	7.021	8.0	0.718	91%
37.8	10.9	0.131	10.755	10.9	0.824	93.5%
37.8	12.0	0.140	12.188	12.0	0.929	93%
37.8	14.0	0.154	1.5E+01			
37.8	16.0	0.169	1.7E+01			
37.8	18.0	0.184	2.0E+01			
37.8	19.0	0.192	2.1E+01			
37.8	22.0	0.214	7.1E+01			
37.8	24.0	0.229	2.2E+02			
37.8	26.0	0.244	9.0E+02			
37.8	28.0	0.259	4.1E+03			
37.8	29.6	0.271	1.4E+04			
37.8	32.0	0.289	8.1E+04			
37.8	34.0	0.304	3.2E+05			
37.8	36.0	0.318	1.1E+06			
37.8	38.0	0.333	3.5E+06			
37.8	40.0	0.348	1.0E+07			
37.8	42.0	0.363	2.7E+07			
37.8	44.0	0.378	6.4E+07			
37.8	46.0	0.417	1.4E+08			
37.8	48.0	0.484	3.0E+08			
37.8	50.0	0.558	5.9E+08			
37.8	52.0	0.640	1.1E+09			
37.8	54.0	0.731	1.9E+09			
37.8	56.0	0.831	3.2E+09			
37.8	58.0	0.940	5.2E+09			
37.8	60.0	1.059	8.0E+09			